THE UNIVERSITY *of* EDINBURGH

Proteolytic processing of the cellular prion protein - its importance in health and as a modulator of TSE disease susceptibility in sheep

Lauren Campbell

Ph.D. by Research

The University of Edinburgh

2013

ABSTRACT

Expression of the cellular prion protein (PrP^C) from the *PRNP* gene is crucial for the development of a group of fatal neurodegenerative disorders called prion diseases. During prion infection a misfolded protein homologue of PrP^C, PrP^{Sc} causes further misfolding on interaction with native PrP^C molecules. PrP^{Sc} is highly resistant to proteinase K and aggregation of this protein is considered a hallmark of infection. Sheep are considered a model of natural infection and susceptibility to scrapie in sheep is defined by polymorphisms in the *PRNP* gene. It is still not fully understood how these polymorphisms regulate the conversion process or which other co-factors are involved. One such factor may be the truncation of PrP^C via proteolytic processing in the form of two main cleavage events, known as α- and β-cleavage. In sheep α-cleavage cuts at amino acid 115, creating two truncated proteins C1 and N1 and represents the main cleavage event in healthy brain. β-Cleavage creates a longer C-terminal fragment, C2 and corresponding N-terminal fragment N2, cutting around amino acid 92 in sheep. Truncated forms of PrP^C have been shown to represent around 50 % of total residual PrP in brain and may be an important determinant of disease through both decreasing the amount of full length PrP^C available for conversion and through functions associated with the truncated fragments. The research presented has shown that increased production of an α-cleavage fragment C1 in brain is associated with TSE resistant genotype ARR/ARR, while the presence of C2 fragment is affiliated with scrapie susceptible *PRNP* genotypes in brain. There was no difference in the levels of full length PrP^C in these genotypes suggesting that PrP expression does not directly correlate to susceptibility in this model. To assess if PrP^C fragments could affect the conversion during disease *in-vitro* fibrillisation assays were performed using novel

truncated recombinant proteins. These truncated proteins, although not thought to convert to PK resistant PrP^{Sc} during disease, can form amyloid fibrils. However, these fibrils appear to be less neurotoxic when compared to fibrils produced by full length PrP^{C}. Only the truncated fragments derived from the ARR allele inhibit *in-vitro* fibrillisation of other allelic PrP^{C} variants. Furthermore, treatment of infected cells in culture with recombinant $C1^{ARR}$ led to a decrease in the formation of disease associated PrP^{Sc}. In conclusion, genetic variations in levels of PrP truncated fragments may add to the complexity of genetic determinants of prion disease. In parallel with polymorphism-dependant conversion abilities, varying α-cleavage of ovine PrP^{C} may help to explain genetic resistance in sheep. The inhibitory effects of C1, illustrated *in-vitro* may represent a therapeutic avenue in the treatment of prion disease.

CONTENTS

ACKNOWLEDGEMENTS

I would firstly like to thank both my Ph.D. supervisors Dr Wilfred Goldmann and Professor Nora Hunter for their continued guidance, shared knowledge, valued criticism and proof reading which made this thesis possible. A special thank you to Wilfred for his day-to-day advice and enthusiasm throughout the last four years. I would also like to thank Dr Andrew Gill for his invaluable help with the creation and purification of recombinant proteins, mass spectrometry and cell free conversion. I am similarly grateful to Dr Sandra McCutcheon for the use of her novel PrP antibodies which were used throughout this thesis, Dr Gillian McGovern for performing Electron Microscopy, Dr Michael Tranulis for the use of his data and making us very welcome in Norway and Bob Fleming for his microscopy expertise. For providing the cell lines used in this work I would like to thank Rona Wilson, Alex Bossers and Didier Vilette. I would also like to thank Paula Stewart, Sonya Agarwal, Fiona Lane, Iain Kennedy, Angie Chong, Barry Bradford and Kayleigh Iremonger for their technical advice and continued support in the lab. A special thanks to Paula Stewart, Fiona Lane and Sonya Agarwal for their friendship and keeping me sane during long days of protein purifications. I would like to thank my parents for their continued support, understanding, advice and love, without whom I would not be half the person I am today. And finally, Richy… no matter how good or bad my work was going you made coming home the best part of the day.

DECLARATION

I have read and understood The University of Edinburgh guidelines on plagiarism and declare that the work presented in this thesis is my own. All experiments were designed in conjunction with my supervisors and performed and analysed by myself unless otherwise stated clearly in the text. A portion of this work has been previously published but none of the work presented in this thesis has, or will be, submitted for any other degree or professional qualification.

Lauren Campbell

PUBLICATIONS

Campbell, L., Gill, A., Hunter, N., Goldmann, W. (2012). ''Alpha-cleavage levels of ovine prion protein in brain are associated with Prnp genotype.'' *Prion 2012 Conference Amsterdam, Netherlands, May 2012, Prion 6 (Suppl), 113*

Stewart, P., L. Campbell, S. Skogtvedt, K. A. Griffin, J. M. Arnemo, M. Tryland, S. Girling, M. W. Miller, M. A. Tranulis and W. Goldmann (2012). "Genetic predictions of prion disease susceptibility in carnivore species based on variability of the prion gene coding region." PLoS One **7**(12): e50623.

Campbell, L., A. C. Gill, G. McGovern, C. M. O. Jalland, J. Hopkins, M. A. Tranulis, N. Hunter and W. Goldmann (2013). "The PrPC Cl fragment derived from the ovine A(136)R(154)R(171) PRNP allele is highly abundant in sheep brain and inhibits fibrillisation of full-length PrPC protein in vitro." Biochimica Et Biophysica Acta-Molecular Basis of Disease **1832**(6): 826-836.

Goldmann, W., Campbell, L., Gill, AC., Hunter, N. (2013) ''The PrPc C1 fragments derived from ovine PRNP alleles exhibit different abundance in brain and in vitro fibrillisation characteristics.'' *Prion 2013 Conference Banff, Canada May 2013, Prion 7 (Suppl.) 86*

S. McCutcheon, J. P. Langeveld, B. C. Tan, A. C. Gill, C. de Wolf, S. Martin, L. Gonzalez, J. Alihabi, A. R. A. Blanco, L. Campbell, N. Hunter and E. F. Houston (2014). ''Prion antibodies that detect multiple TSE agents with high sensitivity and specificity.'' PLoS One in press.

ABBREVIATIONS

APP	Amyloid Precursor Protein
ADAMS	A Disintegrin And Metalloprotease
BASE	Bovine Amyloidotic Spongiform Encephalopathy
BCA	Bicichoninic Acid
BSE	Bovine Spongiform Encephalopathy
CD	Circular Dichroism
CHO	Chinese Hamster Ovary
CJD	Creutzfeldt Jakob Disease
CNS	Central Nervous System
CWD	Chronic Wasting Disease
dH20	Deionised Water
DLS	Dynamic Light Scattering
DMSO	Dimethyl-Sulfoxide
DNA	Deoxyribonucleic Acid
EDTA	Ethylenediaminetetracetic Acid
EGF	Epidermal Growth Factor
EGTA	Ethylene Glycol Tetraacetic Acid
ER	Endoplasmic Reticulum
FCS	Foetal Calf Serum
FFI	Fatal Familial Insomnia
FGF	Fibroblast Growth Factor
FPLC	Fast Protein Liquid Chromatography
FSE	Feline Spongiform Encephalopathy
GFP	Green Fluorescent Protein
GPI	Glycosyl-phosphatidylinositol
GSS	Gerstmann-Sträussler-Scheinker Syndrome
HBSS	Hanks Balanced Salt Solution
HEK	Human Embryonic Kidney
HPLC	High Pressure Liquid Chromatography
HRP	Horseradish Peroxidase
ICC	Immunocytochemistry
IHC	Immunohistochemistry

IPTG	Isopropyl β-D-1-thiogalactopyranoside
LB	Luria Broth
LRP1	Low Density Lipoprotein Receptor Protein
Mte	Montmorrilonite-KSF
NEM	N-Ethylmaleimide
NI-IMAC	Nickel Ion - Immobilized Metal Ion Affinity Chromatography
OCT	Optimal Cutting Temperature compound
OPH	O-phenanthroline
PAGE	Polyacrylamide Gel Electrophoresis
PBS	Phosphate Buffered Saline
PCR	Polymerase Chain Reaction
PDBu	Phorbol 12,13-dibutyrate
PI-PLC	Phosphatidylinositol-specific phospholipase C
PK	Proteinase K
PKC	Protein Kinase C
PMA	Phorbol 12-Myristate 13-Acetate
PMCA	Protein Misfolding Cyclic Amplification
PMSF	Phenylmethylsulfonyl Fluoride
PNGase F	Peptide -N-Glycosidase F
PNS	Peripheral Nervous System
PrP^{C}	Cellular Prion Protein
PrP	Prion Protein
PrP^{Sc}	Misfolded, disease-specific Prion Protein ($PrP^{Scrapie}$)
PrPΔHD	PrP lacking the hydrophobic domain
PVDF	Polyvinylidene Difluoride
QuIC	Quaking-Induced Conversion
RNA	Ribonucleic Acid
Rov9	Rabbit kidney epithelial cells expressing PrP^{VRQ}
ROS	Reactive Oxygen Species
SAF	Scrapie Associated Fibrils
ScN2a	Scrapie infected N2a cell line
sCJD	Sporadic Creutzfeldt Jakob Disease
SD	Standard Deviation
SDS	Sodium Dodecyl Sulphate

SEM	Standard Error of the Mean
SMB	Scrapie Mouse Brain cells
SMB-PS	Scrapie Mouse Brain -Pentosan Sulphate (cured cells)
SSBP/1	Scrapie brain pool/1
TB	Terrific Broth
TBE	Tris Borate EDTA,
TBS (T)	Tris Buffered Saline (Tween)
TFA	Trifluoroacetic Acid
Tg	Transgenic
ThT	Thioflavin T
TSE	Transmissible Spongiform Encephalopathy
vCJD	Variant Creutzfeldt Jakob Disease
w/v	Weight per Volume

FIGURE INVENTORY

TABLE INVENTORY

CHAPTER 1

INTRODUCTION

1.1 AN OVERVIEW OF TSE DISEASE

1.1.1 General Introduction to TSE diseases

TSE's (transmissible spongiform encephalopathy) or prion diseases are a group of neurodegenerative disorders, which are incurable and eventually fatal. The first TSE to be identified around 250 years ago was scrapie in sheep (also known as classical scrapie), but these diseases are now known to affect a wide range of mammals from ruminants to humans in the form of BSE (bovine spongiform encephalopathy) in cattle, CJD (Creutzfeldt-Jakob disease) in humans (Harris 1999) and CWD (chronic wasting disease) in deer and elk (Williams and Young 1992) (Table 1.1) Genetic, sporadic or infectious in nature, these diseases have characteristically long preclinical incubation periods ranging from months to years. Symptoms vary from animal to animal and also depend on the strain of infectious agent but generally include ataxia and loss of neuronal function, which lead to impairment in behavior (Crozet, Beranger et al. 2008). The BSE epidemic in UK cattle of the late 1980's-1990's highlighted the potential for these diseases to cross the species barrier and emphasised the threat to human health in the form of variant CJD (vCJD). The realisation that little was known about the agent of the disease, transmission, pathogenesis and hence how best to implement preventative strategies led to a surge in scientific research. Now with a potential threat of CWD in North America and Canada nearly 30 years on, there are still unknowns and questions to be answered regarding the prion protein along with mechanisms involved in disease development.

DISEASE	PRIMARY HOST	TRAMSMISSION	CLINICAL SYMPTOMS	DISTINCTIVE HISTOLOGY	DISTINCTIVE PrP^{Sc} PATTERN
Classical Scrapie	Sheep, Goats	Animal-to-Animal, Environmental	Pruritus, Ataxia, Weight loss, Hind Limb weakness	*PRNP* genotype dependent	Characteristic
Atypical Scrapie	Sheep, Goats	Unknown	Ataxia, Hind limb weakness	PrP^{Sc} restricted to cerebral cortex and cerebellum	Low molecular weight band
Bovine Spongiform Encephalopathy	Cattle	Ingestion	Weight loss, reduced milk yield, Ataxia, aggressive behavior	PrP^{Sc} deposition in obex, medulla and mid brain	
Atypical BSE (BASE), L- and H-type BSE	Cattle	Unknown	Similar to BSE	Amyloid Plaques, PrP^{Sc} deposition I cortex and thalamus	Decrease in molecular weight of all bands, less di-glycosylated
Feline (F) SE	Domesti c Cats	Ingestion	Ataxia, Behavioral changes, Hyper-Anesthesia	Widespread distinct vacuolation, PrP^{Sc} undetectable in brain	
Chronic Wasting disease (CWD)	Deer and Elk	Animal-to-Animal	Ataxia, Behavioral changes, weight loss	Amyloid Plaques particularly in the cortex, Vacuolation of grey matter	
Creutzfeldt–Jakob disease	Humans	Sporadic, Inherited,	Dementia	Variable PrP^{Sc} deposition	Variable with *PRNP* genotype
Variant CJD	Humans	Ingestion	Behavioral changes, Psychosis, Young age at onset	Florid Plaques, PrP^{Sc} accumulation in lymph	
Gerstmann–Sträussler–Scheinker	Humans	Inherited	Cognitive impairment, Dementia, Limb ataxia and weakness	Widespread circular plaques	Variable PrP isoform pattern
Fatal Familial Insomnia (FFI)	Humans	Inherited, Sporadic	Sleep disruption, Hallucinations, Weight loss	Low PrP^{Sc}, Astrogliosis, Cerebral atrophy	Low molecular weight band
Kuru	Humans	Ingestion	Ataxia, Behavioral changes, Weight loss, Tremors	Widespread micro vacuolation	Variable with *PRNP* genotype and brain region

Table 1.1 – Summary of TSE diseases, including clinical symptoms, characteristic pathology and molecular PrP^{Sc} profiles (Pearson, Wyatt et al. 1992, Cardone, Liu et al. 1999, Collins, McLean et al. 2001, Casalone, Zanusso et al. 2004, Haïk, Peoc'h et al. 2004, Williams 2005, Capobianco, Casalone et al. 2007, Konold, Davis et al. 2007, Martin, Jeffrey et al. 2009, Balkema-Buschmann, Fast et al. 2011).

1.1.2 The prion hypothesis and conversion

There are two main conflicting opinions as to the nature of the infectious agent responsible for the spread of TSEs. Initially it was thought to be a small, 'slow virus' due to features such as long incubation periods and resistance to high temperatures and extreme pH conditions. This resistance to harsh conditions was specifically associated with a small amount of purified infective agent, which for instance could represent a bacteriophage (Chesebro 2003). However, this 'virus' was also resistant to ionizing radiation and ultra violet light, which would suggest a lack of nucleic acids. Moreover, the extremely small predicted molecular weight would render the 'virus' unable to carry the coding information required for replication (Alper, Haig et al. 1966). Continued attempts to view the infectious agent by microscopy were unsuccessful leading to the development of novel hypotheses for the nature of the agent (Gibbons and Hunter 1967).

The now widely accepted prion or 'protein only' hypothesis states that the agent is void of nucleic acids and is instead a protein-like particle inactivated by Proteinase K (PK), phenol, formalin and urea (Pattison 1965, Prusiner, McKinley et al. 1981, Prusiner 1998) This prion, also known as PrP^{Sc} is a conversion product of a cellular form of the prion protein (PrP^{C}), which is encoded by the *PRNP* gene. PrP^{C} is normally expressed in the brain and other parts of the central nervous system (CNS) and at lower levels in peripheral

tissues. It is thought that, on contact with cellular PrP^{C}, misfolded PrP^{Sc} induces a structural shift from a primarily alpha helical PrP^{C} structure to one rich in beta sheet, the latter forming aggregates that accumulate in the brain over the course of the disease (Linden, Martins et al. 2008). It has been concluded from experiments with PrP^{C} null mice that the presence of cellular PrP is essential to propagate PrP^{Sc} (Weissmann, Bueler et al. 1993). The conversion of PrP^{C} to PrP^{Sc} as a process is still not fully understood although, it is thought to involve distinct chronological steps, starting with oligomerisation of PrP^{C} (Rigter, Priem et al. 2009).

Other factors may be involved in the conversion of PrP^{C} to PrP^{Sc}, including the cellular localisation of PrP^{C} such as an increased concentration of PrP^{C} at the cell membrane. High concentrations of PrP^{C} at the cell membrane can cause the protein to form dimers and activate a structural shift towards the formation of β-sheet (Elfrink, Ollesch et al. 2008). Reduction in pH and increased salt concentration can also cause spontaneous conversion of recombinant PrP^{C} from a predominantly alpha helix structure to one rich in β-sheet – a process which is reversible when conditions are returned to normal (Zhou 2009). There are two main accepted models of conversion: the nucleation model and the template assisted model. The first suggests that both PrP^{C} and PrP^{Sc} exist side by side while, the latter indicates that PrP^{C} and PrP^{Sc} can form heterodimers that go on to convert into homodimers of PrP^{Sc} (Noinville, Chich et al. 2008).

1.1.3 Acquisition of disease

TSEs can be transmitted from animal to animal or from the environment by direct feeding of infected animal matter, by ingesting the infectious agent from the environment, by uptake through broken or damaged skin (van Keulen, Bossers et al. 2008), maternally (Foster, McKelvey et al. 1992) and by iatrogenic route for example, by the transfer of blood products, transplanted tissue and peptide hormones (Mabbott, Farquhar et al. 1998). Infection can also be experimentally transmitted by inoculation with tissue from an affected host (CHANDLER and FISHER 1963). However, sporadic diseases are considered the most common in humans, such as CJD with no exposure to known risk factors (Harries-Jones, Knight et al. 1988, Will 1993). Inherited forms in humans include Gerstmann-Straüssler-Scheinker syndrome (GSS), familial CJD and fatal familial insomnia (FFI). By definition these prion diseases are associated with mutations in the *PRNP* gene but perhaps also involve further unknown genetic risk factors (Hsiao, Baker et al. 1989).

1.1.4 The species barrier and strains

There is often a species barrier effect when infectious PrP^{Sc} from one species is introduced to another both in nature and under experimental conditions. For example, there have been no reported cases of scrapie transmission to humans (Moore, Vorberg et al. 2005). Furthermore, although the feeding of BSE contaminated meat and bone meal led to infection of cats and the development of feline spongiform encephalopathy (FSE), there has been no reported infection of dogs fed on a very similar diet. In early experimental transmission experiments rabbits were shown to be resistant to intracranial challenges with scrapie and murine adapted scrapie strains (Gibbs and Gajdusek 1973). However, recently adaptation of scrapie using *in vitro* conversion assays has led to successful infection of rabbits (Chianini, Fernandez-Borges et al. 2012). Along with complete resistance experimental transmission experiments have shown that the species barrier

can also lead to disease adaptations such as longer incubation periods, altered presentation of clinical symptoms and different pathogenesis (Bruce, Chree et al. 1994). This barrier may be explained by differences in the conformation or sequence of the host PrP^{C} protein, which may inhibit or alter interactions with the infecting PrP^{Sc} molecules. Amino acid polymorphisms in the host PrP^{C} can also create a barrier-like effect within in the same species, best illustrated by genetic resistance to classical scrapie in sheep (discussed in more detail in section 1.2.2).

On transmission of naturally occurring scrapie isolates to laboratory mice, numerous different strains of scrapie have been identified which present with different clinical signs or pathologies, varying incubation times and sometimes distinct PrP glycoform patterns created by different ratios of un-, mono- or di-glycosylated forms of PrP^{Sc} or sizes of PK resistant fragments (Somerville 1999, Somerville 2002). Along with different characteristics on transmission, strains also display varying stability and resistance to heat and pH (Somerville 2002). Strain characteristics may be influenced both by the infectious agent and the host protein and as a result strains can present with contrasting phenotypes in different laboratory mouse lines or the phenotype can alter on continued passage. One explanation for changes in strain phenotype is the presence of multiple stains or co-infections, such as classical scrapie and atypical scrapie (Mazza, Iulini et al. 2010). This hypothesis assumes that under diverse conditions, for example in a host with different template PrP^{C} protein and cellular co-factors, different strains become dominant or progress at a faster rate (Somerville 2002).

1.1.5 Atypical scrapie

Atypical scrapie strain primarily causes disease in sheep of classically resistant genotypes (discussed in section 1.2.2), such as ARR/ARR. This strain was identified through a distinct pathology (Benestad, Sarradin et al. 2003) and biochemical signature by immunoblotting. Atypical scrapie has been shown to be infectious under experimental conditions, having been successfully transmitted to sheep and porcine and ovine transgenic mice on intracerebral and oral inoculation (Simmons, Konold et al. 2007, Espinosa, Herva et al. 2009, Andréoletti, Orge et al. 2011, Simmons, Moore et al. 2011). However, natural acquisition of the agent is still under debate. The relatively small number of isolated natural cases has led some to believe that atypical scrapie is a sporadic disease, similar to CJD in humans, only now recognised due to the large scale genetic screening of sheep and wide spread recognition of typical clinical signs.

1.1.6 Pathogenesis and pathology

Oral ingestion is thought to be the most common natural route of infection of sheep with natural scrapie. The infectious agent is thought to be transported though the intestinal epithelia at the Peyer's patches, via M cell or dendritic cells to lymphoid follicles, where PrP^{Sc} accumulates on follicular dendritic cells (Sales 2006, van Keulen, Bossers et al. 2008). In mice follicular dendritic cells play an important role in the replication of PrP^{Sc} in the lymphoid tissue (Bruce, Brown et al. 2000). From the lymph reticular system the infectious agent is transported to the enteric nervous system and finally the central nervous system, where PrP^{Sc} again accumulates, evading clearance by the host immune system throughout (van Keulen, Bossers et al. 2008).

PrP^{Sc} protein aggregation in the brain is considered the hallmark of prion disease, illustrated in Figure 1.1. However, levels of PrP^{Sc} are not always correlated with disease pathogenesis (Piccardo, Manson et al. 2007). Histology at *post mortem* also normally reveals vacuolation (Figure 1.1) and astrogliosis in the CNS (Kuczius, Koch et al. 2007, Linden, Martins et al. 2008). The pattern of pathology is often strain and species dependent (Ligios, Jeffrey et al. 2002). Symptoms are also host dependent and vary according to species and strain of disease (Crozet, Beranger et al. 2008).

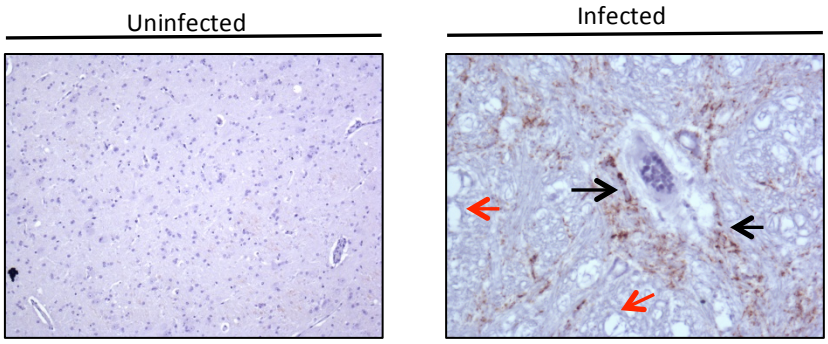

Figure 1.1 – PrP^{Sc} deposition and vacuolation in clinical scrapie infection shown by immunohistochemistry. Magnification of the thalamus from an uninfected and experimentally scrapie (SSBP/1) infected sheep at the clinical stage of disease. PrP^{Sc} deposition (brown staining, black arrows) and vacuolation (red arrows) are highlighted.

1.1.7 Biochemical PrP^{Sc} profiles in scrapie

Although, PrP^{Sc} detection in the brain by IHC is though to be one of the most sensitive methods (Grassi 2002) it is normally used in conjunction with immunoblotting to allow for molecular profiling of PrP^{Sc}. Detection of PrP^{Sc} by immunoblotting relies on the use of PK which degrades cellular PrP^{C} and cleaves misfolded PrP^{Sc} to leave a remaining PK resistant core fragment. As PrP^{C} and hence PrP^{Sc} are present in the brain in three different

forms, un-, mono- and di-glycosylated (see section 1.3.1) this creates a three band pattern in classical scrapie (Figure 1.2). Atypical scrapie can be distinguished from classical scrapie by a distinct biochemical signature of two additional lower molecular weight bands of PK resistant PrP^{Sc} on western blot.

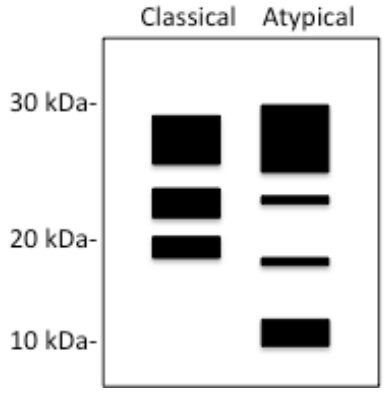

Figure 1.2. – Typical biochemical profile of PK resistant PrP^{Sc} in scrapie by immunoblotting. Diagrammatic representation of Western blot profile of PrP^{Sc} in the brain after PK treatment in both classical and atypical scrapie.

1.1.7 Prion therapeutics

There is currently no preventative therapy, treatment or cure for prion diseases. Although the spread of disease within the periphery could be prevented using immunoregulatory mechanisms, this approach is ineffective after the onset of clinical symptoms and once infection has passed through the blood-brain barrier (Wisniewski, Prelli et al. 2007, Wisniewski and Goni 2012). Some pharmaceuticals, which showed promising results in initial cell culture and animal studies such as the anticoagulant Pentosan polysulfate, did not have desired effects in clinical trials (Dealler and Rainov 2003, Stewart, Rydzewska et al. 2008). Newer potential therapeutics such as Astemizole, currently used in the treatment of rheumatoid arthritis and monocationic phenyl-furan-benzimidazole (DB772) decrease PrP^{Sc} accumulation in both cell culture and mouse models and increase survival time in the latter (Stanton, Schneider et al. 2012, Karapetyan, Sferrazza et al. 2013) but

have yet to be taken to clinical trials. Anti-PrP antibodies have also been shown to block infection and reduce PrP^{Sc} accumulation in cell culture when treated post infection (Perrier, Solassol et al. 2004, Pankiewicz, Prelli et al. 2006). Treatment with antibody post infection in murine models also had a positive effect on survival times and PrP^{Sc} accumulation, both in the CNS and in peripheral tissues. However, this effect was not observed if treatment was started after the onset of clinical signs (White, Enever et al. 2003). This illustrates what could be considered the biggest challenge in regard to the therapeutic treatment of disease. Without an early screening and detection systems these diseases will go unnoticed until the onset of neurological clinical symptoms, at which point infection is systemic and without doubt more difficult to treat.

1.1.8 In-vitro models of conversion

Animal infection experiments and bioassays are considered the most sensitive method to study infectivity, TSE strains and susceptibility but these experiments are long and therefore costly. It is also difficult to identify changes and interactions involving the PrP protein on a molecular level. For these reasons, *in vitro* conversion reactions have been developed, which monitor the formation of either amyloid fibrils or PK resistant PrP^{Sc}. These reactions usually use a small amount of PrP^{Sc} as a seed along with either recombinant PrP protein or the PrP^{C} contained in uninfected brain homogenate as a template, which is then converted on interaction with the PrP^{Sc} seed. In *in vitro* fibrillisation reactions amyloid fibrils can be formed spontaneously from recombinant PrP in the absence of a PrP^{Sc} seed. These fibrillisation reactions are performed under semi-denaturing conditions to aid structural unfolding/refolding, with continuous shaking and in the presence of Thioflavin T (ThT), an amyloid-binding fluorescent dye. The inclusion of ThT allows for the real-time kinetics of the reaction to be monitored in addition to the

analysis of the fibrils formed during the reaction, such as their toxicity to cells in culture (Novitskaya, Bocharova et al. 2006).

The cell-free conversion assay has been shown to mimic polymorphism dependent resistance to classical scrapie and BSE as well as the species barrier and is considered to simulate *in vivo* conversion efficiencies (Kocisko, Priola et al. 1995, Kirby, Goldmann et al. 2006, Eiden, Soto et al. 2011). This reaction uses radio labelled recombinant PrP as a template and a brain derived, purified PrP^{Sc} seed and measures the levels of PK resistant template through autoradiography (Kocisko, Come et al. 1994).

While both these assays strive to shed light on the mechanisms of conversion and the importance of *PRNP* sequence, recently other assays have been developed with the goal of replacing costly bioassays such as the quaking induced conversion (QuIC) and the protein misfolding cyclic amplification (PMCA). The QuIC is performed with intermittent shaking in the presence of ThT and recombinant PrP template. The PMCA uses similar repetitive cycling although the shaking step is replaced with sonication to break up large aggregates. These assays measure the conversion of healthy brain homogenate or recombinant PrP to PK resistant PrP^{Sc} in the presence of a small amount of PrP^{Sc} seed. Both PMCA and QuIC are highly sensitive, amplifying small amounts of PrP^{Sc} from bodily fluids such as blood, saliva, cerebral spinal fluid and urine and represent possible future large-scale screening and monitoring strategies (Wilham, Orrú et al. 2010, Bucalossi, Cosseddu et al. 2011).

1.1.9 Transgenic mouse models

Due to the dominant genetic influence of the *Prnp* gene on TSE susceptibility transgenic mouse models have been used extensively in replacement of costly large animal models,

such as sheep and cattle. In these models, the murine *Prnp* gene is replaced with that of ovine or bovine *Prnp* through transgenesis or by gene replacement using homologous recombination (Weissmann and Flechsig, 2003). These models are often more susceptible to TSE infection than wild type mice and through the creation of overexpressing models such as tg338 and tg20 the role of PrP expression in disease development has also been studied (Vilotte et al., 2001). These overexpressing models display shorter incubation times and higher susceptibility to disease compared to lower expressing models (Crozet et al., 2001). The Tg338 line is homozygous for the ovine VRQ allele, created through a bacterial artificial chromosome (BAC) insert comprised of 125 kb of sheep DNA which was introduced on a mouse $PrP^{0/0}$ background (Vilotte et.al, 2001).

1.2 PRION GENETICS AND DISEASE

1.2.1 The prion gene family

The prion gene family consists of three members; *PRNP* encoding PrP^{C}, *PRND* encoding Doppel and *SPRN*, encoding Shadoo (Shadow of the prion protein). In sheep the *PRNP* gene is located on chromosome 13 and consists of two untranslated exons with the entire open reading frame located within a third long exon (Goldmann, Hunter et al. 1990, Iannuzzi, Palomba et al. 1998). This gene is highly conserved among mammals with variations seen only in the size or number of exons and introns (Baylis and Goldmann 2004). *PRND* is located within 15kb downstream of *PRNP* (Moore, Lee et al. 1999). In contrast to *PrP*, Doppel protein is prominent in the male reproductive system but normally absent in the brain and CNS where it has been shown to be neurotoxic in transgenic mouse models (Genoud, Behrens et al. 2003). In sheep the *SPRN* gene is located on chromosome 22 (Lampo, Van Poucke et al. 2007) and is widely conserved throughout different genomes, from mammals to fish (Premzl, Gready et al. 2004, Stewart, Shen et al. 2009). *SPRN*, like

PRNP, encodes the entire open reading frame on one exon but unlike *PRNP, SPRN* expression appears to be limited to the brain (Lampo, Van Poucke et al. 2007).

1.2.2 Genetic factors in scrapie

In sheep, polymorphisms occurring in the *PRNP* open reading frame specifically at amino acid positions 136 (valine/alanine), 154 (arginine/histidine) and 171 (glutamine/arginine/histidine) predominate in the control of susceptibility and greatly influence incubation period of classical scrapie infection (Goldmann, Hunter et al. 1990, Goldmann 1993, Clouscard, Beaudry et al. 1995). Genotypes with at least one valine at codon 136 (136V) are associated with shorter incubation periods of scrapie infected sheep and an increased risk of acquiring natural infection compared to genotypes homozygous for alanine at the codon 136 (136A) (Goldmann, Hunter et al. 1991, Laplanche, Chatelain et al. 1993, Hunter, Goldmann et al. 1994, Bossers, Schreuder et al. 1996). There is an association between glutamine at position 171 (171Q) and susceptibility to natural scrapie in both Suffolk sheep (Westaway, Zuliani et al. 1994) and Romanov flocks whereas animals with homozygosity or heterozygosity for arginine at position 171 (171R) remained healthy (Clouscard, Beaudry et al. 1995). 171R encoded by at least one *PRNP* gene allele prolonged survival of Cheviot sheep experimentally challenged with CH1641 and BSE by four fold and six fold respectively with many sheep showing no signs of infection (Goldmann, Hunter et al. 1994). More recently, a polymorphism at position 141 (phenylalanine/leucine) has been associated with length of incubation period in BSE and susceptibility to atypical scrapie (Moum, Olsaker et al. 2005, Tan, Blanco et al. 2012). Many more polymorphisms exist in sheep *PRNP* and additional associations have also been established (Goldmann 2008) but for brevity they are not presented in this thesis.

Sheep genotypes are usually described in terms of three codons and combinations of these main resistance associated polymorphisms (codons 136, 154, 171) result in five common alleles: ARR, ARQ, VRQ, AHQ and ARH. These can be categorized depending on their resistance to classical scrapie (Figure 1.3), with genotype VRQ/VRQ being considered the most susceptible and ARR/ARR the most resistant (Hunter 2007). Heterozygote animals with one ARR allele can have a lower frequency of scrapie infection (Baylis and Goldmann 2004) and greatly extended incubation times when compared to heterozygotes of the other alleles (Houston, Halliday et al. 2004). There could be several reasons behind this allele dependent susceptibility, for example, differences in the gene expression of the alleles. However, studies investigating gene expression in different sheep genotypes have not found any evidence that this is the case (Caplazi, O'Rourke et al. 2004). *In vitro* studies indicate that PrP^{ARR} is impossible or difficult to convert to PrP^{Sc} therefore heterozygous sheep with one ARR allele may simply have less readily convertible PrP^{C}. In ARR/ARQ sheep infected with natural scrapie, the majority of PK resistant PrP^{Sc} was found to be that of ARQ allotype (Jacobs, Bossers et al. 2011). PrP^{ARR} is not completely resistant to conversion and under some conditions PrP^{ARR} protein can be converted to PK resistant forms, for example, intracerebral inoculation with BSE has produced TSE disease in ARR/ARR genotype sheep (Houston, Goldmann et al. 2003).

Resistant	Partial Resistance	Susceptible	Highly Susceptible
ARR/ARR	ARQ/ARQ	ARQ/ARQ	ARQ/ARQ
ARR/ARQ	AHQ/ARH	ARR/VRQ	VRQ/ARH
ARR/AHQ	ARH/ARH		VRQ/AHQ
ARR/ARH	ARH/ARQ		VRQ/VRQ

Figure 1.3 - *PRNP* Genotype and spectrum of resistance/susceptibility to natural scrapie. Susceptibility of sheep of different PRNP genotypes to natural scrapie, ranging from the most resistant ARR/ARR to the most susceptible VRQ/VRQ.

1.2.3 In-vitro studies of PRNP polymorphisms in sheep and disease

In order to study the importance of these polymorphisms on the ability of the PrP^{C} protein to convert during disease the use of recombinant proteins and cell culture systems have been adopted. Sabuncu *et al* (Sabuncu, Petit et al. 2003) used transfected rabbit epithelial cells expressing ovine PrP^{ARR} and PrP^{VRQ} (known as Rov cells) and exposed them to scrapie isolated from the brains of terminally infected mice. These cells showed no differences in expression levels, glycoform patterns or proteolytic processing of PrP^{C} prior to infection. No PrP^{Sc} was detected in the cell line expressing PrP^{ARR} whereas a substantial PK resistant band was seen in the PrP^{VRQ} expressing cells (Sabuncu, Petit et al. 2003). Further studies by Sabuncu and colleagues have highlighted the possible importance of varying detergent solubility of PrP variants and the ability of these amino acid changes to cause targeting to different cellular compartments (Sabuncu, Petit et al. 2003). Recombinant ovine PrP 171A and 154H have limited ability to convert to PK resistant PrP^{Sc} in a cell-free conversion assay, seeded with scrapie when compared to 136A. When added to an the assay containing 136A these proteins had an inhibitory effect, reducing the amount of PrP^{Sc} formed (Eiden, Soto et al. 2011). These results support findings from earlier studies in which recombinant PrP^{ARR} showed reduced conversion ability in the cell free conversion assay seeded with both $PrP^{Sc\,ARQ}$ and $PrP^{Sc\,VRQ}$ (Bossers, Belt et al. 1997, Bossers, de Vries et al. 2000). Using PMCA (Protein Misfolding Cyclic Amplification) the conversion ability of PrP^{ARR} and PrP^{ARQ} were compared with calculated amplification factors of 1.4 and 10.1 respectively (Bucalossi, Cosseddu et al. 2011). These polymorphisms, specifically 171R, have the ability to not only influence the susceptibly of the animal but also affect the direct ability of PrP^{C} to convert to PrP^{Sc} on a molecular level.

1.2.4 Genetic factors in other TSE diseases

Genetic predisposition to prion disease is not a phenomenon specifically seen in sheep, but also observed in goats, deer and man. Higher risk of vCJD transmission is associated with the human *PRNP* polymorphism 129M and until 2004 all recorded cases had occurred in patients homozygous at this codon. However, more recently, PrP^{Sc} deposition has been reported in heterozygotes after iatrogenic transmission (Peden, Head et al. 2004). Using transgenic mouse models of human disease Bishop et al 2006 have shown irrespective of the amino acid at position 129 all animals are susceptible to disease, although differences in characteristics were reported (Bishop, Hart et al. 2006). In goats 142M, 146S and 222K are polymorphisms associated with increased incubation periods and reduced susceptibility (Goldmann, Martin et al. 1996, Goldmann, Ryan et al. 2011).

Figure 1.4 – *PRNP* sequence alignment – A comparison of ovine *PRNP* sequence with that of bovine, murine, goat, deer and human. Matching amino acids are represented by a dashed line.

1.3 CELLULAR BIOLOGY OF PrP^C

1.3.1 Structure and Synthesis of the cellular prion protein

PrP^C features an unstructured, flexible N- terminal region with a stretch of octapeptide repeats (PHGGGWGQ) and a structured, globular C-terminal domain with one disulphide bond (Figure 1.5A). PrP^C is attached to the plasma membrane by a GPI (glycophosphotidylinositol)–anchor (Harris 1999, Linden, Martins et al. 2008) and has two N-glycosylation sites, existing in unglycosylated, mono-glycosylated and di-glycosylated forms (Figure 1.8). Glycosylation may influence the stability of the protein and alter protein trafficking but it is not required for the conversion of PrP^C to PrP^{Sc} (Lawson, Collins et al. 2005). Unlike other transmembrane proteins, PrP is not synthesised in a single orientation. Two distinct forms of PrP have been identified, PrP^{sec} – the form which becomes the GPI-anchored, cell membrane associated protein known as full length PrP^C and a transmembrane form (Brockes 1999). This transmembrane form of PrP^C can occur in two different topographies both spanning the membrane at position 112-135, C-transmembrane (PrP^{ctm}) and N- transmembrane (PrP^{ntm}) which are named according to the domain of the protein in the ER lumen (Figure 1.5B).

1.3.2 Trafficking

The trafficking of membrane associated PrP^C is still not fully understood. There is evidence that PrP can be internalised by several routes of endocytosis. Shyng et al (Shyng, Heuser et al. 1994) reported that in N2a cells PrP^C is internalised via copper dependent mechanisms involving clathrin coated vesicles (Figure 1.5B) - a process for which the copper binding octapeptide repeats in the N-terminal are essential (Shyng, Heuser et al. 1994, Shyng,

Moulder et al. 1995). However, depletion of these clathrin coated pits in N2a cells by way of siRNA resulted in no decrease in PrP^C internalisation, indicating there may be an alternative mechanism involved (Kang, Zhao et al. 2009). Alternative candidate mechanisms include the Arf6 associated pathway or a caveolae mediated pathway (Peters, Mironov et al. 2003, Kang, Zhao et al. 2009). Much of the cellular PrP^C produced is recycled as full length protein although a percentage undergoes endoproteolytic cleavage at both the N and C terminals. It is reported that PrP^C is continually recycled in this manner, taking around 60 minutes to travel between the cell surface and endolytic compartments (Shyng, Huber et al. 1993, Harris 2003) but whether this applies to all different forms of the PrP^C protein remains to be established.

1.3.3 Proteolytic processing of PrP – Extreme C-terminal cleavage and shedding

Although the majority of cell associated PrP^C is membrane bound and is recycled within the cell, some may be released from the cell by shedding either through the action of phospolipases on the GPI-anchor or through the proteolysis in the protein C-terminus. The cleavage site which releases secreted PrP^C has been identified at around amino acid 231 (murine) and has been shown to be the result of action by ADAM proteases, specifically ADAM 9 and ADAM10 (Endres, Mitteregger et al. 2009, Taylor, Parkin et al. 2009). The shed protein has been identified in cell culture, human cerebral spinal fluid and in Syrian hamster brain and is thought to have physiological significance (Tagliavini, Prelli et al. 1992) (Borchelt, Rogers et al. 1993, Parkin, Watt et al. 2004).

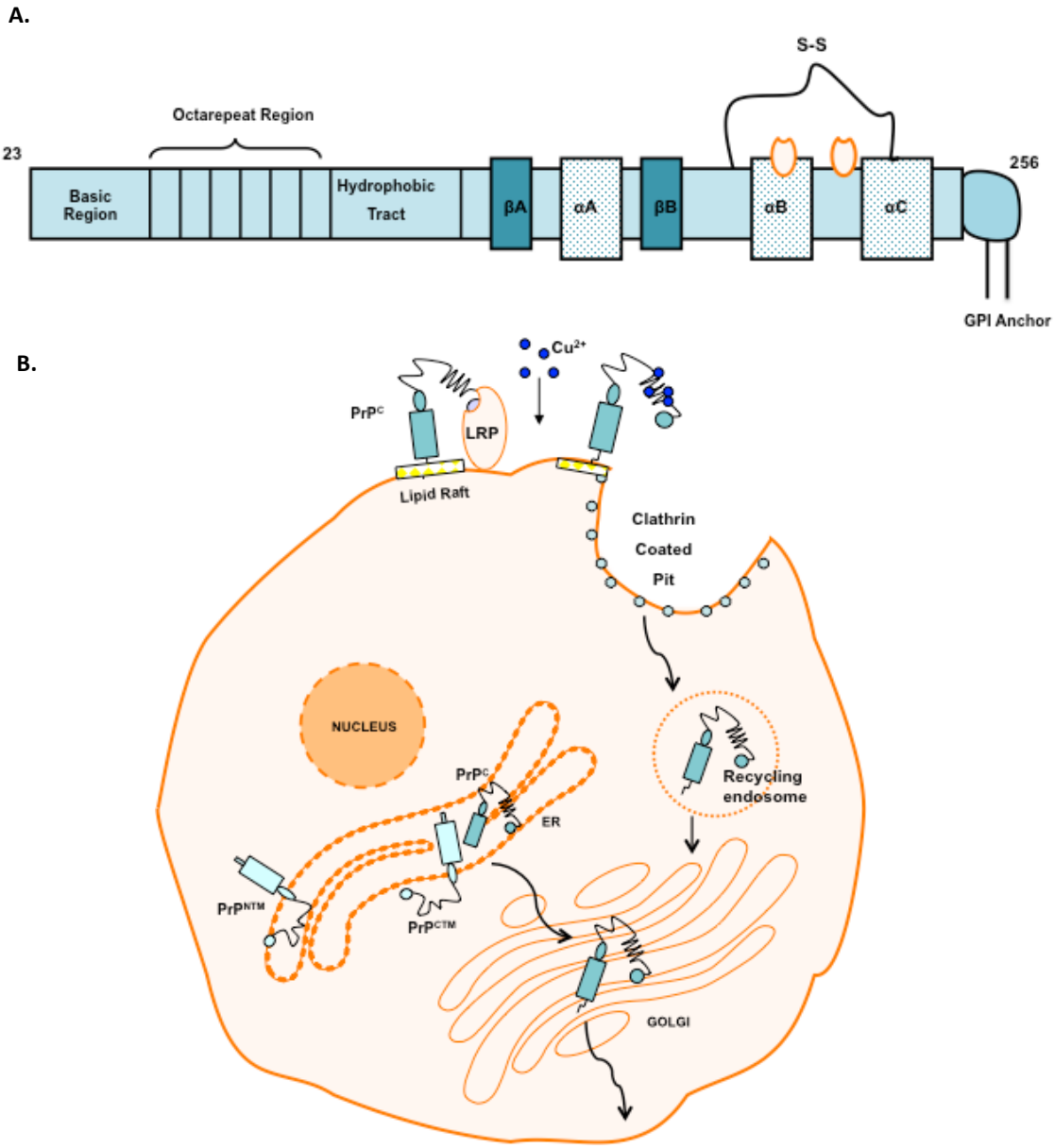

Figure 1.5 - PrP structure and trafficking. A) Linear representation of PrP^C showing N-terminal signal sequence, followed by a basic region, the central domain consisting of octapeptide repeats Arg/Gly rich and the hydrophobic tract. Structured C-terminal with α and β chains, N-glycosylation sites and GPI-anchor. B) Summary of PrP^C trafficking. Full length PrP^C is located on cholesterol rich lipid rafts on the cell surface where it interacts with LRP (laminin receptor precursor) and undergoes copper mediated endocytosis by way of the clathrin coated pit. Once endocytosed it can either be degraded or recycled back to the cell surface. Immediately after synthesis in the nuclease and transport through the ER and Golgi. . Diagram produced using Biomedical PPT toolkit (Motifolio).

1.3.4 Proteolytic processing of PrP – α-cleavage

Proteolytic processing is a common occurrence amongst membrane bound proteins and acts as a mechanism with which to alter biological function or inactivate proteins. In the case of the cellular prion protein 'normal' cellular processing includes an α-cleavage event, severing the peptide bond between 114H and 115V (ovine PrP^C). This cleavage shortens the so-called neurotoxic region (Mange, Beranger et al. 2004, Tveit, Lund et al. 2005). PrP^C fragments equivalent to this α-cleavage have been reported in the brains of a large variety of mammals with diverse susceptibility to TSE diseases including human, mouse, hamsters, rat, marmoset, dog, horse, pig, cow, seal, cat and bear (Jimenez-Huete, Lievens et al. 1998, Laffont-Proust, Faucheux et al. 2005, Diaz-San Segundo, Salguero et al. 2006, Kuczius, Grassi et al. 2007, Kuczius, Koch et al. 2007, Stewart, Campbell et al. 2012). The conserved nature of this event lends to the hypothesis that it is of functional importance within the CNS. α-Cleavage has also been well studied within cell culture systems, allowing further analysis and insight into its functional significance (Vincent, Paitel et al. 2000, Yadavalli, Guttmann et al. 2004, Tveit, Lund et al. 2005, Zhao, Klingeborn et al. 2006).

α-Cleavage creates two truncated proteins. Membrane bound C1 (Figure 1.5B) is the C-terminal fragment with an apparent molecular weight of 17 kDa, which like full length PrP^C can be unglycosylated, mono-glycosylated or di-glycosylated, shown in Figure 1.7 (Chen, Teplow et al. 1995, Laffont-Proust, Faucheux et al. 2005, Kuczius, Grassi et al. 2007). Secreted N1 is the corresponding N-terminal fragment with an apparent molecular weight of 9 kDa (Vincent, Paitel et al. 2000). These truncated proteins were identified through both epitope mapping and sequencing. It has been shown that C1 remains attached to the plasma membrane residing alongside full length PrP^C (Laffont-Proust,

Hassig et al. 2006), whereas N1 is released from the cell (Vincent, Paitel et al. 2000). The lack of cell associated N1 along with its low molecular weight make it difficult to study within the brain and for this reason most observations regarding α-cleavage have been made by measuring the C1 fragment. This said, in cell culture the use of GFP-N1 fusion proteins has allowed the fate of N1 to be documented (Tveit, Lund et al. 2005). The cellular location of the α-cleavage event is still undefined but recent work published by Walmsley *et al.* shows that, by blocking exit of proteins from the endoplasmic reticulum the amount of C1 isoform produced was decreased. This indicates that α-cleavage occurs in a late compartment of the secretary pathway, most likely the Golgi apparatus (Walmsley, Watt et al. 2009).

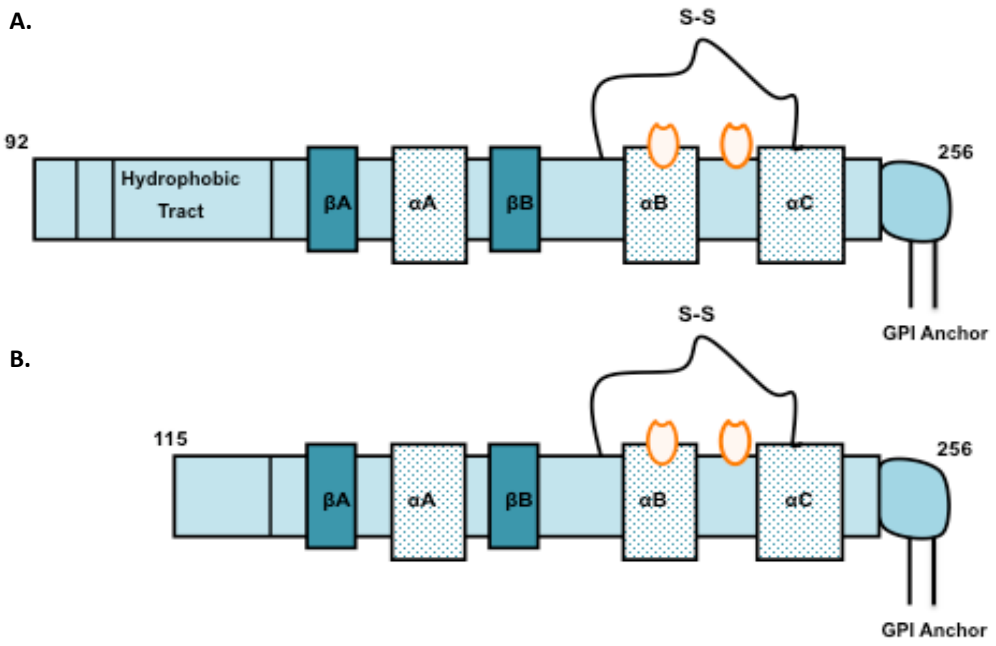

Figure 1.6 - Linear depiction of truncated C-terminal fragments. Diagrammatic representation of C2 and C1, produced by cleavage at position 91/92 and 114/115 respectively (ovine numbering).

α-Cleavage levels are reported to represent around 50 % of total PrP but may be variable both within species groups and between species (Table 1.2). It is unknown what effect cleavage levels may have on incubation times and subgroups of resistance/susceptibility to TSE disease (Laffont-Proust, Hassig et al. 2006). In sheep usually 10-60 % of cellular PrP in brain undergoes α-cleavage (Charmaine Love, PhD Thesis, University of Edinburgh, 2010) and we hypothesize that this may vary between *PRNP* genotype groups, with higher levels of cleavage being associated with resistance to disease. Data on levels of α-cleavage in different brain regions are limited but variation has been reported in both murine and human brain. In the human brain higher C1 levels were found in the cerebellum and the pons, when compared to the cortex, nucleus lentiformis, thalamus, hippocampus and medulla. (Kuczius, Koch et al. 2007). In the mouse the cerebellum was also reported to have higher C1 levels than the cerebrum (Beringue, Mallinson et al. 2003) but this was not confirmed by others (Kayleigh Iremonger, Ph.D. thesis, University of Edinburgh, 2013).

SPECIES	C1 (as a percentage of total PrP)	REFERENCE
Human	30-50%	(Chen et al., 1995)
Human	> 50%	(Jimenez-Huete et al., 1998)
Human (with active ADAM10)	42 % (35-50)	(Laffont-Proust et al., 2005)
Human (without active ADAM10)	17 % (15-20)	(Laffont-Proust et al., 2005)
Human	> 50 %	(Kuczius et al., 2007b)
Sheep	> 50 %	(Kuczius et al., 2007a)
Cattle	> 50 %	(Kuczius et al., 2007a)
Mouse	< 50%	(Kuczius et al., 2007a)
Mouse	< 50%	(Laffont-Proust et al., 2006)
Rat	~ 30 %	(Laffont-Proust et al., 2006)
Hamster	~ 30 %	(Laffont-Proust et al., 2006)
Marmoset	~/< 50%	(Laffont-Proust et al., 2006)
Baboon	~ 80 %	(Laffont-Proust et al., 2006)

Table 1.2 - A comparison of published C1 levels in different species

1.3.5 Proteolytic processing of PrP – β-cleavage

Although α-cleavage accounts for the majority of proteolytic processing, a second alternative cleavage event does occur at low levels in healthy brain, known as β-cleavage. The cut occurs around position 92 in the octapeptide repeat region of the ovine PrP and creates C2 (Figure 1.6A), the slightly longer C-terminal fragment with apparent molecular weight of 21 kDa and the corresponding fragment N2 of around 7 kDa in sheep (Figure 1.7) (Mange, Beranger et al. 2004). In human brain the C2 fragment accounts for around 5 % of total PrP (Chen, Teplow et al. 1995) and there is evidence that this cleavage is not specific to neuronal tissue, with its identification in the human tonsil – another known site of PrP^{Sc} accumulation in the preclinical stage of disease (Monleon, Monzon et al. 2005). Using biotinylation of surface PrP^{C} in cell culture it has been shown that β-cleavage, unlike α-cleavage occurs at the cell surface. This second proteolytic processing event is mediated by reactive oxygen species such as H_2O_2, which on exposure increase the amount of C2 produced. It is thought that β-cleavage represents a mechanism to protect cells against the build up of free-radicals and oxidative stress (Watt and Hooper 2005). Experiments in cell culture demonstrate that α- and β-cleavage are independent events, cleaving different PrP^{C} molecules (Sunyach, Cisse et al. 2007).

A C2-like fragment has also been described in the human brain infected with sporadic CJD and familial GSS and scrapie infected mice and sheep when tested by western blot in the absence of protease K (Chen, Teplow et al. 1995, Jimenez-Huete, Lievens et al. 1998, Owen, Rees et al. 2007). This truncated form was purified in the detergent insoluble fraction along with the PrP^{Sc} and appeared of similar molecular weight to C2 in the 'normal' brain. The origin of this fragment in TSE infected animals is under debate. It is either a result of an increase in production of the cellular PrP^{C} isoform C2 in reaction to increased oxidative

stress during neurodegeneration or a result of a similar *in vivo* cleavage of PrP^{Sc} while accumulating in the brain.

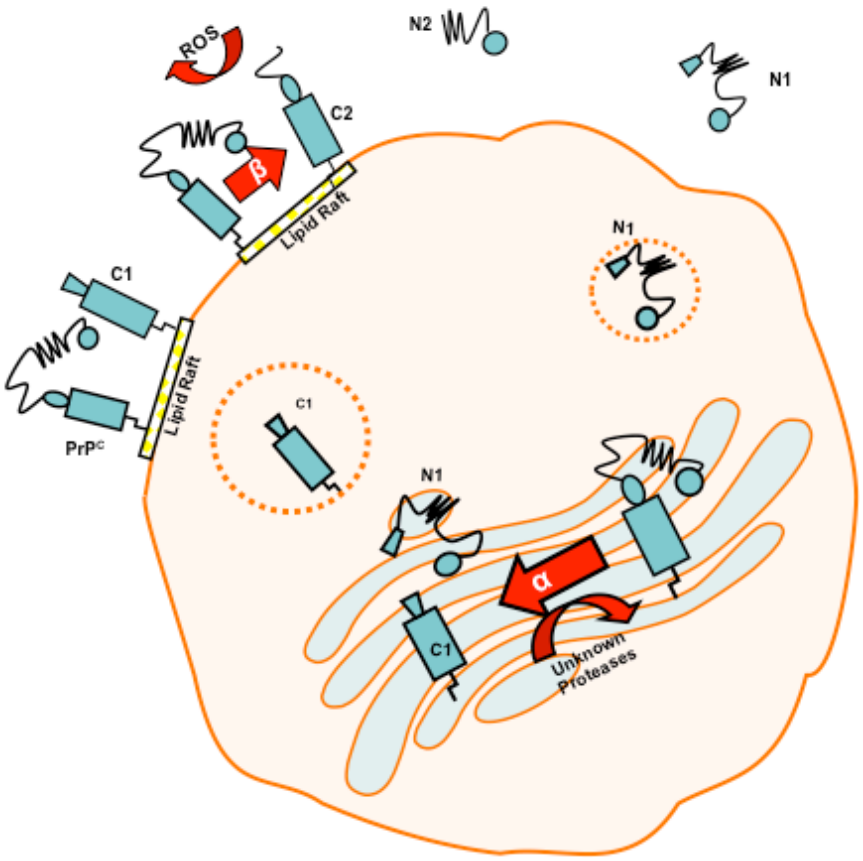

Figure 1.7 - Diagrammatic representation of PrP^C processing within the cell. Full length PrP^C can be cleaved in the Golgi Apparatus (a process known as α-cleavage). The products C1 and N1 are transported to the cell surface where C1 remains anchored and N1 is secreted from the cell. β-cleavage occurs at the cell surface and produces the isoforms C2 and N2. . Diagram produced using Biomedical PPT toolkit (Motifolio).

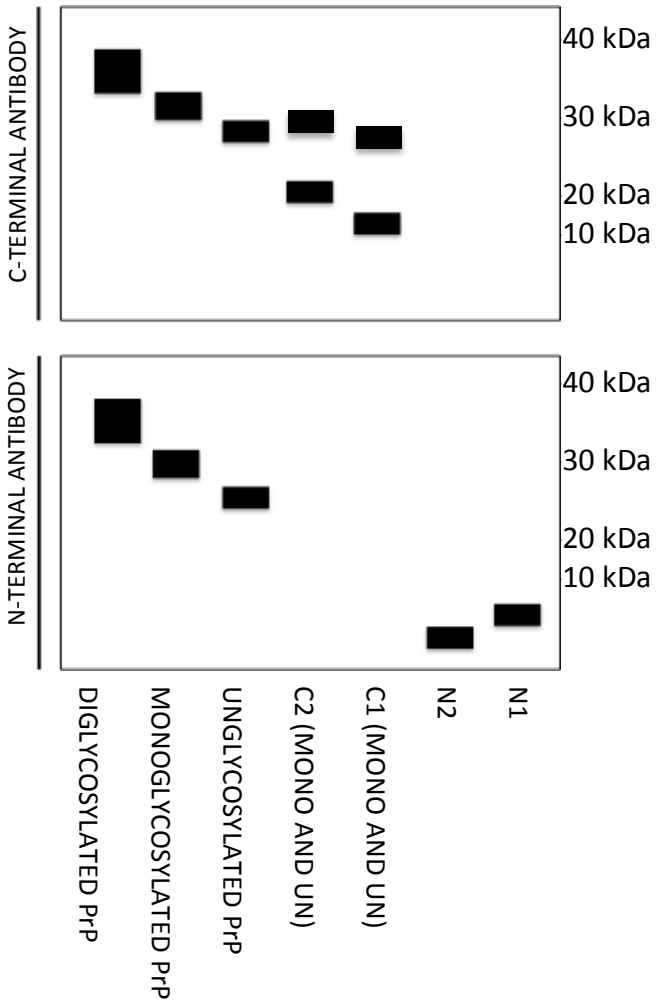

Figure 1.8 – Schematic representation of western blot profiles of PrP and truncated PrP proteins. Showing apparent molecular weights of all forms of PrP found in healthy brain, including glycosylated forms of PrP, unglycosylated PrP and truncated forms produced by α- and β- cleavage and reactivity to N- and C-terminal antibodies.

1.3.6 Proposed functions of PrP^C

The normal role of PrP^C is still undefined although there is evidence that it has many contradictory cellular functions. PrP null mice display no lethal phenotype indicating that PrP is not essential for survival (Bueler, Aguzzi et al. 1993). *PRNP* knockout animals have also been generated in other species such as goats and have even been found as a natural genetic variant in goats without any obvious survival problems (Benestad, Ausbo et al. 2012). However, there are several subtle phenotypes that have been associated with *PRNP*

knockout mice such as disturbances in sleep regulation (Tobler, Gaus et al. 1996, Huber, Deboer et al. 2002), decreased spatial learning and loss of both short and long-term synaptic plasticity leading to decreased memory function (Collinge, Whittington et al. 1994, Criado, Sanchez-Alavez et al. 2005). PrP null mice also have reduced protection against oxidative stress and decreased recovery from ischemic damage (Mitteregger, Vosko et al. 2007, Nicolas, Gavin et al. 2009). It is thought that PrP^{C} has an important role in copper metabolism, binding Cu^{2+} via the octapeptide repeats within the flexible N-terminal region (Hornshaw, McDermott et al. 1995, Kramer, Kratzin et al. 2001) and enabling uptake into the cell. There is a positive correlation between copper uptake and PrP expression in primary cerebellar cells (Brown 1999, Kramer, Kratzin et al. 2001). The cellular prion protein also has further neuroprotective functions within the brain. Normal expression of PrP^{C} reduces Bax induced cell death – an attribute for which the octapeptide repeat region is again essential (Bounhar, Zhang et al. 2001). It has been suggested that pathogenesis associated with TSE infection is partly due to the loss of PrP^{C} function on conversion to PrP^{Sc} (Crozet, Beranger et al. 2008).

1.3.7 Functional importance of truncated PrP produced by cleavage

Independent of the theory that cleavage is important in TSE infection as it represents a mechanism to reduce the amount of full length cellular PrP^{C} available for conversion, the fragments produced during proteolytic processing are biologically active *in vitro* and *in vivo*. As seen with over-expression of full length PrP, C1 induces staurosporine-stimulated caspase-3 activity in several cell types by means of increasing p53 mRNA activation. P53, or tumor suppressor protein p53 induces cell death through apoptosis and is an important factor in the cell cycle. The specificity of C1 is revealed by the fact that C2, longer only by approximately 22 amino acids displayed no such function in this system (Sunyach, Cisse et

al. 2007). α-Cleavage in axons has been linked to maintenance of myelin sheath in the PNS, suggesting a role for C1 in myelin maintenance and cross talk between neurons and Schwann cells (Bremer, Baumann et al. 2010).

Recombinant N1 when added to several cell culture systems resulted in a significant reduction in staurosporine-stimulated caspase-3 activation by down-regulating p53 transcription, in normal expressing, PrP^C over-expressing and C1 over-expressing cells. N1 has also been shown to protect rat retinal cells from pressure-induced ischemia. Surprisingly, N1 had effect without being internalised by the cell indicating that secretion of N1 by some cells may have wider multi-cellular neuroprotective effects. Because N1 has been shown to rescue C1 over-expressing cells from apoptosis, it is concluded that N1 is dominant over C1 function which may partly explain the neuroprotective effects associated with PrP^C. Again, the β-cleavage product N2 did not have similar properties (Guillot-Sestier, Sunyach et al. 2009).

1.3.8 ADAM proteases and α-cleavage

The exact mechanisms of α-cleavage are still undefined and for a long time it was thought that this process involved several metalloproteases of the ADAM class (metalloproteases with a disintigrin domain) – multifunctional transmembrane proteins which when activated can proteolytically cleave other transmembrane proteins and are thought to be of great functional importance within the brain (Novak 2004). There is also contradictory evidence in which these ADAM proteases are held responsible for a different cleavage event, involving the removal of the GPI- anchor and shedding of PrP^C from the cell (Endres, Mitteregger et al. 2009, Taylor, Parkin et al. 2009, Altmeppen, Prox et al. 2011).

Specifically, ADAM proteases 9, 10, 17 (TACE) which are expressed throughout the body and ADAM 23 which is specific to the brain (Novak 2004) are thought to be involved in α-cleavage of PrP and the amyloid precursor protein (APP) (Allinson, Parkin et al. 2003, Asai, Hattori et al. 2003). Although prion and Alzheimer's disease have distinctly different pathologies the similarities in proteolytic processing are evident. Cleavage of APP by α-secretase is thought to occur at the plasma membrane as with PrP^C and sAPPα a product of this event has neuroprotective functions similar to those associated with N1 of PrP^C (Vincent 2004). Cleavage of PrP^C like, APP has been shown to occur independently of sequence around the cleavage site and in the case of PrP is influenced by the distance of the cleavage site from the cell membrane and by charge around the cleavage site (Vincent 2004, Oliveira-Martins, Yusa et al. 2010). Several groups have used general inhibitors of the ADAM metalloproteinases such as O-phenanthroline, which in TMS neurons and HEK293 cells reduced N1 formation by around 40-70 % when compared to control cells (Vincent, Paitel et al. 2001, Cisse, Sunyach et al. 2005). Inhibition by use of protease inhibitors does not completely prevent the formation of N1.

ADAM 9 has been linked to the processing of the cellular prion protein in an ADAM 10 dependent manner, where over expression of ADAM 9 in several cell systems expressing ADAM 10 has led to an increase in the secretion of N1 but no effects were reported in ADAM 10 null cells (Cisse, Sunyach et al. 2005). When both ADAM 10 and 17 were over-expressed independently in HEK293 cells production of the N1 fragment was increased only following the over-expression of ADAM 17. ADAM 17 is thought to cleave PrP^C in a PKC (Protein Kinase C)-mediated manner. Activation of PKC leads to the increase in production of N1 isoform, but not in ADAM 17 null fibroblasts (Alfa Cisse, Louis et al. 2008). This evidence indicates that perhaps α-cleavage may be the result of two separate

mechanisms, one ADAM 10 dependent and the other ADAM 17 and PKC mediated.

Along with investigation into the role of ADAMS in cell culture the ability of recombinant ADAMS to cleave recombinant PrP has also been considered. ADAMS 10 and 17 were incubated in the presence of both full-length recombinant PrP and PrP peptide encompassing the α-cleavage site with no evidence of α-cleavage occurring. Finally it has been shown that there is a positive correlation between higher C1 levels in the human brain and presence of active ADAM 10 (Laffont-Proust, Faucheux et al. 2005). Recently, ADAM 8 has been shown to cleave PrP^C in skeletal muscle but as this protease is not expressed in brain it cannot be similarly involved in the cleavage of PrP^C in the CNS (Liang, Wang et al. 2012).

Despite the mounting evidence for the involvement of ADAMS in the α-cleavage of the cellular prion protein there has been recent evidence which contradicts this hypothesis. Taylor *et al* 2009 have shown that over expression of ADAMS 9, 10 and 17 independently in HEK cells did not alter C1 levels and silencing of the same candidates using siRNA also proved to have no effect on the ratio of full length PrP and C1. The authors suggest that this difference is due to the measurement of the cell associated C1 and not the N1 which is secreted into the media (Taylor, Parkin et al. 2009). This evidence is in agreement with Altmeppen and colleagues, who have shown that C1 levels remain high in ADAM 10 knock out primary neurons (Altmeppen, Prox et al. 2011). It is possible that measurement of secreted N1 may be a misrepresentation of the actual levels of PrP^C cleaved and instead represent the amount secreted from the cell - a process for which ADAM 10 may also play a role. If we hypothesise that ADAM 10 is responsible for the shedding of N1 and not directly involved in the α-cleavage event then it could explain why, by inhibition of ADAM

10, a reduction of N1 is reported but not an alteration in C1 levels. LRP1 (Low-density lipoprotein receptor-related protein 1) is an endolytic, transmembrane receptor protein, with multiple ligand binding sites involved in the endocytosis and trafficking of PrP^C in neuronal cells and it binds to PrP^C through the N-terminal region of the molecule. ADAM proteases 10 and 17 have been shown to result in shedding of LRP1 from the cell (Liu, Zhang et al. 2009), therefore if α-cleavage occurred in unison a N1-LRP1 complex could be released, as illustrated in Figure 1.9.

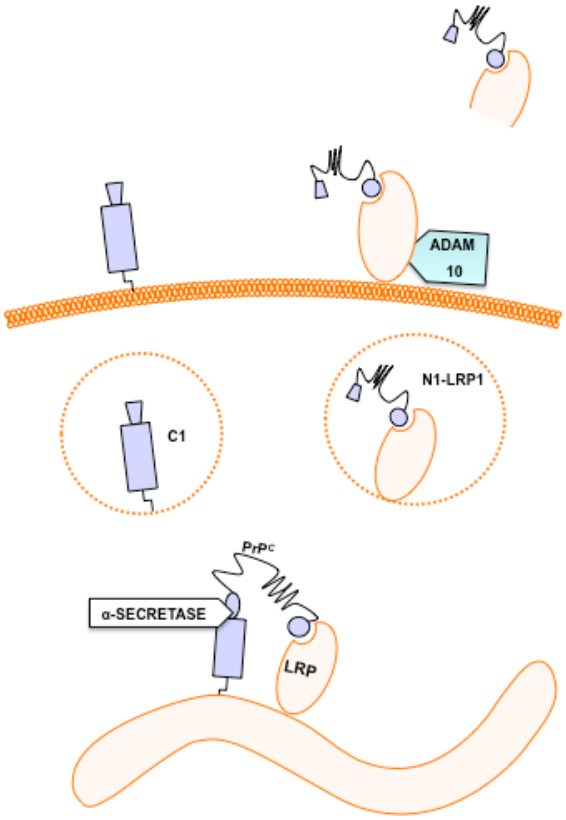

Figure 1.9 – Hypothetical model of ADAM 10 involvement in the shedding of N1 from cells. Full length PrP bound to LRP1 undergoes α-cleavage in the Golgi. C1 is trafficked to the cell membrane where it resides. An N1-LRP1 complex is trafficked to the cell membrane and anchored through LRP1. LRP1 is cleaved by ADAM 10, releasing it from the membrane and subsequently releasing N1 from the cell. . Diagram produced using Biomedical PPT toolkit (Motifolio).

It is also possible that these proteases have to be manipulated in unison as cleavage is a process that requires one or more of the candidate ADAMS to be present. ADAM 10 over-

expressing mice show a dose dependent decrease in PrP^C both at the mRNA level (~70% reduction) and in the amount of protein (~30% reduction), indicating that over expression of ADAM 10 interferes with PrP gene expression. This decrease was mimicked in C1 so that the PrP: C1 ratio remained unchanged (Endres, Mitteregger et al. 2009).

1.3.9 Regulation of α-cleavage by Protein Kinase C

Protein kinase C (PKC) has been shown to be an important mediator of the α-cleavage event. Addition of PKC agonists PMA (phorbol 12-myristate 13-acetate) and PDBu (Phorbol 12,13-Dibutyrate) to HEK293 cells and TSM1 primary neurons led to an dose dependent increase in recovery of the N1 truncated protein (Vincent, Paitel et al. 2000). A general inhibitor of PKC, GF109203X led to a dose dependent decrease in N1 recovery in the same cell lines (Alfa Cisse, Louis et al. 2008). It has also been shown that activation of PKC coupled M1/M3 muscarine receptors leads to phosphorylation of ADAM 17 and an increase in levels of N1 (Alfa Cisse, Sunyach et al. 2007).

The addition of PMA activates PKC and down-regulates LRP1. This would lead to a decrease in cell associated LRP1 available for the transport of PrP^C to the membrane and consequently lead to an accumulation of PrP^C in intracellular compartments (Amos, Mut et al. 2007). Hypothetically the build up of PrP^C in internal compartments would increase the chance of it intercepting the PrP α-secretases responsible for α-cleavage as it has been shown previously that this cleavage event occurs in a late compartment of the secretary pathway (Figure 1.10) (Walmsley, Watt et al. 2009). Increases in ADAM 10 and 17 which shed LRP1 would decrease the amount of cell associated LRP1 available for the transport of PrP to the membrane, leading to an increase in intracellular PrP^C and hence α-cleavage. This model could explain the association of ADAMS 9, 10 and 17 and α-cleavage made by

some (Alfa Cisse, Sunyach et al. 2007, Alfa Cisse, Louis et al. 2008).

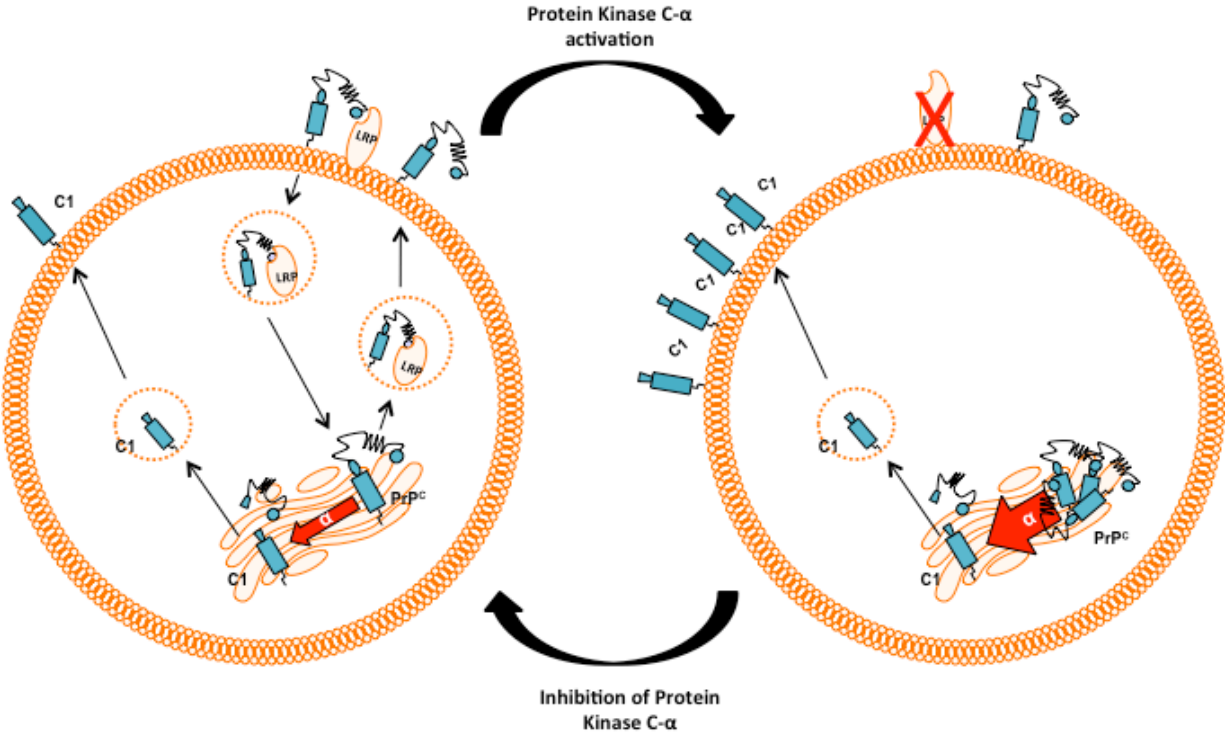

Figure 1.10 - Proposed model of α-cleavage regulation by PKC and LRP1 pathway. Activation of PKC-α leads to a down regulation of LRP1,a known PrP receptor involved in trafficking and endocytosis. The down regulation of LRP1 would lead to an increase in PrP within the intracellular compartments, including the Golgi Apparatus – the proposed site of α-cleavage – increasing the chance of interception with α-secreatases. As LRP1 binds PrP via the N-terminal it is proposed that the C1 fragment is transported to the membrane by an independent pathway. By this mechanism C1 would be the prominent species on the cell surface. Diagram produced using Biomedical PPT toolkit (Motifolio).

1.3.10 PrP^{C} cleavage and its potential effect on conversion to PrP^{Sc}

From a therapeutic angle, it is important to understand what domains of the PrP^{C} protein act as seed for the production of PrP^{Sc} (Table 1.3.). It has been concluded that deletion of the GPI-anchor had no effect on PrP^{Sc} replication *in vivo* (Rogers, Yehiely et al. 1993). Rigter *et al* (2009) suggest that the octapeptide repeat region of the protein stabilises the interaction between PrP^{C} and PrP^{Sc}. When added to the PMCA (Protein Misfolding Cyclic

Amplification) assay this peptide increased formation of PrP^{Sc}. The same authors also stressed the importance of amino acids 89-107 in PrP oligomerisation (Rigter, Priem et al. 2009). From several studies using deletion mutants it appears that essential to the conversion process are amino acids 34-141, deletion of which prevented or decreased conversion (Holscher, Delius et al. 1998, Chabry, Priola et al. 1999, Lawson, Priola et al. 2001, Lawson, Priola et al. 2004). Furthermore, published during the production of this thesis, Westergard *et al* (2011) have shown that transgenic mice expressing only the C1 fragment exhibited no accumulation of PrP^{Sc} or neurological degeneration for up to 1 year after intracerebral inoculation with scrapie. Further recent work also indicates that expression of C1 has an inhibitory effect on disease progression, lengthening incubation times but with no differences in histology or PrP^{Sc} accumulation identifiable at terminal phase (Westergard, Turnbaugh et al. 2011).

If the central amyloidogenic region is crucial in conversion of PrP^{C} to PrP^{Sc} then α-cleavage of PrP^{C} could be an important mechanism in reducing the amount of protein available for conversion to PrP^{Sc} during TSE disease because it cuts at position 115 in sheep (Figure 1.6). β-cleavage, on the other hand, leaves the central region of PrP^{C} intact meaning C2 is a candidate intermediate in the conversion of PrP^{C} to PrP^{Sc}. As briefly mentioned previously there is evidence that a truncated protein similar to C2 can be protease resistant in TSE infected animals but it is unknown whether this is a product of normal cellular PrP (C2) which is then converted to PrP^{Sc}, or the result of cleavage of PrP^{Sc} (Yadavalli, Guttmann et al. 2004, Owen, Rees et al. 2007).

Table 1.3

DELETION/ MUTATION	METHOD	CONVERSION POTENTIAL	REFERENCE
34-94	Cell free conversion assay	Reduced by 35%	(Lawson et al., 2001)
34-113	Cell free conversion assay	Reduced by 60%	(Lawson et al., 2001)
34-120	Cell free conversion assay	Reduced by 70%	(Lawson et al., 2001)
34-124	Cell free conversion assay	Reduced by 70%	(Lawson et al., 2001)
V214I, Q218K	ScN2a cells	No conversion	(Zulianello et al., 2000)
Q171R, V214I, Q218K	ScN2a Cells	No conversion	(Zulianello et al., 2000)
219-232	Cell free conversion assay	conversion	(Horiuchi & Caughey, 1999)
23-88	ScN2a Cells	Conversion	(Supattapone et al., 1999)
23-88	N2a cells	No conversion	(Supattapone et al., 1999)
23-88, 141-176	Tg mice	Conversion	(Supattapone et al., 1999)
23-88	ScN2a Cells	Conversion	(Rogers et al., 1993)
231-254	ScN2a Cells	Conversion	(Rogers et al., 1993)
32-88	Tg mice	Conversion	(Fischer et al., 1996)
A136V	Cell free conversion assay	Increased conversion	(Belt et al., 1995)
Q171R	Cell free conversion assay	Decreased conversion	(Belt et al., 1995)
114-121	Sc1-MNB cells	No conversion	(Holscher et al., 1998)
Peptide 109-141	Cell free conversion assay	Inhibited conversion	(Chabry et al., 1999)
Peptide 119-128	Cell free conversion assay	Partial inhibition of conversion	(Chabry et al., 1999)
Peptide 119-136	Cell free conversion assay	Strong inhibition of conversion	(Chabry et al., 1999)
34-99	Cell free conversion assay	Conversion	(Lawson et al., 2004)
34-102	Cell free conversion assay	Conversion	(Lawson et al., 2004)
34-106	Cell free conversion assay	Some PK resistance, different conformation	(Lawson et al., 2004)
34-110	Cell free conversion assay	Some PK resistance, different conformation	(Lawson et al., 2004)
34-113	Cell free conversion assay	Some PK resistance, different conformation	(Lawson et al., 2004)
34-120	Cell free conversion assay	Some PK resistance, different conformation	(Lawson et al., 2004)
34-124	Cell free conversion assay	Some PK resistance, different conformation	(Lawson et al., 2004)
136A, 154H	Cell free conversion assay	82.5% Reduction	(Eiden et al., 2011)
136A, 171R	Cell free conversion assay	87.5% Reduction	(Eiden et al., 2011)

154H	Cell free conversion assay	>95% Reduction	(Eiden et al., 2011)
171R	Cell free conversion assay	>95% Reduction	(Eiden et al., 2011)
23-111	Tg Mice	No PrP^{Sc} or degeneration	(Westergard et al., 2011)

Table 1.3 – PrP^{C} Deletion and amino acid replacement mutants and their propensity to convert to PrP^{Sc}

1.4 THE PrP^{C} PROTEIN AND OTHER DISEASES

1.4.1 Cancer

PrP^{C} expression in the periphery although likely pivotal to the development of prion diseases has also been implicated in progression and treatment of other diseases such as gastric and breast cancers by promoting cell proliferation and suppressing apoptosis. PrP^{C} is known to be anti-apoptotic in neuronal cells, protecting against Bax mediated apoptosis (Bounhar, Zhang et al. 2001). PrP^{C} expression is unregulated in cancerous gastric tissue in comparison to the healthy equivalent (Du, Pan et al. 2005) and silencing of PrP^{C} expression in cancerous cell lines reduced both cellular adhesion and invasive abilities (Pan, Zhao et al. 2006). Furthermore, PrP^{C} expression levels in breast cancer have been suggested as a marker of treatment outcome, with PrP^{C} expression in tumors associated with resistance to chemotherapy (Meslin, Conforti et al. 2007).

1.4.2 Alzheimer's Disease

Perhaps better understood is the role(s) of PrP^{C} expression in Alzheimer's disease. PrP^{C} has been shown to bind BACE1 (β-site APP Cleavage Enzyme-1), which has a knock-on effect on the availability of BACE to cleave APP. Reduction of BACE mediated cleavage of APP results in a reduction of downstream shedding of toxic Aβ peptides $A\beta_{40}$ and $A\beta_{42}$ (Kellett and Hooper 2009). This relationship is illustrated effectively by the induction of PrP^{C} expression in APP expressing SH-SY5Y cells, resulting in reduced shedding of cleaved

APP. Furthermore, in PrP^C deficient mouse lines production of downstream products of APP $A\beta_{40}$ and $A\beta_{42}$ are increased (Parkin, Watt et al. 2007). This would suggest that expression of PrP^C might help to protect against Alzheimer's pathology by reducing the amount of toxic peptides. However, PrP^C, specifically amino acids 23-90 and 95-110 contained in both N1 and N2 truncated fragments as well as full length PrP^C (murine numbering) can also directly bind to $A\beta_{42}$ oligomers, the most neurotoxic of the Aβ peptides (Chen, Yadav et al. 2010). *In vitro* both full length PrP^C and truncated fragments 23-126 and 91-115 can strongly inhibit fibril formation of both $A\beta_{40}$ and to a lesser extent $A\beta_{42}$ and that addition of PrP^C to fully formed fibrils causes fibril disassembly, favoring the formation of Aβ oligomeric forms. The authors further demonstrate that the binding of PrP^C to Aβ peptides firstly requires misfolding of the peptides (Younan, Sarell et al. 2013). It is Aβ oligomers which are though to be the most neurotoxic of the Aβ aggregates, not larger fibril plaques, therefore PrP^C expression may in fact positively correlate with Alzheimer's induced neuronal toxicity. This hypothesis is supported by studies performed by Gimbel and colleagues (Gimbel, Nygaard et al. 2010) who show that in the absence of PrP^C expression (PrP null murine models) Aβ fibrillar plaques are readily formed however the mice show no behavioral abnormalities or deterioration of memory functions. Revealing that although PrP^C is not required for neuronal aggregation of Aβ, it appears to be essential for the production of small neurotoxic oligomers and hence the subsequent clinical symptoms associated with Alzheimer's disease.

1.6 AIMS

PrP^C protein has both functional importance in the brain and as a determinant in the development of prion diseases. While cleavage of PrP^C has been well characterised its role, if any in prion susceptibility is still inadequately understood. Primarily, this thesis aims to investigate cleavage of PrP^C in the sheep model with the goal of understanding if this could be a contributing factor in the resistance/susceptibility to prion disease and if so, determine the mechanisms behind such effects and how it could influence the outcome of infection.

1. Investigate the proteolytic processing and expression of PrP^C in sheep of different *PRNP* genotypes and assess whether this may contribute susceptibility to classical scrapie.

A. Establish if PrP^C expression and processing is uniform throughout brain regions.

B. Determine if PrP^C expression in the ovine brain correlates with susceptibility to scrapie.

C. Establish if the common polymorphisms in the *PRNP* gene have an effect on proteolytic processing of PrP^C.

2. Determine whether proteolytic cleavage of PrP^C could have a role in fibrillisation and in the conversion of PrP^C to PrP^{Sc} during TSE disease.

A. Establish an approach to isolate or produce truncated PrP^C fragments *in vitro.*

B. Determine if truncated PrP^C fragments can misfold.

C. Investigate if truncated fragments can alter conversion of full length PrP^C.

D. Investigate if truncated fragments can alter TSE susceptibility of cultured cells and hence evaluate the future use of these fragments as therapeutics in the treatment of prion disease.

CHAPTER 2

GENERAL MATERIALS AND METHODS

2.1 ANIMALS AND TISSUES

2.1.1 Sheep and goats

Sheep used in this study were obtained from the Roslin Institute Cheviot flock (formerly known as the NPU Cheviot flock) and from a scrapie free flock (Animal health and Veterinary Laboratory Agency). All scrapie-infected tissues were selected from the Roslin frozen tissue archive and included both naturally and experimentally infected sheep. Following post-mortem all tissue had been immediately stored at -70°C. Goat tissues were obtained from The Roslin Institute goatherd and were uninfected negative control animals from other TSE infection experiments.

2.1.2 Other species

Transgenic mice lines gtARQ (The Roslin Institute, unpublished) and Tg338 (Laude 2001) were used for the creation of primary neuronal cultures. Heads of 17-day-old embryos were provided in Hanks balanced salt solution (HBSS) by The Roslin Institute animal facility, as were rat tissues. The cat brain sample was taken from The Roslin Institute tissue archive where it had been stored at -70 to -90°C.

2.2 PROTEIN EXTRACTION FROM BRAIN

2.2.1 Extraction of PrP^C from brain tissue

Lysis buffer (5 % NP-40 (v/v), 12.1 mM Sodium deoxycholate in PBS) was prepared on ice and stored at 4°C for up to a month. Directly before use protease inhibitors PMSF and NEM

were added (10 µM PMSF, 10 µM NEM final concentration). To make a 10% (w/v) homogenate tissues (100mg) were manually homogenised in 1ml of lysis buffer with protease inhibitors The homogenate was clarified by centrifugation at 2000 rpm at 4 ºC for 10 minutes, the supernatant was collected in 100µl aliquots, flash frozen in liquid nitrogen and stored at -20 °C. Aliquots were subjected to only one freeze thaw cycle.

2.2.2 Deglycosylation of PrP^C

Deglycosylation was performed using a PNGase F kit, New England Biolabs. Brain homogenate (100µl) produced as described in section 2.2.1 (10 % w/v) was denatured with 10µl of denaturing buffer at 100 ºC for 10 minutes. NP40 and G7 reaction buffer (both 10µl) were added and two 25µl aliquots removed from both +PNGase and –PNGase reactions. +PNGase reactions were incubated with 0.125 U of peptide N-glycoside F (PNGase F kit, New England Biolabs) for 2 hours at 37 ºC. -PNGase reactions were incubated with 2µl of pefa bloc (100mM) for 2 hours at 37 ºC Protein was isolated using methanol or acetone precipitation and stored at -20 ºC. Before immunoblotting, the protein was pelleted by centrifugation at 10,400 g for 10 minutes. Prior to electrophoresis, samples were boiled directly in NuPAGE (Invitrogen) sample buffer supplemented with a reducing agent (Invitrogen).

2.3 PROTEIN ANALYSIS BY SDS-PAGE

2.3.1 Western blot immunoassay for detection of PrP^C

Protein was denatured in NuPAGE (Invitrogen) sample buffer supplemented with a reducing agent (Invitrogen) at 70 ºC for 10 minutes and separated by 12% NuPAGE Bis-Tris gels (Invitrogen). Molecular markers spanning 20-220 kDa were used for size reference (MagicMarker XP Western protein Standard, Invitrogen) and electrophoresis

was performed in an Xcell SureLock tank at 150 V for 1 hour using a NuPAGE kit (Invitrogen). Proteins were transferred onto poly (vinylidenedifluoride) membranes (Millipore or GE Healthcare) using wet transfer in the Xcell SureLock tank at 25 V for 1 hour, after which the membranes were washed with TBS (50 mM Tris, 150 mM NaCl, pH 7.5). The membranes were blocked using 0.1 % (v/v) blocking solution (Roche) for 1 hour at room temperature with agitation followed by incubation with anti-PrP antibodies (Table 2.1) diluted in 0.5 % (v/v) blocking solution under the same conditions. Membranes were washed with TBST (0.1 % Tween 20 in TBS) followed by 0.5 % (v/v) blocking solution. The membranes were incubated in horseradish-peroxidase-conjugated rabbit anti-mouse antibody (Stratech, UK) diluted at 1:10000 in 0.5 % (v/v) block for 75 minutes. The membranes were washed in TBST and proteins were visualized using activated chemiluminescence (SuperSignal West Dura Extended Duration Substrate, Thermo Scientific) and Chemiluminescent Detection Film (Lumi-Film, Roche).

2.3.2 Anti-PrP monoclonal antibodies for western blot immunoassay

PrP specific monoclonal antibodies and conditions used unless otherwise stated in text are summarised in Table 2.1. Murine α-tubulin (NeoMarkers, Fisher) was used at a final concentration of 0.01μg/ml in 0.5% blocking reagent.

2.3.3 Stripping and re-probing of PDVF membrane

To allow a western blot membrane to be re-probed with a second monoclonal antibody it was twice washed in TBST, followed by TBS and incubated in 25mLs of Restore western stripping reagent (Roche) for 60 minutes. It was then incubated in fresh Restore overnight with agitation and washed in TBS and TBST. Monoclonal antibody was then applied as previously described in section 2.3.1)

Monoclonal Antibody	PrP Epitope (ovine numbering)	Concentration (ug/ml)	Dilution in 0.5% blocking solution	Source
BC6	144-154	0.3	1:10000	Sandra McCutcheon, Roslin Institute
6H4	144-152	0.1	1:1000	Biopharm Rhone Ltd
FH10	202-210	0.5	1:500	Sandra McCutcheon, Roslin Institute
JB10	216-225	3.1	1:3000	Sandra McCutcheon, Roslin Institute
Barr 224	141-151	0.2	1:1000	Micheal Tranulis Norwegian *School* of Veterinary Science
P4	89-104	0.2	1:5000	Biopharm Rhone Ltd

Table 2.1 – PrP specific monoclonal antibodies as used for western blotting.

2.3.4 Densitometry analysis

For quantitative analysis, blots were scanned and the net intensity of manually selected protein bands representative of full length PrP^C, C1 and C2 were measured by use of Kodak MI software. The combined signal of all bands for each sample was taken as 100% and each band calculated as a percentage of the total signal. For each animal deglycosylation, immunoblotting and densitometry were performed at least twice and any further analysis was based on the average C1 value. For analysis of total PrP protein densitometry measurements of the alpha tubulin loading control were performed. Using these measurements loading was calculated as a factor of the least concentrated lane and PrP^C densitometry values were normalized accordingly.

2.3.5 Protein staining by Instant Blue

Protein samples were denatured at 70 ºC for 10 minutes in a heat block and separated by 12 % NuPAGE Bis-Tris gels (Invitrogen). Electrophoresis was performed in an Xcell SureLock tank at 150 V for 1 hour using a NuPAGE kit (Invitrogen). Gels were incubated with agitation in 20mls of Novexin Instant Blue stain (Gentaur) for 1 hour, allowing blue staining to develop. After which gels were stored in dH_20.

2.3.6 Protein staining by Silver Staining

After electrophoresis 12 % NuPAGE Bis-Tris gels (Invitrogen) were soaked in 25mls fixing solution (30 % v/v ethanol, 10% v/v acetic acid) for 1 hour or overnight and were then incubated for 1 hour in 25mls sensitizing solution (30 % ethanol v/v, 4mls 5% sodium thiosulphate (w/v), sodium acetate 0.84M, 0.5mls 25 % glutaraldehyde) and washed in H_2O. Gels were stained with 25mls silver nitrate (0.25 % w/v) in ddH_2O with Formaldehyde (0.1 % v/v) for 1 hour and developed in 25mls 2.5 % sodium carbonate (w/v) with Formaldehyde (0.04 % v/v) until bands were clear. Gels were then transferred to 25mls stopping solution (1.46 % w/v EDTA).

2.4. IMMUNOHISTOCHEMISTRY/IMMUNOCYTOCHEMISTRY

2.4.1 Haematoxylin and Eosin staining of cultured cells

Cells adhered to glass cover slips were washed twice in PBS (x1) pH 7.8. The cells were fixed in a 4 % paraformaldehyde/0.25 % glutaraldehyde/PBS solution for 10 minutes at room temperature. This step was followed by three five-minute washes in PBS. The slides were then washed with water (2 x 1 minute) and stained with haematoxylin for 2.5 minutes, washed three times with water (1 minute), stained with eosin for 1.5 minutes

and washed again with water. The cover slips were mounted with Vectasheild® hard set (Vector laboratories).

Antibody	Target Antigen	Immunoglobulin Class	Concentration (µg/ml)	Source
BC6	PrP (144-154)	Monoclonal IgG1	0.05	Sandra McCutcheon, Roslin Institute
MAP-2	Microtubule associated protein 2	Monoclonal IgG1	5.0	Abcam
BE12	PrP (23-90)	Monoclonal IgG1		The Roslin Institute, TSE Resource Centre
6H4	PrP (144-152)	Monoclonal IgG1	0.1	Biopharm Rhone Ltd
FH10	PrP (202-210)	Monoclonal IgG2a	0.5	Sandra McCutcheon, Roslin Institute
FH11	PrP (54-58)	Monoclonal IgG2b		
Anti-Syntaxin 6	Syntaxin 6	Monoclonal IgG	1:100	Cell Signaling Technology

Table 2.2 – Primary antibodies used for IHC/ICC.

Antibody	Species and Target	Immunoglobulin Class	Concentration (µg/ml)	Source
Alexa fluor® 488	Rabbit Anti-Mouse	IgG (H+L)	10	Invitrogen
Alexa fluor® 594	Goat Anti-Rabbit	IgG (H+L)	10	Invitrogen

Table 2.3 – Secondary antibodies used for ICC

2.4.2 Immunocytochemistry of cultured neurons

Cells adhered to glass cover slips were washed twice in PBS (x1) pH 7.8. The cells were fixed in 4 % paraformaldehyde (w/v)/0.25 % glutaraldehyde (v/v) in PBS for 10 minutes at room temperature. This step was followed by three five-minute washes in PBS. To permeabilise the cells, coverslips were submerged in 0.1 % Tritron X-100 in PBS (v/v) and

washed a further three times in PBS as above. Block (3 % BSA (w/v) in PBS) was applied and left for 30 minutes. The cells were incubated in monoclonal antibody in a humid chamber at 4 ˚C overnight. Monoclonal antibodies used for ICC are summarised in table 3.2. Following the application of primary antibody the cells were washed in PBS as above and incubated in secondary alexa fluor conjugated antibody (Table 2.3) in a dark humid chamber at room temperature for 1 hour. Again PBS washes were performed and cells were incubated in Hoechst 33342 3µg/ml (Sigma) in water for 10 minutes. This was removed by washing in water twice and the cover slips were mounted with Vectasheild® hard set.

2.5 DNA EXTRACTION AND SEQUENCING

2.5.1 DNA extraction from brain tissues

Genomic DNA was extracted from small sections of tissues (~25mg) using the Qiagen DNA Easy kit according to manufacturers instructions. All solutions were supplied with the kit unless otherwise indicated. DNA was eluted in sterile dH_20 by centrifugation at 13,000rpm for 3 minutes. Concentration was determined by Nanodrop spectrophotometry and genomic DNA was stored at 4ºC.

2.5.2 PRNP Polymerase chain reaction (PCR)

Amplification of the PrP gene from genomic DNA was performed by PCR using Taq polymerase kit (HotStarTaq polymerase (Qiagen)) was performed with oligos forward (5' to 3')' CAAGAGAGAAGCAAGAAATGAGAGACA and reverse GGAATGTGAAGAACATTTATGACCTAGAAT (5' to 3') (Sigma, UK). Reactions were set up as shown in table 2.4. PCR conditions were 95ºC for 10mins, followed by 40 repeats of 95ºC for 1 min, 61ºC for 30 seconds and 72ºC for 1 minute, with a final extension of 72ºC for 10

minutes. The PCR products were purified using activated charcoal, described in section 2.5.3.

REAGENT	VOLUME (µl)
ddH_2O	41.1
X10 Buffer, with 25 mM $MgCl_2$	5.0
Forward and Reverse oligos (100 µM)	0.2
dNTPs (10mM)	1.0
Taq Polymerase (5U/µl)	0.5
Genomic DNA	2.0

Table 2.4 - *PRNP* PCR reaction

2.5.3 Activated charcoal purification of PCR products

To PCR reactions, 30 % (v/v) activated charcoal (1.6 % (w/v) charcoal in ddH_2O) was added, mixed by vortexing and incubated for 20 minutes. The reaction was centrifuged at 13,000 rpm for 15 minutes, supernatant removed and stored at 4ºC.

2.5.4. Agarose gel electrophoresis

To visualise PCR products, reactions were separated on 1.5 % agarose gels (1.5 % agarose, TBE X1 (diluted from 10X stock solution, 0.89M Tris, 0.89M orthoboric acid, 0.2M EDTA) and SYBRsafe® (0.1µl/1ml of agarose/TBE) (Life Technologies). Molecular marker IV (Invitrogen) was used to identify the molecular weights of DNA bands. Gel was run at 10V/cm for approximately 1.5 hours and viewed under U.V. light.

2.5.5 Sequencing of PRNP

The *PRNP* sequencing reaction was set up as shown in table 2.5, using BigDye Terminator v3.1 kit, with supplied BigDye terminator and x5 sequencing buffer (Applied Biosystems) (Oligonucleotide reverse CCCCCAACCTGGCAAAGATTAAGA (3' to 5') (Sigma UK), was diluted 1 to 20 in ddH_2O. Reactions conditions were as follows: 25 repeats of 96ºC for 10 seconds, 53ºC for 15 seconds and 60ºC for 4 minutes. Reactions were purified by adding EDTA (pH 7.5, final concentration 11.3mM) followed by 60µL 100% ethanol, incubated at room temperature for 15 minutes. DNA was pelleted by centrifugation at 2750 rpm for 30 minutes, after which the tubes were inverted and pulse spun upside down to remove residual ethanol from the pellet. The pellet was washed with 60µL of 70% ethanol and centrifugation repeated. Pellets were air-dried, resuspended in 12µl of formamide and 10µl was transferred to 96 well sequencing plates. The samples were sequenced on 3103 Genetic Analyser.

REAGENT	VOLUME (µl)
ddH_2O	11.0
X5 Sequencing Buffer	3.0
F and R Oligos (5µM)	0.2
Big Dye terminator	2.0
Purified PCR reaction	3.0

Table 2.5 – Sequencing reaction

2.6 CELL CULTURE

2.6.1 Cell lines

Cell lines used during this study were kindly gifted as follows; N2a cell line Dr Herbert Baybutt, The Roslin institute; SMB-PS cell line, Dr Rona Wilson, The Roslin Institute; Rov9

cell line, Didier Vilette, (National Institute for Agricultural Research, France); CHO^{VRQ}, CHO^{ARQ} and CHO^{ARR} cell lines, Alex Bossers (Wageningen University, The Netherlands).

2.6.2 Establishing primary neuronal cultures

The following procedure was performed under aseptic conditions. The heads of 17-day-old freshly killed mouse embryos (transgenic lines tg338 and tgARQ) in Hanks Balanced Salt Solution (HBSS) were placed on ice. The brain tissue was removed by carefully peeling back the skin and skull tissue and placed in fresh HBSS. 0.3mLs of TrpyLE™ (GIBCO®) was added per brain and incubated for 15 minutes at 37˚C. TrpyLE™ was removed by pipetting and the brains were washed in HBSS, which was subsequently removed by pipetting. The brains were incubated for 10 minutes in neuronal media (Neurobasal media, 2 % B-27 supplement (v/v), Penicillin (100U/ml), Streptomycin (100µg/ml), 2mM L-glutamine) 1mL per brain and the tissue was dissociated by repeated pipetting using a electronic 10ml serological pipette (PipetteBoy, INTEGRA). At this point the cells were counted using a heamocytometer. For the differentiation of primary neurons, cells were plated at a density of 2.3 x 10^4 cells/mL on cell culture plates or glass cover slips coated in poly-D-lysine hydrobromide (Sigma) and incubated at 37˚C, 0.5 % $C0_2$.

2.6.3 Establishing neurosphere cultures

To establish long-term cultures and reduce the numbers of animals required, neurospheres were created. These are precursor cells, which readily divide in culture and can be later differentiated into neurons. For the production of neurospheres around 5.0x10^6 cells were plated in a 25cm^2 flask along with 8mLs of growth medium with addition of 10 nM epidermal growth factor (EGF) and 10 nM fibroblast growth factor (FGF) and incubated at 37˚C for >20 days. The morphology was monitored and

neurospheres were identified as large round floating aggregates of undifferentiated cells. The suspension was centrifuged at 500rpm for 2 minutes and the supernatant was discarded. For long term storage of neurospheres the pellet was resuspended in modified freezing media (Growth media, 10 % (v/v) DMSO), then frozen at -70˚C for 24 hours in Nalgene® Cryol˚C container, after which they were moved to -180˚C for long-term storage. For direct differentiation into primary neurons neurospheres were pelleted by centrifugation at 500rpm and incubated in TrpyLE™ (GIBCO®) at 37°C for 5 minutes. Cells were transferred to fresh neuronal media, in the absence of EGF and disassociated by pipetting. Cells were plated and cultured as section 2.6.4.

Cell line	Growth media	Reference
N2a	44.5% DMEM (v/v), 45% Opti-MEM (v/v), 10% FCS, Penicillin (100U/ml), Streptomycin (100µg/ml).	Available commercially
SMB-PS	Media 199, 10 % FCS (v/v), Penicillin (100U/ml), Streptomycin (100µg/ml).	Clarke and Haig, 1970
CHO	EMEM, 10% FCS (v/v), Penicillin (100U/ml), Streptomycin (100µg/ml), Hygromycin B (Sigma) (500µg/ml).	Rigter and Bossers, 2005
Rov9	Opti-MEM, 10% FCS (v/v), Penicillin (100U/ml), Streptomycin (100µg/ml). For PrP expression Doxycycline (Sigma) to final concentration of (1µg/ml).	Vilette et al, 2000

Table 2.6 - Cell line specific growth media and supplements.

2.6.4 Maintenance of immortalised cell lines

All cell culture was performed under aseptic conditions. Cells were thawed quickly at 37°C and slowly introduced to preheated specific growth media, indicated in Table 2.6 (All purchased from Invitrogen unless otherwise stated). Cultures were maintained at 37˚C,

0.5 % CO_2 and at around 80 % confluence unless otherwise stated in text. Cells were split when required by removing culture media and washing twice with HBSS. Cells were dislodged from culture flasks by addition of Trypsin-EDTA (X1) and incubating for 10 minutes at 37˚C. An equal volume of growth media was added and cells pelleted by centrifugation at 500rpm for 5 minutes. The cell pellet was resuspended in growth media and plated at desired concentration, approximately calculated by cell counting using a hemocytometer.

2.6.5 Freezing of immortalised cell lines

Cell lines were frozen to create working cell banks. Cells were dislodged from culture flasks by addition of Tripsin-EDTA (X1) and incubating for 10 minutes at 37 ˚C. An equal volume of growth media was added and cells pelleted by centrifugation at 500rpm for 5 minutes. The cell pellet was resuspended in modified freezing medium (45 % (v/v) growth medium, 45 % (v/v) FCS and 10 % (v/v) DMSO) and frozen at -70˚C for 24 hours in a Nalgene® Cryol ˚C container. Cell banks were stored at -170˚C.

2.6.6 Lysis of cultured cells

Media was removed from plates and stored at 4 ˚C. Wells were washed with cold PBS (X1) and 250 µL of lysis buffer (5 % NP-40 (v/v), 12.1 mM Sodium deoxycholate in PBS with protease inhibitors 10 µM PMSF, 10 µM NEM) was added per well of a 6 well plate. The cells were scraped from the surface and suspension was syringed repeatedly to manually lyse the cells. The suspension was clarified by centrifugation at 500rpm for 3 minutes and supernatant collected, flash frozen in liquid nitrogen and stored at -20˚C.

2.6.7 Estimation of total protein concentration in cell lysates by bicinchoninic acid assay (BCA)

As a result of differences in the confluence of cell cultures it was necessary to normailse the protein concentration in cell lysates using the BCA assay (Pierce). All reagents were provided with the kit and the protocol was followed from the manufacturers instructions. Briefly, BSA protein standards were diluted in ddH_2O, ranging from 2 mg/ml – 0 mg/ml. BSA standard or cell lysate (25 µl) was aliquoted into a 96 well plate and diluted with 200 µl of activated reagent (50:1, A: B) per well. The protein concentration of samples was calculated using the BSA standard curve.

2.7 STATISTICAL ANALYSIS

The two-tailed T test was used to test for statistically significant differences between means from two data sets. Errors bars for in vivo data represent calculated standard deviation (SD) from the mean, while for in vitro data error bars are representative of the standard error of the mean (SEM).

CHAPTER 3

PRODUCTION AND EVALUATION OF ANTIBODIES FOR THE STUDY OF PrP^C *IN VIVO*

3.1 INTRODUCTION

Many conventional methods of PrP^C analysis relevant for this study, such as western blotting depend highly on the use of monoclonal antibodies. For example, differential binding efficiencies of antibodies to cellular PrP^C may result from sequence polymorphisms around their epitopes, such as SAF84 which, specifically binds to 171Q allotypes and shows little or no reactivity with 171R or recombinant PrP^{ARR} (Jacobs, Bossers et al. 2011). There are PrP^C specific antibodies which were thought to display different binding affinities to di-, mono-, and un-glycosylated PrP^C but these differences have since been shown to rise from the ability of C-terminal antibodies to recognise di- and mono-glycosylated truncated proteins C1 and C2 which in the absence of PNGase F, are similar in size to un and mono-glycosylated PrP^C (Figure 1.7) (Kuczius, Grassi et al. 2007). To ensure correct comparisons of both full length protein and truncated protein between samples from sheep of different *PRNP* genotypes antibodies are required which show minimal variability in their affinities.

3.2 AIMS AND OBJECTIVES

The aim of this chapter was to assess and select the most sensitive anti-PrP antibody for which affinity was not affected by the most important ovine *PRNP* polymorphisms. Firstly, to ensure that PrP^C protein levels could be accurately measured throughout this thesis several new in-house anti-PrP monoclonal antibodies were purified and compared for

binding to both full-length PrP^C and truncated forms isolated from brain tissue. Additionally, protocols were optimised and assessed for reproducibility.

3.3 MATERIALS AND METHODS

3.3.1 Harvesting and purification of monoclonal antibodies

Working cell bank stocks of hybridoma cell lines JB10 (773/2/7- 10/03/10), FH10 (772/2/6 4403) and BC6 (F782/2/7) were kindly donated by Sandra McCutcheon (The Roslin Institute). Cells were thawed quickly and slowly introduced to preheated growth media (RPMI + L-glutamine, 10 % FCS (v/v), 2% HT supplement (v/v) and 1% penicillin/streptomycin (v/v, Penicillin (100U/ml), Streptomycin (100µg/ml)). These were cultured until confluent and left for 10 days to die and release intracellular antibody. The suspension was clarified by centrifugation at 4000 rpm for 10mins and the supernatant was concentrated to 10% of initial volume using Vivaflow 50 (Sartorius Mechatronics) according to manufactures instructions. Monoclonal antibodies were purified by using a HiTrap protein G column by FPLC and dialysed in PBS (pH 7.5).

3.3.2 Storage of hybridoma cell lines

Hybridoma cell lines were frozen when cultures were around 60% confluent. Cells were dislodged from the surface of the flask and pelleted by centrifugation at 1200rpm for 10 minutes. The cell pellet was re-suspended in modified freezing medium (45% (v/v) growth medium, 45 % (v/v) FCS and 10 % (v/v) DMSO) and frozen at -70˚C for 24 hours in a Nalgene® Cryol˚C container. Cells were stored at -170˚C.

3.4 RESULTS

3.4.1 Regrowth, purification and testing of PrP monoclonal antibodies

Monoclonal antibodies BC6, JB10 and FH10 were quality tested to ensure conserved binding efficiencies with previous batches of antibodies. FH10 and JB10 show reactivity to sheep PrP^C - both cellular and PK resistant - but with greatly reduced binding efficiency to murine PrP^C whereas BC6 shows strong affinity to both murine and ovine PrP^C. None of the three antibodies show any non-specific reactivity to PrP^C null mouse tissue, indicating no binding to proteins other than PrP^C under these conditions (Figure 3.1).

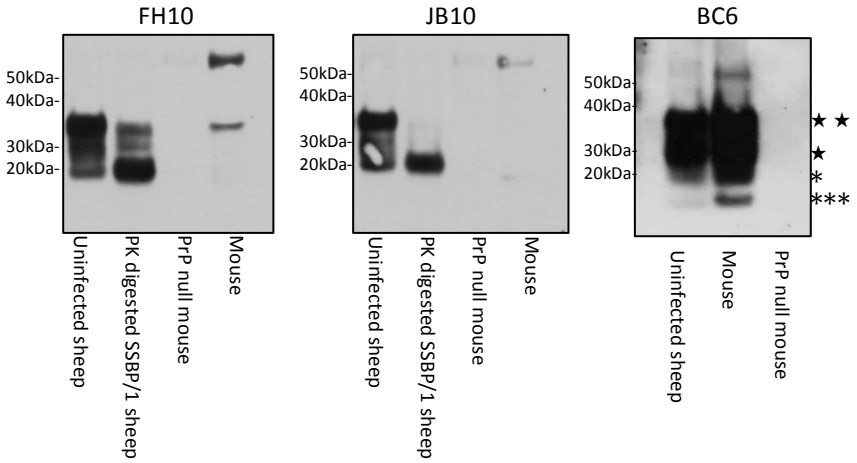

Figure 3.1 – Testing of monoclonal antibodies. Mouse and sheep brain homogenate (10 %) was subjected to western blotting and probed with newly produced batches of monoclonal antibodies FH10, JB10 and BC6. Di-glycosylated PrP (★★), Mono-glycosylated PrP (★), Unglycosylated PrP (*), unglycosylated C1 (***).

3.4.2 Antibody binding to PrP^C in sheep

A panel of four monoclonal antibodies were compared for binding efficacy to PrP^C from sheep of four common *PRNP* genotypes. It was important that the antibody chosen would consistently reflect the levels of both full length and truncated PrP in all samples tested. This panel included commercially available 6H4 (Prionics) and those produced in-house BC6, FH10 and JB10 (sections 3.3.1 and 3.4.1). The individual epitopes for each antibody used are shown in Figure 3.3A. As both 6H4 and BC6 share very similar binding epitopes the sensitivity of these antibodies to PrP^C from sheep brain was firstly compared (Figure 3.2). Homogenate (10 %w/v) from the ovine cortex was diluted to 0.0625 % homogenate in lysis buffer and treated with PNGase F (as described in section 2.2.2). The diluted samples were subjected to western blotting with both 6H4 and BC6 antibodies. 6H4 could detect PrP^C in 100 μg of ovine brain but not at lower dilutions whereas BC6 identified both bands of full length PrP^C and C1 in 50 μg of ovine brain and C1 in 25 μg of ovine brain.

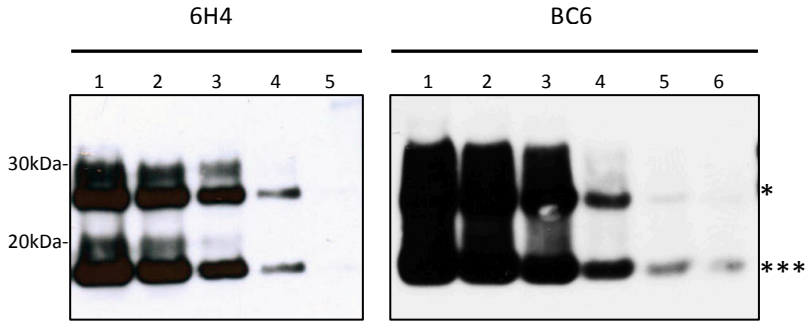

Figure 3.2 – Comparison of PrP^C detection limit in ovine brain tissue using BC6 and 6H4 monoclonal antibodies. Cortex was sampled from an ARQ/ARR (61X13) sheep brain. A 10 % homogenate (w/v) was prepared and a range of dilutions were made from neat to 0.625 %. Samples were treated with PNGase F, subjected to western blotting as described in section 2.3.1 with monoclonal antibodies 6H4 and BC6 and images were exposed for 1 minute. Lane 1 (400 μg), Lane 2 (300 μg), Lane 3 (200 μg), Lane 4 (100 μg), Lane 5 (50 μg), Lane 6 (25 μg). Full length PrP^C (*), C1 (***).

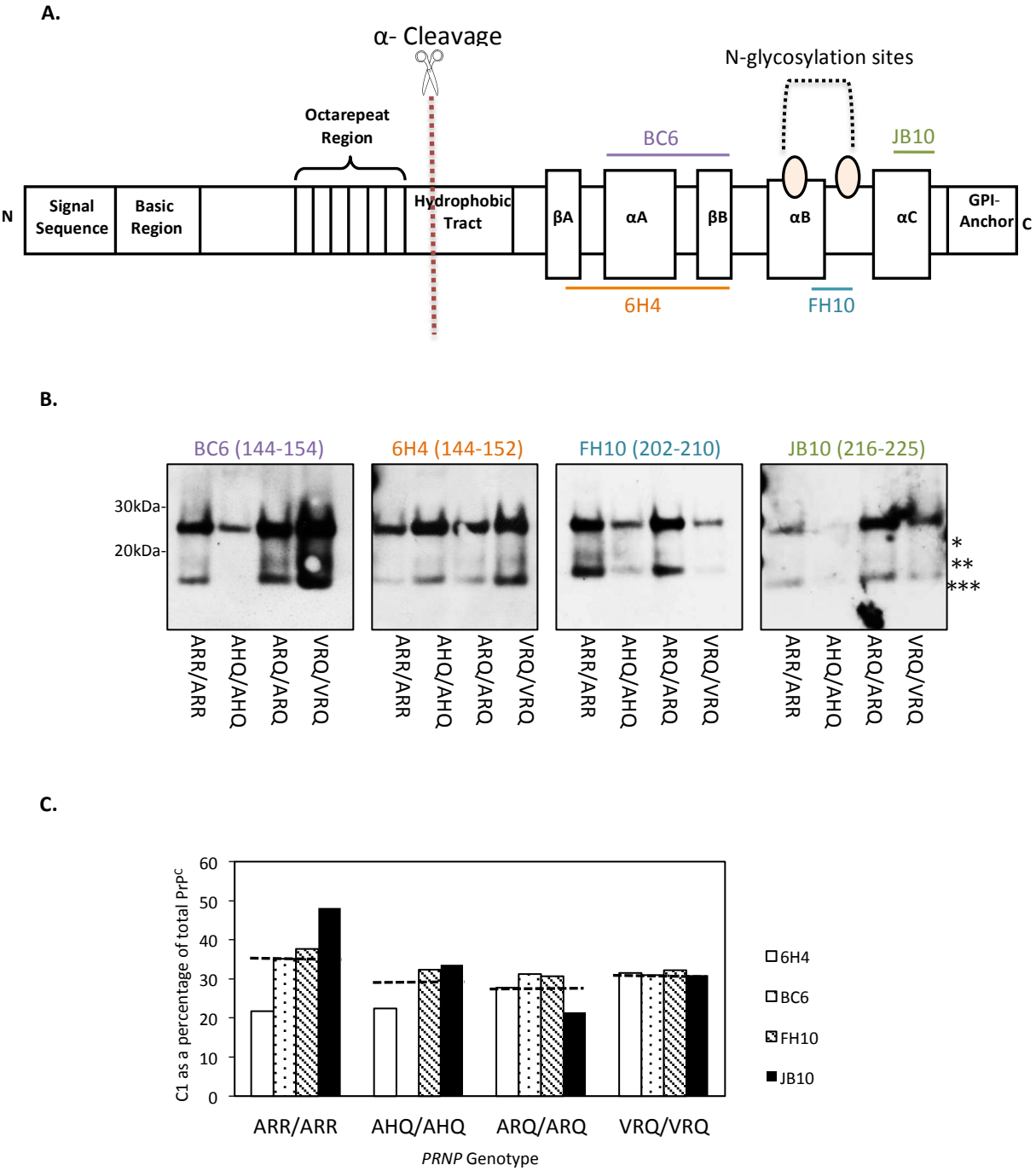

Figure 3.3 – Comparison of monoclonal antibody binding to ovine PrP^C of various *PRNP* genotypes by western blotting. A) Linear diagram of the PrP^C protein, with epitopes for monoclonal antibodies 6H4, BC6, FH10 and JB10. Showing the site of α-cleavage, areas of helical structure (αA-C), areas of beta sheet structure (βA-B)) and two glycosylation sites. B) Western blotting of one animal from each *PRNP* genotype was performed as described in section 2.3.1 and probed with the four selected antibodies. These blots were subjected to densitometry measurements and C1 levels calculated. Full length PrP^C (*), C2 (**), C1 (***). C) Graph representing densitometry results for western blots shown in Figure 3.2B. The average value for all antibodies for each animal is represented by the dashed line.

Brain tissue homogenate from one animal of each of the following *PRNP* genotypes: ARR/ARR, ARQ/ARQ, AHQ/AHQ and VRQ/VRQ was tested by western blot and probed as described in section 2.3.1. The level of C1 was calculated as a percentage of total PrP^{C}, measured by densitometry. An average value was calculated for each animal from two replicate experiments shown in Figure 3.3C with the average C1 value calculated as an average of results from all antibodies tested, represented by the dashed line (Figure 3.3C). The BC6 antibody epitope has been mapped using peptide scanning (Dr Sandra McCutcheon, personal communication, The Roslin Institute), which defined the epitope in sheep PrP^{C} as encompassing amino acids 144-154 and figure 3.3B indicates that BC6 has reduced binding to PrP^{C} and C1 with the 154H allele. To further investigate this observation total protein levels of 10 % brain homogenate from ARQ/ARQ, ARQ/AHQ and AHQ/AHQ sheep were measured by BCA assay, loading normalised and subjected to western blotting with both BC6 and anti-α tubulin antibodies (Figure 3.4). BC6 shows strong reactivity to $PrP^{ARQ/ARQ}$, decreased reactivity to $PrP^{ARQ/AHQ}$ and no binding to $PrP^{AHQ/AHQ}$ with equal amounts of brain homogenate loaded per well.

It is also apparent from both comparing data collected previously using 6H4 antibody (Charmaine Love, Ph.D. Thesis, University of Edinburgh, 2010) and from Figure 3.5 that monoclonal antibody 6H4 binds less efficiently to the C1 truncated protein in ARR/ARR animals compared to the other three antibodies tested. To further investigate the reduced binding of 6H4 to $C1^{ARR}$, 10 % brain homogenate from gene targeted (gt) transgenic mice expressing the same level of either sheep PrP^{ARR} or sheep PrP^{ARQ} (The Roslin Institute, unpublished) were subjected to western blotting with both 6H4 and BC6 antibodies (Figure 3.5). Using densitometry, C1 was calculated as a percentage of total PrP^{C} and an

average taken from two repeat experiments. With BC6 antibody C1 was calculated in gtARR mice to represent 42 % of total PrP^C whereas with 6H4 C1 was calculated as 20 % of total PrP^C. In contrast in gtARQ mice C1 was calculated as 40 % of total PrP^C with BC6 antibody and 31 % with 6H4.

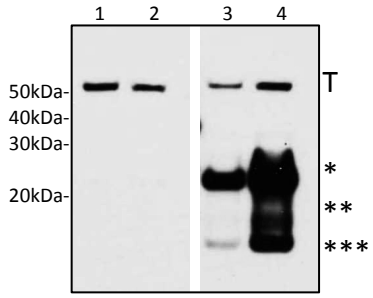

Figure 3.4 – BC6 has reduced binding to PrP^{AHQ}. Equal concentrations of 10 % brain homogenate from sheep of genotypes AHQ/AHQ (Lanes 1 and 2), ARQ/AHQ (Lane 3) and ARQ/ARQ (Lane 4), were treated with PNGase F and subjected to western blotting with BC6 monoclonal antibody and anti-α tubulin as described in section 2.3.1. Full length PrP (*), C2 (**), C1 (***) and -α tubulin (T).

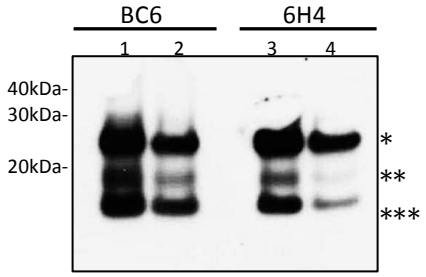

Figure 3.5 – 6H4 has reduced binding to truncated PrP^{ARR} produced in in transgenic mice. 10 % brain homogenate from gtARQ (Lanes 1 and 3) and gtARR (Lanes 2 and 4) were treated with PNGase F and subjected to western blotting with 6H4 and BC6 monoclonal antibodies, as described in section 2.3.1. Full length PrP (*), C2 (**), C1 (***).

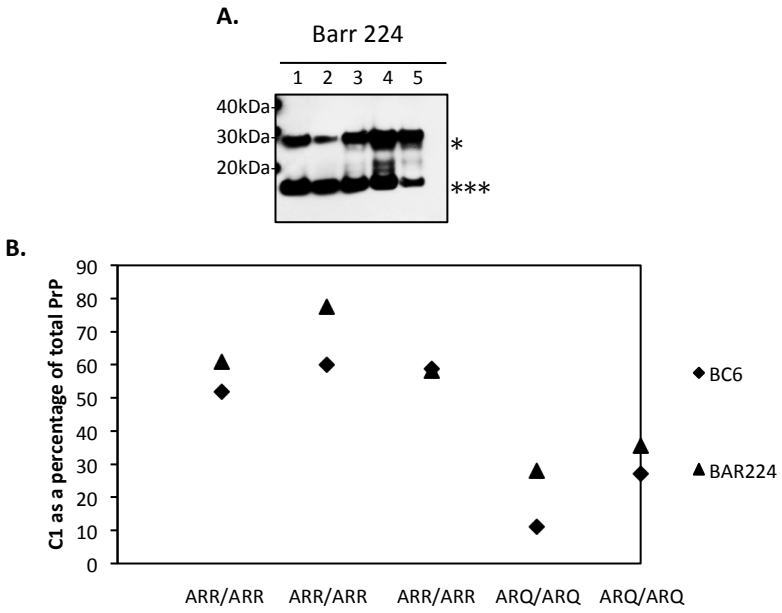

Figure 3.6 – Comparison of C1 levels in the cortex of ARR/ARR and ARQ/ARQ sheep using different monoclonal antibodies A) Western blots of ovine cortex probed with monoclonal antibody Barr 224 as described in section 2.3.1; Lane 1(O22, ARR/ARR), Lane 2 (O30, ARR/ARR), Lane 3 (61x04, ARR/ARR), Lane 4(Pg0443, ARQ/ARQ), Lane 5 (Pg0877, ARQ/ARQ). B) Graph showing C1 levels calculated for each animal when probed with each monoclonal antibody.

To allow comparison of the data presented in this thesis with other results from scientific collaborators, C1 levels calculated from western blotting in sheep brain with Bar224 monoclonal antibody were compared to those calculated from BC6 (Figure 3.6). In four out of five sheep use of Bar224 resulted in slightly higher C1 levels compared to BC6 but the differences between animals remained relatively consistent.

3.4.3 Quantification of western blotting analysis by densitometry

To semi-quantify protein levels from western blots, gel images were scanned and analysed by densitometry using the Kodak IM software. The method of manual band selection was chosen to take into account irregularities in shape, size and spacing of bands and lanes. The net intensity was taken for bands of full length PrP^C, C2 and C1 and levels of the truncated isoforms were calculated as a percentage of total PrP^C (100 %). It was important to ensure that selection of western blot bands using this manual region of interest setting was reproducible and was not subject to human error. To test reproducibility, the same gel image (Figure 3.7A) was subjected to four separate analyses on non-consecutive days. Figure 3.7B shows the calculated C1 levels for each repeat. The largest margin of variability was 5 % from the mean of 37.25 % in lane 4.

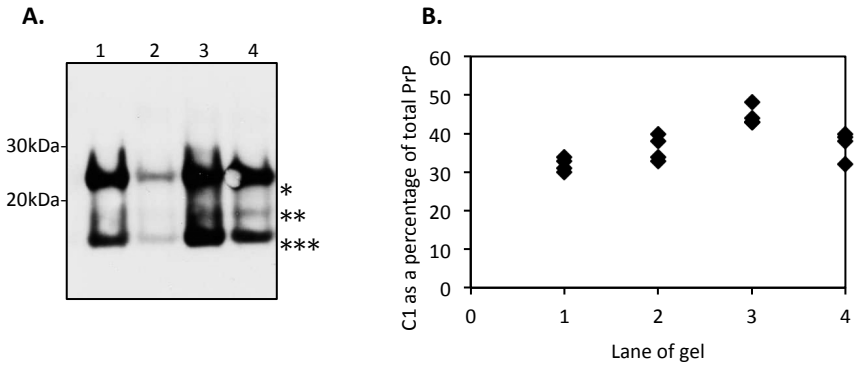

Figure 3.7 - Reproducibility of densitometry method for analysis of western blots. A) Sheep cortex from four animals (Lane 1-4) treated with PNGase F, tested by western blot, and probed with monoclonal antibody BC6 as described in section 2.3.1. Full length PrP^C (*), C2 (**), C1 (***). B) C1 levels calculated as a percentage of total PrP^C. Each marker is representational of an independent single reading taken on consecutive days.

As pre-loading total protein assays were not performed before western blotting it was accepted that loading concentrations would vary slightly between samples. Although care was taken to accurately prepare 10 % (w/v) homogenates for each sample the brain tissue in some cases was taken from a frozen tissue archive. As a result, over time this may have been subjected to desiccation, increasing the protein concentration/mg. A dilution experiment was performed to assess if changes in the mass of protein loaded per lane would have an effect on antibody binding or densitometry analyses. Dilutions of the same sample were made in lysis buffer ranging from undiluted (10 % w/v) to 1 % (w/v) and subjected to western blotting and densitometry. In this specific case the C1 level was calculated to be 52 % of total PrP^C in the 10 % (w/v) sample, 57 % in the 5 % (w/v) sample, 59 % in the 2 % (w/v) sample and 52 % in the 1 % (w/v) sample. This finding was important as it showed that C1 levels calculated using this methodology were not influenced by the amount of homogenate loaded onto a gel. These four measurements resulted in a standard deviation of ± 3.55 from the mean of 55 % (Figure 3.8). Therefore, the standard variation of this method exclusive of biological and sample preparation variation- equals (densitometry variance^2 + dilution variance^2) $^{1/2}$; in this case ± 10 %.

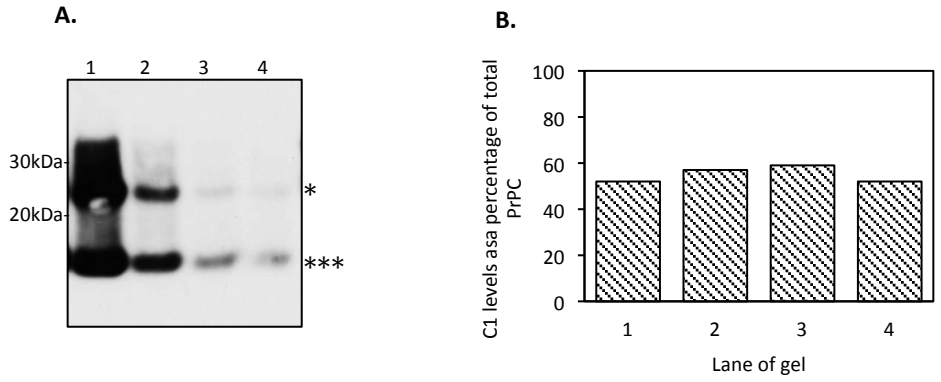

Figure 3.8 - The effects of protein loading on calculated C1 levels. A) Western blot of sheep cortex sample diluted and probed with BC6 antibody as described in section 2.3.1. Full length PrP^C (*), C1 (***). Lane 1 (Undiluted, 10 % w/v), Lane 2 (5 % w/v), Lane 3 (2 % w/v), Lane 4 (1 % w/v). Densitometry was performed and C1 levels calculated as a percentage of total PrP^C. B) Graph of densitometry results for each lane.

3.5 DISCUSSION

3.5.1 The selection of an antibody for detection of PrP^C in brain by immunoblotting

The antibodies newly assessed for their binding to PrP^C were created within The Roslin Institute (BC6, FH10, JB10), reviewed by McCutcheon (2014) and new batches were produced for the purpose of this thesis. This ensured that all immuno-blotting was performed using one batch to avoid variation in concentration or efficacy sometimes associated with batches of commercially available antibodies. BC6, JB10 and FH10 represent useful C-terminal antibodies, which recognise both full length PrP^C and truncated proteins C1 and C2 in brain tissue. BC6 was found to have less unspecific background when compared to both JB10 and FH10 and had higher sensitivity to ovine PrP^C and truncated proteins when compared to 6H4, particularly concerning ARR/ARR. It was therefore preferential to use BC6 for the purpose of studying PrP^C in ovine brain for the genotypes selected for this study. For applications involving cell culture derived PrP^C JB10 has the advantage of having no or very low reactivity to murine or hamster PrP^C. For example, this antibody was used to distinguish between ovine and hamster PrP^C in transfected CHO cells (data not shown).

3.5.2 Ovine PRNP polymorphisms and antibody binding

With one of the main aims of this thesis to investigate the levels of full length PrP^C and truncated proteins in sheep of different *PRNP* genotypes it was imperative that the antibody used for immunoblotting showed no loss of binding as a result of *PRNP* sequence polymorphisms. PrP: C1 ratios were compared in the cortex of sheep of genotypes ARR/ARR, AHQ/AHQ, ARQ/ARQ and VRQ/VRQ by probing with 6H4, BC6, FH10 and JB10 antibodies. BC6 showed reduced immunoreactivity to PrP^C from AHQ/AHQ sheep brain. It is likely that the variation (arginine or histidine) of the amino acid at position 154 alters

the affinity of BC6. Binding may be disrupted by variation in charges at the antibody epitope for example, arginine is fully positively charged at cellular pH whereas only 50 % of histidine will be charged. Secondly, arginine and histidine differ structurally. Histidine is both smaller in size compared to arginine and has an aliphatic ring which could affect antibody binding to proteins with 154H. This is an important finding if we consider that BC6 has previously been used for the detection of PrP^{Sc} (Tan, Blanco et al. 2012) and may also fail to recognise PrP^{Sc} from AHQ carriers. This data suggests that ovine genotype should be considered before immunological detection of PrP^{Sc}/PrP^{C} in ovine tissues. Moreover, it would be advised that new antibodies should be tested on all known alleles or as new alleles become of interest in prion research they be screened with a selection of available antibodies.

Antibody 6H4 which is used for rodent and ruminant prion protein studies has a light but consistent reduction of binding affinity to the truncated C1 171R ($C1^{ARR}$) compared to C1 171Q ($C1^{ARQ}$ or $C1^{VRQ}$) which does not appear to affect the full-length protein affinity. This is difficult to understand as the epitope of 6H4 DYEDRYYRE in helix 1 (codon 147-155) should not be directly affected by the truncation of the protein at amino acid 115. Although, the mechanism of this altered binding cannot yet be explained this antibody should not be used for the study of PrP^{C} processing in sheep with 171R.

3.5.3 Evaluation of densitometry as a method to calculate PrP:C1 ratio in brain tissue

To allow quantification of relative levels of truncated proteins in brain samples western blot images were subjected to densitometry. Using manual band selection, which accounted for abnormalities in band shape, there was little variation between separate readings, henceforth it was thought sufficient to analyse gel images only once with this

technique. These experiments have also shown that amount of protein loaded onto a gel has little influence on C1 level when calculated relative to the amount of total PrP^C using this method. This method was used throughout this thesis to maintain consistency with results however it is envisaged that in the future direct detection based on fluorescence will be employed.

3.5.6 Conclusions

The aim of this chapter was to assess and select a sensitive anti-PrP antibody with which affinity was not affected by ovine *PRNP* polymorphisms. The selection of appropriate antibodies for the study of protein expression is pivotal to ensuring findings accurately represent the *in vivo* situation. In the case of PrP^C, BC6 was selected to use for all further western blotting. This antibody has high sensitivity and specificity to ovine PrP^C and truncated PrP^C C-terminal fragments within brain tissue - an important factor as some of the truncated PrP^C proteins, such as C2 are present at very low concentrations. The inability of BC6 to bind 154H was not considered to hinder this study as the animals selected were all homozygous 154R.

CHAPTER 4

EXPRESSION AND PROTEOLYTIC PROCESSING OF THE CELLULAR PRION PROTEIN IN BRAIN

4.1. INTRODUCTION

PrP^C Processing

As described in section 1.3.4 and 1.3.5 cellular processing of PrP^C involves two well-documented proteolytic cleavage events (Mange, Beranger et al. 2004, Tveit, Lund et al. 2005). In the case of α-cleavage both cleavage fragments, C1 and N1, appear to have additional or possibly supplementary functions to those of full length PrP^C. It is a long held view that prion disease incubation periods are correlated with the amount of PrP^C. This has been demonstrated in various transgenic mouse models in which incubation periods of experimentally induced prion diseases are inversely correlated with the PrP^C protein expression (Manson, Clarke et al. 1994, Weissmann, Bueler et al. 1994). However, often in these studies the levels of full-length PrP^C and its proteolytic fragments have not been differentiated. Recently it was shown conclusively that the murine C1 fragment itself does not convert into a protease-resistant isoform in scrapie challenged transgenic mice expressing only C1. Furthermore, when the C1 fragment was co-expressed with full-length PrP^C incubation periods were extended (Westergard, Turnbaugh et al. 2011). It has also been shown that cell lines with naturally higher levels of α-cleavage show enhanced resistance to prion infection (Lewis, Hill et al. 2009). This raises the possibility that PrP^C cleavage may control disease by either reducing the amount of full length PrP^C available for conversion or by producing different levels of the C1 fragment, which would act as inhibitory modulators of conversion. Additionally, in sheep the natural host of scrapie,

highly complex genetic variation and disease association of *PRNP* could be the result of processing differences of the many PrP^C protein variants.

Experimental considerations

During this study it was vital that the tissues tested were scrapie free to allow for investigations into 'normal' cellular process to be made. In the Roslin Institute flock scrapie is endemic producing disease in VRQ/VRQ and VRQ/ARQ sheep generally over two years of age. As a result healthy sheep tissue of the most susceptible *PRNP* genotype, VRQ/VRQ was sourced from a scrapie free sheep flock (AHVLA). For this reason numbers of sheep in this group are lower than in other genotype groups. It was also imperative that the animals used were homozygous for the resistance/susceptibility haplotype in order to generate clear results, reducing sample size considerably. Low sample size was considered to be of secondary importance to the benefits of using a large animal model, naturally infected with scrapie over ovine transgenic mouse models.

It was previously thought that PrP^C cleavage products may accumulate after death, representing an artifact produced on tissue degradation or fragmentation of the protein on storage and freeze/thaw cycles. However, this has been investigated by several research groups through the incubating of tissue samples at different temperatures over increasing time periods in the absence of protease inhibitors, with no differences in levels of C1 isoform observed (Laffont-Proust, Hassig et al. 2006) (Charmaine Love, PhD Thesis, University of Edinburgh). It has also been shown that there is no significant correlation between α-cleavage and age at death or time of post-mortem interval in humans (Laffont-Proust, Faucheux et al. 2005). To distinguish these cleavage fragments from full length PrP^C PNGase F was used to remove the N-glycans. This assay involves the incubation of

homogenates at 37°C for 2 hours, which could induce degradation of PrP^C and affect levels of truncated proteins. In previous experiments within our laboratory 10 % homogenates were incubated with PNGase F for up to 24 hours at 37 °C without any effects on the PrP: C1 ratio (Kayleigh Iremonger, PhD Thesis, University of Edinburgh, 2013). Despite the indication that tissue storage has little effect on C1 levels relative to PrP^C several precautions were taken to minimize tissue degradation. These included the freezing of tissue at -70°C at the time of post mortem, followed by removal of tissue which was used to prepare 10 % homogenate. This homogenate was aliquoted into small volumes, flash frozen in liquid nitrogen and thawed only once immediately before use.

4.2 AIMS AND OBJECTIVES

This chapter presents data with the aim of exploring both the expression and proteolytic processing of PrP^C throughout the sheep brain, in animals with varying susceptibility to TSE disease defined by *PRNP* genotype. Both expression and proteolytic processing of PrP^C were compared in seven ovine brain areas and proteolytic processing was compared in the cortex of sheep of ARR/ARR, ARQ/ARQ and VRQ/VRQ genotypes. To assess if levels of PrP^C cleavage in sheep brain was comparable with other species, several species were tested, along with transgenic mouse models expressing ovine PrP alleles. Furthermore, manipulation of α-cleavage in cell lines was attempted to produce an inducible model of PrP^C processing.

4.3 MATERIALS AND METHODS

4.3.1 Sectioning of ovine brain

For a small selection of sheep 1cm sections were cut from the left side of ovine brain midsection at post mortem (Wim Bosma, Roslin NPD farm). Cores were removed using

Harris Unicore 3mm (Ted Pella Inc.) from the cortex, cerebellum, medulla, thalamus, hypothalamus, mid brain and pons, as shown in Figure 4.1.

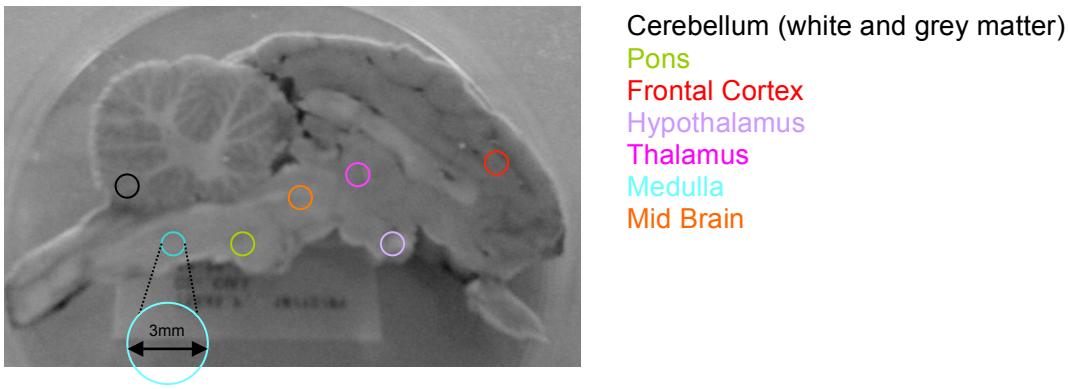

Figure 4.1 – Coring from the ovine brain. Photograph of section from ovine brain, taken before sampling. Circles indicate areas where 3mm cores were removed for protein extraction.

4.4 RESULTS

4.4.1 Levels of PrP^C fragments in different areas of ovine brain

During TSE disease PrP^{Sc} selectively accumulates in certain brain areas and displays varying rate of spread within the brain (van Keulen, Schreuder et al. 1995, Wemheuer, Benestad et al. 2011). It was hypothesised that this may be influenced by varying levels of α-cleavage throughout the ovine brain as a mechanism, which inadvertently reduces the amount of PrP^C available for conversion during TSE disease. Variation in cleavage levels between brain areas may also indicate a change in expression of the protease(s) involved in cleavage, of which there remain several candidates.

Animals were re-genotyped as described in section 2.5.2 to section 2.5.5 prior to experimental use for confirmation of ARR/ARR, ARQ/ARQ and VRQ/VRQ carriers and to exclude any of AHQ/AHQ genotype (see antibody reactivity, section 3.4.2). The removal of brain slices at *post mortem* to extract tissue samples from specific brain areas was a new procedure and as a result the number of sheep available to be culled for this thesis was limited. These included three ARQ/ARQ, two ARR/ARR and two ARQ/ARR sheep. Seven brain areas were selected; cortex, cerebellum, medulla, thalamus, hypothalamus, mid brain and pons to give coverage throughout the whole brain. These samples were removed from specific areas by coring and tested by western blot using BC6 antibody and α-tubulin as a loading control. To visualise the cleavage products of PrP^C, the samples were treated with PNGase F to remove N-glycosylated sugars. This produced three characteristic bands, one representing full-length unglycosylated PrP^C of around 27 kDa, truncated C1 17kDa and in some of the animals tested a faint band of around 21 kDa was also evident which most likely represented C2, the product of β cleavage – known to occur at lower levels in healthy animals (Jimenez-Huete, Lievens et al. 1998).

An example of PrP^C banding patterns in each area from ARR/ARR and ARQ/ARQ sheep when visualised by immunoblotting are shown in Figure 4.1. In all sheep α-cleavage was observed in all brain areas tested (Figure 4.2). The average C1 levels for all animals tested were as follows; hypothalamus 36.3 % (SD ± 9.7), thalamus 36.3 % (SD ± 9.9), cortex 34.5 % (SD ± 7.1), mid brain 33.1 % (SD ± 9.6), medulla 28.5 % (SD ± 13), cerebellum 25.1 % (SD ± 11.4), and pons 18.5 % (SD ± 8.1), (Figure 4.3A). Relative C1 levels varied considerably between animals (e.g. levels of C1 in the cortex ranged from 12-48 %).

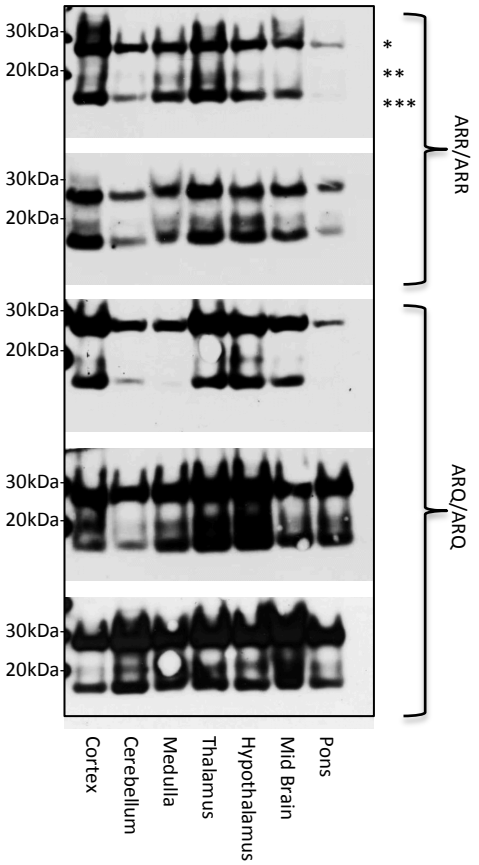

Figure 4.2 – PrP^C and C-terminal fragments in seven brain areas from ARR/ARR and ARQ/ARQ sheep. Cores were removed from specific areas and 10 % homogenates were made and treated with PNGase F. Samples were subjected to western blotting with monoclonal antibody BC6 as described in section 2.3.1. Full length PrP (*), C2 (**), C1(***).

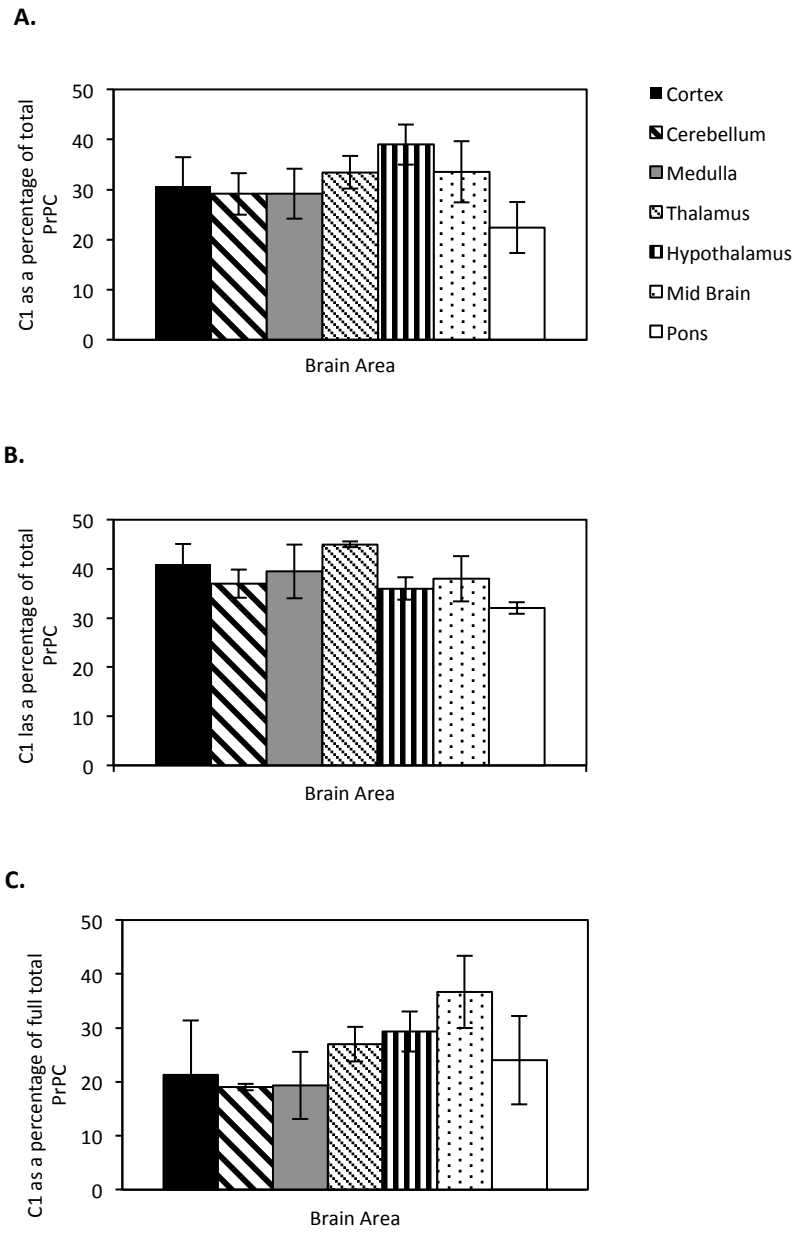

Figure 4.3 – Levels of C1 throughout the ovine brain. A) Average C1 levels in seven brain areas of sheep of mixed *PRNP* genotypes (ARR/ARR, ARQ/ARQ and ARQ/ARR, n = 7). B) Average C1 levels in seven brain areas of ARR/ARR sheep (n = 2). C) Average C1 levels in seven brain areas of ARQ/ARQ genotype sheep (n = 3). Error bars represent standard deviation from the mean

We normalised C1 levels for all brain areas against the cortex (cortex = 1) for each animal and for a further four unrelated homozygote Norwegian sheep. C1 levels in cerebellum (0.78 ± 0.23) and brainstem (0.9 ± 0.54), relative to cortex in the Norwegian sheep, did not differ significantly from the Roslin sheep (Figure 4.4). Overall, we found that relative C1 levels were similar across different brain regions for individual animals.

The ARQ/ARQ (n = 3) and ARR/ARR (n = 2) genotype animals were assessed separately (Figure 4.3B and 4.3C). Brain areas were ranked by the percentage of C1 as a percentage of total PrP^C. In sheep of ARQ/ARQ genotype the mid brain had the highest average level of C1 with 36.7% of total PrP^C, followed by hypothalamus (29.3 %), the thalamus (27.0 %), the pons (24.0 %), the cortex (21.3 %) and the cerebellum (19.0 %). For the ARR/ARR animals average C1 levels ranged from high to low as follows; thalamus (45.0 %), cortex (41.0 %), medulla (39.5 %), mid brain (38.0 %), cerebellum (37.0 %), hypothalamus (36.0 %) and pons (32.2 %). The ARR homozygote group showed less variation in C1 levels in the different brain areas and C1 levels were higher throughout.

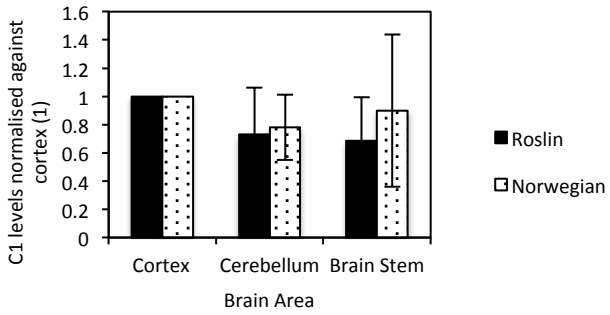

Figure 4.4 – Comparison of C1 levels in three brain areas from sheep taken from two unrelated flocks. Brain tissue was treated with PNGase F and western blotted with either antibody BC6 (Roslin) or Barr 224 (Norwegian). C1 levels calculated by densitometry were normalised against the cortex for each animal and averages calculated. Error bars represent standard deviation from the mean.

As there were no significant differences in cleavage levels between the brain areas levels of full length PrP^C were measured in the same brain areas of three sheep (one ARQ/ARQ and two ARR/ARR). For each brain (n = 3) PrP^C levels were normalized to the cortex to allow for relative expression levels to be compared. The cortex had significantly ($p \leq 0.02$) higher average levels of full length PrP^C when compared to the mid brain (48.4 % of cortex, SD ± 5.3) and pons (42.6 % of cortex, SD ± 3.6) but there was no significant difference between any of the other areas tested (Figure 4.5E). To investigate if there was a relationship between C1 levels and full length PrP^C the net intensity of the full length band as a percentage of the highest value was plotted against C1 levels as a percentage of total PrP^C for two sheep. In the ARR/ARR animal there was a significant positive correlation ($p \leq 0.02$), indicating higher PrP^C levels are associated with higher α-cleavage levels in this animal. However, in the ARQ/ARQ animal there was no such relationship found (Figure 4.5C and D).

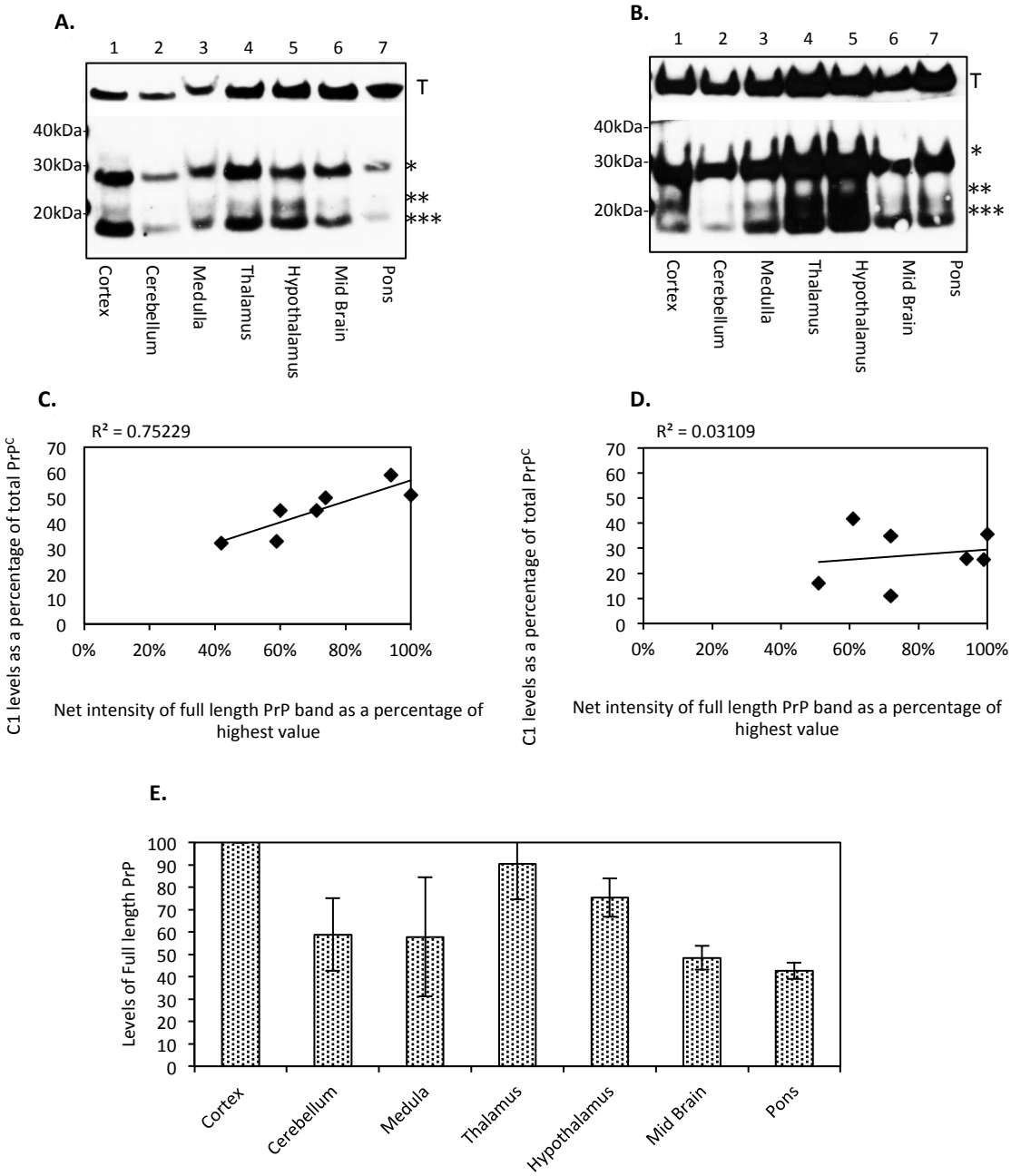

Figure 4.5– Comparison of full length PrP^C throughout the ovine brain. A) Western blot of seven brain areas from an ARR/ARR genotype animal, probed with BC6 and α-tubulin (T) as described in section 2.3.1. Full length *PrP^C, **C2,***C1. B) Western blot of seven brain areas from an ARQ/ARQ genotype animal, probed with BC6 and α-tubulin. C) Net intensity of full length PrP^C plotted against C1 levels throughout the ovine brain for the ARR/ARR animal. D) Net intensity of full length PrP^C plotted against C1 levels throughout the ovine brain for the ARQ/ARQ animal. E) Average levels of full length PrP^C in seven brain areas from three sheep (2 of ARR/ARR and 1 ARQ/ARQ). Normalized to PrP level in the cortex (100 %).

4.4.2 Polymorphisims in the PRNP gene and α-cleavage of PrP^C in the ovine cortex

It appeared that the ARR/ARR animals tested during the brain areas study had higher levels of truncated C1 than ARQ/ARQ sheep, which supported the hypothesis of a genetic association between α-cleavage and *PRNP* genotype. To verify the putative link between *PRNP* genotype and PrP processing a more detailed investigation was carried out. A larger number of ovine brain samples were taken from homozygous sheep of the following genotype groups ARR/ARR, ARQ/ARQ and VRQ/VRQ with varying resistance/susceptibility to natural scrapie.

Cortex samples were treated with PNGase F and subjected to western blotting with BC6 antibody. Sheep of ARR/ARR genotype – associated with resistance to natural scrapie - have significantly higher levels of C1 in cortex when calculated as a percentage of full length PrP^C when compared to sheep of ARQ/ARQ ($p \leq 0.0001$) and VRQ/VRQ ($p \leq 0.002$) genotypes, with an average of 52.6 % (SD ± 11.9) (Figure 4.6B). Figure 4.6A illustrates the different western blot profiles seen when comparing an ARR/ARR sheep in which a more pronounced band of C1 was detected in comparison to examples of the other *PRNP* genotypes. There was no significant difference between C1 levels in the remaining genotypes, which have varying levels of susceptibility to natural scrapie. For these groups the average C1 values were as follows: ARQ/ARQ 27.7 % (SD ± 14.5) and VRQ/VRQ 32.6 % (SD ± 8.8). The standard deviation from the mean was higher than the calculated range for experiential variation (10-15 %), indicating that this represents natural animal-to-animal variation, which appears to be larger in the ARQ/ARQ genotypes.

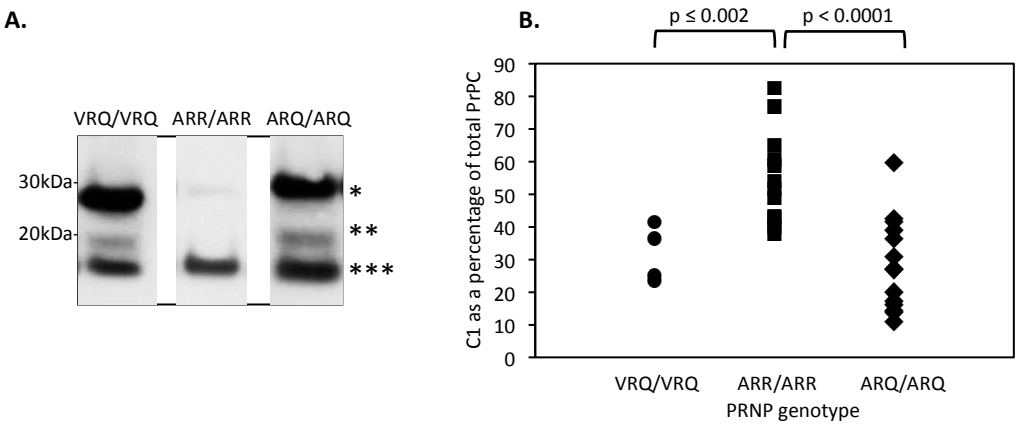

Figure 4.6 – *PRNP* genotype and C1 levels in the ovine cortex. A) Examples of one animal from each *PRNP* genotype tested by western blot with BC6 antibody as described in section 2.3.1. *Full length PrP. ** C2, ***C1. B) Graph showing the average C1 values as a percentage of total PrP as measured by densitometry for each animal in each genotype group.

To further investigate this correlation the effects of one ARR allele was investigated by comparing C1 levels in ARR homozygotes and ARR heterozygotes with other genotypes. Both the ARR/VRQ (49.5 % SD ± 12.3) and ARR/ARQ (53.4 % SD ± 20.3) heterozygotes have higher C1 levels than homozygotes of the VRQ/VRQ (32.6 % SD ± 8.8) and ARQ/ARQ (27.7 % SD ± 14.5) genotypes, $p = 0.060$ and $p = 0.039$ respectively (Figure 4.7).

The sheep used in this study came from two different flocks as explained in section 2.1.1. To rule out any flock specific effect on C1 levels the ARQ/ARQ and VRQ/VRQ animals were grouped depending on the flock they resided in and average C1 levels were taken for each group. There was no significant difference between flocks with average C1 values of 29.9 % (SD ± 16.4) and 28.4 % (SD ± 10.0).

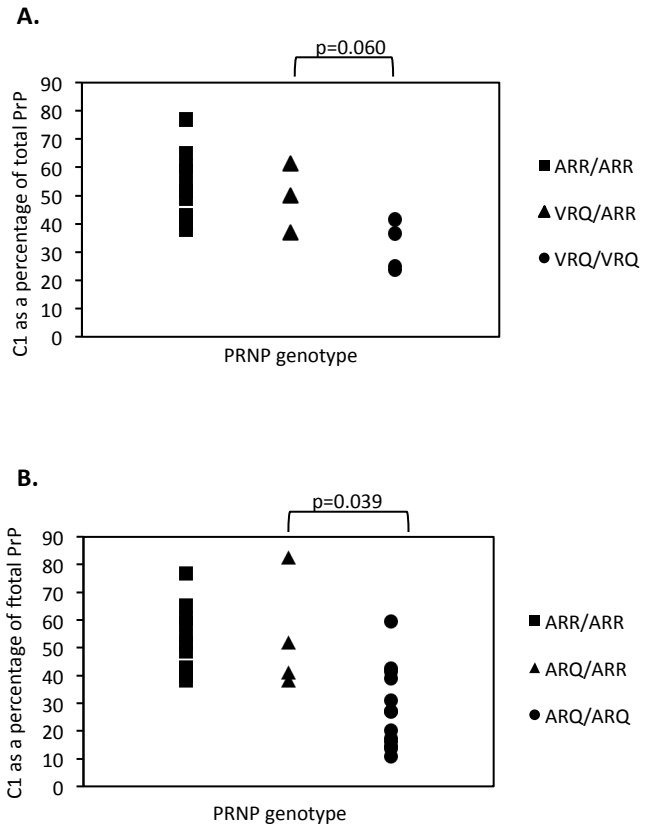

Figure 4.7 – Effects of one ARR allele on levels of C1 in the ovine cortex. A) Histogram comparing average C1 levels in ARR/ARR homozygotes ARR/VRQ heterozygotes and VRQ/VRQ homozygotes. B) Histogram comparing average C1 levels in ARR/ARR homozygotes ARR/ARQ heterozygotes and ARQ/ARQ homozygotes.

Alleles at amino acid 141 have been shown to influence susceptibility to BSE in sheep inoculated intravenously. LL141 was associated with shorter incubation periods, while both LF141 and FF141 were associated with prolonged incubation periods when inoculated intravenously (Tan, Blanco et al. 2012). It was investigated if there was any association of incubation period length and C1 levels within the ARQ/ARQ genotype with a polymorphic codon 141. Illustrated in Figure 4.8, there was a trend but no significance ($p = 0.06$, in both cases) towards higher levels of C1 in LF141 heterozygotes with an average C1 level of 44 % (SD ± 14.5, n = 3), compared to the LL141 and FF141 animals, with average C1 levels of 24.1 % (SD ± 10.8, n = 4) and 23.5 % (SD ± 12.9, n = 4) respectively.

This trend could explain the larger varaiation in C1 levels seem in the ARQ/ARQ genotype group compared to VRQ/VRQ and ARR/ARR. (Figure 4.6).

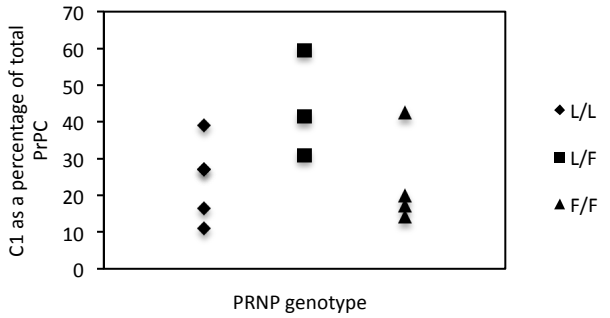

Figure 4.8 –Alleles at position 141 and levels of C1 in ovine cortex of ARQ/ARQ sheep. Histogram showing average C1 levels in the cortex of ARQ/ARQ sheep with alleles at amino acid 141.

4.4.3 Polymorphisims in the PRNP gene and β-cleavage of PrP^C in the ovine cortex.

While collecting C1 data from these animals it was observed that some but not all had a second C-terminal truncated protein C2. Therefore levels of C2 were calculated as a percentage of total PrP^C in the genotype groups. Using the densitometry method as described in section 2.3.4 detection of bands as low as 1 % of the total PrP can be identified. In the animals in which no C2 band could be visualised, even after over exposure the levels of C2 were taken as 0 %.

Across sheep of all genotypes, the mean C2 level (for C2 ≠ 0) was 7.8 % (SD ± 4.8) of total PrP^C (n = 11), but 17 samples had no detectable C2 (defined here as ≥ 1% of total PrP^C). A single ARR/ARR sample out of 11 showed detectable C2, representing 3 % of total PrP^C. Of the ARQ/ARQ animals tested 46 % had a visible C2 band, with an average value of 7.9 %.

(SD ± 4.3) C2 was produced more frequently in the VRQ/VRQ group, within which 80 % of animals had a visible C2 band with an average value of 8.9 % (SD ± 6.2) (Figure 4.9). Although the production of C1 and C2 is thought to be unrelated it was investigated if there was any link between levels of production of either truncated protein. Average C1 and C2 levels were plotted for all animals, independent of genotype with no correlation found (Figure 4.10A). When C2 levels were plotted against levels of full length PrP^C there was a significant negative correlation ($p = 0.01$), indicating that as expected higher levels of C2 result in lower levels of full length PrP^C (Figure 4.10B).

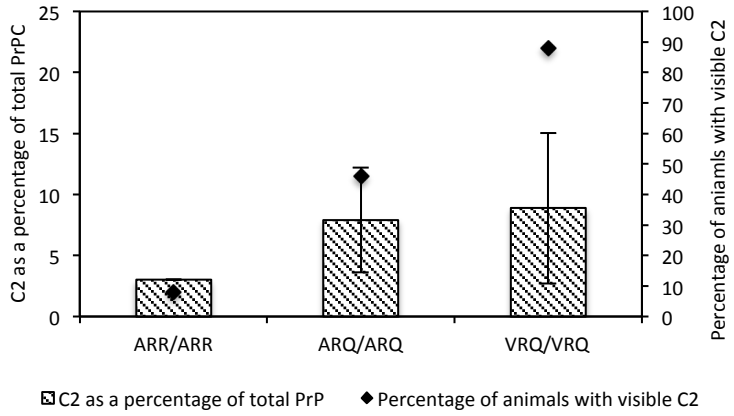

Figure 4.9 - *PRNP* genotype and levels of C2 in the ovine brain. Graph showing the percentage of animals in each genotype group with visible C2 band and comparing the average levels of C2 as a percentage of total PrP in the cortex from each of the genotype groups, omitting animals with no visible bands of C2.

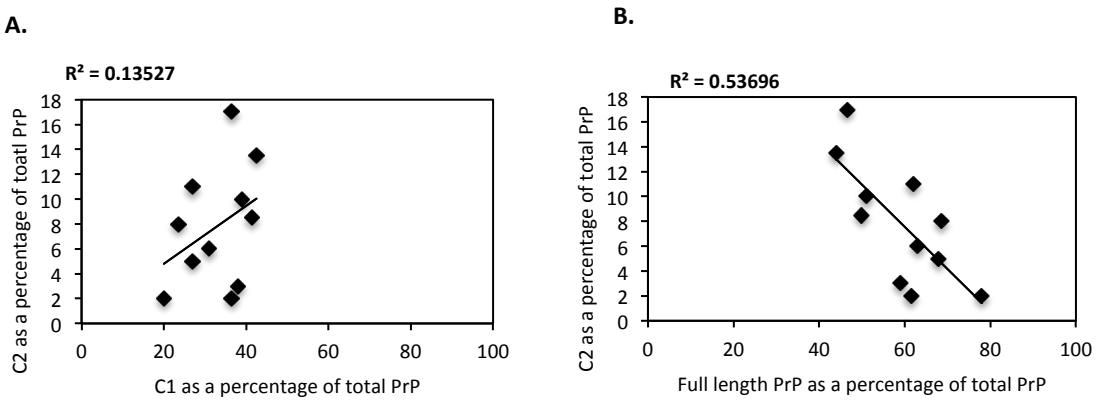

Figure 4.10 – The relationship between C2 levels and other forms of PrP in the ovine cortex n=11. A) Average levels of C2 for each animal were plotted against C1 as a percentage of total PrP. B) Average levels of C2 for each animal were plotted against full length PrP as a percentage of total PrP.

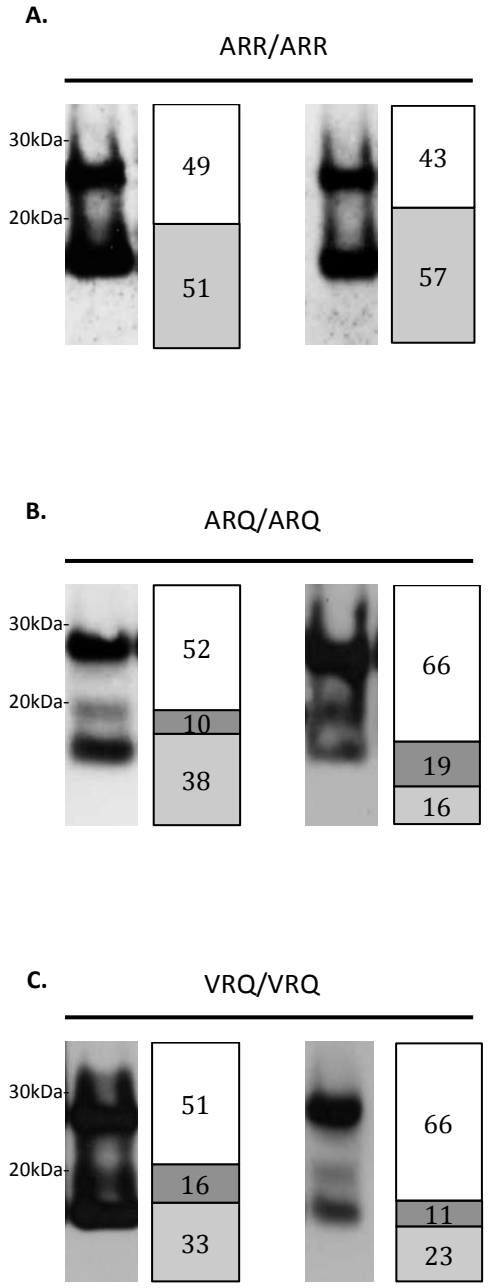

Figure 4.11 – Differential PrP^C processing in *PRNP* genotypes A) Examples of PrP banding patterns from samples of the cortex of two ARR/ARR animals, subjected to western blotting as described in section 2.3.1 and probed with BC6. The densitometry readings are represented in the opposing bar chart. B) ARQ/ARQ animals as described in A. C) VRQ/VRQ animals as described in A.

Animal ID	Genotype	C1 (%)	Average C1	C2 (%)	Average C2
66x48	ARR/ARR	38, 31, 45	38	0, 0, 9	3
O14	ARR/ARR	53, 55	54	0, 0,	0
O22	ARR/ARR	51, 52	51.5	0, 0	0
O30	ARR/ARR	64, 57	60.5	0, 0	0
O51	ARR/ARR	48, 38	43	0, 0	0
77x94	ARR/ARR	53, 32	42.5	0, 0	0
75x49	ARR/ARR	45, 35	40	0,0	0
O17	ARR/ARR	85, 47	65	0, 0	0
81X28	ARR/ARR	72, 82	77	0, 0	0
82X77	ARR/ARR	47, 50	48.5	0, 0	0
61X04	ARR/ARR	62, 56	58.75	0, 0	0
PG0443/03	ARQ/ARQ	11, 11	11	0, 0	0
PG0854/03	ARQ/ARQ	20, 13	16.5	0, 0	0
PG0856/03	ARQ/ARQ	27, 27	27	3, 7	5
75X68	ARQ/ARQ	25, 9	17	0, 0	0
69X67	ARQ/ARQ	10, 18	14	0, 0	0
83X13	ARQ/ARQ	58, 60	59	0, 0	0
72X75	ARQ/ARQ	42, 43	42.5	14, 13	13.5
67x79	ARQ/ARQ	45, 38	41.5	0, 0	0
79x99	ARQ/ARQ	19, 9, 15	14.3	0, 0	0
78x80	ARQ/ARQ	12, 28	20	0, 4	2
78x74	ARQ/ARQ	25, 37	31	12, 0	6
PG0877/03 85	ARQ/ARQ	31, 23	27	11, 11	11
PG0416/03	ARQ/ARQ	40, 38	39	10, 10	10
PG0216/04	VRQ/VRQ	43, 30	36.5	4, 0	2
PG0109/08	VRQ/VRQ	39, 34	36.5	12, 22	17
PG0224/04	VRQ/VRQ	14, 36	25	0,0	0
PG0225/04	VRQ/VRQ	33, 14	23.5	16, 0	8
PG0114/08 85	VRQ/VRQ	39, 44	41.5	8, 9	8.5

Table 4.1 – Summary of C1 and C2 levels in the cortex of all homozygote sheep included in analyses**.**

Animal ID	Genotype	C1 (%)	Average C1	C2 (%)	Average C2
61x13	ARR/ARQ	62, 51.9	57	0, 3.5	1.5
72x38	ARR/ARQ	41.3	41.3	0,0	0
74x00	ARR/ARQ	37.6	37.6	0,0	0
63x51	ARR/ARQ	76.7, 88.3	82.5	0,0	0
60x68	ARR/VRQ	63.5, 55.4	59.5	0,0	0
67x26	ARR/VRQ	64.6, 58	61.3	0,0	0
73x23	ARR/VRQ	41.1, 33.1	37.1	0,0	0

Table 4.2 – Summary of C1 and C2 levels in all heterozygote sheep included in analyses**.**

4.3.4 Proteolytic processing in other species

Although data on C1 levels has been previously published for a range of species often these are simply reported as over/under 50 % total PrP^C (Table 1.2). For more specific values allowing for a direct comparison to our sheep data goat, rat and cat cortex was extracted, treated with PNGase F and subjected to western blotting as with previous ovine samples (Figure 4.12). Five goats of ARQ/ARQ genotype all showed visible bands of C1 with an average C1 level of 29.1 % (SEM ± 4.6). This value, when compared to ARQ/ARQ sheep (average of 27.7 % SEM ± 4.0) was found to be very similar. Samples from the cortex of five rats were also tested. C1 values ranged from between 16.4 % and 25.0 %, with an average of 18.8 % (SEM ± 1.63), this was significantly lower than ARQ/ARQ sheep ($p = 0.03$) and goats ($p = 0.04$). The one cat sample was found to have a C1 level of 47.2 % which has been compared to a second by Stewart *et al* 2012, with very similar western blotting profiles (Stewart, Campbell et al. 2012).

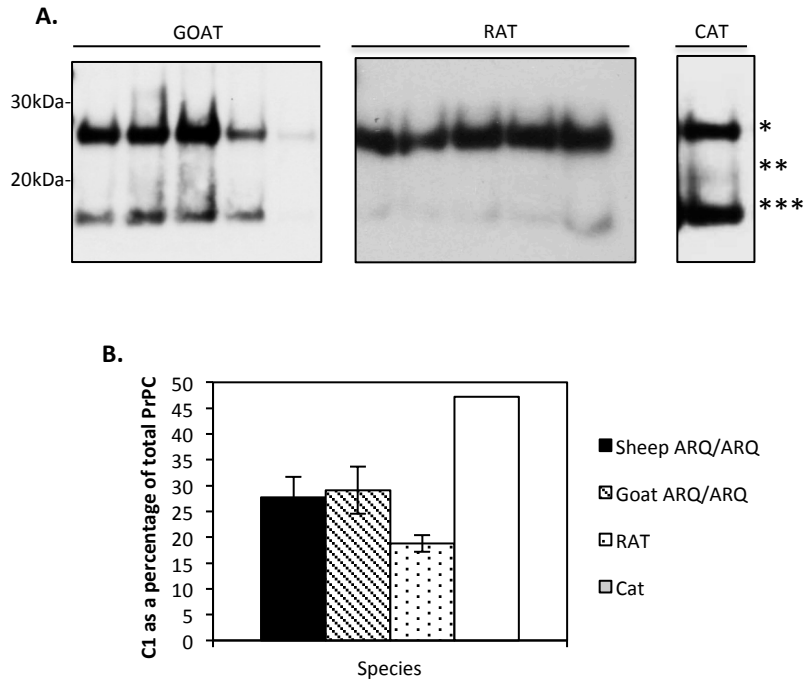

Figure 4.12 - C1 levels in other species. A) Western blot of goat, cat and rat probed with BC6 monoclonal antibody. B) Graph comparing average C1 levels for ARQ/ARQ sheep with average C1 levels in other species tested.

Ovine transgenic mouse models express ovine PrP^C with the purpose of modeling the genotype specific incubation times and disease profiles seen in sheep. In these models ovine PrP^C is produced under the murine gene expression control, therefore there is no evidence that levels of genotype specific expression seen in sheep will be mimicked. Two-day-old Tg338 transgenic mice, expressing PrP^{VRQ} reportedly around 6-8 times that seen in sheep (Le Dur, Beringue. et al 2005) showed very similar levels of truncated C2 protein as seen in VRQ/VRQ sheep (13.9 %, SEM ± 7.2) (Figure 4.13B). The average C1 level of 21.8 % (SEM ± 6.0) in Tg338 mice (n = 3) is lower than seen in VRQ/VRQ sheep, while levels of

C2 are similar, meaning that relative levels of full length PrP^C protein are higher in Tg338 mice.

Gene targeted gtARR and gtARQ transgenic mice were also tested. These express ovine PrP^{ARR} or PrP^{ARQ} at levels comparable to that in sheep. Although only one brain of each line could be sourced PrP^C expression and processing appeared to be almost identical in both models and no genotype effect was observed (Figure 4.13). GtARQ mice and ARQ/ARQ sheep produce strikingly similar levels of C1 protein, while gtARR mice have lower levels compared to ARR/ARR sheep. C2 is present in both models at higher levels than ovine equivalents, 9.8 % in gtARQ and 14.1 % in gtARR. In ovine brain this fragment was found at a measureable level in only 46 % of ARQ/ARQ and 3 % of ARR/ARR sheep brains.

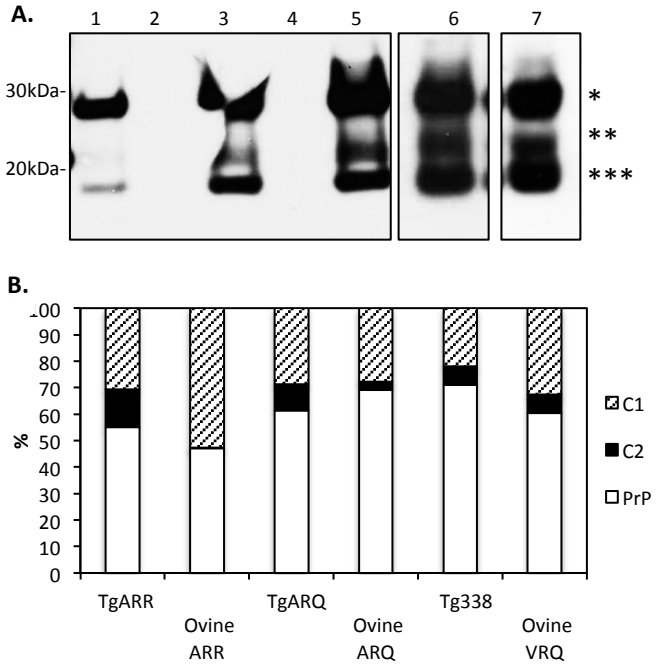

Figure 4.13 – Proteolytic processing in ovine transgenic mice. A) 10 % whole brain homogenate from 3 Tg338 (Lanes 1,3 and 5), gtARQ (Lane 6) and gtARR (Lane 7) was treated with PNGase F and subjected to western blotting with BC6 antibody, as described in section 2.3.1. B) Graph comparing levels of PrP truncated proteins in transgenic mice to sheep expressing corresponding allotype of PrP. For transgenic analysis densitometry was performed on western blots and average levels of both C1 and C2 were calculated as a percentage of total PrP^C.

4.4.5 Levels of PrP^C in the ovine cortex and polymorphisms in the PRNP gene.

In parallel to measuring PrP^C processing, levels of total PrP^C were also measured as it was hypothesised that varying levels of PrP^C protein in the brain may influence the amount of PrP^{Sc} accumulation and susceptibility to disease. This was based on evidence that in $PrP^{0/0}$, $PrP^{+/0}$ and $PrP^{+/+}$ mouse models disease susceptibility and incubation period was inversely correlated with PrP^C expression (Bueler, Aguzzi et al. 1993). Homozygotes from genotype groups ARR/ARR, ARQ/ARQ and VRQ/VRQ were used in this study and both full length PrP^C levels and total PrP^C levels (taken as a sum of all bands visible) were measured. To compare the bands of full length PrP the net intensity of the loading control band of alpha tubulin was measured by densitometry. All values were calculated as a factor of the lowest net intensity and this was used to determine the level of full length PrP^C if loading was exactly equal between all samples. This method allowed for all samples in a gel to be included for measurement despite varied loading. Shown in Figure 4.14, animals of the VRQ/VRQ genotype have significantly higher levels of full length PrP^C than animals of the ARQ/ARQ genotype ($p = 0.012$) but not ARR/ARR genotype animals ($p = 0.43$).

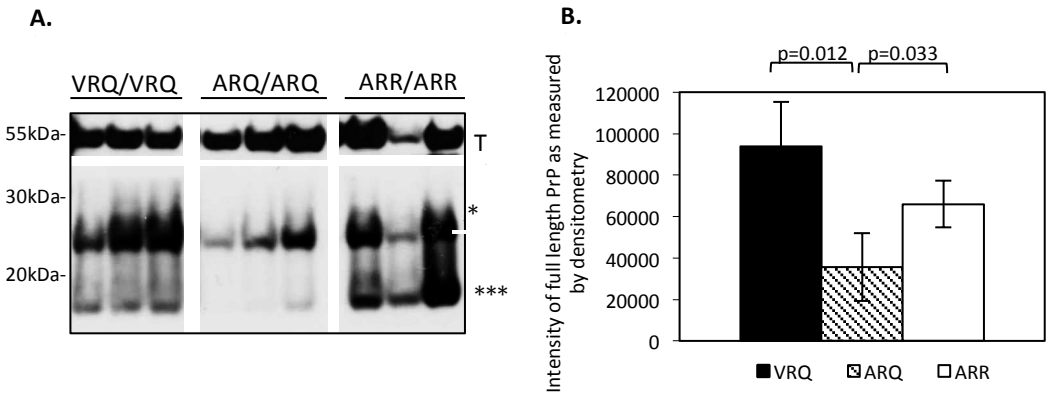

Figure 4.14 – Full length PrP^C expression in *PRNP* genotype groups. A) 10 % homogenate from homozygous animals of the following *PRNP* genotypes VRQ/VRQ, ARQ/ARQ and ARR/ARR, treated with PNGase F and subjected to western blotting with BC6 and alpha tubulin antibodies. Full length PrP*, C1***, alpha tubulin T. B) Average full length PrP^C levels (calculated from net intensity) for each *PRNP* genotype (n=3) when probed with monoclonal antibody BC6.

The total PrP^C level in the cortex of each sheep was determined by measuring densitometry of all bands and calculating an average for each genotype group. There is a significant difference between the average levels of total PrP^C in VRQ/VRQ and ARQ/ARQ sheep ($p = 0.006$). PrP^C levels in animals of the ARR/ARR genotype were also found to be significantly higher than those of the ARQ/ARQ genotype ($p = 0.009$), representing around a three-fold decease.

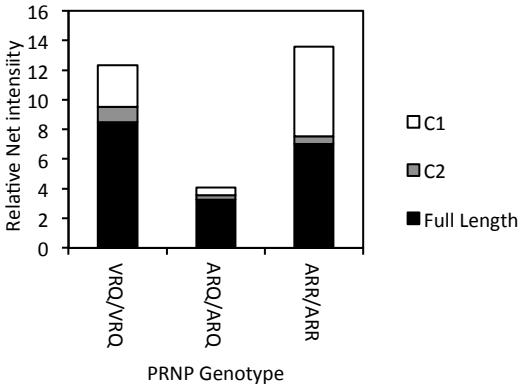

Figure 4.15 – *PRNP* genotype and levels of total PrP^C in the ovine brain Average total PrP levels for each *PRNP* genotype (n=3) when probed with monoclonal antibody BC6. Highest levels are seen in the VRQ/VRQ and ARR/ARR groups.

4.4.6 PrP^C expression in peripheral lymphoid tissues

Due to the involvement of lymphoid organs such as the tonsils and spleen in early prion infection it was of interest to study both PrP^C expression and processing in these tissues. Any variation in levels of either full length PrP^C or truncated C1 fragment could have influence over the initial stages of infection and explain the lack of PrP^{Sc} accumulation in resistant animals before nervous system involvement. 10 % (w/v) homogenates of tonsil, mesenteric lymph node (MLN) and popliteal lymph node (PLN) were produced from one ARR/ARR sheep and subjected to western blotting. PrP^C expression levels in the peripheral lymphoid organs were expected to be around 100 times lower than in brain

(Moudjou, Frobert et al. 2001). After extended exposure a band of ~ 27 kDa, thought to represent full length unglycosylated PrP^C, can be seen in the tonsil sample (Figure 4.16A), which becomes more defined on increased concentration of homogenate. At higher concentration of homogenate the lanes become overloaded and smearing occurs. Examples from MLN and PLN are shown in Figure 4.16B, after treatment with PNGase F. Again, there is a band of possible unglycosylated PrP^C, but no smaller truncated fragments. This sheep is of ARR/ARR genotype which has around 50 % C1 in brain tissue. As full length PrP^C is visible but no C1 we can surmise that levels of α-cleavage are lower in these peripheral tissues when compared to brain.

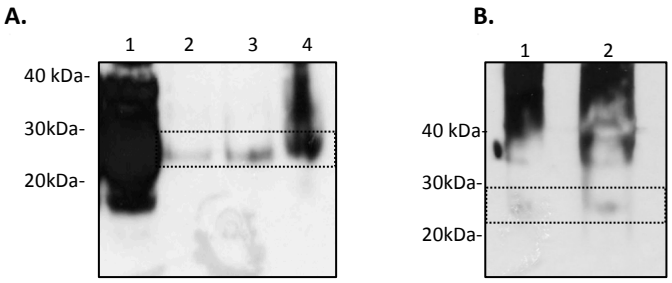

Figure 4.16 – Visualisation of PrP^C in peripheral lymphoid tissues by western blotting. A) 10 % homogenate of brain (Lane 1) and tonsil (Lanes 2-4) from sheep O51, were subjected to western blotting with antibody BC6 as described in section 2.3.1. Three concentrations of tonsil homogenate were tested. 10 % homogenate (Lane 2), 20 % homogenate (Lane 3) and 50 % homogenate (Lane 4). B) 20 % homogenates from MLN (Lane 1) and PLN (Lane 2) from sheep O51, were treated with PNGase F and subjected to western blotting with BC6 antibody. Dashed box highlights possible band of full length unglycosylated PrP^C.

4.4.7 ADAM protease inhibition and α-cleavage in Tg338 derived primary neuronal cells

Although there are many immortalised cell lines that express ovine PrP, few of these are neuronal. Primary cell lines often maintain the same physiology and metabolic

characteristics to cells *in vivo* and therefore represent a more attractive *in vitro* model for the study of cellular processing. Primary neuronal cultures were established under selection of growth factor B-27 from embryonic stem cells derived from mouse line Tg338, which has truncated PrP^C fragments at similar levels to VRQ/VRQ sheep and from gtARQ, which are thought to express PrP^C at levels comparable to that in sheep.

Neuronal differentiation in cell cultures were identified by characterisation of morphology and ICC with an antibody against microtubule associated protein-2 (MAP-2), a neuron specific marker (Figure 4.17). Axons and dendrites can clearly be seen indicating that most cells have fully differentiated into neuronal cells. Differentiated cells from these cultures were lysed 7 days post plating, treated with PNGase F and immuno-blotted with BC6 antibody to assess PrP^C expression (Figure 4.18A). Tg338-derived cells had around 40 % C1, slightly lower than the Tg338-derived line created by Cronier and colleagues in which C1 represented around 60 % of total PrP^C (Cronier, Laude et al. 2004). Total PrP^C expression was around 4-fold higher in Tg338-derived primary neurons compared to gtARQ-derived cells (Figure 4.18B). Expression of full length PrP^C was only 2.5-fold higher in Tg338 primary neurons compared to gtARQ-derived cells. It has previously been reported that Tg338 mice express PrP^C at a level of 6 x higher than found in sheep brain (Laude, Vilette et al. 2002). However, it is important to note that PrP^C expression in neurons alone may not be representative of PrP^C expression in other cell types in the brain.

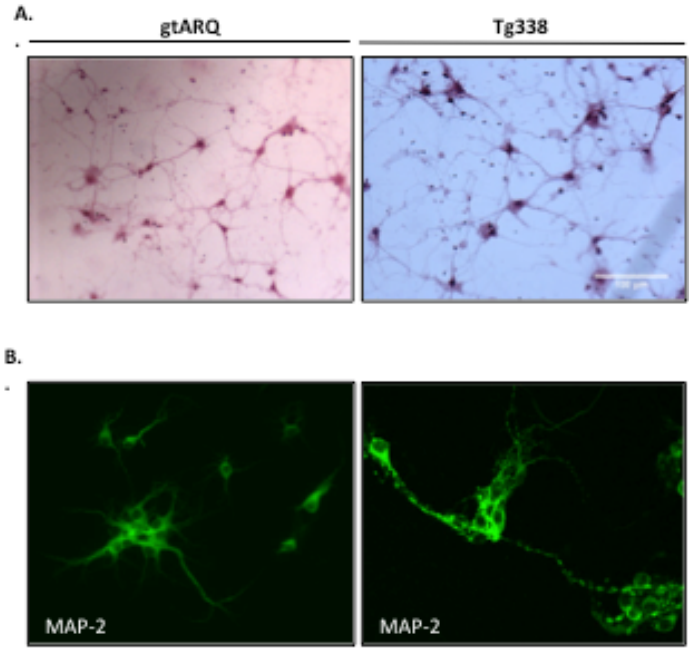

Figure 4.17 – Morphology of primary neuronal cells Tg338 and gtARQ. A) Primary neurons extracted and differentiated from the brains of 17d embryos, cultured on poly-ornithine treated glass slides at 37˚C for around 14 days as described in section 2.6.2. Haemolysin and Eosin staining performed as described in section 2.4.1 shows typical neuronal morphology. Images were taken on a Nikon 800E B) Anti-MAP-2 is specific for microtubule-associated protein-2, a marker for neurons. IHC was performed as described in section 2.4.4Visible staining of neuronal bodies and dendrites. Images were taken on a Zeiss LSM Pascal confocal microscope.

As PrP^C glycosylation has been shown to influence both susceptibility to TSEs and cellular localisation and trafficking (Cancellotti, Wiseman et al. 2005, Cancellotti, Mahal et al. 2013) we compared PrP^C glyco-profiles from Tg338 derived neuronal cell lysates to whole brain lysate of a 2-day-old Tg338 mouse and found them to be very similar (Figure 4.18C), with di-glycosylated PrP^C as the most prominent band.

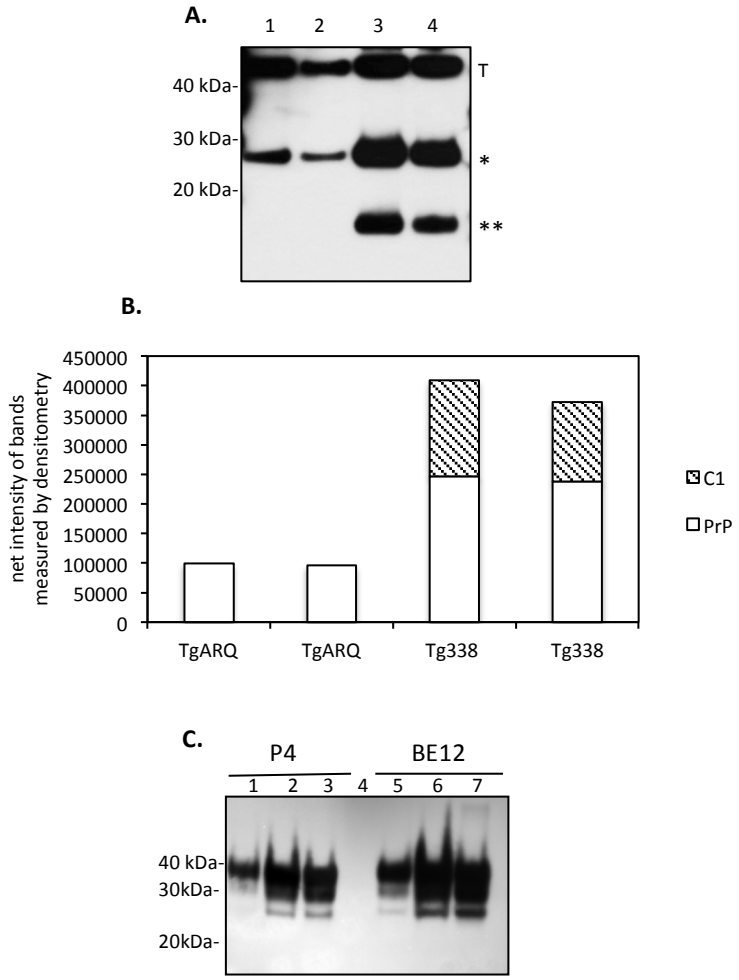

Figure 4.18 – Comparison of PrP^C expression in primary neurons by western blot A) Cell lysates were prepared day 7 post plating as described in section 2.6.2 and samples were treated with PNGase F. Alpha tubulin was used as a loading control (T) and the blot was probed with BC6 antibody, as described in section 2.3.1; Lane 1 and 2 (cell lysate gtARQ); Lane 3 and 4 (cell lysate Tg338). B) PrP bands were measured by densitometry and loading was normalised to the alpha tubulin loading control. C) Tg338-derived cell lysate as A) and brain homogenate from a 2 day old Tg338 mouse, in absence of PNGase F were probed with two monoclonal antibodies P4 and BE12. Lanes 1 and 5 (10 µg total protein, Tg338 cell lysate), Lanes 2 and 6 (25 µg total protein, Tg338 cell lysate), Lane 3 and 7 (Tg338 brain homogenate ,300 µg).

ICC was performed as described in section 2.4.2 to establish the localisation of both PrP^C and truncated C1 on primary neuronal cell lines using a panel of specific monoclonal antibodies with epitopes in both the C-terminal (BC6, FH10), reactive with C1, C2 and full

length PrP^C and the N-terminal (BE12, FH11), specific to full length PrP^C (Figure 4.19, Table 2.2). All antibodies showed reactivity to these primary neurons, shown in Figure 4.18 but the patterns of expression varied considerably depending on the primary antibody used. N-terminal antibody BE12 showed strong immuno-reactivity with the cell body alone and less pronounced staining along projections while FH11 shows less cell body specific reactivity and has strong tropism with the nucleus. C-terminal antibodies BC6 and FH10 both stained projections strongly and showed deposition in the cell body similar to that seen with BE12.

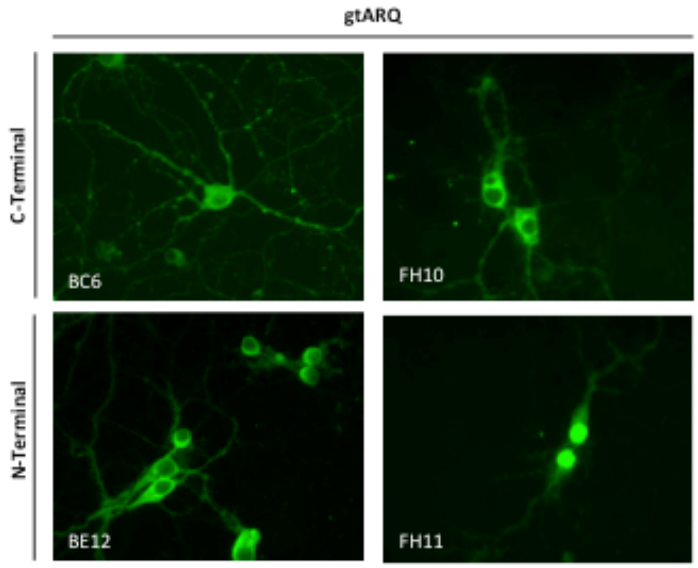

Figure 4.19 – Expression of PrP^C in gtARQ derived primary neurons using a panel of PrP specific antibodies. Primary neurons extracted and differentiated from the brains of 17d gtARQ embryos, cultured on poly-ornithine treated glass slides at 37˚C for around 14 days as described in section 2.6.2 ICC was performed using a panel of PrP specific antibodies (see section 2.4.2), to both the C-terminal and the N-terminal. Images were taken on a Zeiss LSM Pascal confocal microscope, with LSM image analysis software.

It has been reported that general inhibitors of the ADAM metalloproteinase such as O-phenanthroline (OPH) reduced N1 formation by around 40 % - 70 % in TMS neurons and HEK293 cells (Vincent, Paitel et al. 2001, Cisse, Sunyach et al. 2005). However, the involvement of the ADAM proteases in α-cleavage is still under debate. A cell line with manipulative levels of C1 could also act as a model to study the mechanisms linking C1 to TSE pathology. In an attempt to create such a system a general ADAM protease inhibitor OPH (10 μM – 1 mM) was added to the Tg338 primary neuronal cell line at day 23, when full differentiation was observed and incubated for 24 hours. The cells were then lysed and subjected to western blotting with monoclonal antibodies BC6 and anti-ADAM 10 with α-tubulin as a loading control (Figure 4.20A and 4.21A). Three wells (12 well plate format) were set up for each of conditions tested and the experiment was repeated twice. All C1 values calculated are averaged from both experiments.

To confirm inhibition of ADAM proteases the levels of ADAM 10 were measured by western blotting with ADAM 10 specific monoclonal antibody (Abcam UK) and anti-α-tubulin as a loading control. OPH is a zinc metalloproteinase inhibitor, which means the mechanism of inhibition involves the removal of a zinc ion which inactivates the ADAM protease but does not destroy it. Figure 4.20 illustrates the build up of this inactivated form of ADAM 10 with increased concentrations of inhibitor.

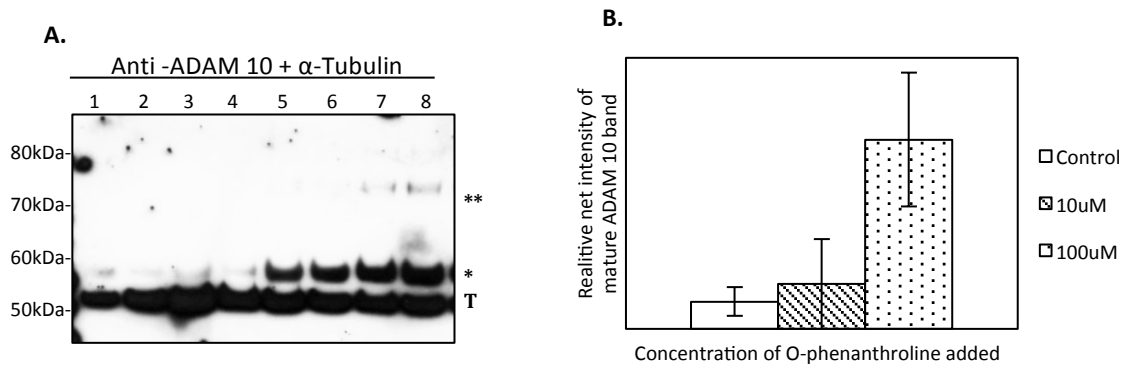

Figure 4.20 – Levels of ADAM 10 after addition of O-phenanthroline. A) Western blot of cell lysate, produced as described in section 2.6.6, probed with anti ADAM 10 and anti-alpha tubulin antibodies. Lanes 1 and 2, control; lanes 3-5, O-phenanthroline 10μM; Lanes 6-8, O-phenanthroline 100μM. Mature ADAM 10 *, Inactivated ADAM 10**, alpha tubulin **T.** B) Graph illustrating relative levels of mature ADAM 10 in O-phenanthroline treated Tg338 primary neurons.

Addition of OPH at 1mM concentration appeared toxic to cells, indicated both from visible cell death and morphological change. Therefore no further analysis was performed for that concentration. The control cells had an average C1 level of 26.0 % (SEM ± 2.2) and 10μM and 100μM OPH treated cells had levels of 29.0 % (SEM ± 2.4) and 34.1 % (SEM ± 2.6) respectively (Figure 4.21). Addition of OPH at a concentration of 100 μM therefore led to s small but significant increase of C1 ($p = 0.03$), suggesting that inhibition of ADAM proteases does not prevent or reduce α-cleavage as reported for other cell lines. It has also been suggested that ADAMs may be directly involved in the extreme C-terminal shedding of PrP^C therefore levels of total PrP were measured using α-tubulin as a loading control. Addition of 10 μM OPH significantly increases the levels of total PrP to 170 % of control cells ($p = 0.027$). With the higher concentration 100μM OPH the increase (140 % of control cells) is not found to be significant.

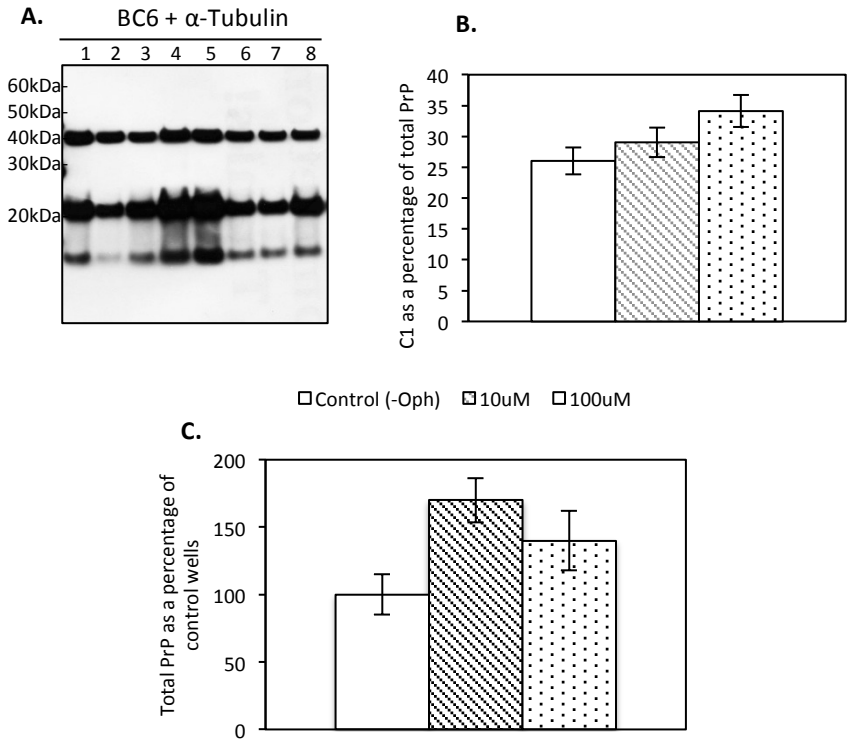

Figure 4.21 – PrP^C and α-cleavage levels on addition of O-phenanthroline. A) Western blot of cell lysate taken after 24 hour incubation, performed as described in section 2.3.1 with 0 (Lanes 1-2), 10µM (Lanes 3-5), or 100µM (Lanes 6-8) O-phenanthroline, treated with PNGase F and probed with BC6 and α-tubulin antibodies. B) Graph of average C1 levels as a percentage of total PrP by densitometry for each concentration. C) Graph of average total PrP (net intensity of all visible bands) calculated as a percentage of control wells.

4.4.11 PrP^C processing in the cortex of scrapie-positive sheep

It has been shown that N1 the corresponding product of α-cleavage has neuroprotective functions by inhibition of staurosporine induced caspase-3 activation through the p53 pathway and that this function is dominant over any pro-apoptotic C1 function (Guillot-Sestier, Sunyach et al. 2009). It can therefore be supposed that any decrease in production of this fragment could have negative effects and may aid the neurodegeneration associated with TSE disease. To look for α-cleavage in the cortex of scrapie infected animals, protein

was extracted and subjected to western blotting using BC6 antibody as previously described. All scrapie cases had been confirmed as PrP^{Sc} positive in the brain (Angie Chong, The Roslin Institute). PK, which would normally be used for the analysis of scrapie infected tissue was omitted as this would cause degradation of cellular PrP^{C}, C1 and C2. It can therefore be noted that, the detected bands on the immunoblot may include both cellular and disease-associated forms of the protein. However, PrP^{Sc} isolated from classical scrapie cases does not normally contain PrP fragments of the size range in which C1 is detected even after PK digestion. Specific genotypes were not considered here but all scrapie infected animals were VRQ carriers.

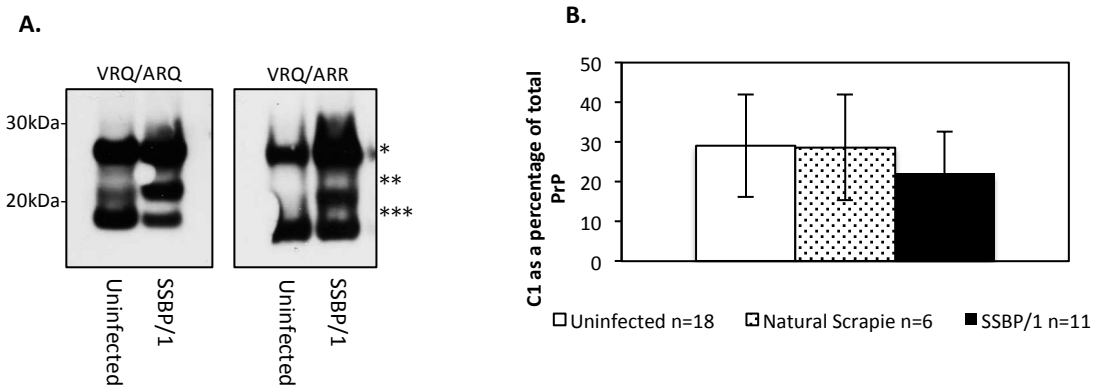

Figure 4.22 – C1 is present in scrapie infected sheep brain at similar levels as in uninfected brain. A) Western blots of animals of VRQ/ARQ and VRQ/ARR genotypes, uninfected and infected with SSBP/1, treated with PNGase F and probed with BC6 monoclonal antibody (section 2.3.1) Full length PrP/PrP^{Sc} (*), C2(**) and C1(***). B) Average C1 values were calculated as a percentage of total PrP for SSBP/1 and classical scrapie infected sheep and these values were compared to average C1 levels in uninfected sheep, omitting ARR/ARR genotype.

In all infected animals tested (n = 17) there was a visible band of C1 protein, running at the same molecular weight as C1 isolated from uninfected brain (Figure 4.22A). Normal

loading controls such as alpha tubulin cannot be used to compare the loading of samples from healthy and brains undergoing neurodegeneration, as neuronal death will alter levels of housekeeping proteins (Dr Barry McColl, The Roslin Institute, personal communication). Total PrP includes both cellular PrP^{C} and PrP^{Sc} as at the present we had no means to accurately separate the two forms of the protein from tissue. However, it was calculated from SSBP/1 infected sheep brain by blotting with a standard curve dilution of recombinant PrP protein (Data not shown) that there is around 2μg of SAF/g of sheep brain. Using this calculation we can assume there will only be around 0.5ng of SAF loaded per lane of gel, which is unlikely to present a visible change in the density of the full length PrP band.

Omitting ARR carriers as we have shown the presence of one ARR allele is associated with higher level of C1, ARQ/ARQ and VRQ/VRQ uninfected sheep were compared to scrapie infected sheep. There was no significant difference in C1 levels in scrapie infected and uninfected ovine brain (Figure 4.22B), indicating that at clinical stage of disease C1 is not reduced at measureable levels.

In the SSBP/1 and classical scrapie infected animals there is an increase or appearance of C2, with an apparent molecular weight of 20-21 kDa (Figure 4.22). It is unknown at present whether this protein represents an increase in production of the cellular form seen at low levels in healthy animals (Chen, Teplow et al. 1995, Jimenez-Huete, Lievens et al. 1998, Mange, Beranger et al. 2004) mediated by reactive oxygen species (Watt and Hooper 2005, Watt, Taylor et al. 2005) or a cleavage product of disease related PrP^{Sc}. This C2 protein was observed at a higher frequency in infected sheep with 100 % of SSBP/1 infected animals and 66.7 % of classical scrapie infected animals with visible bands of C2, compared to 37.9 % of uninfected. To characterise the C1 and C2 proteins in infected tissue western blots were performed with N-terminal antibody P4 (Table 2.1). P4 showed

no reactivity to C1, confirming this is N-terminally truncated, while both BC6 and P4 antibodies bound the C2 fragment as shown in Figure 4.23.

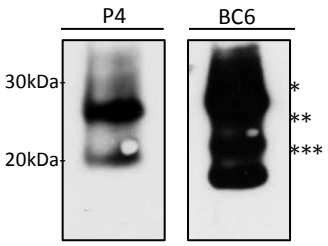

Figure 4.23 –Antibody binding to truncated fragments in infected brain. A) A western blot of SSBP/1 infected brain first probed with BC6, stripped and then probed with P4 as described in section 2.3.3 (Full length PrP*, C2**, C1*).

4.5 DISCUSSION

4.5.1 Distribution of PrP^C and truncated fragments in the ovine brain

It was speculated that different ovine brain regions would have different levels of PrP^C expression as a result of both physiological and functional regional variation and the high diversity of cell types. PrP mRNA expression levels in neurons in mice are higher when compared to glial cells (Ford, Burton et al. 2002). Although protein levels may not correlate directly with mRNA expression we can speculate that areas known to have a relatively high density of neurons, such as the cerebellum, would have higher levels of PrP^C expression, compared to areas where neurons are thought to represent less than 1 % of cells, such as the mid brain and pons (Azevedo, Carvalho et al. 2009). Our data from sheep partially complies with this model, with very low relative levels of residual full length PrP^C in the mid brain and pons. However, in the three sheep tested average levels of full length PrP^C were highest in the cortex and thalamus and relatively low in the cerebellum. If we consider the cellular composition of ovine brain to resemble that of

primates this finding would suggest that neuronal density is not associated with high PrP^{C} expression, illustrated by low levels of PrP^{C} in the cerebellum. This also suggests that glial cells express measureable PrP^{C}, confirming in sheep that mRNA levels in glia and neurons do not directly correlate to PrP^{C} expression in the brain, or that not all neuronal cells in areas such as the cerebellum express PrP^{C} measureable by western blotting.

Furthermore, it was thought that regional variations in PrP^{C} expression may partly explain the distinct phenotypes and regions of PrP^{Sc} accumulation in scrapie (Spiropoulos, Casalone et al. 2007). However, low average levels of residual full length PrP^{C} were found in the pons and midbrain which are primary sites of PrP^{Sc} accumulation during disease (Wemheuer, Benestad et al. 2011). This indicates that PrP^{C} expression levels, although important in the development of scrapie in murine transgenic models are unlikely to be the only defining factor in PrP^{Sc} deposition throughout the ovine brain. In the periphery, PrP^{C} expression in tissues and organs alone is not correlated with ability to accumulate PrP^{Sc} or involvement in infection. PrP^{C} expression is relatively low in the spleen and tonsil when compared to areas thought to be absent of PrP^{Sc} accumulation, such as lung, heart and skeletal muscle (Moudjou, Frobert et al. 2001, Komolka, Ponsuksili et al. 2013).

To further understand the discrepancies with regional PrP^{C} expression and PrP^{Sc} accumulation proteolytic processing was investigated in these seven brain areas - the first most detailed study of PrP processing in a ruminant brain. It was hypothesised that areas with higher levels of C1 would be less likely to accumulate PrP^{Sc} as C1 is not a sufficient substrate for conversion and may act as a dominant inhibitor of conversion, as illustrated in murine models (Westergard, Turnbaugh et al. 2011). α-Cleavage, represented by steady state levels of C1 protein, was evident in all of the seven brain areas tested and there were

no significant differences in C1 levels between these areas. Firstly, this indicates that the unknown protease(s) responsible for cleavage is (are) ubiquitously expressed throughout the brain. Additionally, the possibility cannot be excluded that different proteases are responsible for cleavage in different cell types. For example, in skeletal muscle, ADAM 8 has been linked to α-cleavage (Liang, Wang et al. 2012) but there is no evidence that ADAM 8 is directly involved in α-cleavage in brain tissue. Even CNS specific ADAM proteases are more likely to be involved in cleaving at the extreme C-terminus, shedding PrP^C from the cell surface (Parkin, Watt et al. 2004). Secondly, this suggests that the function of C1 is not area specific or that C1 may play several different roles within the brain as the range of brain areas tested are both structurally and functional diverse.

C1 levels have been previously investigated throughout both the murine and human brain. In agreement with our findings, C1 distribution in wild type mice showed no significant regional differences when measured by western blotting (Kayleigh Iremonger, Ph.D Thesis, University of Edinburgh, 2013). However, in human brain C1 levels were reportedly highest in the cerebellum and pons (Kuczius, Koch et al. 2007). Whether this is a true difference between species or due to differences in preparations and measurements remains to be shown. It is likely that ovine brain, like that of primates has distinctly different regional cell populations. As levels of proteolytic processing in ovine brain regions are remarkably similar despite their cellular composition we can postulate that neurons and glial cells may have comparable levels of PrP^C processing. This would indicate that processing of PrP^C is an important feature of cellular function in general rather than specifically neuronal.

4.5.2 PrP^C expression in the ovine brain and susceptibility to scrapie

It is currently very difficult to measure PrP^C expression and cleavage in the brain prior to infection with scrapie and during scrapie infection, due to the physiology of the brain and the difficulties involved with sampling from this organ. Hence it is not possible to directly correlate these variables with susceptibility and incubation of disease. PrP^C expression and processing was therefore investigated in known models of resistance and susceptibility, determined by *PRNP* genotype. Although there was a trend for average full-length PrP^C levels in VRQ/VRQ sheep to be slightly higher, both ARR/ARR and VRQ/VRQ animals had similar levels, while expression in ARQ/ARQ animals was lower. A separate study which looked at PrP^C expression in brain from two sheep of each *PRNP* genotype (ARR/ARR, ARQ/ARQ and VRQ/VRQ) reported no significant differences in total PrP^C expression (Thackray, Fitzmaurice et al. 2006). We know from *in vitro* studies that PrP^{ARR} cannot be easily converted to PrP^{Sc} therefore perhaps small variations in PrP^C expression between VRQ/VRQ and ARQ/ARQ can go someway to explaining the varying susceptibility to scrapie (Bossers, Belt et al. 1997, Kirby, Agarwal et al. 2010).

This study has primarily looked at PrP^C expression and processing in the brain. Although the brain is the major site of PrP^{Sc} accumulation and pathology it is not the main site of PrP^{Sc} conversion during scrapie infection via the natural oral route. PrP^{Sc} can accumulate in the digestive tract, lymphoid organs, (Andreoletti, Berthon et al. 2000) and circulating blood prior to the onset of clinical disease (Terry, Howells et al. 2009). It is the latter, along with PrP^{Sc} presentation on migrating immune cells, which is though to promote the spread of prion infection throughout the body. PrP^C expression and processing as a factor of susceptibility/resistance may be more important in these early sites of conversion rather than in the brain. During this study attempts were made at visualising PrP^C truncated fragments from tonsil and lymph node (section 4.4.6). The sheep used for this study had an

average C1 level of 43 % in brain therefore we can surmise that although C1 cannot be measured it represents sufficiently less than 50 %. This suggests that α-cleavage levels in the lymphoid organs may be lower compared to levels seen in ovine brain. PrP^{C} expression was too low in these tissues to allow for clear visualisation of PrP^{C} truncated forms using conventional blotting methods. Using immunoprecipitation or similar enrichment techniques analysis of PrP^{C} and truncated proteins in these tissues may be possible, however at the time of completing this work the importance of C1 in scrapie susceptibility was unknown and hence the time was not spent to develop these techniques. PrP^{C} expression has been compared on ovine blood cells of varying *PRNP* genotypes. Total expression of PrP^{VRQ} was found to be higher than both PrP^{ARR} and PrP^{ARQ}, while surface expression of PrP was found to be similar in all genotypes (Halliday, Houston et al. 2005, Thackray, Fitzmaurice et al. 2006), indicating that there may be *PRNP* genotypic differences in the periphery, which needs to be further explored.

Although, we have found no direct association between levels of PrP^{C} expression and scrapie susceptible genotypes, if we postulate that ovine C1 may be a dominant negative inhibitor of conversion of PrP^{Sc} as suggested for mice by Westergard et al (Westergard, Turnbaugh et al. 2011) more relative C1 in the brain of ARR/ARR sheep could negate or prevent much of the full length PrP converting to PrP^{Sc} during TSE disease. Figure 4.24 models such an effect in a deliberately simplified linear manner. Convertible forms of PrP (full length PrP^{C} and C2) are shown in black for each *PRNP* genotype. If C1 (white) could inhibit conversion at a 1:1 molecule: molecule ratio the level of convertible PrP in ARR/ARR sheep is greatly reduced compared to VRQ/VRQ.

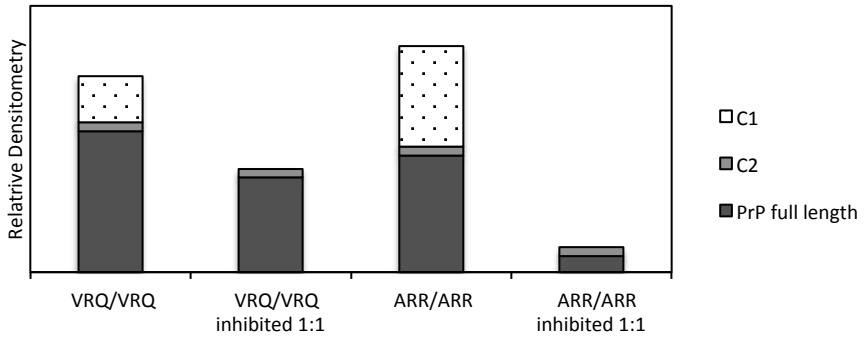

Figure 4.24 – The hypothetical effect of C1 as inhibitor of conversion on levels of convertible PrP in *PRNP* genotype groups with varying susceptibility to scrapie. Levels of full length PrP, C2 and C1 were taken from average levels as shown in Figure 3.19A, using BC6 antibody. 1:1 inhibition assumes that every molecule of C1 can inhibit one molecule of PrP or C2, shown in grey.

4.5.3 PrP^C processing in the ovine brain and susceptibility to scrapie

ARR/ARR sheep, which are naturally resistant to classical scrapie, have significantly higher average levels of C1 fragment in the cortex than ARQ/ARQ and VRQ/VRQ sheep. In heterozygous sheep the presence of one ARR allele led to higher C1 levels in the ovine brain which could be attributed to an increased susceptibility of more PrP^{ARR} to take part in α-cleavage. In sheep the presence of one ARR allele greatly reduces the risk of acquiring natural scrapie and increases incubation period of infection (Baylis, Chihota et al. 2004, Hunter 2007). If antibodies specific to PrP^C variants were available these could have been used to determine if the C1 present in the brains of heterozygotes is predominantly produced from PrP^{ARR}.

The correlation between a high C1 levels and scrapie resistance is supported by similar evidence from cell culture assays and transgenic mouse models. Lewis *et al* (Lewis, Hill et al. 2009) showed that neuronal and non-neuronal cell lines with higher levels of α-cleavage show more resistance to prion infection and concluded that this cleavage is the most important factor in the selective vulnerability to prions (Lewis, Hill et al. 2009). Scrapie challenges in transgenic mice expressing only C1 protein (Westergard, Turnbaugh et al. 2011) have shown that C1 alone does not act as a substrate for conversion to PrP^{Sc}. Over-expression of C1 in the presence of full length PrP^{C} slowed accumulation of PrP^{Sc} and extended the incubation period of disease in these transgenic mice, supporting the view that C1 may inhibit some unknown pathway in the conversion of PrP^{C} to PrP^{Sc} (Westergard, Turnbaugh et al. 2011).

Although N1 levels were not measured in sheep brain samples, its production can be inferred from the levels of the corresponding C1 fragment and it is likely, therefore, that the increased levels of this fragment in disease-resistant animals will represent an additional benefit in protection against the neurodegeneration associated with prion disease. For example, N1 can inhibit staurosporine induced caspase-3 activation through the p53 pathway (Sunyach, Cisse et al. 2007). Addition of a recombinant N1 to cultured cells also shows dose dependent neuroprotective effects (Guillot-Sestier, Sunyach et al. 2009). N1 has also been shown to bind to early stage Aβ oligomers which may inhibit the formation of amyloid fibril formation and reduce fibril associated toxicity and associated effects in both neuronal cell culture and in murine Alzheimer's models (Tagliavini, Prelli et al. 1992).

In TSE infected mice it is reported that there is a decrease in C1 (Nicot and Baron 2010) which could be indicative of an alteration in cellular homeostasis, disrupting an upstream signaling pathway such as protein kinase C. It could also signify increased degradation of C1, possibly due to attempts by the cell to clear misfolded PrP^{Sc}. In contrast, all infected sheep brain tested had C1 present and levels of C1 were relatively similar to those in uninfected ovine brain of susceptible *PRNP* genotypes. Although the amount of PrP^{Sc} accumulation in the brain changes during disease and varies from sheep-to-sheep, affecting the total PrP levels, PrP^{Sc} was not thought to be present at sufficient levels to alter the appearance of PrP by conventional immunoblotting. The use of α-tubulin loading control, as used in other aspects of this thesis, was explored. However, this and other similar 'house-keeping' markers can decrease with neuronal loss (Barry McColl, personal communication), a key feature of scrapie infection.

Although C1 represented the major truncated fragment in ovine brain, C2 was also observed in some samples. It is though that C2 may be an intermediate which is subsequently converted to PrP^{Sc} and there were clearly more infected sheep in this study that showed C2 compared to uninfected sheep. Rather unexpectedly, ARR/ARR animals had both a significantly lower average C2 level and were much less likely to have detectable C2 than the more susceptible genotypes. Truncated recombinant PrP^{90-231}, representing truncated C2 protein have similar ability to aggregate and form amyloid fibrils as full length recombinant PrP^{23-231} (Stohr, Elfrink et al. 2011) indicating C2 may represent an alternative substrate for conversion to PK resistant PrP^{Sc}. It is possible that this increase in production of C2 during disease is specific to the brain region tested – the cortex – as cell culture experiments have show production of this fragment to be dependent on cell type, finding higher levels of C2 produced in scrapie infected astrocytes

when compared to neurons (Dron, Moudjou et al. 2010). However, ovine PrP^{C} expressing neuronal and non-neuronal cell lines tested during this thesis showed no evidence of C2 fragment.

4.5.4 Potential mechanisms of PRNP polymorphism dependent PrP^{C} processing

The C1 fragment is produced by the action of an unknown PrP-secretase (as discussed in section 1.3.8) and high C1 levels in ARR/ARR sheep may result from an increased proteolytic processing of PrP^{ARR} compared to PrP^{ARQ} or PrP^{VRQ}. This may be explained by conformational differences leading to increased presentation of the cleavage site for the PrP secretase or by the extended presence of PrP^{ARR} within intracellular compartments increasing the chance of interacting with the PrP secretase. Slight conformational variations could lead to differences in the half-lives of the C1 fragments, as suggested by Thackray *et al* in the case of full length PrP (Thackray, Yang et al. 2004). Furthermore, PrP^{ARR} may have a higher propensity to form homodimers, compared to other variants of PrP^{C}. It has been shown that forced homodimerisation of PrP^{C} in cell culture increased α-cleavage levels and it may be the case that PrP^{C} homodimerisation is required for binding to or recognition by the unknown PrP secretase (Tagliavini, Prelli et al. 1992, Béland, Motard et al. 2012). In agreement with this hypothesis, mutations within the dimer binding site (amino acids 112-133, murine) but not directly at the alpha cleavage site (111/112, murine) have been shown to reduce production of C1 (Oliveira-Martins, Yusa et al. 2010).

It is yet unknown if the formation of homodimers containing two variants of PrP^{C} (for the purposes of this discussion from now on referred to as heterodimers) have the same effects on levels of α-cleavage as the formation of homodimers of the same PrP^{C} variants.

However, if this increase in cleavage was homodimer specific it would be expected that levels of α-cleavage in heterozygote sheep would be much lower than in homozygotes, which was not the case in the sheep tested. Polymorphisms at position 136, 154 and 171 are out with the dimer binding site and therefore dimerisation should be irrespective of polymorphisms at these positions. However, if we speculate that PrP^{ARR} has an increased propensity to form dimers other factors may be involved, such as conformational differences which would affect outward facing regions for binding. It has been shown that polymorphisms at positions 136 and 171 can have an effect on the secondary structure and stability of PrP^{C}. On comparison of 171Q to 171R it was found that the latter results in a more flexible structure and as a result PrP^{ARQ} and PrP^{VRQ} are more compact, ridged and stable (Rezaei, Choiset et al. 2002, Wong, Thackray et al. 2004, Bujdoso, Burke et al. 2005). If PrP^{ARR} is more flexible we can surmise that perhaps the dimer binding regions are more likely to intercept when compared to other PrP^{C} variants.

It also has to be considered that the high levels of α-cleavage associated with the Roslin Institute ARR carriers may be a result of inbreeding within a closed flock. If high levels of C1 are a result of a separate genetic factor such as mutation of another gene, perhaps the unknown PrP-secretase, high levels in these animals may in fact be inadvertently passed from generation to generation in parallel with the R171 polymorphism. This would explain the lack of a strong association of higher levels of C1 in ARR-heterozygotes in the Norwegian sheep, clearly seen within the Rosin sheep flock (Michael Tranulis and Wilfred Goldmann, personal communication), while there was little difference when we compared ARQ/ARQ sheep in both flocks. Unfortunately, we have not yet been able to obtain brain tissue from any ARR/ARR homozygote sheep from the Norwegian flock to directly compare to ARR/ARR homozygotes from Roslin.

4.5.5 Levels of α-cleavage fragments in sheep relative to other species.

C1 levels account for around 50 % of the total PrP in brain of several other species, such as humans, cats, brown bear and primates, indicating that the ARR/ARR sheep tested in this thesis do not have abnormally high levels of α-cleavage (table 1.2, Chapter 1)(Stewart, Campbell et al. 2012). In particular, baboon brain shows very high levels of C1, of ~ 80 % (Laffont-Proust, Hassig et al. 2006), similar to the highest levels found in ARR/ARR sheep, whereas C1 levels found in ARQ/ARQ and VRQ/VRQ sheep are more similar to those in rats, mice and goats (Laffont-Proust, Hassig et al. 2006). These data suggest that high levels of α-cleavage is not an anomaly associated with the ARR/ARR genotype of sheep but it may be unusual to have such variation within a species and I am currently unaware of other studies in which α-cleavage levels have been investigated in a large number of animals out with transgenic or laboratory mice populations.

4.5.6 Cell culture models of PrP^C processing

Although sheep represent excellent large animal models of disease it was advantageous to identify a model of ovine PrP^C expression that would accurately mimic proteolytic PrP^C processing observed in ovine brain, as it would be open for manipulation. Therefore PrP^C expression and processing were investigated in cell culture models expressing ovine PrP^C. Primary neuronal cell lines were derived from ovine transgenic mice Tg338 and gtARQ. PrP^C expression in gtARQ derived primary neuronal cells was lower in comparison to Tg338 and truncated fragments were not visible by western blotting of cell lysates. Primary neurons derived from the PrP^C overexpressing Tg338 line had measureable full

length PrP^C protein and truncated fragment C1 at levels comparable with Tg338 murine brain and VRQ/VRQ ovine brain. With the goal of using Tg338 derived neuronal cells as a basis to create an inducible model of α-cleavage to study conversion ADAM proteases were inhibited by addition of OPH. This had no inhibitory effect on the levels of α-cleavage and at the highest concentration resulted in a significant increase in cell associated, truncated C1. In agreement with these findings Taylor et al (2009) have shown that over expression of ADAMS 9, 10 and 17 independently in HEK cells did not alter C1 levels and silencing of the same candidates using siRNA also proved to have no effect on the levels of C1. Altmeppen and colleagues also show that C1 levels remain high in ADAM 10 knock out primary neurons (Altmeppen, Prox et al. 2011). In contrast, in cultures of TMS neurons and HEK293 cells addition of OPH resulted in a significant reduction in N1 secretion by 40 -70 % when compared to untreated cells (Vincent, Paitel et al. 2001, Cisse, Sunyach et al. 2005). It is possible that this difference is due to the measurement of secreted N1 and not the cell associated C1 and can be explained using our hypothetical model of ADAM 10 involvement in the shedding of N1 through the cleavage and shedding of LRP1 and not the direct cleavage of PrP^C (Chapter 1, Figure 1.9). Further attempts at manipulating the processing of PrP^C in the Tg338 derived primary cell model were hindered both by the availability of embryonic tissues as a result of low mating success and problems with reproducibility in production of primary neuronal cultures.

Interestingly, there was no measureable band of C2 found in any of the cell lines tested throughout this study. This may indicate that production of C2 is specific to some neuronal cells or the conditions in which the cells are grown suppress C2 production. This could be investigated by inducing oxidative stress or by addition of reactive oxygen species to these

cells in culture and measuring effects on C2 production, as described by Watt *et al* for neuronal cells (Watt, Taylor et al. 2005).

4.5.7 Conclusions

This chapter firstly aimed to investigate the proteolytic processing and expression of PrP^{C} in the ovine brain. Regional differences in residual full length PrP^{C} levels could be further understood by investigating PrP^{C} protein expression in different neuronal cell types. However, the lack of an association between high PrP^{C} expression and areas of known PrP^{Sc} accumulation during scrapie disease led us to conclude that regional PrP^{C} expression in the ovine brain is not a defining factor in the pattern of spread. Perhaps, the ability of different cell types to support and accumulate PrP^{Sc} or variable susceptibility of neuronal cell types to PrP^{Sc} related neurotoxicity might better explain the characteristic pathologies. Contrastingly, there was no major regional variation in the levels of residual C1 protein throughout the ovine brain which may reflect the functional importance of this fragment. However, levels of C1 in the cortex were found to vary extensively between sheep, which may have consequences on normal cellular/brain function.

Secondly, this chapter aimed to assess whether variations in PrP^{C} expression and processing could contribute to scrapie disease susceptibility in sheep. We identified an association of high levels of α-cleavage fragment C1 with scrapie resistant genotype ARR/ARR although, it is unknown if this is a result of an altered ability of the PrP secretase to cleave PrP^{ARR}, higher stability of $C1^{ARR}$ or of another heritable genetic factor. The development of *in vitro* assays of conversion with C1 will be essential to fully understand the role of C1 in the conversion of PrP^{C} to PrP^{Sc}.

CHAPTER 5

CHARACTERISATION AND MISFOLDING OF PRION PROTEINS *IN-VITRO*

5.1. INTRODUCTION

As discussed in great detail in sections 1.3.2, 1.3.8 and 1.3.10 there is growing evidence that C1 cannot be converted to PrP^{Sc} and that the presence of C1 may lead to increased resistance to TSE infection. This raises the possibility that PrP^{C} cleavage may control disease by either reducing the amount of full length PrP^{C} available for conversion or by producing different levels of the C1 fragment, which would act as an inhibitory modulator of conversion. In sheep, this control may be associated with *PRNP* genotype. To investigate the conversion potential of ovine C1 *in vitro* fibrillisation assays were performed.

Experimental considerations

Recombinant proteins have been extensively used to represent cellular PrP^{C} in prion research; hence a system was developed here to produce bacterially expressed recombinant proteins representing truncated C1 and C2 proteins with various sequence variations. Ideally, these experiments using recombinant C1 would be followed by using C1 purified either from the ovine brain or mammalian cells in culture as this would be both glycosylated, carry the GPI-anchor and be naturally folded. However, using unglycosylated recombinant PrP^{C} is not entirely artificial as a fraction of cellular PrP^{C} isolated from tissue is unglycosylated and can be found in PrP^{Sc} preparations supported by *in vivo* studies also showing that glycosylation is not essential for conversion (Tuzi, Cancellotti et al. 2008).

In vitro fibrillisation assays are discussed in detail in section 1.1.8. They allow for the kinetics of conversion to be monitored through the use of ThT, a fluorescent dye that specifically binds to amyloid and which can be used to follow the conversion reaction in real time. Furthermore, this assay has been well characterised for PrP and does not involve a PrP^{Sc} seed. Fibrillisation reactions have been shown to mimic the interspecies barrier (Panza, Luers et al. 2010) and may, as reported from other *in vitro* conversion assays, display variation in fibrillisation abilities associated with resistance associated polymorphisms (Kirby, Agarwal et al. 2010, Eiden, Soto et al. 2011).

5.2 AIMS AND OBJECTIVES

Previous chapters have shown that levels of truncated PrP^{C} protein in ovine brain are highly variable. It has also been suggested that murine C1 is not converted to PK resistant PrP^{Sc}. This chapter aimed to investigate whether truncated ovine PrP^{C} proteins with sequence variation have the potential to misfold *in vitro.* Recombinant proteins were produced and characterised. These recombinant proteins were subjected to fibrillisation assays to assess their potential to contribute to conversion during disease.

5.3. MATERIALS AND METHODS

5.3.1 Production of PET19B/ C1 and C2 plasmids

To produce truncated recombinant PrP proteins representative of the C1 fragment the open reading frame between codons 115 and 234 of the ovine *PRNP* gene alleles ARR, VRQ and ARQ was amplified each by PCR from ovine genomic DNA (homozygous genotypes) with oligonucleotide primers Nde_C1F (CATCATATGGTGGCAGGAGCTGCTG, 3' to 5') and BamH1_C1R (AGTGGATCCTCAACTTGCCCCCCTTTG, 3' to 5') and high fidelity Taq

polymerase. For production of C2 fragments the open reading frame between codons 92 and 234 of ovine *PRNP* from gene alleles ARR and VRQ were amplified each by PCR from genomic DNA with oligonucleotide primers Nde_C2F (CATCATATGGGCTGGGGTCAAGGTG) and BamH1_C1R (AGTGGATCCTCAACTTGCCCCCCTTTG) and high fidelity Taq polymerase. The PCR reactions are summarised in Table 2.4 and conditions are as follows 95ºC for 10minutes, followed by 40 repeats of 95ºC for 1 minute, 61ºC for 30 seconds and 72ºC for 1 minute, with a final extension of 72ºC for 10 minutes. PCR products and PET-19b plasmids were digested with Nde and BamH1 restriction enzymes (both New England Biolabs) in a double digest reaction at 37°C for 1 hour. Digested products were then gel purified using QIAquick gel extraction kit (QIAGEN, UK) to manufacturers instructions and eluted in ddH_2O. PCR products were ligated into the digested PET 19b plasmids using the rapid DNA ligation kit (Roche, UK) at a ratio of plasmid: insert 1:3 as to manufacturers instructions.

5.3.2 Transformation of PET-19b plasmids into E.coli

PET-19b plasmids with inserts were transformed into competent *E.coli* DHα cells (Invitrogen) as follows; 40µL of cells: 5µL of ligation reaction was incubated on ice for 30 minutes, heat shocked at 42ºC for 45 seconds, incubated on ice for 2 minutes and diluted in 0.9mLs of SOC medium (Invitrogen). Cells were grown for 1 hour at 37 ºC and plated onto agar/ampicillin plates (100µg/ml) and incubated at 37 ºC. Colonies, which had grown overnight, were picked and inoculated in to LB broth (6mls, ampicillin 100µg/ml). These were again grown overnight and the plasmids were purified from cultures using QIAminiprep kit (Qiagen, UK) according to manufacturer's instructions and eluted in H_2O. For protein expression the QIA minipreps were transfected into competent *E.coli* BL21(DE3) competent *E.coli* cells (Invitrogen) under the same conditions as described

above. The sequences of all plasmid constructs were confirmed by sequencing with T7 oligonucleotide (TAATACGACTCACTATAGG) on an AB3130 Genetic Analyser with the BigDye® terminator v3.1 cycle sequencing kit (Applied Biosystems, USA) as described in section 2.5.5.

5.3.3 Expression of recombinant proteins

For expression of recombinant full length PrP variants glycerol bacterial stocks were kindly provided by Dr Andy Gill (The Roslin Institute). These were *E.coli* strain Rosetta (DE3) with pTrcHis B vector containing the PrP open reading frame (codons 25-233 inclusive) of the ARR, ARQ, and VRQ alleles (Kirby, Goldmann et al. 2006). Individual *E.coli* clones were cultured over night in 10mls of LB/ampicillin (100µg/ml) at 37°C with shaking. Overnight cultures (4ml) were then cultured in Terrific Broth (TB, 400mls)/ ampicillin (100µg/ml) to an optical density of between 0.6 - 0.8 and PrP protein expression was induced by addition of isopropyl β-D-1-thiogalactopyranoside (IPTG) to a final concentration of 1 mM and cultures were grown for 16-18 hours. To harvest the cells, the cultures were centrifuged at 10,000rpm for 15 minutes and pelleted *E.coli* were frozen at -20°C to aid cell lysis. Pellets were resuspended in 50 mM Tris-HCl, pH 8.0, 1 mM EDTA and 100 mM NaCl, (9mls/g of pellet) and mixed for 1 hour. Lysozyme (20µl/ml) and PMSF (4mM) was added to each pellet mix and cultures were then incubated at 4˚C with continued stirring for 40 minutes. Sodium Deoxycholate was added (1mg/ml) and each mixture was stirred for a further 30 minutes, followed by addition of DNase (10 µg/ml) and stirring for 40 minutes. Inclusion bodies were pelleted by centrifugation at 15,000rpm for 15 minutes and stored at -20 ˚C

5.3.4 NI-IMAC purification

NI-IMAC purification was performed as described in Kirby et al, 2010. Inclusion body pellets containing recombinant protein were resuspended in a urea based buffer NI-A (urea 8 M, Na_2HPO_4 0.1 M, Tris-base 10 µM, pH8 with 2-mercaptoethanol) 5 ml/g and centrifuged at 15000rpm for15 minutes. The supernatant was collected. Affinity purification was performed using Ni-NTA resin (QIAGEN) equilibrated in buffer NI-A by gravity flow. Proteins were eluted in buffer NI-B (buffer NI-A, pH 4 with 2-mercaptoethanol). Fractions were collected and analysed by general protein staining with instant blue (Sections 2.3.1) or PrP-specific immunoblotting (Section 2.3.2).

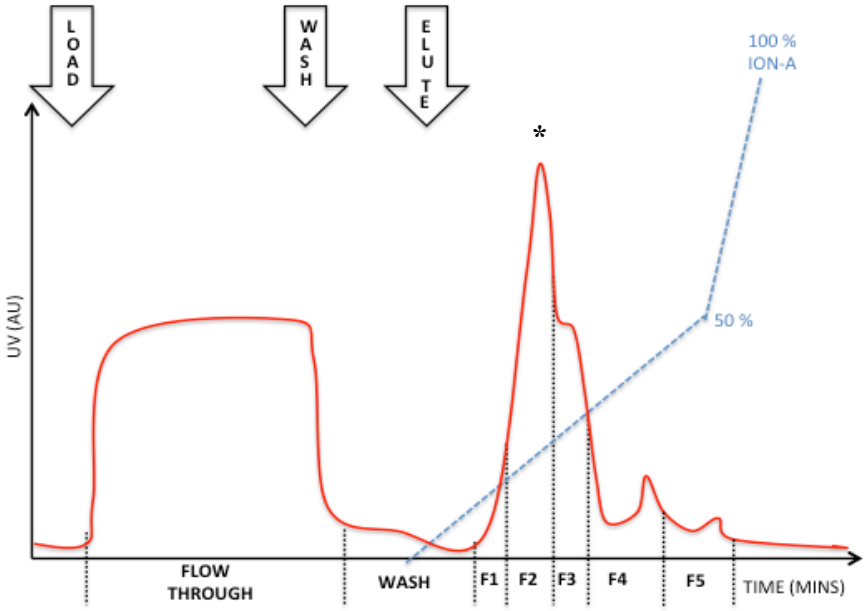

Figure 5.1 – Ion Exchange purification. Typical chromatogram of the purification of recombinant PrP^C and truncated proteins using a Sepharose™ column. The sample was loaded (1 :1 in ION-A) and unbound proteins were collected in the flow through. The column was washed in ION-A and when the U.V. returned to baseline bound proteins were eluted with a graduated increase of ION-B from 0-50 % over 20 minutes. PrP protein was eluted in a single major peak (*).

5.3.5 Ion Exchange Purification

Elutes collected from NI-IMAC chromatography containing the protein of interest were subjected to Ion exchange chromatography using a Sepharose™ column (GE healthcare) and FPLC machine (AKTA, GE Healthcare) equilibrated with buffer ION-A (8M urea, HEPES 50μM, pH 8). Proteins were eluted in buffer ION-B (buffer ION-A with NaCl 1.5M) over a linear gradient with buffer ION-A of 0-50% and UV peaks were collected and analysed and fractions containing the protein of interest were pooled.

5.3.6 Refolding of truncated PrP C1

To induce the formation of the di-sulphide bond in recombinant protein molecules, recombinant protein was diluted to a concentration of 0.1mg/ml in urea (9M). $CuCl_2$ was added at a molar ratio $CuCl_2$: protein of 5:1 and incubated at 4 ˚C with stirring overnight. The protein was dialysed in 2l of 50mM sodium acetate, 10mM EDTA, pH 5.5, with a second dialysis step of 50mM sodium acetate only, pH 5.5 and then stored at -80°C.

5.3.7 NI-IMAC purification for fibrillisation

For the use in fibrillisation reactions an alternative protocol was used for the purification of recombinant proteins. Inclusion body pellets containing protein were resuspended in a urea based buffer NIF-A (urea 8 M, Na_2HPO_4 0.1 M, Tris-base 10 μM, reduced glutathione, 12mM, pH8) 10mL/g for 1 hour and centrifuged 15000rpm, 15 minutes. The supernatant was collected and Ni-NTA resin (QIAGEN) equilibrated in buffer NIF-A was added (10 % v/v) and incubated with stirring for 1 hour. Affinity purification was performed by gravity flow using disposable polypropylene 10 ml columns (Pierce), purifying around 50ml of supernatant/resin suspension per column. Proteins were eluted in buffer NIF-B (buffer A,

pH 4) and 5ml fractions were collected with addition of 50µl EGTA (5mM), pH 8. Fractions were analysed by NuPAGE electrophoresis with gels either stained with instant blue (Section 2.3.1) or western blot (Section 2.3.3).

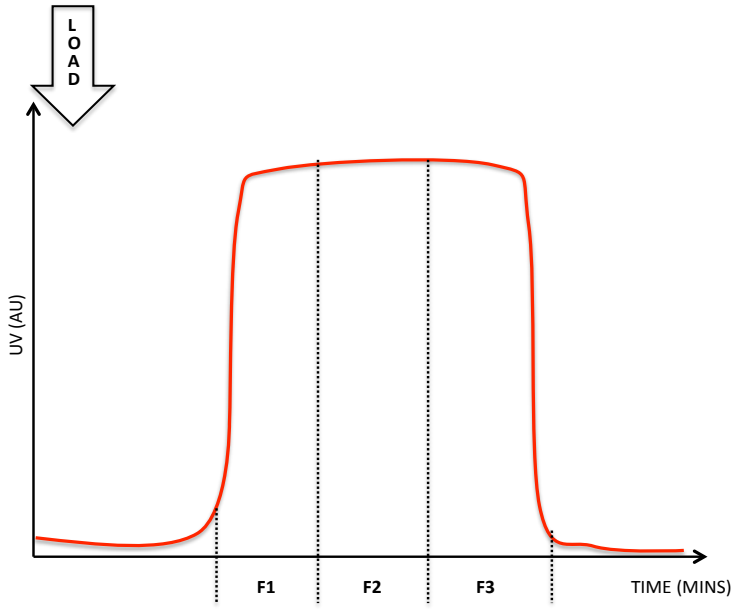

Figure 5.2 – Desalting purification. A characteristic chromatogram of desalting purification of recombinant PrP^C and truncated PrP^C with a HiPrep Desalting column. The sample was loaded 1:1 in desalting buffer and fractions (10mls) were collected when the U.V. started to rise above base line, indicating that protein had been eluted. Once the sample had been loaded Desalting buffer is continually rinsed through the column and fractions are collected until the U.V. returned to base line.

5.3.8 Desalting purification for fibrillisation

Fractions containing the protein of interest after NI-IMAC purification were pooled. Using an FPLC machine (AKTA, GE Healthcare) the desalting column (HiPrep) was equilibrated with desalting buffer (urea 6M, Tris 100mM, pH 7.5). Pooled fractions were loaded onto the column at a rate of 1ml/minute. Fractions were collected when the U.V. strated to rise as illustrated in Figure 5.2. Fractions were analysed by NuPAGE electrophoresis with gels

either stained with instant blue (Section 2.3.1) or western blot (Section 2.3.3). Fractions containing the protein of interest were pooled, the concentration was determined by nanodrop spectrophotometry as described in section 5.3.10 and the protein was diluted to 0.3mg/ml in desalting buffer, EGTA (5mM) and oxidised glutathione (0.2μM) and incubated overnight, at 4°C, with stirring.

5.3.9 Reverse Phase purification for fibrillisation

After desalting the protein was purified further using a reverse phase HPLC (Ultimate 3000, Dionex) with a Vydac HPLC column #4 protein (GRACE) equilibrated in H_2O with 0.1 % (v/v) Trifluoroacetic Acid (TFA). Prior to loading purified protein from desalting was diluted to 0.1mg/ml in H_2O 0.1 % (v/v) TFA and loaded onto the column at a rate of 3ml/ minute. After loading the column was washed with H_2O 0.1 % (v/v) TFA until U.V. had returned to baseline and bound proteins were eluted over a gradient with acetyl nitrate 0.1 % TFA (v/v), as illustrated in figure 5.3 the gradient was as follows; 0-20% in 0-5 minutes, 20-50% in 5-45 minutes and 50-100% in 45-60 minutes. Again, fractions were analysed by NuPAGE electrophoresis with gels either stained with instant blue (Section 2.3.1) or western blot (Section 2.3.3). Fractions containing the protein of interest were pooled, the concentration was determined by nanodrop spectrophotometry as described in section 5.3.10 and the protein was lyophilised and stored at -20°C.

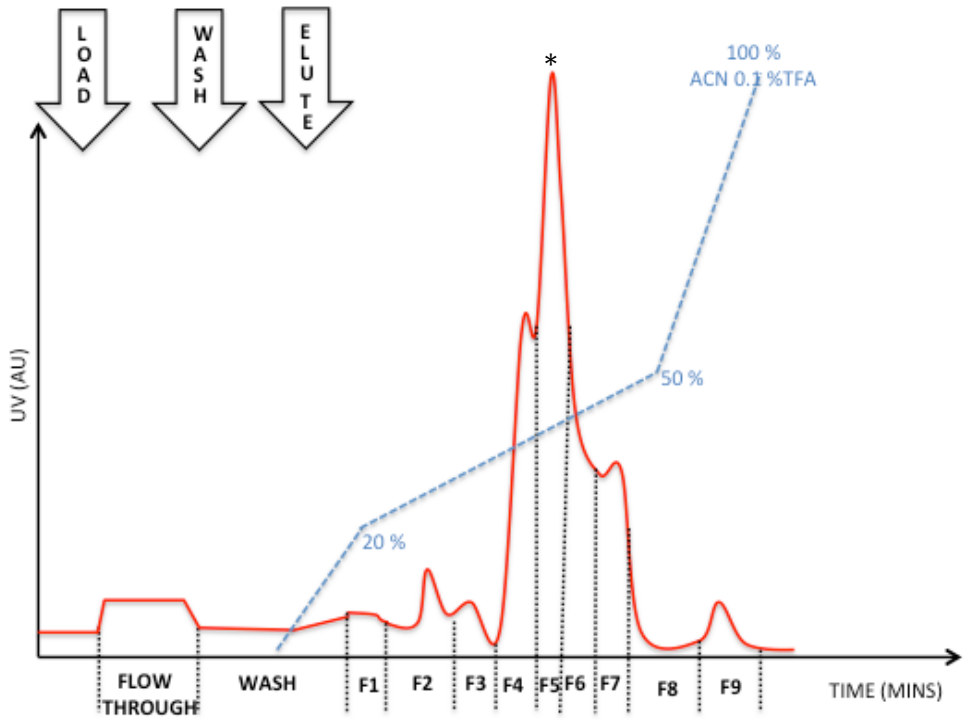

Figure 5.3 – Reverse Phase purification of recombinant proteins. Typical chromatogram of reverse phase of recombinant PrP^C and truncated proteins. The sample was loaded (0.3mgs/ml, in H_2O 0.1 % TFA) and the column was washed with H_2O 0.1 % TFA until U.V. returned to baseline. Bound protein was eluted with a gradient of ACN 0.1 % TFA as follows; 0-20 % in 5 minutes, 20-50 % in 30 minutes, 50-100 % in 10 minutes. Typically PrP (*) started to elute around 35 % ACN 0.1 %TFA.

5.3.10 Measuring recombinant protein concentration by nanodrop spectrophotometry

The concentration of recombinant protein was measured using a nanodrop (Thermo Scientific). Readings were taken at both 280nm and 320nm. The concentration of recombinant protein was calculated using the following equations;

$$Extinction\ co-effifficent$$
$$= (number\ of\ cysteine\ residues \times 120)$$
$$+ (number\ of\ tyrosine\ residues \times 1280)$$
$$+ (number\ of\ tryptophan\ residues \times 5690)$$

$$concentration(mg/ml) = \left(\frac{OD\ 280 - OD\ 320}{Extinction\ co-efficient}\right) \times molecular\ weight$$

5.3.11 Circular Dichroism

For circular dichroism studies measurements of purified protein (~0.5 mg/ml) in 50 mM sodium acetate were made using a Jasco J-710 spectropolarimeter with a path length of 0.2 mm. Readings were collected from 260 nm to 200 nm, with 20 scans repeated for each reading at a rate of 100 nm/min. Observations were made about protein secondary structure by comparison of the spectral output with those characteristically associated with proteins of known secondary structure.

5.3.12 Mass Spectrometry

Mass spectrometry was performed by Dr Andy Gill, (The Roslin Institute) with lyophilised protein samples, purified for fibrillisation. These methods are described in full in Campbell et al. 2013.

5.3.13 Fibrillisation of recombinant C1 and C2

The fibrillisation studies followed a method previously published by Breydo *et al* 2008 (Breydo, Makarava et al. 2008, Graham, Agarwal et al. 2010). In summary, lyophilised recombinant C2 and C1 and full length PrP were reconstituted in 6 M guanidine-HCl (pH 6.0) to a concentration of 3 mg/ml. Reaction mixtures were prepared contained 2 M guanidine-HCL, 50 mM MES, 10 mM thiourea and 100 μg/ml recombinant protein. For assays with two proteins, each was added to a final concentration of 50 μg/ml. To account for background fluorescence, fibrillisation reactions were also set up in the absence of PrP protein. To monitor fibrillisation kinetics, Thioflavin (ThT) was added (10 μM). T reaction

mix (167 µl) was dispensed into each well of a 96 well plate along with 3 Teflon balls (2.381 mm diameter, The Precision Plastic Ball Company). The plate was incubated at 37 °C with shaking at 900rpm in a fluorescent plate reader (Fluoroskan Ascent, Thermo Scientific). ThT fluorescence was measured every 5 minutes for 24 hours (excitation at 444 nm, emission at 485 nm). Data was analysed and lag times calculated as previously described (Graham, Agarwal et al. 2010). The number of repeat fibrillisation assays (n) varied for each protein variant and is stated in the corresponding results sections. For analysis of fibrils by other methods, separate reactions were set up without ThT. Post-fibrillisation, these reactions were dialysed into 10 mM sodium acetate and stored at 4 °C.

5.3.14 Maturation and PK digestion of fibrils

This protocol was followed directly from Breydo *et a*l (Breydo, Makarava et al. 2008). Proteins were visualised by gel electrophoresis (12 % NuPAGE Bis-Tris gel, Invitrogen) and silver staining (Section 2.4.2).

5.3.15 Dynamic Light Scattering (DLS)

Fibrils of recombinant PrP and C1 were produced as described in 5.3.13 in the absence of ThT and dialysed into sodium acetate. To analyse smaller aggregates and oligomers dialysed fibrillisation reactions were centrifuged at 16,000rpm for 30 minutes and the supernatant was collected. A sample (60µl) of fibril preparation (0.5mg/ml) was loaded to a 384 well plate and run on a Zetasizer APS (Malvern) at 10 °C. Between readings the instrument was washed with 5 % (v/v) Decon and sodium acetate buffer (pH 5.5). Each sample was scanned ≥ 13 times per reading and 5 repeat readings were performed. Average curves were fitted and size distribution by mass was used to compare estimated aggregate sizes.

5.3.16 Electron Microscopy

Electron microscopy was performed by Dr Gillian McGovern (AHVLA-Lasswade). Formvar coated copper grids were placed onto a 50 µl drop of fibril preparation (60 µg/ml in 10 mM sodium acetate, pH 5). After 45 seconds, the grid was removed, touched to a filter paper to remove excess fluid, and then placed onto a drop of filtered 2 % aqueous phosphotungstic acid for 2 minutes. Grids were then air dried before storage and examined using a Jeol 1200EX transmission electron microscope.

5.4. RESULTS

5.4.1 Expression and purification of recombinant C1 proteins

Several different methods of separating C1 from full length PrP in brain homogenate and cell culture were investigated during the production of this thesis for example exploiting the differential binding affinities to soil and the purification of C1 from transfected PrP expressing CHO cells (Rigter and Bossers, 2005). Complete separation of C1 from full length PrP was not accomplished therefore alternatively recombinant C1 proteins were produced. As described in sections 5.3.1-5.3.9 the *PRNP* open reading frame DNA was amplified from genomic DNA and a truncated fragment covering amino acids 115-234 was inserted into a protein expression vector (PET-19b) with a His-Tag to aid purification of the protein, in absence of the charged N-terminal. As these proteins had previously never been produced samples were harvested at several time points after induction to check both the expression of the protein and for bacterial degradation. Sampling at 1 hour, 2 hours, 3 hours and 4 hours showed increased production of a 16.5 kDa molecular weight band (predicted molecular weight 16.6642 kDa), confirmed as C1 by western blotting

using BC6 C-terminal antibody (Figure 5.5 and 5.6). C1 proteins were purified either using NI-IMAC (Figure 5.7A) followed by Ion exchange (Figure 5.7B) and dialysed into sodium acetate, or for fibrillisation, by NI-IMAC, followed by Desalting (Figure 5.7C) and Reverse Phase chromatography (Figure 5.7D), summarised in Figure 5.8. Both methods resulted in production of pure recombinant protein as shown in eluted fractions.

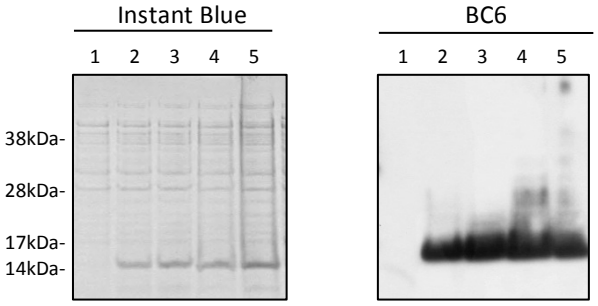

Figure 5.4 – Expression of C1^{VRQ} protein in bacteria. Sampling of bacteria after induction of expression, stained with both Instant Blue as described in section 2.3.5 for total protein and BC6 C-terminal antibody confirming the presence of truncated PrP species. Lane 1 (Before induction), Lane 2 (After 1 hour), Lane 3 (After 2 hours), Lane 4 (After 3 hours), Lane 5 (After 4 hours). Slight smearing seen in western blot is attributed to viscous consistency of the pellet samples.

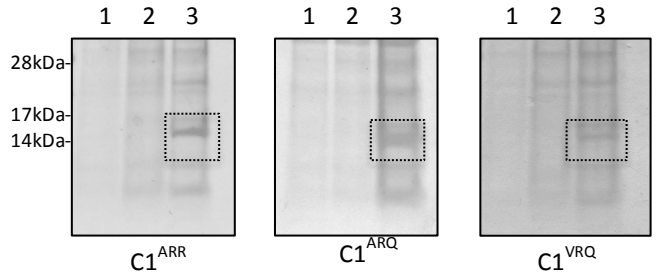

Figure 5.5 – Expression of C1 recombinant proteins. SDS –page gel stained with instant blue as described in section 2.3.5. Bacterial cultures were pelleted by centrifugation and denatured in sample buffer and reducing agent at 90 °C. Before induction (Lane 1), 1 hour post induction (Lane 2), ~ 18 hours post induction (Lane 3).

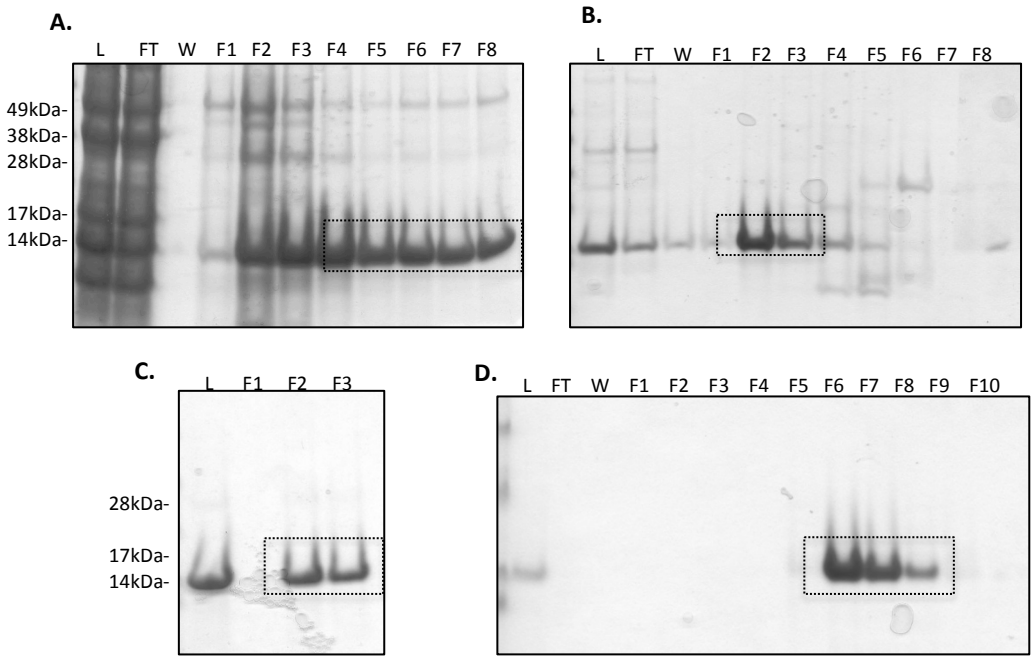

Figure 5.6 – Purification of recombinant C1^{VRQ} protein. SDS –page gels stained with instant blue as described in section 2.3.5. A) NI-IMAC purification of C1 protein by gravity flow. 16.7 kDa protein is eluted in fractions 2-8 (Lanes 5-11). B) Ion exchange chromatography purification of C1 protein by FPLC. C) Desalting purification of C1^{VRQ} by FPLC. D) Reverse Phase purification by HPLC. Load (L), Flow through (FT), Wash (W), Collected fractions (F1-F10). Recombinant C1^{VRQ} protein is highlighted dashed box.

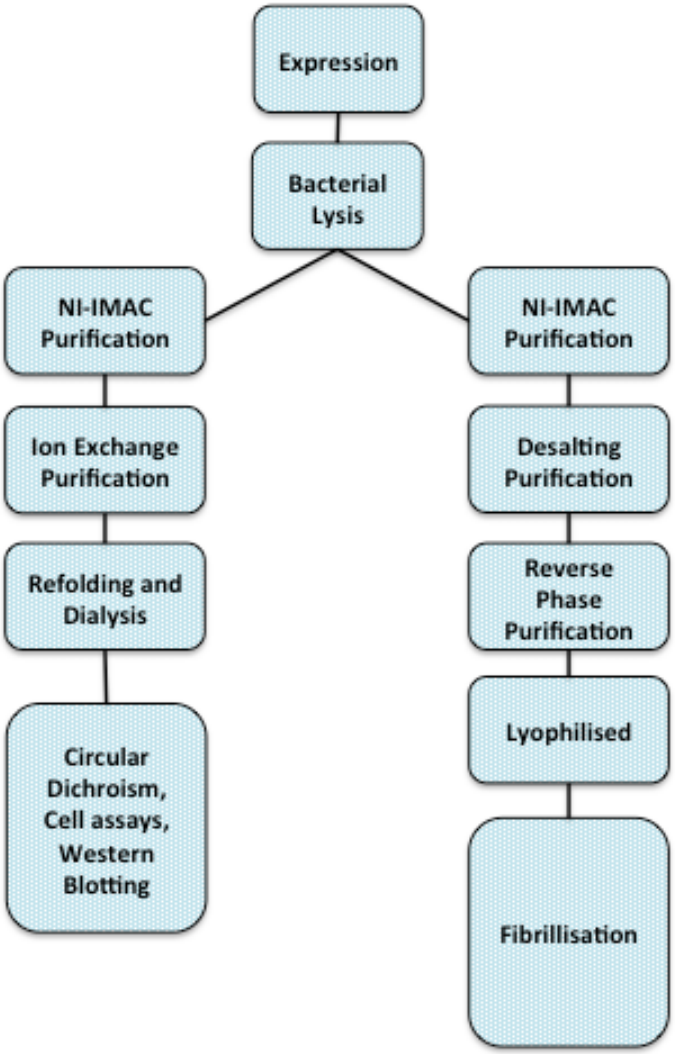

Figure 5.7 – Recombinant protein purification. An overview of recombinant protein production using two different methods. Both result in pure protein suitable for different applications.

5.4.2 Characterisation of recombinant C1 proteins

As expected, the recombinant C1 proteins were detected by immuno-blotting with the C-terminal antibody, BC6, but no reactivity was observed with the N-terminal antibody P4 (Figure 5.9A). The purity of protein was confirmed both by SDS-PAGE stained with Instant Blue (Figure 5.9B) and by mass spectrometry. Mass spectrometry revealed that the C1 proteins had been correctly expressed, but also indicated small amounts of the protein

that had been modified causing mass shifts of +178Da and +258Da (Figure 5.8). Such modifications have been previously documented and are attributed to spontaneous alpha-N-6-phospho-gluconoylation of the His-tag (Geoghegan, Dixon et al. 1999). These modifications were slightly more abundant in the $C1^{ARR}$ variant, but since the levels of these modifications are already low and the modifications are within the octa-histidine tag, they are unlikely to impact on protein misfolding or stability. To check this secondary structure was analysed using circular dichroism spectra (CD) for the three C1 protein variants, which appeared to exhibit a primarily alpha-helical structure, characterized by spectra showing two minima at 222 nm and 208 nm, as shown in Figure 5.9C.

CD analysis programs were used to confirm this observation. Four were deemed suitable for this data; K2D, CDSTTR, SELCON and CONTIN (Compton and Johnson 1986, Manavalan and Johnson 1987, Sreerama and Woody 2000, Sreerama and Woody 2004, Whitmore and Wallace 2004, Whitmore and Wallace 2008). Three independent readings were analysed for each variant with each program and average values are shown in Table 5.1. Estimation of secondary structure varied depending on the program used therefore average values for all four programs were calculated for comparison.

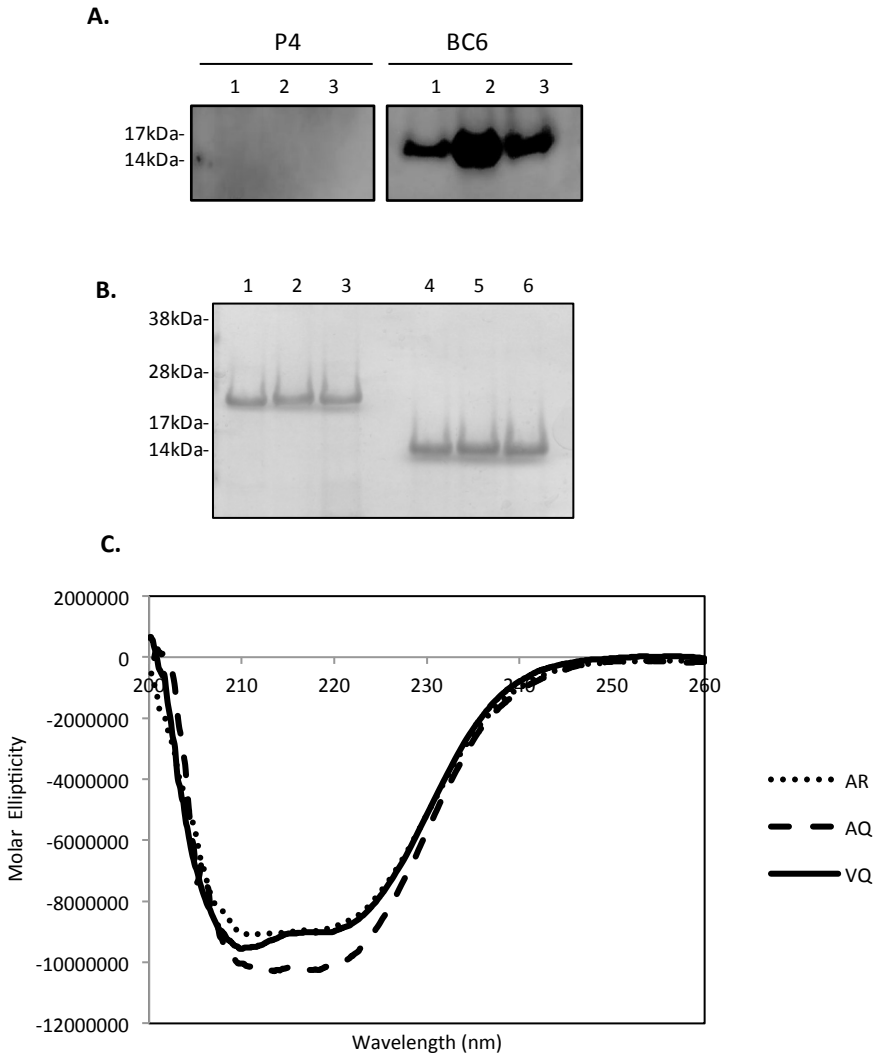

Figure 5.8 – Characterisation of recombinant C1 proteins. A) Western blots of rC1 proteins, probed with monoclonal antibodies P4 (epitope 89-104) and BC6 (epitope 146-154).C1 variants $C1^{ARR}$ (Lane 1), $C1^{ARQ}$ (Lane 2) and $C1^{VRQ}$ (Lane 3) were immunoblotted with both BC6 and P4 antibodies. B) All variants of recombinant protein expressed were separated by SDS-page and stained with Instant Blue to confirm purity. PrP^{ARR} (Lane 1), PrP^{ARQ} (Lane 2), PrP^{VRQ} (Lane 3), $C1^{ARR}$ (Lane 4), $C1^{ARQ}$ (Lane 5), $C1^{VRQ}$ (Lane 6). C) Circular Dichroism was performed as described in section 5.3.11 of three C1 variants to assess secondary structure. ~ 0.5mg/ml in sodium acetate.

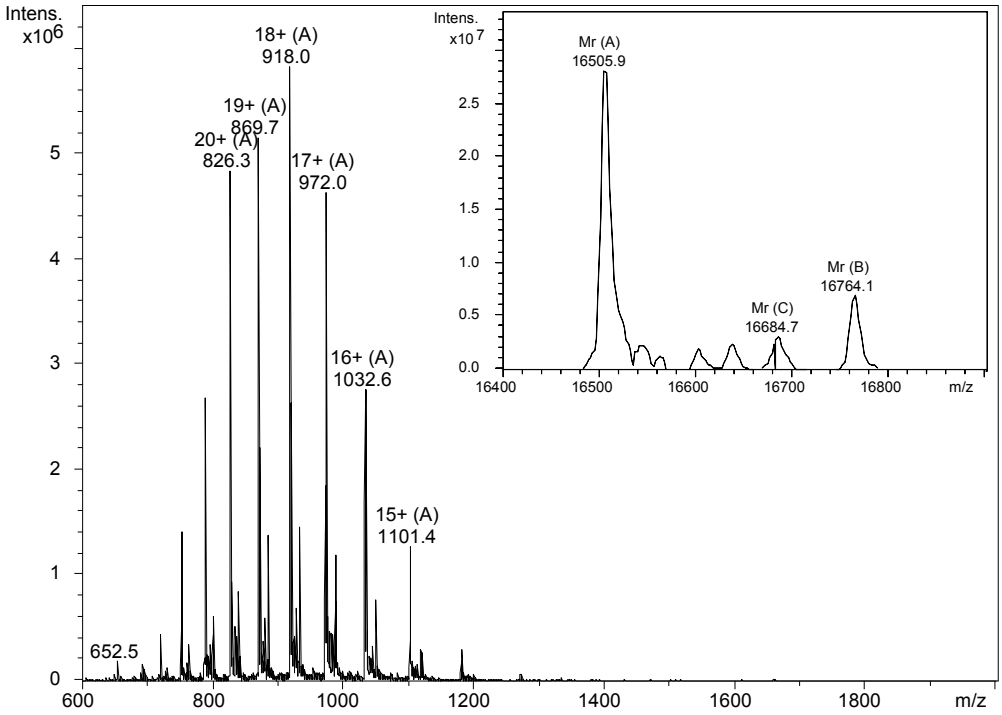
Intens.
x10^6
18+ (A)
918.0
19+ (A)
869.7
20+ (A)
826.3
17+ (A)
972.0
16+ (A)
1032.6
15+ (A)
1101.4
652.5
m/z
Intens.
x10^7
Mr (A)
16505.9
Mr (C)
16684.7
Mr (B)
16764.1
m/z

B.

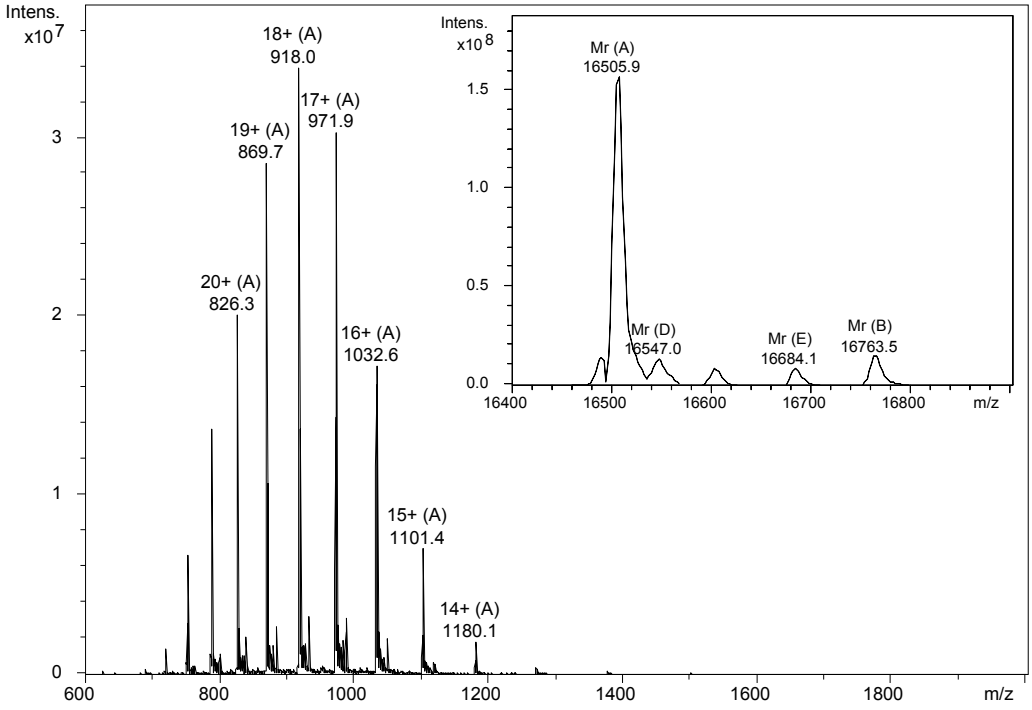
Intens.
x10^7
18+ (A)
918.0
17+ (A)
971.9
19+ (A)
869.7
20+ (A)
826.3
16+ (A)
1032.6
15+ (A)
1101.4
14+ (A)
1180.1
m/z
Intens.
x10^8
Mr (A)
16505.9
Mr (D)
16547.0
Mr (E)
16684.1
Mr (B)
16763.5
m/z

Figure 5.9 – Mass Spectrometry of recombinant C1 proteins. A) rC1$^{ARR.}$ The spectrum consists of a single major charge envelope, labelled with 'A' along with the charge state of each of the species (20+, 19+ etc) and the mass/charge ratio at which each peak occurs. Deconvolution of the spectrum shows the presence of a single major species (labelled Mr(A) 16505.9) which represents the unmodified protein. The measured molecular weight of the unmodified protein (16505.9 Da) is in excellent agreement with the theoretical molecular weight calculated from the sequence of 16506.1 Da. A second species (labelled Mr(B) 16764.1) occurs at a molecular weight of 258 Da higher than the unmodified protein whilst a third (labelled Mr (C) 16684.7) is 178 Da higher in mass than the unmodified protein. These species are consistent with previously reported modifications within the His Tag region of the protein, specifically attributed to spontaneous alpha-N-6-phospho-gluconoylation. B) The spectrum consists of a single major charge envelope, labelled with 'A' along with the charge state of each of the species (20+, 19+ etc) and the mass/charge ratio at which each peak occurs. Deconvolution of the spectrum shows the presence of a single major species (labelled Mr(A) 16505.9) which represents the unmodified protein. The measured molecular weight of the unmodified protein (16505.9 Da) is in excellent agreement with the theoretical molecular weight calculated from the sequence of 16506.1 Da. A second species (labelled Mr(B) 16763.5) occurs at a molecular weight of 258 Da higher than the unmodified protein whilst a third (labelled Mr (E) 16684.1) is 178 Da higher in mass than the unmodified protein.

Program	C1 ARR			C1 ARQ			C1 VRQ		
	α	β	Un-ordered	α	β	Un-ordered	α	β	Un-ordered
K2d	36	13	51	14	35	50	30	15	54
CDSTTR	30	18	28	44	19	28	47	20	33
SELCON	28	21	51	28	16	58	42	13	46
CONTIN	28	22	51	34	17	49	38	18	44
Mean	30.5	18.5	45	30	22	47	39	16.5	44

Table 5.1 – Comparison of CD analysis of recombinant C1 using four independent programs

On average it was estimated that $C1^{ARR}$ has 30.5 % alpha helix and 18.5 % beta-sheet, $C1^{ARQ}$ has 30.0 % alpha helix and 22.0 % beta-sheet and $C1^{VRQ}$ has 39% alpha helix and 16.5 % beta sheet. Alpha helix is the dominant structure in all three variants, confirming that most molecules have been refolded correctly (Haire, Whyte et al. 2004).

5.4.3 Expression and purification of recombinant C2 proteins

As with production of C1, *PRNP* open reading frame DNA (encoding amino acids 92-234) was amplified from genomic DNA and inserted into an expression vector (PET-19b) with a His-Tag to aid purification of the protein as described in sections 5.3.1-5.3.9. After induction of expression a band with apparent molecular weight of 20 kDa was produced (Figure 5.11A), this was similar to the predicted molecular weight of 19.171 kDa. To confirm this was C2 these bacterial samples were immuno blotted with BC6 (Figure 5.11B). C2 is visible 1 hour post induction and is increased by ~18 hours. The bacterial pellet sample shows strong staining with BC6 and smearing attributed to the viscous consistency of the pellet. C2 proteins were purified similar to C1 variants, illustrated in Figure 5.12.

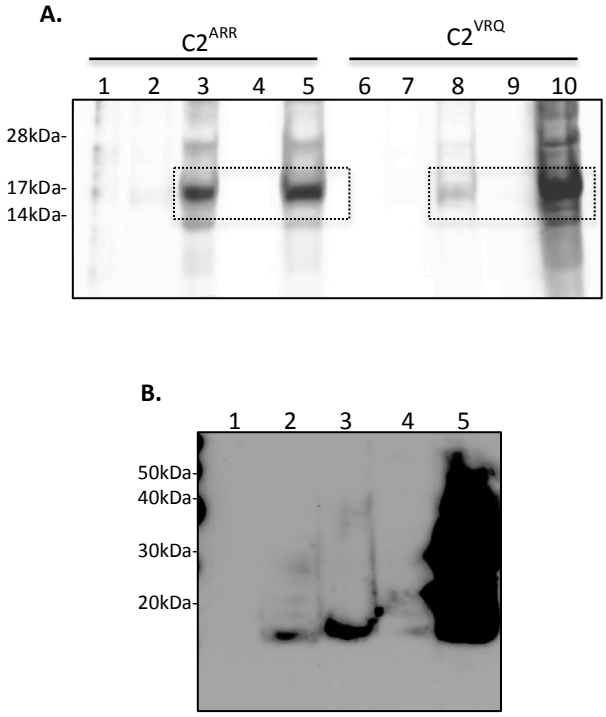

Figure 5.10 – Expression of recombinant C2 proteins. A) SDS –page gel stained with instant blue, as described in section 2.3.5. Samples of bacterial cultures were pelleted by centrifugation and denatured in sample buffer and reducing agent at 90 °C. Before induction (Lane 1 and 6), 1 hour post induction (Lane 2 and 7), ~ 18 hours post induction (Lane 3 and 8), bacterial supernatant (Lane 4 and 9), bacterial pellet (Lane 5 and 10). Recombinant C2 is highlighted by a dashed box B) Western blot (section 2.3.2) of bacterial culture samples as in A), probed with BC6 antibody.

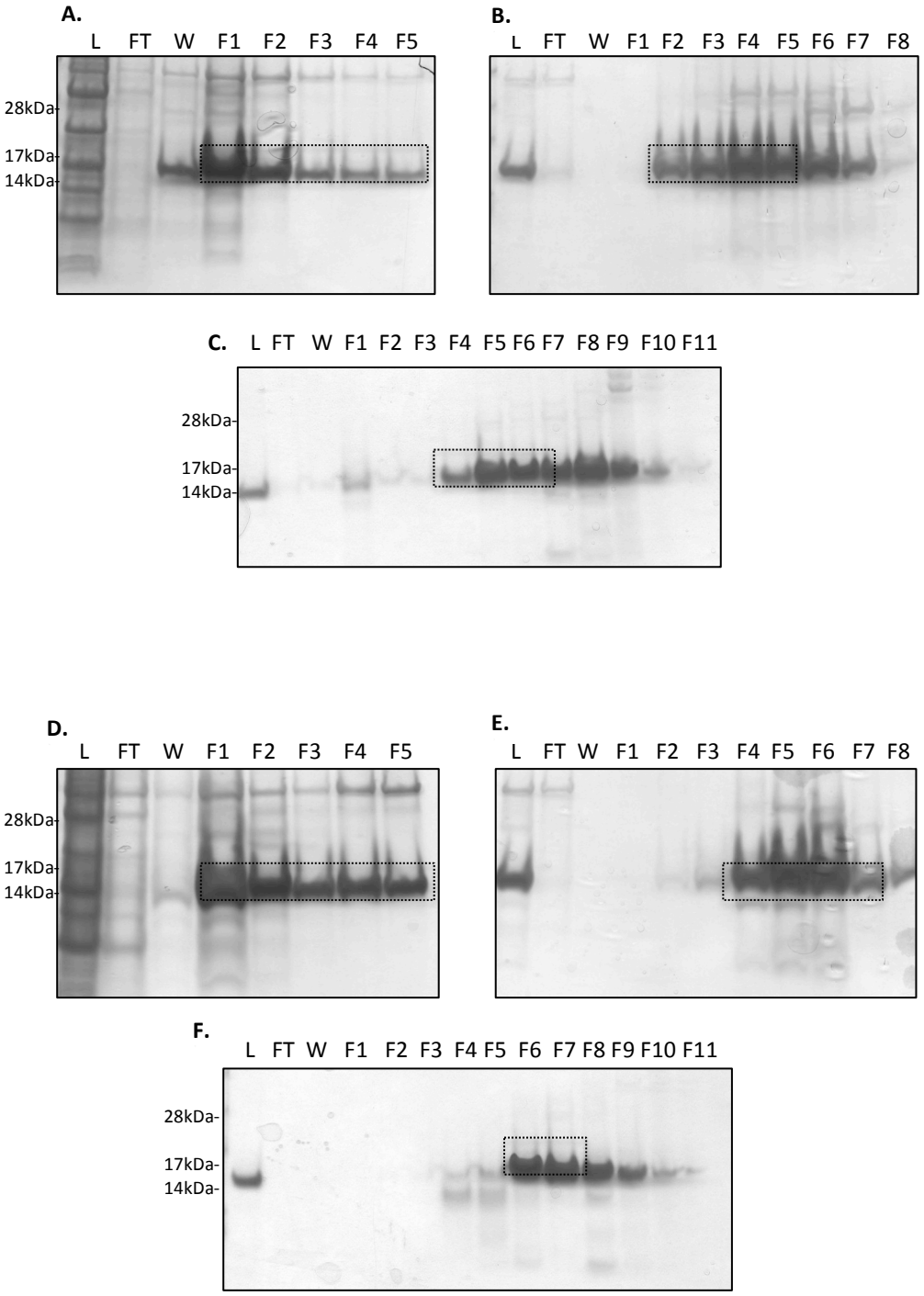

Figure 5.11 – Purification of recombinant C2 proteins. A) SDS –page gel stained with instant blue, as described in section 2.3.5. NI-IMAC purification of $C2^{ARR}$ protein by gravity flow. B) Ion exchange chromatography purification of $C2^{ARR}$ protein by FPLC. C) Reverse phase purification of C) Fractions F4, F5 and F6 were considered pure and were pooled and lyophilsed. D) NI-IMAC purification of $C2^{VRQ}$ protein by gravity flow. E) Ion exchange chromatography purification of $C2^{VRQ}$ protein by FPLC. F) Reverse phase purification of $C2^{VRQ}$. Fractions F6 and F7 were considered pure and were pooled and lyophilsed. Load (L), Flow through (FT), Wash (W), Collected fractions (F1-F10).

5.4.4 Characterisation of recombinant C2 proteins

To assess the secondary structure of recombinant C2 proteins circular dichroism spectra (CD) were measured for each variant. Both appeared to exhibit a primarily alpha-helical structure similar to the recombinant C1 variants. However, the characteristic minima at 222 nm and 208 nm are less pronounced, as shown in Figure 5.13. The same panel of CD analysis programs were used to estimate secondary structure elements, although K2d was deemed unsuitable to analyse this data as resulting readings reported 100 % alpha helix (Compton and Johnson 1986, Manavalan and Johnson 1987, Sreerama and Woody 2000, Sreerama and Woody 2004, Whitmore and Wallace 2004, Whitmore and Wallace 2008). Three independent readings were analysed for each variant with each remaining programs and average values are shown in Table 5.2. Estimation of secondary structure varied depending on the program used therefore average values were taken from all three programs and compared.

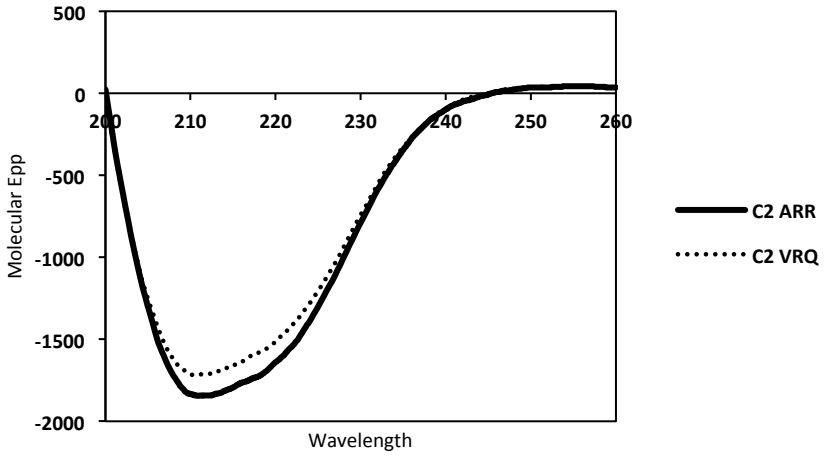

Figure 5.12 – Secondary structure of recombinant C2 proteins by circular dichroism. Circular Dichroism was performed as described in section 5.3.11. Recombinant proteins ~ 0.5mg/ml in sodium acetate.

Program	C2 ARR			C2 VRQ		
	α	β	Un-ordered	α	β	Un-ordered
CDSTTR	63	13.5	21.5	45	28	27
SELCON	35	18	55	80	1	23
CONTIN	65	2	33	97	3	0
Mean	54.3	11.2	36.5	74	10.7	16.7

Table 5.2 - Comparison of CD analysis of C2 using three independent programs

On average it was estimated that $C2^{ARR}$ has 54.3 % alpha helix and 11.2 % beta-sheet, while $C2^{VRQ}$ has 74 % alpha helix and 10.7 % beta sheet. Average alpha helical content in recombinant $C2^{VRQ}$ appears to be higher than $C2^{ARR}$, although in both proteins helix is the dominant secondary structure. It should be noted that the VRQ variant of recombinant C1 is also predicted to have slightly higher alpha helical content when compared to ARR (Table 5.1).

5.4.5 Amyloid fibril formation of recombinant C1 protein

The mechanisms involved in conversion itself are still fairly unknown as is the role of C1 in this process. C1 proteins were assessed for their ability to form amyloid fibrils *in vitro* and to investigate genotype specific effects associated with the folding pathways of the C1 fragment. For comparison, truncated proteins and full length PrP^{ARR} and PrP^{VRQ} were expressed and purified from bacterial glycerol stocks provided by Dr Andy Gill (The Roslin Institute). Using these full-length PrP^{C} proteins along with three variants of recombinant C1, fibrillisation assays were set up in the presence of thioflavin T (ThT) as described in section 5.3.13. Fibril formation kinetics were measured over a 24-hour period and lag times were calculated as described in Graham *et al.* (Graham, Agarwal et al. 2010).

Fibrillisation experiments were repeated multiple times (n) and typical fibrillisation curves for C1 fragments are shown in Figure 5.14B, whilst typical curves for the full-length proteins PrP^{VRQ} and PrP^{ARR} are shown in Figure 5.14D. Fibrillisation of PrP^{ARR} and PrP^{VRQ} showed an initial lag phase (nucleation) followed by a rapid increase in fluorescence on fibril growth (elongation) as reported previously for murine full length PrP^{C} (Bocharova, Breydo et al. 2005, Graham, Kurian et al. 2011) and human full length PrP^{C} (Almstedt, Nystrom et al. 2009). PrP^{VRQ} had an average lag time of 5.57 hours (SEM +/- 0.40, n =16) while with PrP^{ARR} the lag time was significantly longer ($p \leq 0.002$), averaging 8.32 hours (SEM +/- 0.69, n = 16). Fibrillisation of $C1^{VRQ}$ (n = 24) and $C1^{ARQ}$ (n = 14) produced curves that were qualitatively similar to those of the full length variants, with shorter average lag times of 3.98 (SEM+/- 0.34) and 3.96 (SEM +/- 0.22) hours respectively (Figure 5.12E). Once maximum fluorescence was reached, ThT fluorescence curves tended to fall to around 60 % of the maximum (Figure 5.12D). This phenomenon of reducing fluorescence signal following fibril formation has previously been reported during the fibrillisation of human PrP^{90-231}. The reasons for it are yet to be fully explained, but Almstedt *et al.* suggested that aggregation of fibrils was the most likely cause, thereby reducing the outward facing regions available for ThT binding (Almstedt, Nystrom et al. 2009).

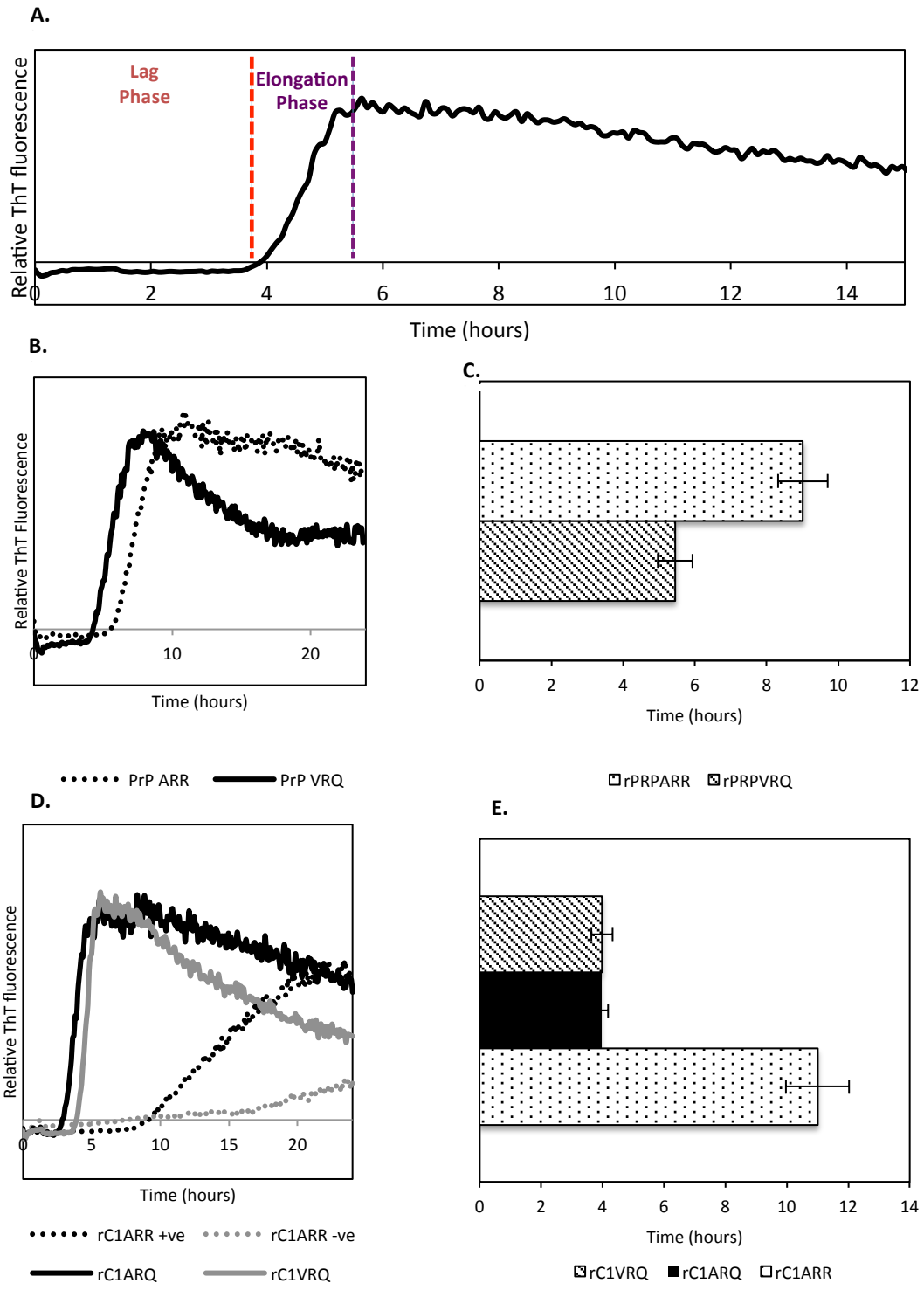

Figure 5.13 – Fibrilisation kinetics of PrP and C1 recombinant proteins. A) Expected curve representing fibril formation, with lag time or nucleation phase followed by elongation phase. B) Typical fibrillisation curves for PrP variants. Background ThT fluorescence from no PrP controls subtracted from raw data. C) Average lag time of fibrillisation for PrP variants in reactions which fibrillisation occurred within the time frame of the experiment. PrP^{ARR} n = 18, PrP^{VRQ} n = 20. D) Typical fibrillisation curves for C1 variants. E) Average lag time of fibrillisation for C1 variants in reactions which fibrillisation has occurred within the time frame of the experiment. $C1^{ARR}$ n = 12, $C1^{ARQ}$ n = 24, $C1^{VRQ}$ n = 24.

Compared to the other two C1 proteins, $C1^{ARR}$ (n = 24) showed a modified fibrillisation profile comprising a significantly longer lag time (taken as an average of all reactions in which fibrillisation had occurred within 24 hours, $p \leq 2.5 \times 10^{-6}$), on average 11.0 hours (SEM +/- 1.0) (Figure 5.14E) and a longer period of elongation after nucleation. Indeed, complete fibrillisation did not occur in 50 % of these reactions within the 24-hour time frame of the experiment; in these cases the lag times could not be calculated, since this calculation depends on maximal levels of ThT fluorescence being achieved. Figure 5.14D shows an example of two $C1^{ARR}$ reactions, one positive and one negative for complete fibrillisation.

It has been suggested that the maximum level of fluorescence is dependent on protein concentration (Biancalana and Koide 2010). However, Alvarez-Martinez et al (2011) show that structurally diverse amyloid can be formed with the same concentration of protein under the same conditions (Alvarez-Martinez, Fontes et al. 2011). This is thought to be a factor of differential initial conformational changes at the nucleation stage, which are then propagated during fibril formation. The resulting fibrils may appear to differ structurally and ability to bind ThT may vary, hence explaining the different ThT fibrillisation profiles. When protein from the two distinct pathways is seeded the characteristics seen in the unseeded reaction are mimicked (Alvarez-Martinez, Fontes et al. 2011). Similar discrepancies in maximum fluorescence between wells have been observed during this experiment. For example Figure 5.15 represents four repeat wells containing $C1^{VRQ}$, in which two wells reach a maximum relative fluorescence of double the other two wells. There is little variation between the lag time or the rate of elongation between wells.

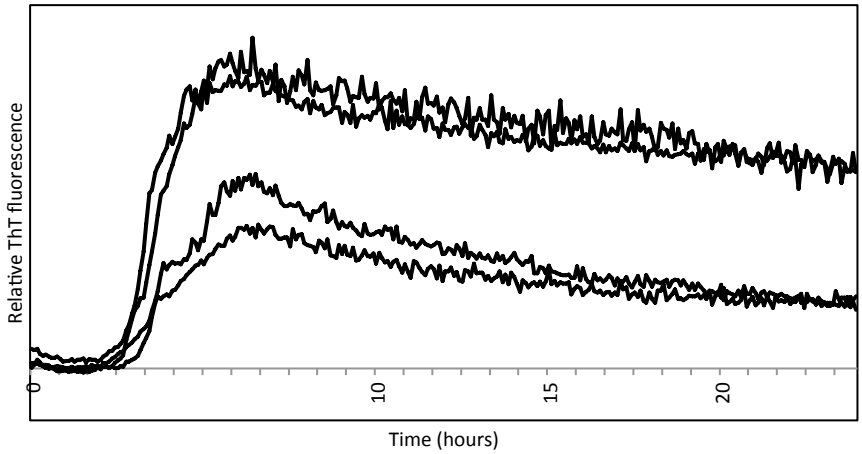

Figure 5.14 – Differential fibrillisation profiles under the same experimental conditions. Raw data of $C1^{VRQ}$ fibrillisation, showing ThT fluorescence obtained from four repeat wells. All four wells have similar lag times however maximal fluorescence readings show two patterns.

5.4.6 Characterisation of C1 amyloid fibrils

To confirm that C1 proteins were producing fibrils rather than non-fibrillar, ThT-binding aggregates an assay originally described by Bocharova *et al* (Bocharova, Makarava et al. 2006) know as the fibril maturation assay was performed. Fibrils composed of PrP have a PK resistant core of 10-12 kDa, but by heating PrP amyloid fibrils to 80 ˚C a structural change is initiated such that the PK-resistant core is extended to 16 kDa. Protease-resistant PrP can be detected by SDS-PAGE and silver staining (Figure 5.16). For the full length PrP samples, a well-defined 16 kDa band is evident after maturation along with the characteristic 12 and 10 kDa fragments, consistent with previously reported results (Bocharova, Makarava et al. 2006, Breydo, Makarava et al. 2008) and confirming the presence of fibrils. In C1 fibrillisation reactions, along with the three bands described above two additional PK-resistant fragments appeared after maturation, one of the similar size to the intact C1 protein (~16.6 kDa) and one of ~13 kDa. The 16 kDa band was less

intense in C1 fibril preparations compared to recombinant PrP preparations, suggesting that a reduced amount of fibrils may be produced in C1 fibrillisation reactions. To further characterise C1 amyloid fibrils, preparations were analysed by electron microscopy, as shown in Figure 5.17. Fibrils were observed in all preparations and there were no clear morphological differences between fibrils from different samples. It appeared that there were fewer fibrils in the $C1^{ARR}$ and $C1^{ARQ}$ preparations but using this technique it was not possible to accurately quantify the number of fibrils.

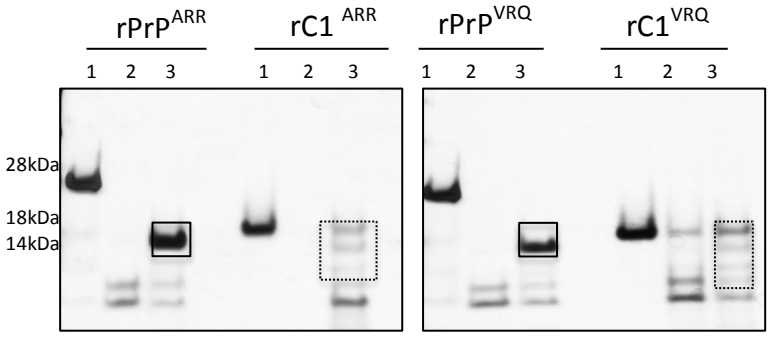

Figure 5.15 – Maturation and PK digestion of PrP and C1 fibrils. Maturation and PK digestion of fibrils were performed as described in section 5.3.14. 0.5 µg of recombinant protein was untreated (Lane 1), PK treated at a ratio 100:1 of PrP:PK (Lane 2), or matured by heating to 80°C followed by PK treatment (Lane 3). Matured fibrils (Lane 3) show increased PK resistance relative to non-matured fibrils. rPrP reactions show a 16 kDa band after maturation which confirms the presence of fibrils, highlighted by the black box. In rC1 preparations, bands with increased PK resistance of 16.6 kDa, 16 kDa and 13 kDa are present, highlighted by the dotted box.

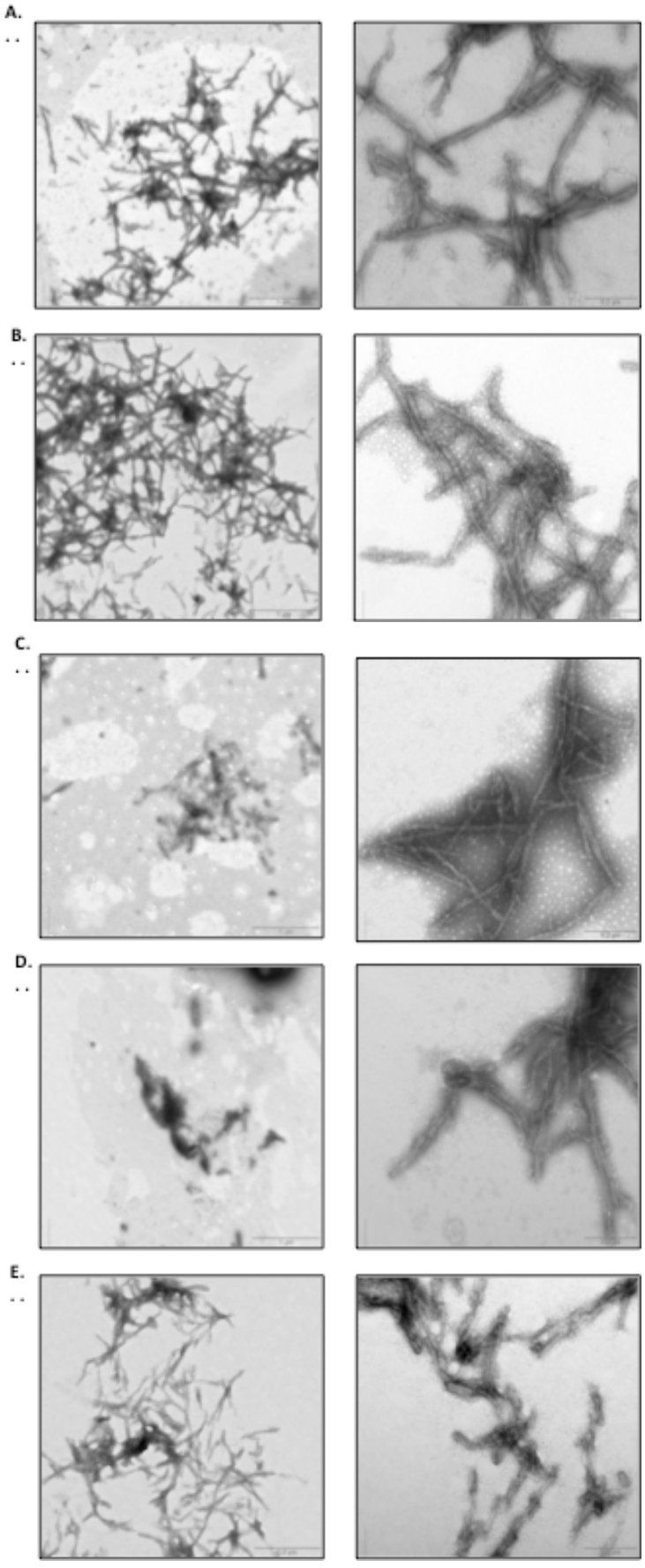

Figure 5.16 – Electron microscopy of PrP and C1 amyloid fibrils. Electron microscopy was performed as described in section 5.3.16. Fibrils were produced in the absence of ThT and dialysed into sodium acetate. Fibrils were viewed on a transmission electron microscope. Images were taken at x 5000 (right panel) and x 20000 (left panel). A: $rPrP^{ARR}$, B: $rPrP^{VRQ}$ C: $rC1^{ARR}$ D: $rC1^{ARQ}$, E: $rC1^{VRQ}$

To shed some light on both the numbers of fibrils present in these preparations and the smaller intermediates and/or aggregates dynamic light scattering (DLS) was used, as described in section 5.3.13. This technique measures the amount of light scattered from particles in a solution and predicts particle size and distribution using the theory of Brownian motion. C1 fibrils ~0.5mg/ml were compared either directly to full length PrP fibrils (Figure 5.18A) or preparations were centrifuged to remove the larger fibrils and aggregates to allow analysis of the smaller particles (Figure 5.18B). The size estimates are based in a globular protein model and therefore will not accurately represent fibril size. However, the predicted sizes allow for comparisons between fibril preparations. Figures 5.18A and B represent average traces taken from 5 separate repeats of 13 or more readings calculated by Zetasizer software.

The C1 fibril preparations appear to have less large sized aggregates when compared to PrP preparations represented by the lower percentage volume of protein species (Figure 5.18A). The size of the most prevalent protein aggregates in PrP and C1 preparations also vary, with C1 reactions forming aggregates equivalent to the largest of full length PrP. In $C1^{ARR}$ fibril preparations the dominant species were around 253.8 (SD ± 21.12), 374.6 (SD ± 46.50) and 602 (SD ± 72.27) d.nm and in $C1^{VRQ}$ preparations the dominant species are estimated at 422.2 (SD ± 40.77) and 611.7 (SD ± 56.77). In comparison, in PrP^{ARR} preparations the dominant species were 58.72 (SD ± 5.229), 115.3 (SD ± 19.60) and 480.27 (SD ± 125.1) d.nm and in full length PrP^{VRQ} reactions the dominant species were around 90.23 (SD ± 9.605) and 365.2 (SD ± 84.43).

A.

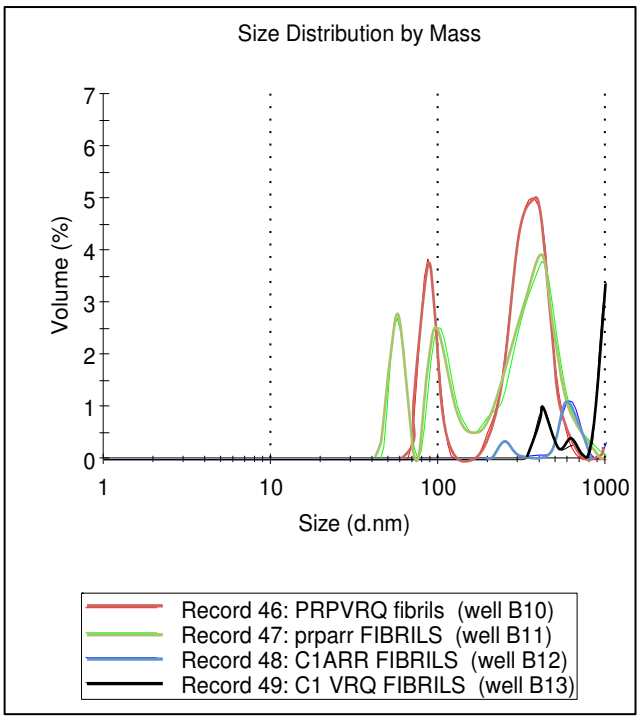

B.

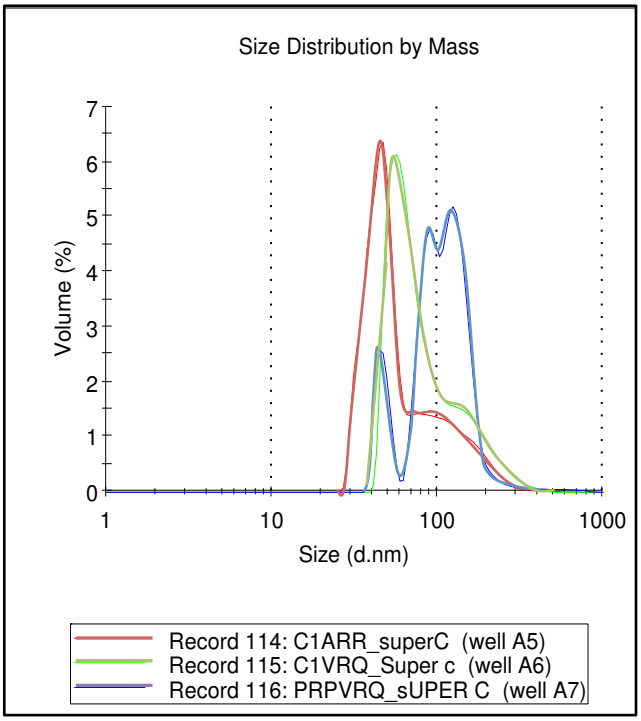

Figure 5.17 – Fibrils size distribution by mass using DLS. As described in section 5.3.15, C1 fibrils ~0.5mg/ml were compared either directly to full length PrP fibrils (Figure 5.16A) or preparations were centrifuged to remove the larger fibrils and aggregates to allow analysis of the smaller particles (Figure 5.16B) Figures 5.16A and B represent average traces taken from 5 separate repeats of 13 or more readings calculated by Zetasizer software.

When the larger aggregates were removed by centrifugation C1 preparations were found to be very similar to each other with $C1^{ARR}$ dominant species around 47.74 (SD ± 8.290) and 186.2 (SD ± 75.07) and $C1^{VRQ}$ around 62.86 (SD ± 9.278) 196.7 (SD ± 71.89) (Figure 5.18B and 5.19). Full length PrP^{VRQ} had a small amount of 48.18 (SD ± 4.688) and major species of 157.4 (SD ± 72.90) and 630 (SD ± 89.66). These readings indicate that C1 fibril preparations vary from full length PrP both in the sizes of large aggregates and smaller oligomers. This could be important in neuronal toxicity as it is still unknown which form of misfolded protein causes cell death during TSE disease.

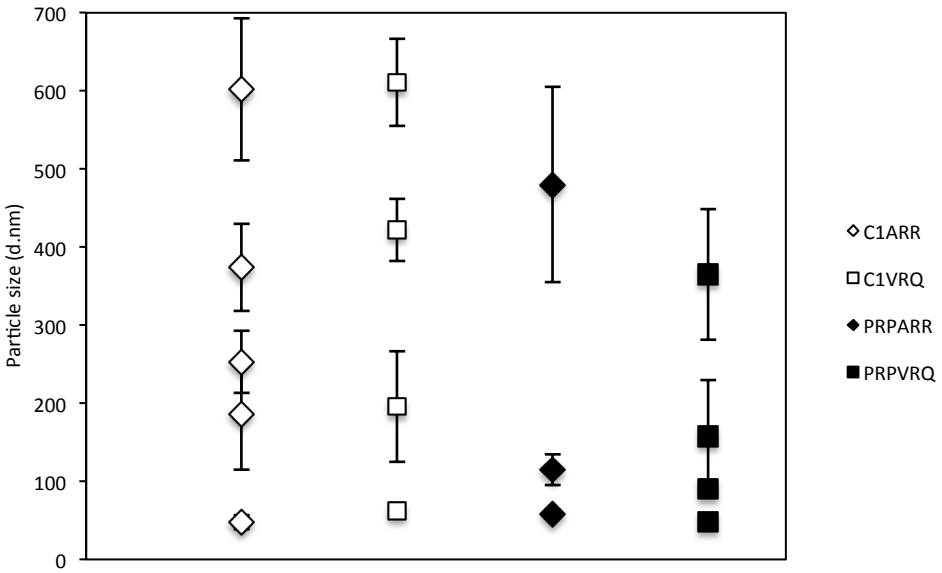

Figure 5.18 – Estimation and comparison of average particle size in fibril preparations. Fibrils were produced in the absence of ThT at ~0.5mg/ml and analysed by DLS using a Zetasizer APS as described in section 5.3.15. The size of dominant protein species were calculated from the average of five readings of multiple repeats. Error bars represent variations in size around each peak. This graph combines data from 5.18A and 5.18B.

5.4.7 Amyloid fibril formation of recombinant C2 protein

It was also assessed if recombinant C2 proteins could form amyloid fibrils. Although found at low levels in healthy animals and more common in ARQ and VRQ homozygotes compared to ARR homozygotes, as illustrated in section 4.4.3 (Chapter 4) the frequency of C2 is increased in infected brain tissue (section 4.4.11, Chapter 4). $C2^{ARR}$ and $C2^{VRQ}$ fibrillisation assays were set up in the presence of thioflavin T (ThT). Fibril formation kinetics were measured over a 24-hour period and lag times were calculated as described in Graham *et al.* (Graham, Agarwal et al. 2010). Fibrillisation experiments were repeated multiple times (n) and typical fibrillisation curves for C2 fragments are shown in Figure 5.18. $C2^{VRQ}$ produced curves similar to those of the full-length variants, $C1^{ARQ}$ and $C1^{VRQ}$ with an average lag time of 4.3 hours (SEM +/- 0.4). $C2^{ARR}$ reactions had a significantly longer average lag time of 9.1 hours (SEM +/- 1.6, p = 0.01) taken from only 7 repeat reactions as 80 % of reactions failed to fibrillise within the 24 hour time frame of the experiment. Fibrillisation curves of $C2^{ARR}$ tended to mirror those of $C1^{ARR}$ with slow elongation rates and low maximum fluorescence indicating that $C2^{ARR}$, like $C1^{ARR}$ has reduced potential to form amyloid fibrils *in-vitro.*

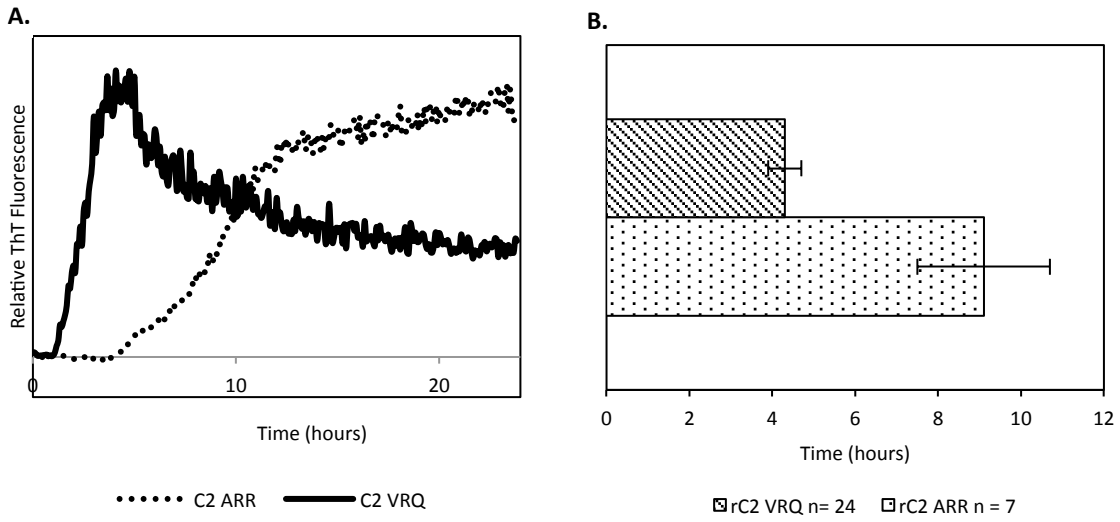

Figure 5.19 – Fibrillisation kinetics of C2 recombinant proteins. Fibrillisation was performed as described in section 5.3.13 A) Typical fibrillisation curves for PrP variants. Background ThT fluorescence from no PrP controls subtracted from raw data. B) Average lag time of fibrillisation for C2 variants

To confirm that C2 proteins were producing fibrils rather than non-fibrillar, ThT-binding aggregates, a fibril maturation assay was performed. Like full length PrP, recombinant C2 proteins display a 16 kDa band evident after maturation along with the characteristic 12 and 10 kDa fragments (Figure 5.21).

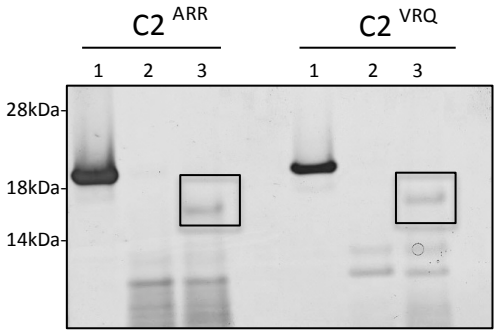

Figure 5.20 – Maturation and PK digestion of C2 fibrils. Maturation and PK digestion of fibrils were performed as described in section 5.3.14.. 0.5 μg of recombinant protein was untreated (Lane 1), PK treated at a ratio 100:1 of PrP: PK (Lane 2), or matured by heating to 80°C followed by PK treatment (Lane 3). Matured fibrils (Lane 3) show increased PK resistance relative to non-matured fibrils. Reactions show a 16 kDa band after maturation which confirms the presence of fibrils, highlighted by the black box.

5.4.8 Comparison of fibril formation kinetics between PrP and truncated cleavage fragments C1 and C2

All prior fibrillisation reactions were performed at a protein concentration of 100 μg/ml. To compare fibril formation kinetics between proteins of different molecular weights, reactions were set up at a single molar concentration of 4.4nM (equal to 100 μg/ml of full length recombinant PrP protein) ensuring the same numbers of protein particles were added into each reaction. Full length PrP reactions were as previously described in section 5.4.6 and Figure 5.14. For both $C1^{ARR}$ and $C2^{ARR}$ all reactions at 4.4nM (both, n = 4) failed to fibrillise within the time frame of the experiment, therefore lag times could not be calculated. The higher frequency of failed reactions compared to the prior experiment can

be explained by the reduction in molecules put in to the reaction. C1^{VRQ} at 4.4 nM had an average lag time of 2.11 hours (SEM ± 0.27) while for C2^{VRQ} the average lag time was slightly longer at 3.47 hours (SEM ± 0.27). Lag time of fibrillisation for PrP and truncated PrP representing the VRQ allele seems to positively correlate with molecular weight (Figure 5.21A). Reactions at lower protein concentration of C1^{VRQ} and C2^{VRQ} also have shorter lag times of fibrillisation than the equivalent more concentrated reactions (Figure 5.21B).

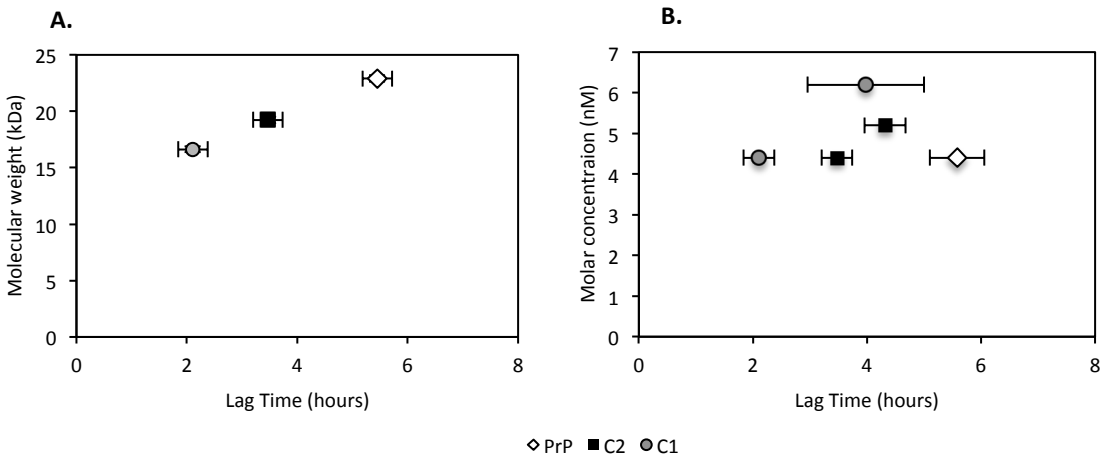

Figure 5.21 – Fibrilisation lag time and molar concentration. A) The relationship between average fibrillisation lag time and protein molecular weight for recombinant VRQ variants. B) The relationship between fibrillisation lag time and molar concentration of recombinant VRQ proteins.

5.5 DISCUSSION

5.5.1 Generation and characterisation of truncated PrP^{C} recombinant proteins

A number of *in vitro* studies investigating the molecular aspects of scrapie-associated polymorphisms in the *PRNP* gene have examined the initial binding of PrP^{C} to PrP^{Sc} prior to conversion (McCutcheon, Hunter et al. 2005, Rigter and Bossers 2005) and the relative convertibility of prion protein variants (Kirby, Goldmann et al. 2006, Eiden, Soto et al. 2011). Others have tried to explain disease resistance by allele-specific expression profiles (McCutcheon, Hunter et al. 2005, Rigter and Bossers 2005), different protein conformations or different characteristics of fibrillisation and thermal stability (Kirby, Agarwal et al. 2010). These studies have shown that alterations in the sequence of *PRNP* are pivotal in defining the ability of the PrP^{C} protein to convert. However, at this time there have been no *in vitro* models which have taken truncated PrP^{C} proteins into account albeit levels of C1 have been shown to be an important determinant of scrapie susceptibility in cell culture (Lewis, Hill et al. 2009). Moreover, we have shown that levels of C1 and C2 can be highly variable in ovine brain and can account for a large proportion of cellular PrP^{C} (sections 4.4.2 and 4.4.3).

It was felt that the production of recombinant proteins C1 and C2 and consequent fibrillisation would be the best method to directly determine if truncated PrP^{C} proteins C1 and C2 could be misfold and whether misfolding was associated with protein allotypes. Recombinant full length PrP^{C}, three variants of C1 (C1^{ARR}, C1^{ARQ}, C1^{VRQ}) and two variants of C2 (C2^{ARR} and C2^{VRQ}) were produced. In the case of C1 variants, mass spectrometry was performed which confirmed high purity but did highlight slight modifications in the His-tag which has been previously reported (Geoghegan, Dixon et al. 1999). These proteins

were primarily alpha-helical in secondary structure as indicated by CD. Interestingly, when estimates were compared between the $C1^{ARR}$ and $C2^{ARR}$ variants it was found that the C2 variants had more molecules of α-helical structure. The same was observed on comparison of VRQ variants. Both $C1^{VRQ}$ and $C2^{VRQ}$ had higher estimates of α-helix than the corresponding ARR variants. It is unknown if similar structural variations will be present *in vivo*. These findings are somewhat unexpected as during conversion α-helices undergo a structural shift into β-sheet, therefore it would be assumed that a protein with a higher propensity of β-sheet would more easily undergo conversion.

The isolation of mammalian expressed truncated protein from full length PrP^{C} would allow for the misfolding of these proteins to be investigated using *in vitro* as the majority of ovine C1 appears to be mono-or di-glycosylated, as indicated by the lack of substantial 17 kDa band in the absence of PNGase F by western blotting. Glycosylation of truncated $PrP^{175\text{-}195}$ fragment has been shown to alter the kinetics of fibrillisation reactions (Bosques and Imperiali 2003), indicating that glycosylation of C1 and C2 may be an important consideration for fibrillisation studies. Furthermore, complete separation of C1 from full length PrP^{C} protein in brain would allow for direct quantification of C1 levels by DELFIA, which has previously been performed for total PrP^{C} (Charmaine Love, Ph.D. Thesis, University of Edinburgh, 2010).

5.5.2 C1 and C2 recombinant proteins can form amyloid fibrils in vitro

The pure and refolded recombinant proteins were subjected to fibrillisation assays to determine if they had the potential to undergo structural misfolding and form amyloid fibrils under semi-denaturing conditions All variants tested had the ability to form amyloid fibrils, confirmed by the presence of mature PK resistant cores after fibrillisation

Full-length PrP variants and C2 variants had typical banding after maturation and PK digest in the form of 16 kDa, 12 kDa and 10 kDa bands, indicating that C2 forms the same PK resistant C-terminal core as full length PrP, encompassing amino acids 173-224 (murine numbering) (Tycko, Savtchenko et al. 2010). In contrast, recombinant C1 fibrils had additional bands of 16.6 kDa and 13 kDa. The presence of a 13 kDa band was also evident in maturation assays of human PrP^{90-231}, representative of the C2 fragment (Lu, Wintrode et al. 2007) and may indicate formation of disordered aggregates with increased PK resistance. The 16.6 kDa band could represent an increase in core expansion or a structural change, which alters available PK digestion sites. Whether this fragment is ovine sequence related or can also be found in recombinant C1 fibril preparations from other species remains to be established. The fibril associated 16 kDa band was fainter in all preparations of truncated PrP proteins indicating that less fibrils were being formed during these reactions compared to full-length proteins: an observation which fitted in with findings from both electron microscopy and DLS of recombinant C1 proteins. Further discrepancies in fibrillisation reactions were observed and hence, fibrillisation kinetics were investigated in detail to determine if there were allotype specific differences in fibril formation of PrP^{C} truncated proteins.

5.5.3 Amyloid fibril formation kinetics

ARR/ARR sheep are considered resistant to classical scrapie infection and do not accumulate PrP^{Sc}, although they can do so after BSE infection (Houston, Goldmann et al. 2003). *In vitro* PrP^{ARR} has the ability to form fibrils. However, longer lag times, representing the time taken for protein misfolding to commence, indicate that PrP^{ARR} has reduced potential to form amyloid fibrils compared to PrP^{VRQ} with a significantly longer lag time. $C1^{ARR}$ and $C2^{ARR}$ also had a significantly longer average lag time of fibrillisation.

However unlike full length PrP^{ARR} these variants also showed an extended or slowed elongation phase when compared to other allotypic forms of C1 and PrP^{C}. Often in reactions truncated ARR variants would fail to fibrillise fully within the time frame of the experiment indicating that these proteins have a reduced potential to form fibrils. Truncated ARR variants most likely take a different aggregation pathway to that of the other variants tested. Previous work looking at kinetic pathways of aggregation in course-grain peptide models have shown that small differences in sequence can lead to extremely different structural outcomes (Bellesia and Shea 2009). Similar polymorphism-dependent differences have been reported with *in vitro* conversion of recombinant human PrP^{90-231} (Apetri, Vanik et al. 2005, Baskakov, Disterer et al. 2005, Nystrom, Mishra et al. 2012). It appears that only in the absence of the N-terminal of PrP does the inhibitory effect associated with the presence of an arginine at position 171 become important in delaying fibril formation (Figure 5.28), while, polymorphisms at 136 appear to have no effect on fibrillisation of PrP. The primary binding site of PrP-to-PrP interaction is likely to be situated on the N-terminal of the protein and therefore we can hypotheses that when proteins bind via this site under specific conditions the structure is favorable to fibril formation. In the absence of this binding site, for example, in truncated C1 and C2 a secondary, lower affinity binding site must be adopted. If this site is in close proximity to amino acid 171, then polymorphisms at this position could be important in defining interaction and binding.

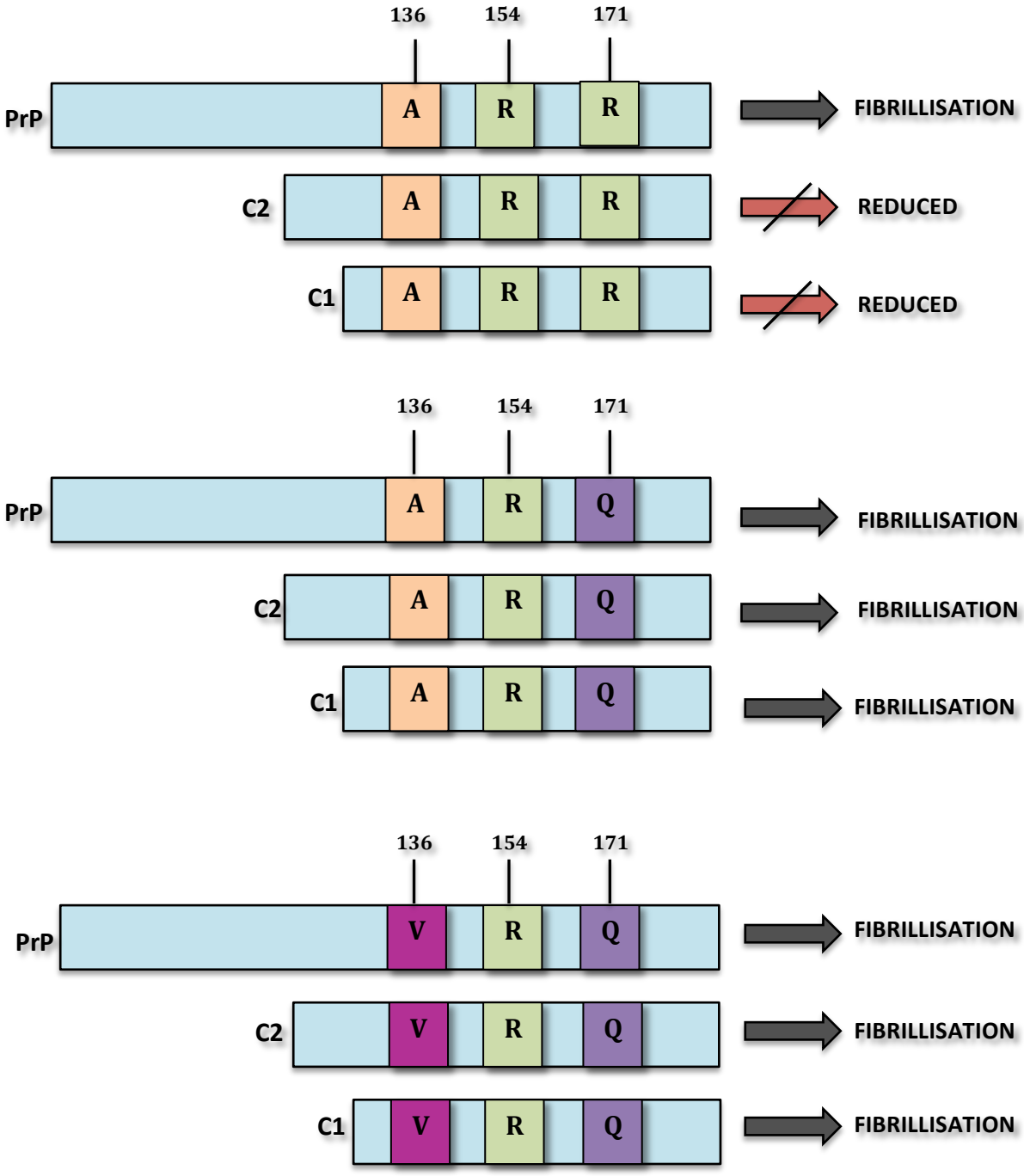

Figure 5.22 – Diagrammatic illustration of allele-dependent variation in ability to form amyloid fibrils *in-vitro*.

It has been previously suggested that lag time is a factor of concentration and that the more concentrated a protein the shorter the lag time, explained through proteins at higher density having more chance of intercepting each other in the correct susceptible conformation. To understand the effect of concentration on lag time, fibrillisation reactions were set up at two different molar concentrations. At lower concentrations to that originally tested (100 μg/ml) all ARR truncated variants failed to fibrillise within the time frame of the experiment. In contrast to ARR and against expectation, lowering the concentration of recombinant $C1^{VRQ}$ and $C2^{VRQ}$ proteins resulted in shorter lag times of fibrillisation. Furthermore, it was observed that lag times of PrP and truncated PrP proteins representing the VRQ allele appeared to positively correlate with protein molecular weight, indicating that the shorter the PrP^{VRQ} fragment the faster it was misfolded. This may directly reflect the α-helical content of these proteins, as calculated by CD, of which $C2^{VRQ}$ was found to have a higher proportion of helically folded protein in comparison to C1. We can hypotheses that the longer lag time of fibrillisation associated with C2 may reflect the time taken for a more helically folded protein to fully adopt a beta-sheet formation, compared to a protein with less alpha helix (C1). However, the direct reasons for this remain to be established.

5.5.5 Fibrillisation as a tool to unravel molecular mechanisms of PrP conversion

The formation of amyloid fibrils *in vitro* has been important in shedding light on the early stages of conversion at a molecular level. Fibrils formed using these assays have, like PrP^{Sc}, have increased resistance to PK and produce characteristic truncated species and PK cleavage patterns (Bocharova, Breydo et al. 2005, Sajnani, Pastrana et al. 2008). Perhaps, most importantly amyloid fibrils formed *in vitro* have been shown to generate disease (Legname, Baskakov et al. 2004). Although *in vitro* fibrils are likely to be formed by

different misfolding pathways and misfolded proteins are therefore structurally different to PrP^{Sc} formed *in vivo,* structural similarities must be sufficient to bind native PrP^{C} and induce misfolding. During this study fibrillisation was performed using recombinant PrP and truncated proteins. Considering the results with the various allotypes, it may be important to repeat these misfolding assays using purified mammalian PrP with its GPI-anchor and/or glycosylation intact. The purification and fibrillisation of full length PrP^{VRQ} from CHO cells proved to produce fibrillar structures morphologically different from that produced by recombinant protein, with similar properties to PrP^{Sc} isolated from brain (Stohr, Elfrink et al. 2011).

Fibrillisation assays, while able to produce fibrils with PrP^{Sc}-like properties, cannot account for cellular conditions such as PrP^{C} localisation in the cell or cellular co-factors for their importance in conversion. These assays are performed under semi-denaturing conditions to promote protein unfolding and with intense and continuous shaking these assays do not mimic physiological conditions, limiting their relevance *in vivo*. Furthermore, these assays measure the formation of amyloid alone and do not account for the formation of smaller oligomers and intermediates. These smaller aggregates may be PK sensitive, infective and could be responsible for prion associated cellular toxicity (Sanghera, Wall et al. 2008) - hypothesis supported by transgenic models with little or no PK resistant PrP^{Sc} but high titers of infectivity (Barron, Campbell et al. 2007, Piccardo, Manson et al. 2007). Despite these limitations, fibrillisation represents a useful assay to study the ability of proteins to misfold and can be used as an indicator of *in vivo* behavior.

5.5.6 Conclusions

In contrast to previous assumptions the work described in this chapter has shown that C1 and C2 proteins have the potential to form amyloid fibrils. It is unknown whether this is strictly an event occurring *in-vitro* or whether this can also occur in the brain during disease. Moreover, it is unknown how variation in the potential of these truncated proteins to misfold could effect the conversion and misfolding of full length PrP^{C}. To fully understand the role of these proteins in disease it is essential that these questions be answered. If these truncated proteins of TSE susceptible allotypes could also take part in conversion whereas, truncated ARR variants representing on average ~50 % of total PrP could not, this may be partially responsible for the resistance effect

CHAPTER 6

A ROLE FOR C1 IN TSE DISEASE?

6.1. INTRODUCTION

Recombinant ovine C1 can form amyloid fibrils *in-vitro,* but does not convert into PrP^{Sc} in scrapie challenged Tg mice expressing only C1 (Westergard, Turnbaugh et al. 2011). I have also presented data in chapter 5 showing that recombinant $C1^{ARR}$ has reduced potential to form amyloid fibrils compared to other C1 variants and full-length PrP^{C}. These findings leave many unanswered questions as to the role of C1 during scrapie disease but indicate that the C1 fragment may be an inhibitory modulator of conversion. In sheep, this control is likely to be associated with *PRNP* genotype. Inclusion of recombinant C1 proteins into well-characterised *in vitro* fibrillisation assays may shed some light on this possible inhibitory effect. If C1 can delay or inhibit conversion of PrP^{C} to PrP^{Sc} it may be a possible therapeutic target in the treatment of prion disease either by exogenous application C1 at the site of infection or by increasing the levels of α-cleavage through manipulating of the yet unknown PrP secreatase.

6.2 AIMS AND OBJECTIVES

Previous chapters presented data showing that animals of the ARR/ARR genotype have higher average levels of C1 protein compared to ARQ/ARQ and VRQ/VRQ and that all variants of recombinant C1 tested can form amyloid fibrils in vitro, although $C1^{ARR}$ appears to have a reduced potential to do so. This chapter aimed to investigate the role C1 may play in the conversion of PrP^{C} to PrP^{Sc} using *in vitro* fibrillisation assays and to assess the potential protective effects of C1 in a cell culture model of infection.

6.3 MATERIALS AND METHODS

6.3.1 Mixed fibrillisation assays

Fibrillisation assays were performed as described in section 5.3.13 with two recombinant proteins. For 1: 1 (w/w) PrP: C1 reactions each protein was at a final concentration of 50 µg/ml. For reactions at 4: 1 (w/w) PrP: C1 recombinant protein were at a final concentration of 80 µg/ml and 20 µg/ml.

6.3.2 Addition of fibrils to cell culture

Growth media (Table 2.6) was aspirated from N2a or SMB cells 24 hours after plating. Recombinant protein fibrils, produced as described in section 5.4.6 in sodium acetate (10mM, pH 5.5) were added to cells at a concentration of 1, 2 or 5µM (20µl volume) in 80µl of cell specific growth media along with sodium acetate (10mM, pH 5.5) only and α-helical recombinant protein before fibrillisation (at 1,2, or 5 µM). Plates were incubated at 37°C, 0.5% CO_2 for 24-72 hours.

6.3.3 Live/Dead cell assay

To measure the cell toxicity associated with addition of fibrils to cells in culture fibril suspension was aspirated and the cells were then washed twice in HBSS (Hanks Balanced Salt Solution). Hoechst 33342 (Thermo Scientific) and Sytox orange (Molecular Probes) were diluted in H_2O at a final concentration of 4 µg/ml and 3 µM, respectively. Then 100 µl was applied per well and incubated for 15 minutes at room temperature. The stain was aspirated from the cells and replaced with 500 µl of HBSS. Plates were viewed on Zeiss Live Cell Observer at x10 and two images taken at random in grey scale for each well. Live and dead cells were counted using image J and results were exported to Microsoft Excel

for analysis. Cell viability was calculated as the percentage of live cells in the total cell count.

6.3.4 Isolation of scrapie associated fibrils (SAF)

Natural scrapie infected sheep brain (1.5g) was manually homogenised in 15ml brain lysis buffer (365 mM N-Sarkosyl, 0.85mM Trisodium phosphate, pH 7) with protease inhibitors PMSF (1.3 µM) and NEM (1.3 µM). The homogenate was clarified by centrifugation at 13,500rpm at 10 °C for 30 minutes (R5B Ultra Centrifuge) and pellets discarded. The supernatant was transferred to 70Ti glass tubes and centrifuged at 46000rpm at 10 °C for 2.5 hours and the pellet stored over night at 4 °C. The pellet was resuspended in ddH_2O (6ml/pellet) and incubated at 37 °C with shaking for 30 minutes. An equal volume of 15 % Iodine HSB (0.9 mM Potassium iodide, 6 µM Sodium Thiosulfate Pentahydrate) was added and the suspension was further incubated for 45 minutes. Per pellet 6ml of 10 % Iodine HSB (0.6 mM Potassium iodide, 6 µM Sodium Thiosulfate Pentahydrate) was added and the mixture was over-laid on a 20 % sucrose bed (w/v in 10 % IHSB). Tubes were centrifuged at 40000rpm at 10 °C for 1.5 hours and the supernatant removed. The pellet was washed with ddH_2O, further centrifuged at 50000rpm 10 °C for 1 hour and stored at 4°C.

6.3.5 Determining SAF concentration

SAF pellets were resuspended in ddH_2O. PK was added to a small sample at a final concentration of 60 µg/ml and incubated at 37 °C for 1 hour. To stop the PK reaction Pefabloc (Sigma) was added at a final concentration of 25mM. Several dilutions of PK treated SAF were loaded onto an SDS-PAGE gel along with dilutions of recombinant PrP^{VRQ} (100-5 ng) in sample buffer (Invitrogen) with reducing agent (Invitrogen) and western

blotted as described in section 2.3.1. To detect PrP^{Sc} monoclonal antibody P4 (Biopharm Rhone Ltd) was used at a concentration of 0.2 µg/ml in 0.5 % blocking reagent (Roche) and incubated for 1 hour. Densitometry was performed as described in section 2.3.4 using Kodak MI software and PrP^{Sc} concentration was calculated from a recombinant protein standard curve.

6.3.6 Preparation of sterile SSPB/1 positive brain homogenate

All steps were performed in a biological safety cabinet. Sterile brain tissue from a SSBP/1 infected VRQ/VRQ sheep was defrosted and immediately mechanically homogenised (M protein program, gentle MACs disassociator, Miltenyl Biotec)) in Opti-MEM media (Invitrogen) to make a 10 % (w/v) homogenate and stored at -20 °C. Homogenate was diluted to 2.5 % (v/v) in Rov9 cell growth media (pre-warmed to 37 °C, Table 2.6) prior to application.

6.3.7 Testing sterility of brain homogenate

To ensure brain homogenate were sterile and hence suitable for cell culture, 100µl of undiluted homogenate and dilutions at of 10^{-1}, 10^{-2}, 10^{-3}, 10^{-4} and 10^{-5} in Opti-MEM media (Invitrogen) were plated on both LB agar (Roslin Institute central services) and chocolate agar plates (E and O Laboratories). Plates were incubated at 37 °C for ~ 48 hours and monitored for growth.

6.3.8 Scrapie infection of Rov9 cells

Rov9 cells were cultured as described in Table 2.6, in a 12 well plate format. Growth media was aspirated and replaced with 500 µl of 2.5 % SSPB/1 positive homogenate (section 6.3.6) or for negative control wells growth media alone and incubated at 37 °C for

2 hours, after which a further 500 µl of growth media was added. After 48 hours the homogenate was aspirated from the cells and replaced with normal growth media. Recombinant $C1^{ARR}$ (5µg/well) was added into the growth media at 24 hours prior to infection, pre-mixed with the homogenate at time of infection or 24 hours post infection. The wells in which $C1^{ARR}$ was added 24 hours post infection were given further doses of $C1^{ARR}$ after splitting and re-plating at day 2, 5, and 11.

6.3.9 Lysis of infected cell lysate

All steps were performed in a biological safety cabinet. Wells were washed with cold HBSS and 500 µl of lysis buffer (5 % NP-40 (v/v), 12.1 mM Sodium deoxycholate in PBS with protease inhibitors 10 µM PMSF, 10 µM NEM) was added per well of a 12 well plate. The cells were scraped from the surface. The suspension was syringed repeatedly to promote cell lysis. Suspension was clarified by centrifugation at 500rpm for 3 minutes and the supernatant collected, flash frozen in liquid nitrogen and stored at -20˚C.

6.3.10 PK digestion of infected cell lysate

Cell lysate (30 µg total protein, as measured by BCA assay) in an equal volume of lysis buffer was treated with PK (50 µg/ml) and incubated at 37 °C with shaking for 1.5 hours. To stop PK reaction Pefabloc was added at a final concentration of 25mM. To precipitate the protein, 5 x volume of ice-cold acetone was added to precipitate the protein and incubated at -20 °C for at least 1 hour. Protein was pelleted before use by centrifugation at 13000rpm, 4 °C and air-dried. For western blotting the pellet was resuspended in equal volumes of sample buffer and dH_2O with reducing agent and denatured at 80 °C for 10 minutes.

6.3.11 Dot blotting for detection of PrP^{Sc}

PVDF membrane was wetted in methanol, H_2O and soaked in TBS for 15 minutes. The dot blotting apparatus (Biorad) was set up to the manufacturers instructions with pre-wet PVDF membrane. TBS was applied to all wells and vacuum pumped through the membrane. The membrane was re-wet with TBS and 2.5µg of cell lysate was applied per well diluted in 100µl TBS or in wells with no sample a 100µl of TBS alone was added. The sample was allowed to drip through the membrane by gravity flow and was replaced by two further washes with TBS. The membrane was removed from the apparatus, washed in TBS for 5 minutes and blocked using 0.1 % (v/v) blocking solution (Roche) for 1 hour at room temperature with agitation followed by incubation with anti-PrP antibody P4 at a final concentration of 0.2µg/ml diluted in 0.5 % (v/v) blocking solution under the same conditions. Membranes were washed with TBST (0.1 % Tween 20 in TBS) followed by 0.5 % (v/v) blocking solution. The membranes were incubated in horseradish-peroxidase-conjugated rabbit anti-mouse antibody (Stratech, UK) diluted at 1:10000 in 0.5 % (v/v) block for 75 minutes. The membranes were washed in TBST and proteins were visualized using activated chemiluminescence (SuperSignal West Dura Extended Duration Substrate, Thermo Scientific) and Chemiluminescent Detection Film (Lumi-Film, Roche).

6.4 RESULTS

6.4.1 Characterisation of PrP^C in SMB-PS and N2a cell lines

SMB (Scrapie Mouse Brain) cells were originally isolated as primary culture from the brains of scrapie infected mice and can sufficiently maintain infection in culture (Clarke and Haig 1970). The cell line used in this thesis has been cured of scrapie infection by treatment with pentosan polysulphate (subsequently named SMB-PS) and can be re-infected (Birkett, Hennion et al. 2001), indicating this could be an excellent model to investigate processing prior to and post infection. The morphology of SMB-PS cells were first examined by ICC, stained with Haematoxylin and Eosin (Figure 6.1A). At higher densities a large percentage of the cells appeared to have flat wide cell bodies, however at lower densities more neuronal morphology can be seen with extending neurites. These cells were stained with neuronal specific marker MAP-2 (Figure 6.1B). Reactivity is varied with some cells expressing high levels of microtubule associated protein, while in others staining is limited, confirming this may be a mixed population.

PrP^C expression was investigated by both western blotting and ICC and is shown in Figure 6.2. The most prevalent form of PrP^C in these SMB-PS cells is di-glycosylated. On removal of N-glycans with PNGase F the C1 fragment becomes visible indicating that PrP^C undergoes α-cleavage in these cells, representing 20-30 % of total PrP^C protein, similar to mouse brain tissue.

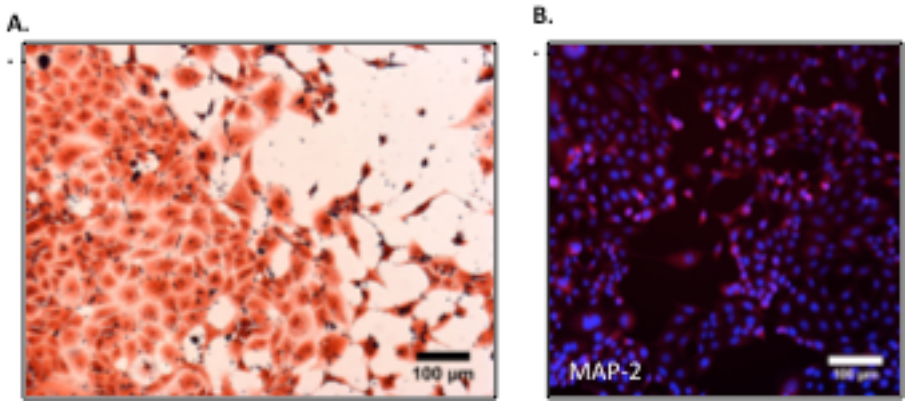

Figure 6.1 – SMB cell morphology. A) SMB cells cultured on glass slides at day 5 after plating, fixed and stained with Haematoxylin and Eosin. Image was taken on a Nikon 800E. B) SMB cells days 6 after plating on glass slides were stained with MAP-2 neuronal marker (1:200) with secondary alexa fluor 568 anti-mouse and DAPI (1:10000). Images were taken on Nikon EC1 inverted confocal microscope at x20.

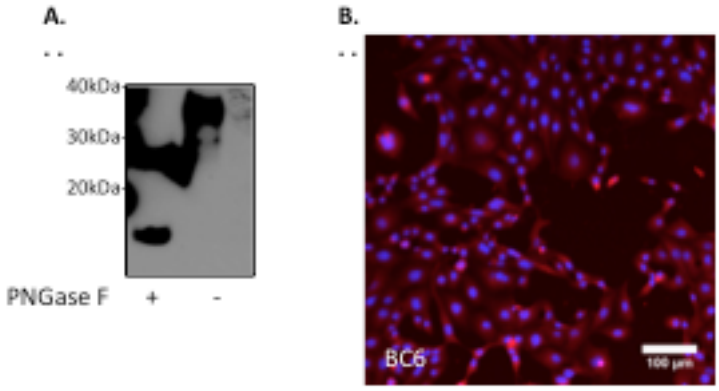

Figure 6.2 – PrP Expression in SMB-PS cell line. A) Cells were lysed, treated with or without PNGase F and subjected to western blotting with BC6 antibody. B) SMB cells days 6 after plating on glass slides were stained with BC6 (1:200) with secondary alexaflour 568 anti-mouse and DAPI (1:10000). Image was taken on Nikon EC1 inverted confocal microscope at x20.

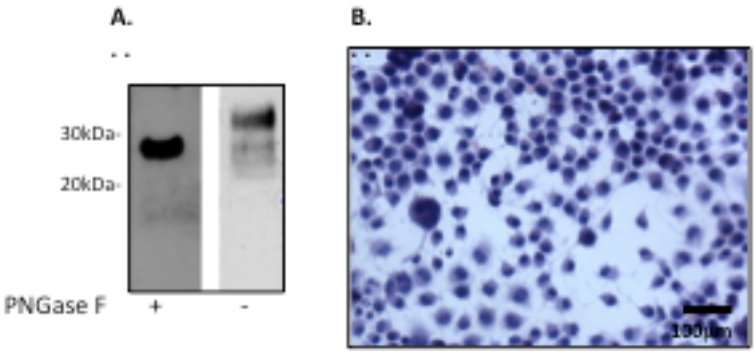

Figure 6.3 – Morphology of and PrP expression in N2a cell line. A) Cells were lysed, treated with or without PNGase F and blotted with BC6 antibody. B) N2a cells days 3 after plating on glass slides were stained Haematoxylin and Eosin. Image was taken on Nikon 800E.

N2a cells are a neuroblastoma cell line isolated from murine neuronal crest, which are frequently, used in general neurobiology research and in the TSE field as they differentiate into cells with neuronal-like morphology and can be infected with prions. The morphology of N2a cells was examined by ICC, stained with Haemolysin and Eosin, showing flattened cell bodies and long extensions (Figure 6.3B). As PrP^C expression has been shown to be essential for PrP fibril toxicity (Novitskaya, Bocharova et al. 2006) and N2a cell lines can have variable levels of PrP^C expression (Tagliavini, Prelli et al. 1992) PrP^C expression and α-cleavage was tested by western blotting of cell lysate with BC6 antibody (Figure 6.3A). This showed that the most prevalent band of PrP^C is di-glycosylated, as expected. After PNGase F digest C1 is present but only as a very faint band, indicating α-cleavage may be much lower in the N2a cell line compared to the SMB cell line.

6.4.2 Toxicity of C1 fibrils in cell culture

It has been shown that fibrils made up of full length PrP^C are toxic to neuronal cells in culture (Novitskaya, Bocharova et al. 2006) and we have established (Chapter 5) that all three variants of ovine C1 have the potential to form amyloid fibrils *in-vitro*. Although it in unknown whether C1 fibril formation occurs *in vivo*, any additional misfolding during disease could potentially add to neurodegeneration and toxicity. For this reason, C1 fibril preparations were tested for potential toxicity to two cells lines, SMB-PS and N2a. Both cell lines were selected as they both express PrP^C but showed different residual levels of α-cleavage (Figures 6.2 and 6.3). Along with recombinant C1 fibril preparations full length PrP^C fibril preparations were included as positive controls against which C1 fibril toxicity would be compared and α-helical recombinant C1 or buffer only were added as negative controls.

Examples of live/dead staining with Hoechst 33342 and Sytox orange of SMB-PS cells treated with a 2μM concentration of fibrils or α-helical C1 are shown in Figure 6.4. Recombinant protein concentrations of 1 μM, 2 μM and 5 μM were tested with incubations of 24 hours, 48 hours and 72 hours. Cell viability was calculated as a percentage of buffer only control wells and average values for each are summarised in Figure 6.5, 6.6 and Table 6.1.

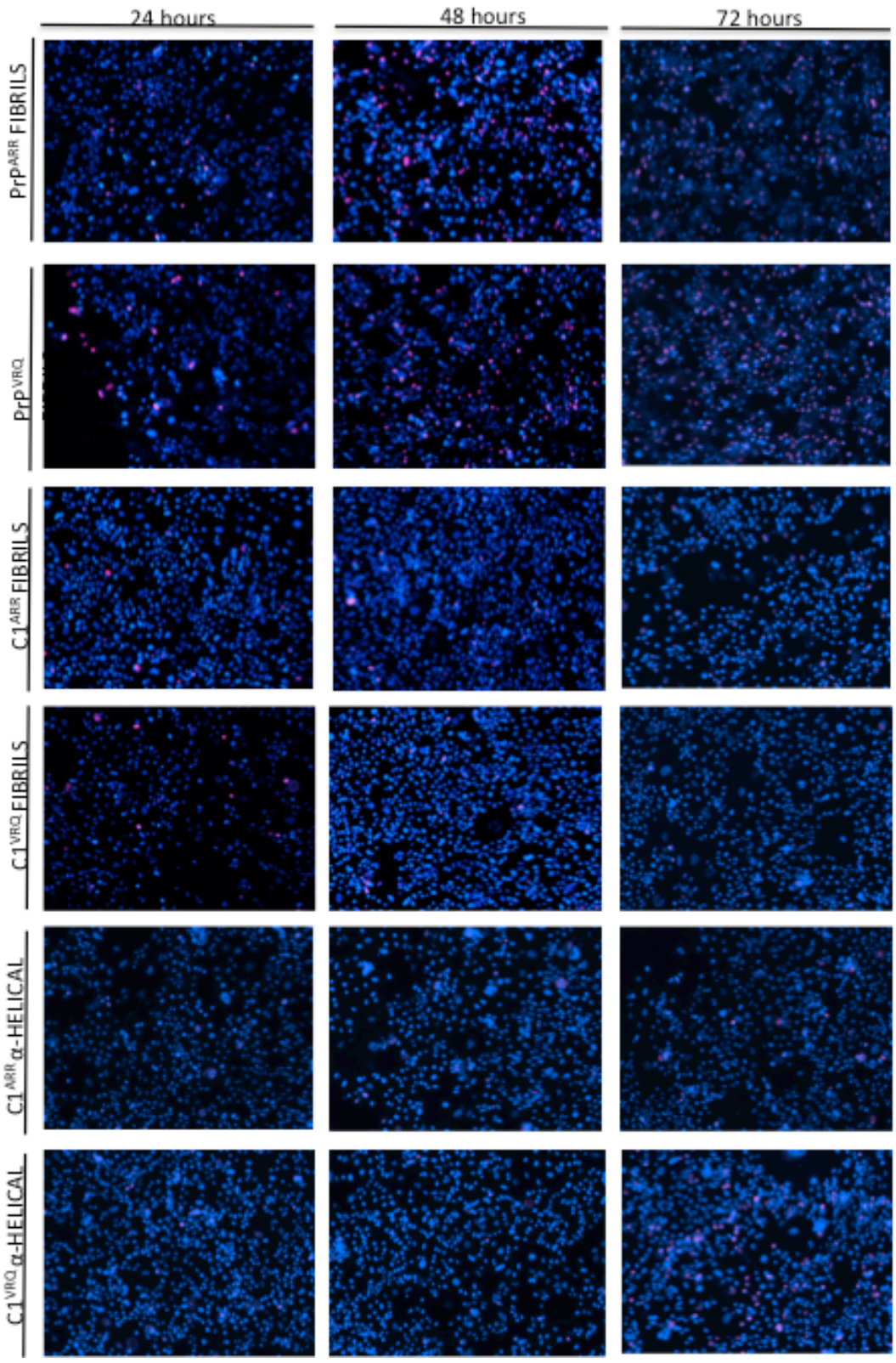
24 hours
48 hours
72 hours
PrP^ARR FIBRILS
PrP^VRQ
C1^ARR FIBRILS
C1^VRQ FIBRILS
C1^ARR α-HELICAL
C1^VRQ α-HELICAL

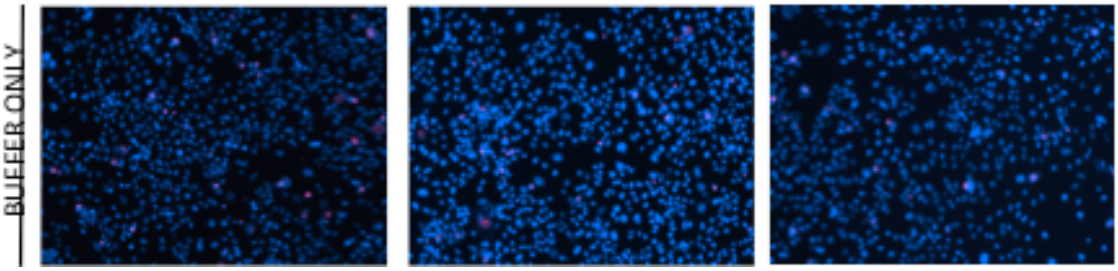

Figure 6.4 – Fibril toxicity in SMB cell line by live/dead staining. Fibrils or α-helical recombinant protein was added to SMB cells in culture at 2μM concentration along with buffer only controls. After incubations of 24-72 hours live cells were stained with Hoechst 33342 (blue) and dead cells were stained with Sytox orange (red). Images were taken on Zeiss live cell observer x10.

At 24 hours incubation at 1 μM or 2 μM neither full length PrP fibril preparations nor C1 fibril preparations had any significant effect on cell viability compared to buffer only controls. At 5 μM concentration of full length PrP fibril preparation cell viability decreased significantly compared to 1 μM and 2 μM concentrations (both $p \leq 0.03$). No such concentration dependent toxicity was seen with C1 fibril preparations or α-helical $C1^{ARR}$. However, decreased cell viability on addition of α-helical $C1^{VRQ}$ was positively correlated with concentration ($p \leq 0.0004$), suggesting that there may be allotype specific toxicity of α-helical C1. To assess if incubation time had an effect on toxicity the 2 μM concentration was selected. Full length PrP fibril preparations appear to have increasing toxicity with increasing incubation time. In the case of PrP^{ARR} cell viability at 72 hours is significantly lower than at 24 hours and 48 hours ($p \leq 0.007$ and $p \leq 0.05$, respectively). On addition of PrP^{VRQ} cell viability at 72 and 48 hours was significantly lower than at 24 hours ($p \leq 0.02$ and $p \leq 0.001$, respectively). Average cell viability on addition of recombinant C1 fibril preparations showed no significant difference at any time points tested. There was also no significant difference between cell viability on incubation of α-helical C1 variants at any of the time points tested.

Variant	Concentration	Incubation Time	Repeat Wells	Average Cell Viability	SEM
PrP ARR FIBRILS	1μM	24	3	98.2	0.03
	2μM	24	11	96.1	2.69
	2μM	48	11	90	2.45
	2μM	72	4	81.8	3.38
	5μM	24	3	89.6	1.7
PrP VRQ FIBRILS	1μM	24	2	98.7	0.5
	2μM	24	11	98.6	2.4
	2μM	48	12	88.02	1.72
	2μM	72	7	80.4	6
	5μM	24	2	82.7	2.85
C1 ARR FIBRILS	1μM	24	3	97.6	1.51
	2μM	24	11	100.3	1.28
	2μM	48	11	95.5	1.73
	2μM	72	4	93.5	5.74
	5μM	24	3	97.7	1.63
C1 VRQ FIBRILS	1μM	24	2	97.6	0.95
	2μM	24	11	99.4	1.84
	2μM	48	12	96.6	1.1
	2μM	72	7	94.9	6.33
	5μM	24	3	96.5	3.17
α C1 ARR	1μM	24	2	100.2	0.1
	2μM	24	12	97.2	2.6
	2μM	48	12	96.1	1.28
	2μM	72	5	100.8	2.73
	5μM	24	3	101.7	1.08
α C1 VRQ	1μM	24	3	99.4	0.26
	2μM	24	10	93	3.06
	2μM	48	11	94.5	1.73
	2μM	72	6	100.6	3.02
	5μM	24	3	77.4	1.13

Table 6.1 – Cell viability of SMB cells with addition of PrP, C1 fibrils and recombinant α-helical C1 proteins.

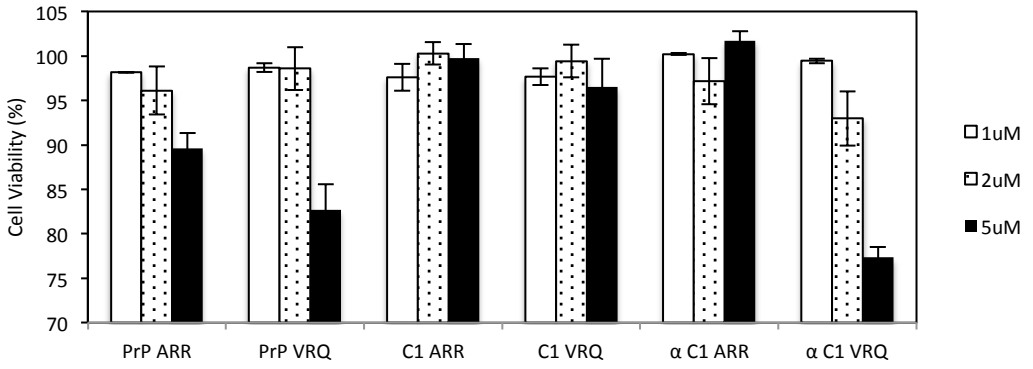

Figure 6.5 –The effect of fibril concentration on toxicity to SMB-PS cell line. Graph summarising cell viability for concentrations of fibrils/recombinant protein of 1 µM, 2 µM and 5µM incubated for 24 hours. Cell viability was calculated as a percentage of average cell viability of buffer only control wells.

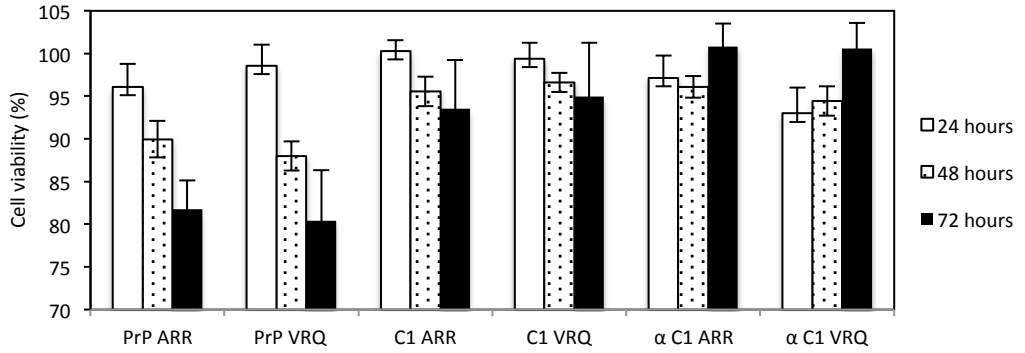

Figure 6.6 – The effect of incubation time on fibril toxicity to SMB-PS cell line. Graph summarising cell viability for fibrils/recombinant protein 2µM incubated for 24, 48 or 72 hours. Cell viability was calculated as a percentage of average cell viability of buffer only control wells.

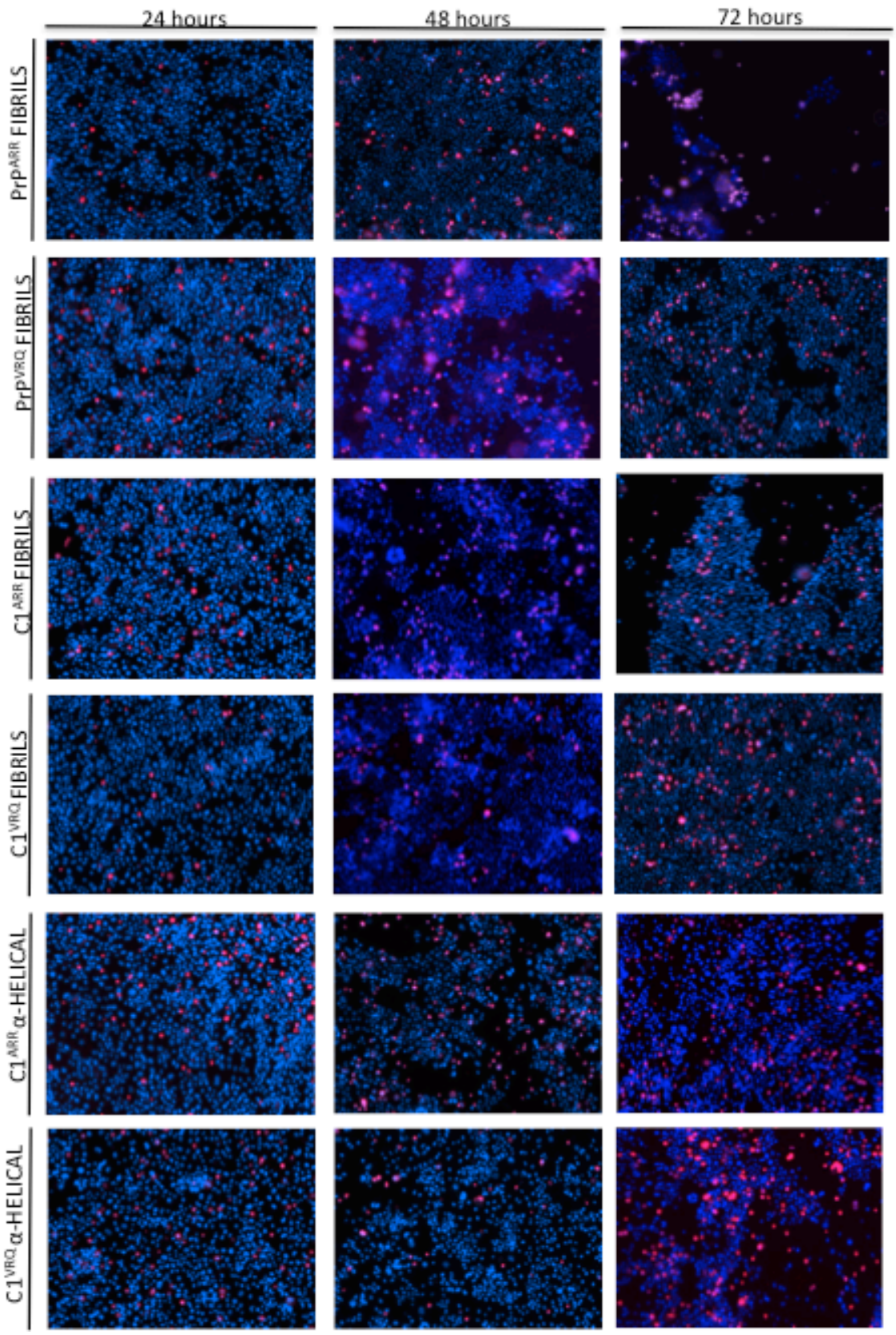
24 hours
48 hours
72 hours
PrP^ARR FIBRILS
PrP^VRQ FIBRILS
C1^ARR FIBRILS
C1^VRQ FIBRILS
C1^ARR α-HELICAL
C1^VRQ α-HELICAL

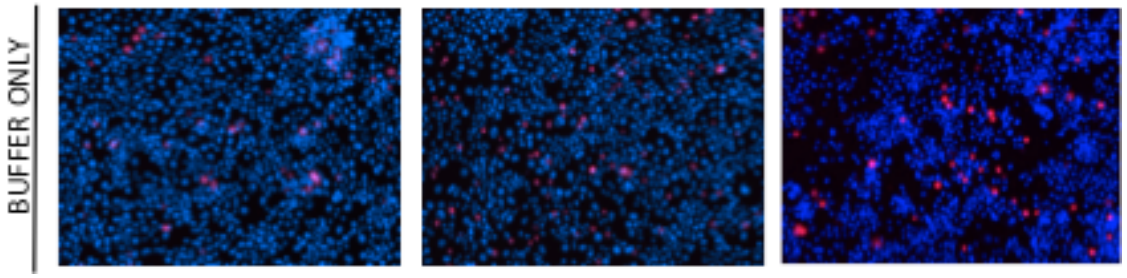

Figure 6.7 – Fibril toxicity in N2a cell line by live/dead staining. Fibrils or α-helical recombinant protein was added to N2a cells in culture at 2μM concentration along with buffer only controls. After incubations of 24-72 hours live cells were stained with Hoechst 33342 (blue) and dead cells were stained with Sytox orange (red). Images were taken at random on Zeiss live cell observer x10.

Examples of live/dead staining of N2a cells treated with 2 μM concentration of fibrils or α-helical protein are shown in Figure 6.7. In the case of N2a cells buffer only controls showed higher cell death in comparison to assays in SMB-PS cells. Recombinant protein concentrations of 1 μM and 2 μM were tested along with incubations of 24 hours, 48 hours and 72 hours. Cell viability was calculated as a percentage of buffer only controls, represented as 100 % and average values for each are summarised in Figure 6.8 and Table 6.2. There was no significant difference between cell viability when fibrils or α-helical proteins were added at a concentration of 1 μM or 2 μM at any of the time points tested, indicating this difference in concentration is not sufficient to alter toxicity to N2a cells. At 24 hours incubation full length PrP fibril preparations, C1 fibril preparations and α-helical protein controls show no alteration in cell viability. At 48 hours again, there is no reduction in cell viability associated with addition of full length PrP or C1 fibril preparations. At 72 hours all variants of fibrils and α-helical proteins cause substantial reduction in cell viability compared to wells treated with buffer only.

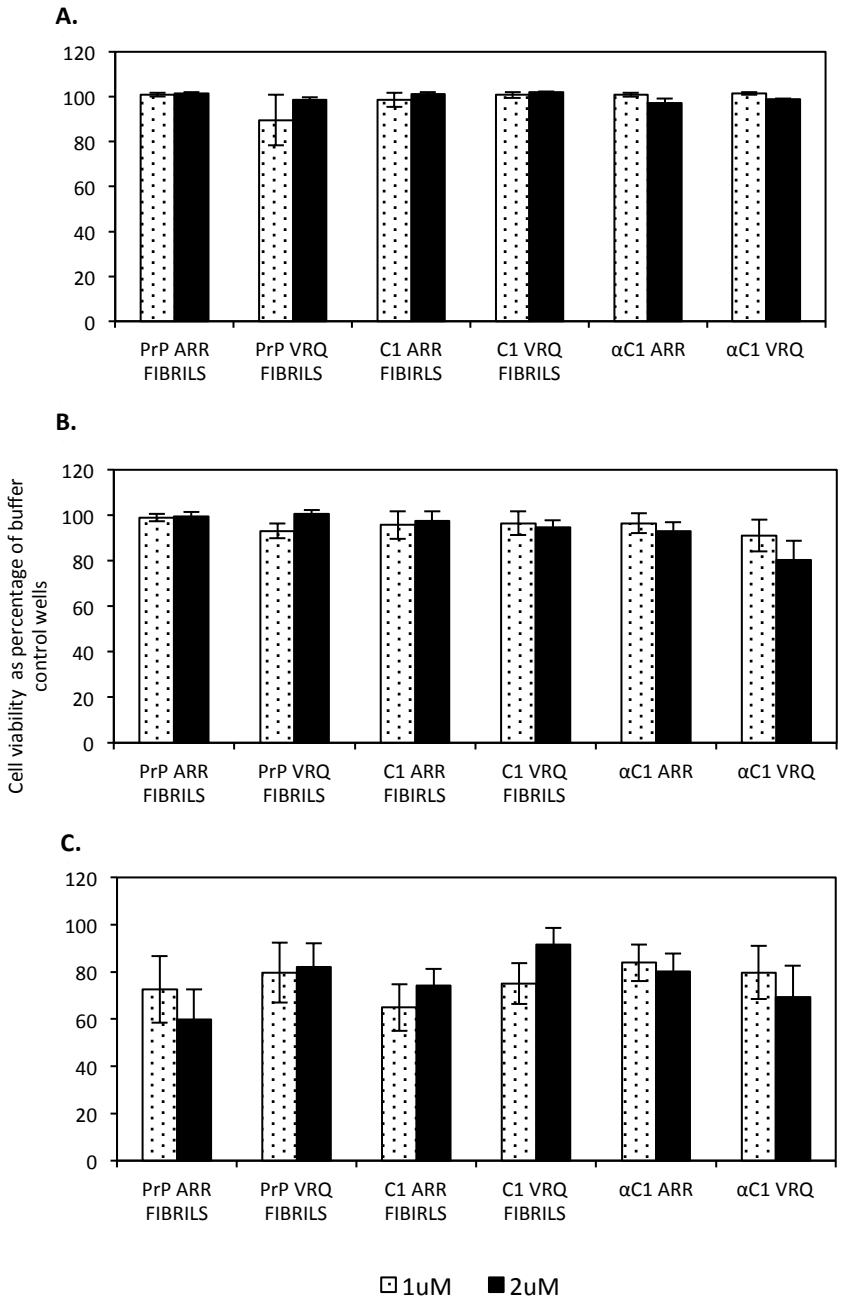

Figure 6.8 – Cell Viability of N2a cells on addition of PrP fibrils. Graphs summarising cell viability for concentrations of fibrils/recombinant protein of 1 µM, and 2 µM. Cell viability was calculated as a percentage of average cell viability of buffer only control wells, represented as 100 %. A) After 24 hour incubation. B) After 48 hour incubation. C) After 72 hours incubation.

Variant	Concentration	Incubation Time	Repeats	Average Cell Viability	SEM
PrP ARR FIBRILS	1µM	24	9	101	0.88
	1µM	48	9	98.9	1.56
	1µM	72	6	72.6	14.15
	2µM	24	9	101.4	0.65
	2µM	48	9	99.6	1.79
	2µM	72	6	59.9	12.68
PrP VRQ FIBRILS	1µM	24	8	89.6	11.33
	1µM	48	9	93.2	3.25
	1µM	72	6	79.8	12.76
	2µM	24	9	98.6	1.23
	2µM	48	9	100.5	1.85
	2µM	72	6	82.1	10
C1 ARR FIBRILS	1µM	24	6	98.6	3.23
	1µM	48	9	95.7	6.13
	1µM	72	6	64.9	9.87
	2µM	24	6	101.3	0.82
	2µM	48	8	97.5	4.22
	2µM	72	6	74.2	7.01
C1 VRQ FIBRILS	1µM	24	9	100.8	1.33
	1µM	48	9	96.5	5.19
	1µM	72	6	75	8.58
	2µM	24	9	101.9	0.49
	2µM	48	9	94.7	3.13
	2µM	72	6	91.5	7.18
α C1 ARR	1µM	24	6	100.9	0.9
	1µM	48	9	96.5	4.3
	1µM	72	6	83.8	7.77
	2µM	24	6	97.3	1.9
	2µM	48	8	93	3.86
	2µM	72	6	80.1	7.71
α C1 VRQ	1µM	24	6	101.33	0.57
	1µM	48	9	91.1	6.92
	1µM	72	6	79.8	11.37
	2µM	24	6	98.8	0.46
	2µM	48	9	80.4	8.41
	2µM	72	6	69.2	13.28

Table 6.2 - Cell viability of N2a cells with addition of PrP, C1 fibrils and recombinant α-helical C1 proteins.

6.4.3 The effect of C1 on fibrillisation of full-length PrP

All sheep tested during the preparation of this thesis have measureable levels of C1 protein present in their brains. Depending on their *PRNP* genotype, ovine cells will contain a mixture of full length PrP^{C} molecules and C1 fragments with identical or different protein sequences at varying ratios. To partially mimic this *in vivo* scenario, mixed fibrillisation assays were performed as described for single variants alone (Chapter 5) with both truncated and full length recombinant proteins at two ratios (1:1, equivalent to 50 % C1 and 4:1, equivalent to 20 % C1), representative of ratios found *in vivo*. Fibrillisation reactions were repeated multiple times (n) and typical results for selected reaction mixtures are show in Figure 6.9. PrP^{VRQ} was mixed at a 1:1 ratio with $C1^{ARR}$ (n = 10), $C1^{ARQ}$ (n = 6) or $C1^{VRQ}$ (n = 10). The lag time of fibrillisation was measured as an indicator of the delay in nucleation along with the growth rate of fibrillisation, measured by the rate constant of the elongation phase (k). There was no significant change in lag time with addition of $C1^{ARQ}$ (5.46 hours, SEM ± 0.67) or $C1^{VRQ}$ (5.13 hours, SEM ± 0.50) compared to PrP^{VRQ} alone (Figure 6.10). However, $C1^{ARR}$ addition at 1:1 significantly increased the lag time of fibrillisation of PrP^{VRQ} from 5.57 hours (SEM ± 0.48) to 10.6 hours (SEM ± 1.12) ($p = 5.2 \times 10^{-5}$). As observed with fibrillisation of $C1^{ARR}$ alone, 80 % of the mixed assays did not result in full fibrillisation within the time frame of the experiment and therefore lag times could not be calculated in these cases. When full fibrillisation was achieved reactions had around an 80 % lower maximum fluorescence and there was a trend for the elongation phase of fibrillisation to be slower (k = 1.29, SEM ± 0.38) compared to PrP^{VRQ} alone (1.91, SEM ± 0.24) (Table 6.3). The growth rate is measured by the rate constant (k) and is independent of maximum fluorescence and lag time of fibrillisation (Graham, Agarwal et al. 2010).

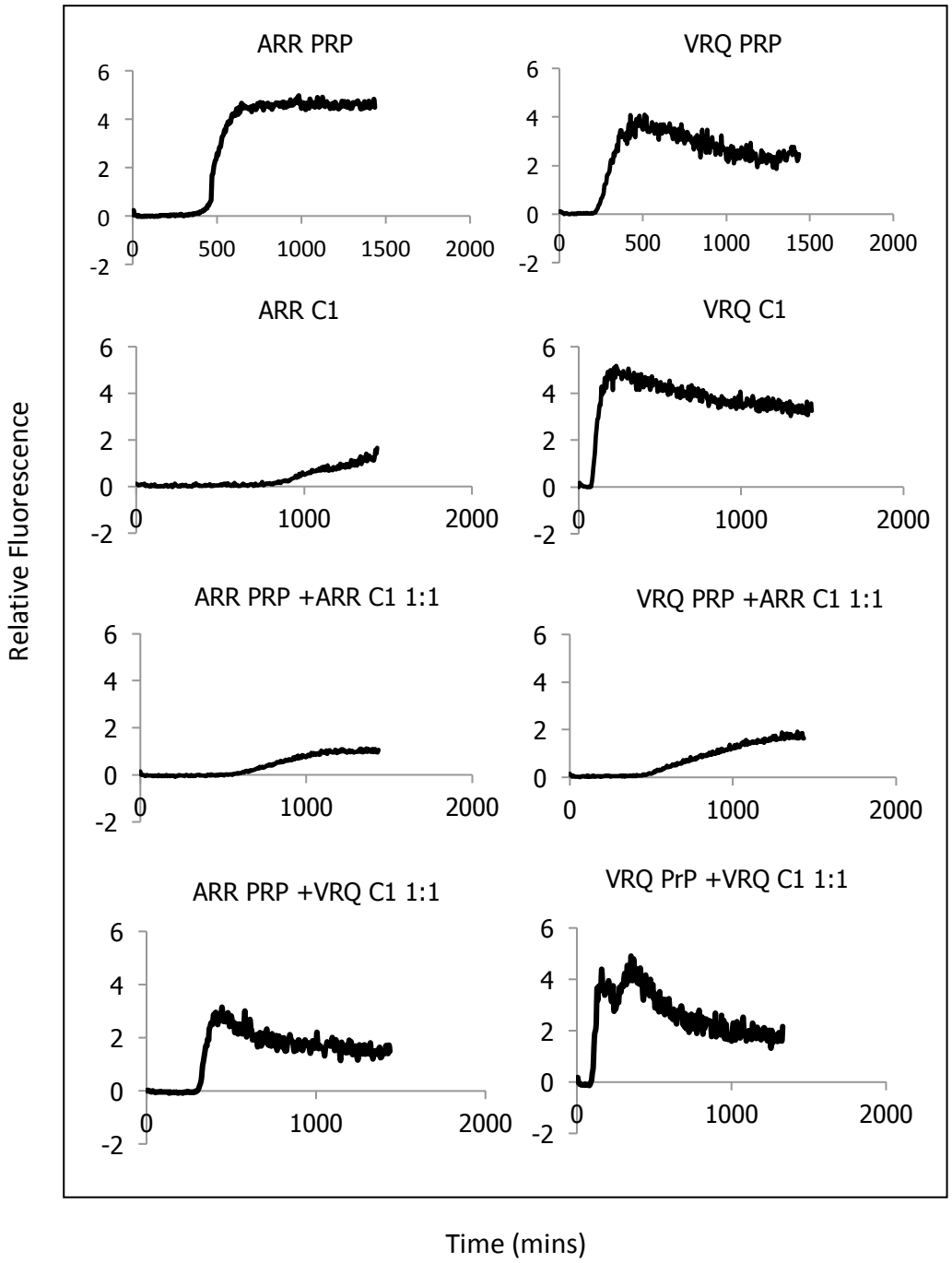

Figure 6.9 – Fibrillisation kinetics of PrP and C1 mixed reactions. Fibrillisation was performed as described in sections 5.3.13 and 6.3.1. Typical fibrillisation curves for PrP variants. Background ThT fluorescence from no PrP controls subtracted from raw data.

Reactions at a 4:1 PrP^{VRQ}: $C1^{ARR}$ ratio were also performed (n = 7), in in which lag times for fibrillisation of PrP^{VRQ} were increased to an average of 6.6 hours (SEM ± 1.36). In these reactions, fibrillisation of PrP^{VRQ} was inhibited to less of an extent compared to the 1:1 reactions. Maximum fluorescence was again lower than seen with full length protein alone, with 3 out of 7 replicates failing to fibrillise fully within the time frame of the experiment.

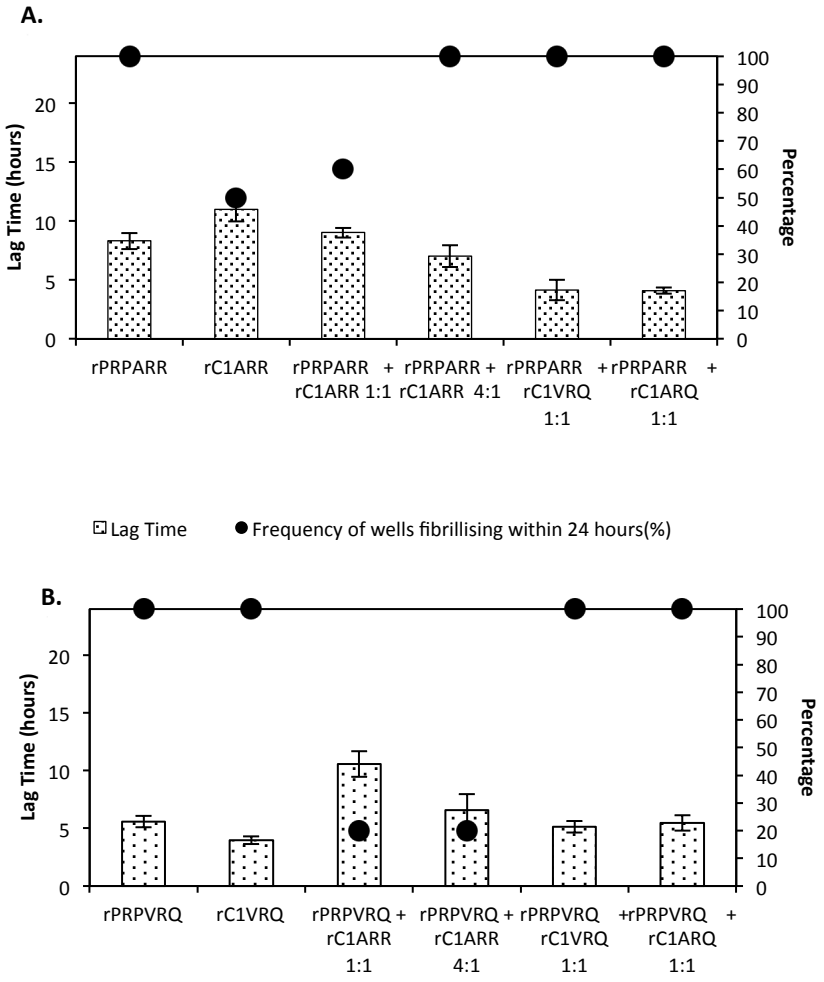

Figure 6.10 – Average lag times for mixed fibrillisation reactions. The lag time of fibrillisation was measured for each well repeat in which fibrillisation was complete within the time frame of the experiment and an average was calculated. A) Average lag time of fibrillisation for PrP^{ARR} reactions with C1 variants along with the percentage of reactions completing fibrillisation within the time frame of the experiment. B) Average lag time of fibrillisation for PrP^{VRQ} reactions along with the percentage of reactions completing fibrillisation within the time frame of the experiment.

Mixed reactions with PrP^{ARR} and all three variants of C1 at a 1:1 ratio were performed. Addition of $C1^{ARR}$ to PrP^{ARR} (n = 10) increased the average lag time only marginally from 8.3 (SEM ± 0.69) to 9.0 (SEM ± 0.41) (Figure 6.10). However, the rate of fibril elongation (k) was significantly decreased by 2.6 times from 1.60 (SEM ± 0.22) to 0.45 (SEM ± 0.10) $p \leq 3.0^{-5}$ (Table 6.3), which was similar to the rate for $C1^{ARR}$ alone. In contrast, addition of $C1^{VRQ}$ or $C1^{ARQ}$ to PrP^{ARR} shortened the lag time of fibrillisation (Figure 6.10) and increased the rate of elongation (Table 6.3). The early ThT fluorescence increase may represent C1 fibrillisation and mask the slightly later fibrillisation of PrP^{ARR} or the addition of these C1 variants may increase the rate of nucleation and elongation of PrP^{ARR}. Further evidence to support the first of these hypotheses is the observation, in some mixed reactions, of two peaks of fluorescence, illustrated in the PrP^{VRQ} + $C1^{VRQ}$ fibrillisation curve in Figure 6.9. In these cases, curves of best fit could not be produced and lag times were not calculated. It appears that $C1^{ARR}$ but not $C1^{ARQ}$ or $C1^{VRQ}$ can inhibit fibrillisation of full length PrP^{C} variants by either extending the lag time of fibrillisation or by altering the elongation stage.

The presence of fibrils in these mixed assays was confirmed using the maturation assay, as described in Chapter 5 and shown in Figure 6.12. Resulting gels showed 10 and 12 kDa bands as described for full length PrP species along with a prominent 16.6 kDa band associated with C1 fibrils alone after maturation. The 16 kDa band which would confirm the presence of full length PrP fibrils is very faint when compared to maturation and PK digestion of full length PrP alone, indicating that full length PrP^{C} may have formed les amyloid fibrils, indicating that mixed reactions may favor the production of C1 fibrils.

Variant	Mean Rate Constant of Elongation (k)
$C1^{ARR}$	0.46 (SEM ± 0.09)
PRP^{ARR}	1.6 (SEM ± 0.22)
PRP^{ARR} +$C1^{ARR}$ 1:1	0.45 (SEM ± 0.10)
PRP^{ARR} +$C1^{ARR}$ 4:1	1.04 (SEM ± 0.10)
PRP^{ARR} +$C1^{ARQ}$ 1:1	2.28 (SEM ± 0.09)
PRP^{ARR} +$C1^{VRQ}$ 1:1	4.53 (SEM ± 0.71)
$C1^{VRQ}$	5.78 (SEM ± 0.53)
PRP^{VRQ}	1.91 (SEM ± 0.24)
PRP^{VRQ} +$C1^{VRQ}$ 1:1	3.09 (SEM ± 0.39)
PRP^{VRQ} +$C1^{VRQ}$ 4:1	1.71 (SEM ± 0.84)
PRP^{VRQ} +$C1^{ARR}$ 1:1	1.29 (SEM ± 0.38)
PRP^{VRQ} +$C1^{ARQ}$ 1:1	2.9 (SEM ± 0.31)

Table 6.3 – Average rate of elongation for mixed fibrillisation reactions

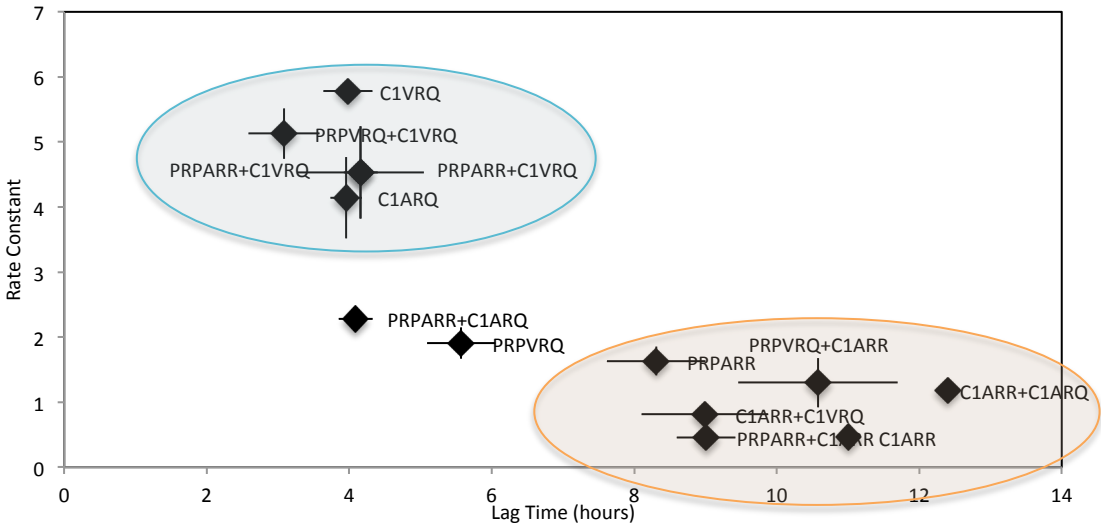

Figure 6.11 – The relationship between average rate constant and average lag time for fibrillisation reactions. Average rate constant plotted against average lag time of fibrillisation for recombinant PrP, C1 and mixed reactions at a ratio of 1:1. Error bars represent SEM.

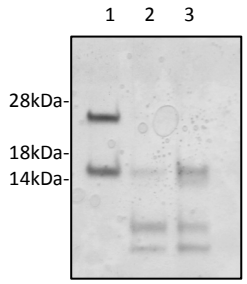

Figure 6.12 – Maturation and PK digest of PrP^{VRQ} and $C1^{ARR}$ mixed reaction. Maturation and PK digestion was performed as described in section 5.3.14. 0.5 µg of recombinant protein was untreated (Lane 1), PK treated at a ratio 100:1 of PrP: PK (Lane 2), or matured by heating to 80°C followed by PK treatment (Lane 3). Matured fibrils (Lane 3) show increased PK resistance relative to non-matured fibrils.

It was investigated if $C1^{ARR}$ could also inhibit fibrillisation of other C1 variants as observed for full length PrP^{C} variants (Figure 6.13). Mixed reactions at a 1:1 ratio were set up as previously described. Addition of $C1^{ARR}$ to $C1^{ARQ}$ significantly increased the lag time of fibrillisation from 3.96 hours (SEM ± 0.22) to 12.44 (SEM ± 0.1) ($p \leq 2.0^{-10}$), as illustrated in Figure 6.10 and significantly reduced the elongation rate (k) from 4.14 (SEM ± 0.34) to 1.18 (SEM ± 0.16) ($p \leq 4.0^{-7}$). Similar inhibition was also observed in mixed reactions with $C1^{ARR}$ and $C1^{VRQ}$, where lag time of fibrillisation was significantly increased from 3.98 hours (SEM ± 0.34) to 8.99 hours (SEM ± 0.89) ($p \leq 2.0^{-5}$) in mixed reactions and elongation rate was decreased from 5.12 (SEM ± 0.69) to 0.82 (SEM ± 0.12) ($p \leq 6.0^{-6}$). In both cases 75 % of mixed reactions failed to fibrillise within the 24 hour time frame of the experiment, indicating that $C1^{ARR}$ can also inhibit fibril formation of other C1 variants.

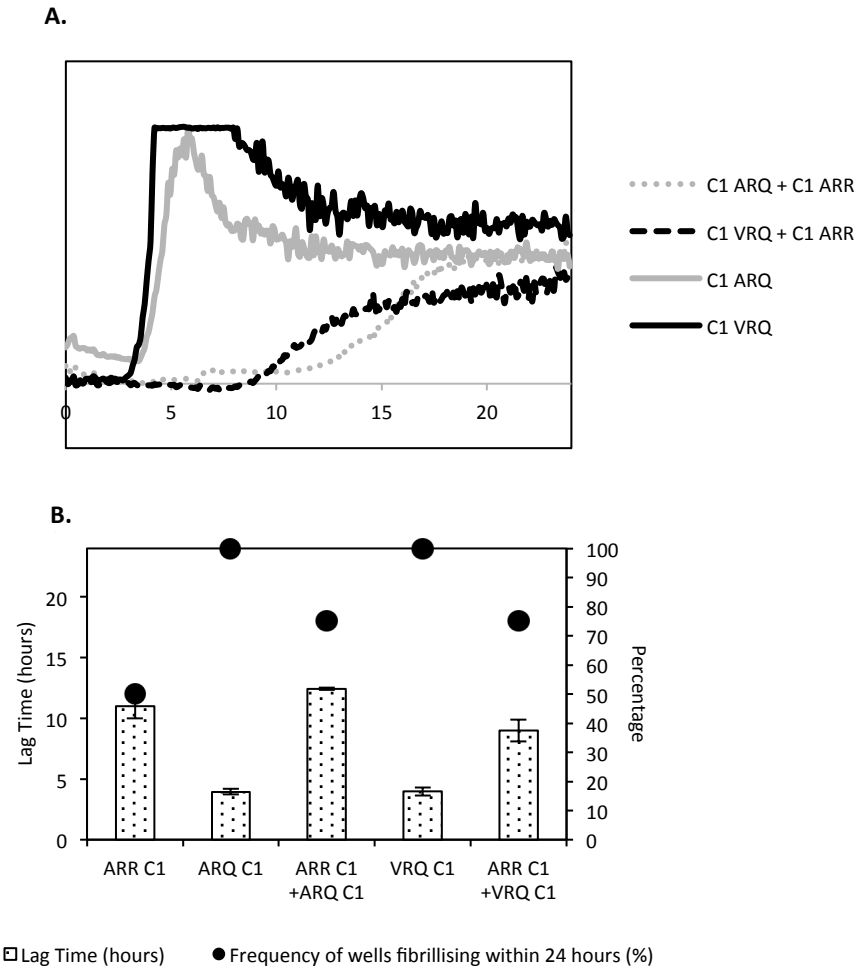

Figure 6.13 – Fibrillisation kinetics for C1 mixed fibrillisation reactions. A) Typical fibrillisation curves for $C1^{ARQ}$ and $C1^{VRQ}$ alone and with $C1^{ARR}$ at a 1:1 ratio. B) The lag time of fibrillisation was measured for each repeat in which fibrillisation was complete within the time frame of the experiment and an average was calculated along with the percentage of reactions completing fibrillisation within the time frame of the experiment.

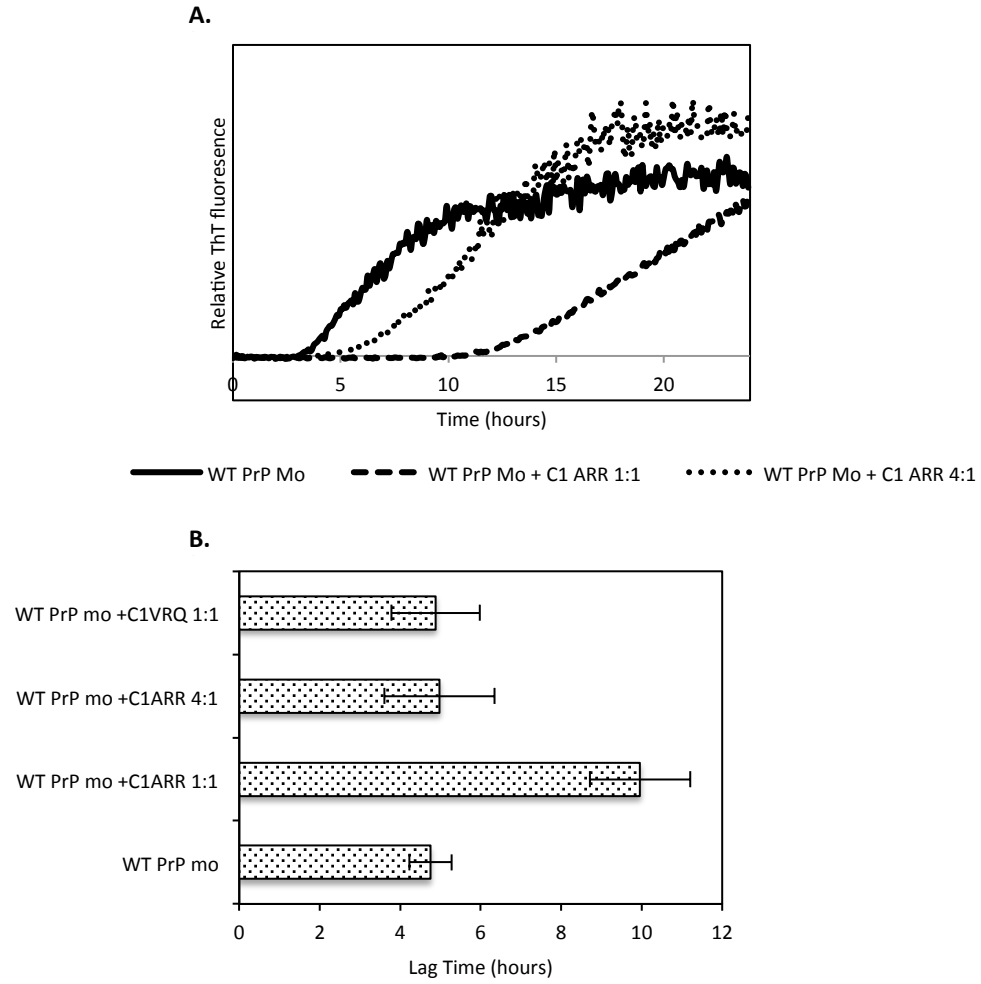

Figure 6.14 – Fibrillisation kinetics for murine PrP with ovine recombinant C1. A) Typical fibrillisation curves for wild type murine recombinant PrP, with $C1^{ARR}$ at both 1:1 and 4:1 ratios. B) The lag time of fibrillisation was measured for each repeat in which fibrillisation was complete within the time frame of the experiment and an average was calculated along with the percentage of reactions completing fibrillisation within the time frame of the experiment.

Does $C1^{ARR}$ have the ability to also inhibit fibrillisation of murine PrP^C? This question is important as the cell lines used to assess fibril toxicity (N2a and SMB-PS) were of mouse origin and other *in vitro* conversion reactions, such as the cell free conversion are more effective using murine derived PrP^C. Mixed reactions with either $C1^{ARR}$ or $C1^{VRQ}$ were set up at ratios of 1:1 and 4:1 with murine recombinant PrP (kindly provided by Fiona Lane,

The Roslin Institute). Figure 6.14 shows typical fibrillisation curves for these reactions along with the average lag times of fibrillisation. Murine PrP^C alone has an average lag time of 4.57 hours (SEM ± 0.52), however on addition of $C1^{ARR}$ at a 1:1 ratio the lag time was significantly increased to 9.96 hours (SEM ± 1.25) ($p \leq 0.003$). There was no significant difference to lag times when $C1^{ARR}$ was added at a 4:1 ratio or on addition of $C1^{VRQ}$ at a 1:1 ratio the rate of elongation (k) did not significantly differ in any of the mixed reactions when compared to murine PrP^C alone..

Protein variant 1:1	Inhibition of lag phase	Inhibition of growth phase	Reduction in maximum fluorescence
PrP^{ARR}	✗	✓	✓
PrP^{VRQ}	✓	✗	✓
$C1^{ARQ}$	✓	✓	✓
$C1^{VRQ}$	✓	✓	✓
Murine PrP	✓	✗	✓

Table 6.4 – Summary of inhibition of mixed fibrillisation reactions at a ratio of 1:1 by $C1^{ARR}$.

6.4.4 Infection of Rov9 cells with SSBP/1 scrapie isolate

To allow for the inhibitory effects of recombinant $C1^{ARR}$, illustrated in fibrillisation assays to be further investigated a cell culture model of infection was essential. Comparison of PrP expression in eight different cell lines was performed to determine the line expressing highest levels of PrP^C protein. This was felt to be advantageous as high levels of PrP^C expression have been linked to susceptibility in mouse models (Bueler, Aguzzi et al. 1993) and the VRQ allotype expressed by these cells is most prone to conversion (Sabuncu, Petit et al. 2003). These cells have also been successfully infected with scrapie on several occasions (Sabuncu, Petit et al. 2003, Neale, Mountjoy et al. 2010).

PrP^C expression was quantified in the N2a neuroblastoma cell line by western blotting of cell lysate along with dilutions of recombinant murine wild type (kindly provided by Fiona Lane, The Roslin Institute). Densitometry was performed and PrP^C expression was quantified in N2a cells using a recombinant protein standard curve. Assuming that the affinity of BC6 was similar for recombinant and cellular murine PrP^C protein it was estimated from three dilutions that N2a cells express 6.5 ng of PrP for every 1 µg of total protein in cell lysate. Cell lysates from other cell lines (gtARQ derived, Tg338 derived, SMB-PS, Rov9, CHO^{ARR}, CHO^{ARQ} and CHO^{VRQ}) were then subjected to western blotting (100 µg/ lane), probed with BC6 antibody along with alpha tubulin loading control and subjected to densitometry. PrP^C expression levels relative to N2a cell expression were used to calculate the actual quantity of PrP^C expressed per µg of total protein (Figure 6.15). Cell lysates were created on two separate occasions and average expression of PrP^C relative to N2a cells was calculated as an average of the two experiments. Graphed values represent the average calculated PrP^C expression for each cell line. Rov9 cells express the most PrP/ µg of total protein, 31.2 ng/µg (SEM ± 1.3), followed by CHO^{VRQ} at 22.2 ng/µg (SEM ≠ 0) and Tg338 derived primary neurons expressing 18.9 ng/µg (SEM ± 1.9). N2a and SMB-PS express the lowest levels of PrP per µg of total protein and levels are very similar between the two cells lines, an observation also reported by Mays et al (Mays, Yeom et al. 2011).

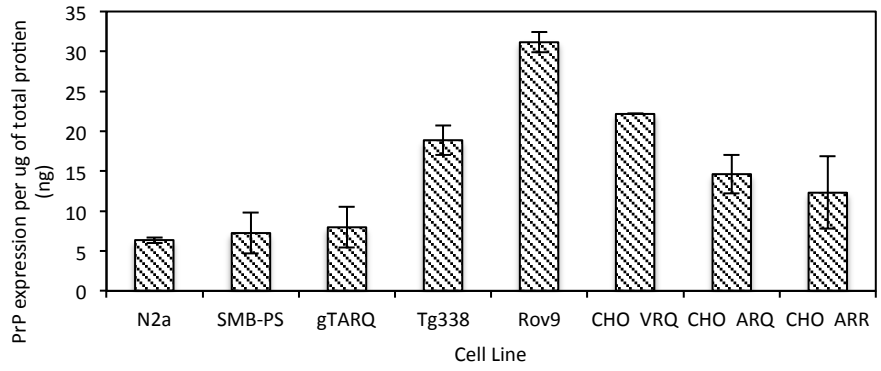

Figure 6.15 – Quantification of PrP expression in cell lines by western blotting. 100µg of cell lysate was tested by western blot with BC6 and anti-alpha tubulin as a loading control. Densitometry was performed and loading was normalised against alpha tubulin. PrP expression was quantified for each cell line relative to N2a PrP expression and repeated twice.

Sterile brain homogenate from a VRQ/VRQ genotype SSBP/1 infected sheep (final concentration of 2.5 % w/v) was added to Rov9 cells 48 hours post Doxycycline induction of PrP^{C} expression. The cells were continually passaged 1:4 and lysed at 2 (passage 1), 5 (passage 2), 11 (passage 3) and 14 (passage 4) days post infection. To confirm infection, 30 µg of cell lysate was treated with PK at concentration of 50 µg/ml (Protein: PK ratio of 25:1). Control cells show no PK resistant protein both at Day 2 and Day 14 (Figure 6.16). In contrast, cells exposed to SSBP/1 homogenate had bands of PK resistant PrP^{Sc} at all time points. The banding pattern produced after treatment with PK in Rov9 cells is slightly different to that characteristically observed in the scrapie infected brain with the molecular weight shift seen primarily in the di-glycosylated high molecular weight band. Similar band patterns in infected Rov9 cells have been reported by Vilette and colleagues (Vilette, Andreoletti et al. 2001) who also show that the PrP^{Sc} produced by Rov9 cells appears to be a lower molecular weight when compared to PrP^{Sc} from scrapie infected brain homogenate. At day 14 it is unlikely that the PK resistant PrP^{Sc} visible is residual

infected brain homogenate as homogenate will have been diluted to 1/64 of the original inoculum through passaging of the cells.

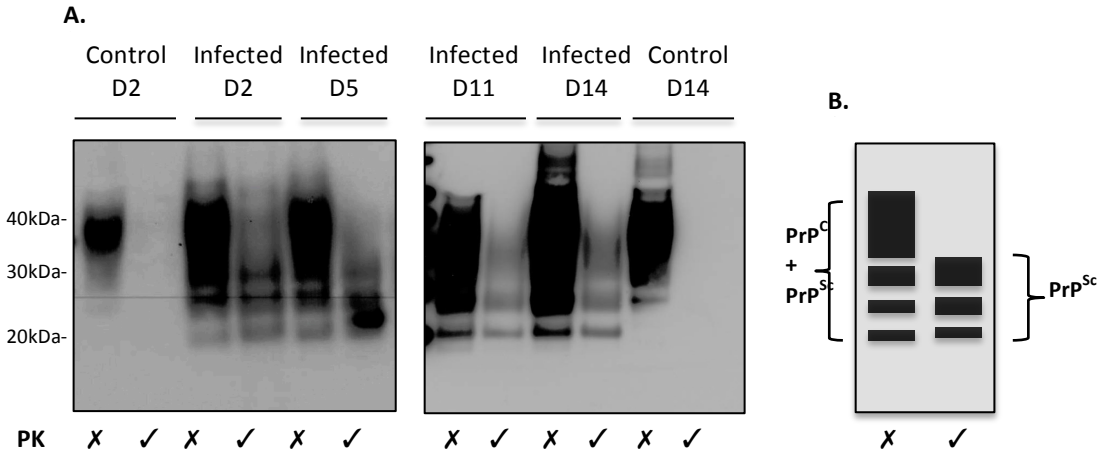

Figure 6.16 – PrP^{Sc} accumulation in SSBP/1 infected Rov9 cells. A) 30μg of cell lysate was treated with or without PK (50μg/ml) for 1.5 hours at 37 °C. Protein was acetone precipitated and separated on a 12% NuPAGE Bis-Tris gel and immunoblotted with anti-PrP antibody P4. B) Illustration of characteristic molecular weight shifts associated with PK resistant PrP^{Sc}.

6.4.5 The effect of C1 on scrapie infection in cell culture

Following confirmation that in our hands Rov9 cells can maintain scrapie infection and produce PrP^{Sc} in culture it was explored if $C1^{ARR}$ could alter or inhibit PrP^{Sc} accumulation when applied exogenously. This was performed as a small-scale pilot experiment to highlight a potential area for future study. It was unknown if recombinant $C1^{ARR}$ would be up taken up by the cell or would be quickly degraded in the cell culture media. Therefore, recombinant C1 was added to Rov9 cells at 5 μg/well and incubated for 24 hours. Both media and cell lysate were collected, acetone precipitated and immunoblotted with an anti-His-Tag monoclonal antibody. A small amount of recombinant C1 seems to have been taken up into the cells or has bound to the surface while the majority remains in the media (Figure 6.17).

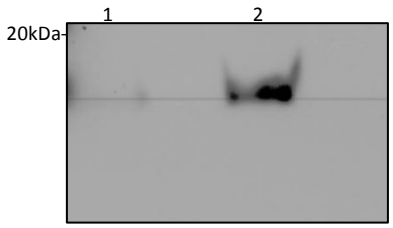

Figure 6.17 – The fate of recombinant C1^{ARR} in cell media after 24 hours. 5μg of recombinant C1^{ARR} was added/well of Rov9 cells and incubated for 24 hours. Lysate and media were collected and analysed by immunoblotting with Anti-His-Tag antibody. Lane 1 (media), Lane 2(Cell lysate).

Recombinant C1^{ARR} (5μg/well) was added to Rov9 cells 24 hours before infection with SSBP/1 infected homogenate (n =4), mixed with the infected homogenate (n = 4) or added at 24 hours post infection (n = 4). The wells treated with C1^{ARR} post infection were continually treated at every subsequent passage. Positive control wells without recombinant C1 but with homogenate (n = 4) and negative control wells with media only (n = 4) were also included. At day 2 post infection 2 wells from each were passaged (1:4). Cell lysate was collected from the remaining 2 wells and pooled. This was repeated at day 5, day 11 and day 14. The total protein concentration of cell lysates were measured by BCA assay, normalised and treated with PK (50μg/ml). To allow for densitometric comparison of PrP^{Sc} levels a dot blotting method was adopted as described in section 6.3.11.

Dot blotting was carried out with PK treated samples (2.5μg), with two repeats of each sample included (Figure 6.18). In control wells there was no evidence of PK resistant PrP^{Sc} at any time point. At day 2 all samples treated with infected homogenate have evidence of PK resistant PrP^{Sc}, which is most likely residual PrP^{Sc} from the homogenate. By the second passage (day 5) levels of PK resistant PrP^{Sc} are reduced, corresponding with the removal of the homogenate and replacement of growth media. In both the infected control wells

and in the wells that had been treated with $C1^{ARR}$ prior to infection PrP^{Sc} levels are increased at day 11 and 14 indicating these cells are now producing misfolded PrP^{Sc} independent of the initial homogenate. Wells that had been treated with $C1^{ARR}$ at the time of infection and post infection with continued application with every passage show no evidence of PK resistant PrP^{Sc} at later time points.

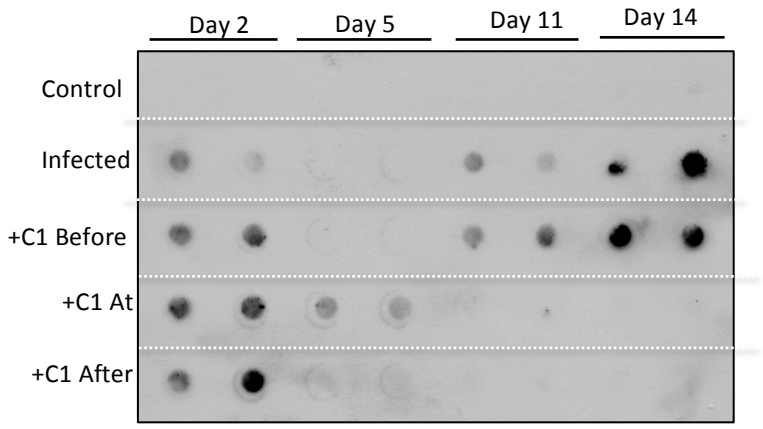

Figure 6.18 – PK resistant PrP^{Sc} in SSBP/1 infected Rov9 cells in the presence of $C1^{ARR}$. Rov9 cell lysates (2.5 μg) were treated with PK (50μg/ml), subjected to dot blotting and probed with P4 monoclonal antibody as described in section 6.3.11.

6.5 DISCUSSION

6.5.1 C1 fibril preparations have reduced toxicity to SMB-PS cells in culture compared to PrP^{C} fibril preparations

It is unknown at present the precise form of misfolded PrP^{C} responsible for causing cellular toxicity during disease. It has been shown that oligomers and pre-fibrillar aggregates cause neurotoxicity to cells in culture (Sanghera, Wall et al. 2008) and that neuronal loss can occur before the accumulation of measureable levels of amyloid,

indicating that perhaps it is a smaller oligomer or intermediate aggregates that have a prevailing toxic effect. However, full-length PrP fibrils are also toxic to primary neurons in culture (Novitskaya, Bocharova et al. 2006). In previous chapters we have shown that recombinant PrP fragments equivalent to naturally occurring truncated PrP^{C} proteins can form amyloid fibrils *in vitro* and that these truncated variants have different populations of fibrils and smaller aggregates when compared to full length PrP^{C} fibril preparations. Although it is unknown if these truncated proteins have the potential to misfold and aggregate *in vivo* the toxicity of C1 fibril preparations was tested in two cell culture models with variable results.

In SMB-PS cells full length fibrils of both PrP^{ARR} and PrP^{VRQ} caused a significant reduction in cell viability, positively correlated with both concentration and incubation time while no reduction was seen with either of the C1 fibril preparations. Potentially, this variation may be attributed to a lower number of toxic fibrils or misfolded aggregates present in the C1 preparations, as suggested by the data collected from Dynamic Light Scattering (DLS). Full length variants appear to form different populations of smaller protein aggregates when compared to truncated C1, perhaps with the higher propensity to form stable toxic oligomers or intermediates. DLS also revealed that polymorphisms in the PrP^{C} protein had little effect on the size of fibrils or aggregates that were produced. If the size and number of smaller aggregates are linked to toxicity then this observation correlates with the similar levels of toxicity seen on addition of PrP^{ARR} and PrP^{VRQ} to cell culture. However, it has also been suggested that aggregate and oligomer size is not accountable for toxicity which is instead determined by the conformation and folding of the individual protein fragments (Lee, Savtchenko et al. 2011). It may be a combination of both variable

aggregate size and formation of different small intermediate oligomers and aggregates that contributes to the variable toxicity of full length PrP and C1 fibril preparations.

At the highest concentration of α-helical $C1^{VRQ}$ (5μM) tested cell viability was reduced to an average of 77.4 % of buffer only control wells. $C1^{VRQ}$ related cell death might occur in a p53 dependent manner as over-expression of murine C1 in a cell culture has been shown to modulate and increase sensitivity to p53 dependent apoptosis through the caspase 3 pathway (Sunyach, Cisse et al. 2007). Whether these pathways are indeed activated in SMB-PS cells remains to be investigated, for example by monitoring caspase 3 activity in cells and through pharmacologically blocking of the p53 pathway in cells which have been incubated with α-helical $C1^{VRQ}$. Equally important would be to test the toxicity of $C1^{ARQ}$ as a PrP with different sequence could clarify whether this effect is VRQ specific or whether the absence of toxicity from ARR is unique.

6.5.2 Fibril toxicity is cell line dependent

There was no such protein specific fibril toxicity in the N2a cell line at the concentrations used in this study and high proportions of dead cells were observed in the buffer only control wells compared to that seen in the SMB-PS line. This is indicative that N2a cells may be more susceptible to the addition of sodium acetate buffer. In our hands the N2a cell line naturally had a faster cell cycle when compared to SMB-PS and perhaps increased in cell death in control wells can be attributed to dense culture conditions. At 72 hours incubation addition of all fibril variant preparations and α-helical recombinant protein led to decreased cell viability as a percentage of control wells. This indicates that PrP fibril preparations are toxic to N2a cells and that unlike that seen with SMB-PS cells C1 fibrils are equally toxic to N2a cells. Furthermore, a reduction in cell viability is seen with both α-

helical $C1^{ARR}$ and $C1^{VRQ}$ proteins, in contrast to $C1^{VRQ}$ only in the case of SMB-PS cells. The mechanisms of toxicity caused by either α-helical C1 and fibril preparations may differ. If we surmise that after 72 hours of culture N2a cells, as a result of their faster cell cycle, become stressed these cells will be more sensitive to p53 mediated apoptosis due to overcrowding and lack of available nutrients. As C1 expression in cell culture has been shown to enhance p53 transcription and activation this could explain why these cells display reduced viability and higher sensitivity to α-helical C1 (Sunyach, Cisse et al. 2007).

Varying susceptibility of cell lines to fibril related toxicity couldn't be explained by differences in PrP^C expression as SMB-PS and N2a cell lines both expressed similar levels of total PrP^C. However, these cell lines do have different levels of α-cleavage, with less residual C1 in N2a cell compared to SMB cells. It is possible that reduced levels of α-cleavage in the N2a cell line make it more susceptible to C1 fibril toxicity. Cell lines with low residual levels of α-cleavage have previously been associated with cellular susceptibility to scrapie infection (Lewis, Hill et al. 2009). Furthermore, as total PrP^C expression is comparable in both cell lines different levels of α-cleavage would impact on the amount of residual cell associated full length PrP^C.

6.5.3 Truncated $C1^{ARR}$ recombinant proteins can alter fibrillisation of full length PrP^C

The aim of this chapter was to understand the role of C1 in prion disease and explore the possible dominant negative inhibitory effects described by Westergard and colleagues (Westergard, Turnbaugh et al. 2011) on overexpression of murine C1 *in vivo*. To demonstrate if these inhibitory effects associated with C1 are likely to occur in normal ovine brain fibrillisation reactions were performed at relative ratios of recombinant full length PrP and C1 to represent a situation similar to *PRNP* homozygous and heterozygous

brain tissue. When mixed with other protein variants at a ratio of 1:1, $C1^{ARR}$ inhibited fibril formation of both PrP variants whilst $C1^{ARQ}$ and $C1^{VRQ}$ did not. In fibrillisation reactions with a PrP^{C}: C1 ratio of 4:1, inhibition was reduced suggesting that the PrP: C1 ratio could be an important factor if similar inhibitory mechanisms apply *in vivo* in brain during the formation of disease associated amyloid fibrils. In the case of ovine C1 it appears that *PRNP* sequence is an important factor in the inhibition of fibril formation. However, it is unclear if *PRNP* sequence is also important for inhibition of conversion during disease as mouse wild type C1, which is different from sheep $C1^{ARQ}$ by only nine amino acid changes - has a delaying effect on development of TSE disease *in vivo* (Westergard, Turnbaugh et al. 2011). Perhaps, if the amount of $C1^{ARQ}$ and $C1^{VRQ}$ in fibrillisation reactions were increased to that relative to the ratios observed in overexpressing murine models then C1 would have the same inhibitory effects on fibrillisation as reported on conversion. It also remains to be established whether this variation in inhibition between murine and ovine C1 indicates that the inhibition mechanism for seeded and un-seeded nucleation or elongation is different or that the effects of C1 on prion replication are amplified in an *in vivo* situation.

The dominant negative inhibitory effect in fibrillisation of $C1^{ARR}$ is not specific to ovine full-length PrP^{C}, but crosses the species barrier to also delay fibril formation of recombinant mouse PrP^{C}. Following these results and considering the large number of other known polymorphisms in PrP^{C} it would be of further interest to produce recombinant C1 proteins to test for inhibitory characteristics, particularly with other species specific resistance associated polymorphisms such as human M129V. For example, addition of different C1 variants into reactions with recombinant full length PrP expressing 129M has been shown previously to readily form amyloid fibrils *in vitro* (Lewis, Tattum et al. 2006).

6.5.4 Potential mechanisms of fibril inhibition

C1 can directly inhibit the formation of PrP amyloid fibrils in the absence of PrP^{Sc}. Our findings suggest that $C1^{ARR}$ can either inhibit the initial nucleation of amyloid fibrils or slow the elongation phase of fibrillisation when mixed with full length PrP^{C}, while when mixed with other variants of C1 it appears to inhibit both stages of fibrillisation. Therefore we believe that there may be two mechanisms explaining this inhibition as illustrated in Figure 6.19. The C1 protein may bind to PrP^{C} and prevent further interaction with other recombinant PrP^{C} proteins thereby inhibiting the formation of an initiating nucleus. Alternatively, the C1 protein may become incorporated into amyloid fibrils of PrP^{C}, which would interfere with subsequent elongation of the fibrils, perhaps by inducing the formation of disordered aggregates. Knowles and colleagues (Knowles, Waudby et al. 2009) state that once in the elongation stage fibrils fragment and re-nucleate. A further possible mechanism leading to a slower growth rate in mixed $C1^{ARR}$ reactions would be the reduced potential of $C1^{ARR}$ containing fibrils to fragment. It appears that both putative mechanisms may occur independently and/or simultaneously. $C1^{ARR}$ clearly inhibits fibrillisation of all variants with exception of full length PrP^{ARR} via binding prior to nucleation, extending the lag time of fibrillisation. As PrP^{ARR} has an already longer relative lag time and hence a slower propensity to nucleate C1 interactions prior to nucleation may be masked.

.

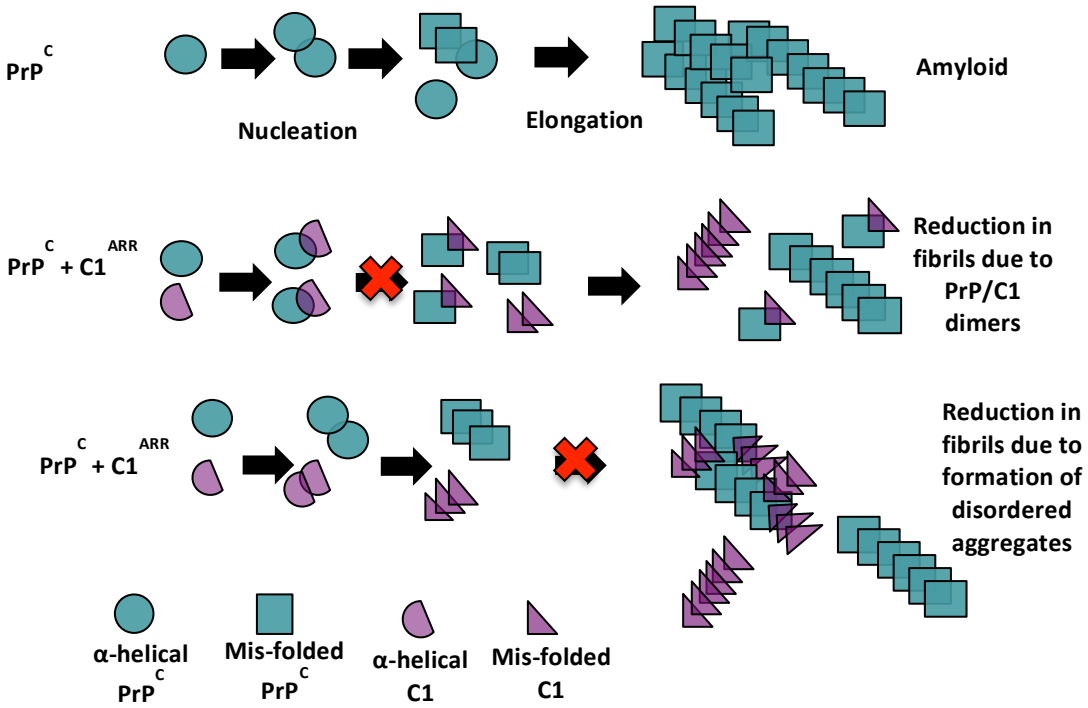

Figure 6.19 – Theoretical models of $C1^{ARR}$ associated inhibition of *in-vitro* fibrillisation. Diagrammatic representation of possible mechanisms of inhibition, through either direct binding to PrP^{C} prior to misfolding or through production of homogeneous aggregates or pro-fibrils which then bind.

6.5.5 A cell culture model of C1 related inhibition of conversion

Although only a small pilot study this experiment aimed to address the effects of C1 on conversion in a physiological system. The major challenge was to find a suitable method to compare PrP^{Sc} accumulation in a large number of independent cultures. Western blotting and dot blotting were adopted as these techniques required little optimisation and have been well characterised for visualising infected brain homogenate. On reflection perhaps a different assay would have given more consistent results, such as the cell blotting assay, described by Bosque and Prusiner (Bosque and Prusiner 2000). A further problem with analysing data from a small cell infection experiment such as this is that infection is not

always guaranteed to affect the same number of cells in each culture. Of the cells that are infected PrP^{Sc} production/accumulation may not be equivalent. To address this, two wells were pooled at each passage/lysis step.

Despite these limitations and being aware of the small number of experiments that were performed, these assays did show variable PrP^{Sc} accumulation, with some dependents to addition of C1. It was hypothesised from fibrillisation experiments that $C1^{ARR}$ would bind to PrP^{C} and subsequently prevent dimerisation and binding to incoming PrP^{Sc}. However, addition of $C1^{ARR}$ before infection did not appear to effect PrP^{Sc} accumulation. It appeared that application of $C1^{ARR}$ both at time of infection and after infection and at every passage led to a reduction in the accumulation of PrP^{Sc} in Rov9 cells. This confirms the hypothesis presented earlier for a role for C1 in binding to PrP^{Sc} and preventing further aggregation or binding to PrP^{C} and suggests that exogenous application of C1 may be a possible therapeutic in the treatment of prion disease, representing an important area for future study.

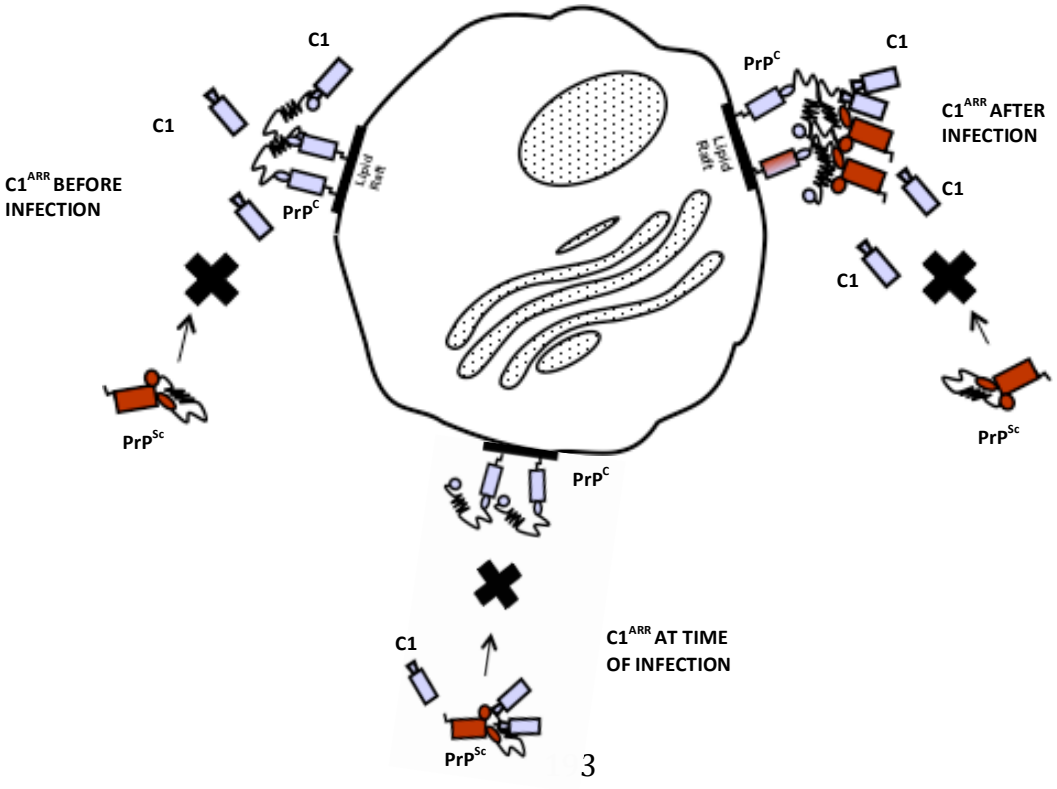

Figure 6.20 – Theoretical models of $C1^{ARR}$ associated inhibition of conversion in Rov9 cell culture model. Diagrammatic representation of possible mechanisms of inhibition

6.5.6 Conclusions

This chapter aimed to investigate the role C1 may play in the conversion of PrP^{C} to PrP^{Sc} using two *in vitro* conversion assays. In previous chapters truncated C1 proteins were converted to amyloid fibrils *in vitro.* These fibrils were shown to have reduced toxicity to SMB-PS cells when compared to full length PrP^{C} fibrils and moreover it has been shown that cells lines expressing very similar levels of PrP^{C} but different levels of C1 can have different susceptibility to fibril toxicity. $C1^{ARR}$ but not $C1^{ARQ}$ or $C1^{VRQ}$ could inhibit fibril formation of other recombinant protein variants by at least two independent mechanisms. Using the cell free conversion both variants of C1 appeared to reduce the production of PK resistant PrP^{Sc}. A small pilot study suggested that addition of $C1^{ARR}$ exogenously to a cell culture model of infection had the potential to influence the outcome of infection and needs to be further investigated.

CHAPTER 7

DISCUSSION

Primarily, this thesis aimed to investigate cleavage of PrP^C in the sheep model both in health and with the goal of understanding if it is a contributing factor in the resistance/susceptibility to prion disease. The experimental approach was to use *in vivo* investigations into PrP^C expression and processing in sheep brain and *in vitro* modeling of misfolding and cellular toxicity. There were no significant regional differences in PrP^C processing throughout the ovine brain, but levels of both α-cleavage and β-cleavage were found to vary significantly between animals, associated with polymorphisms in the *PRNP* gene. Recombinant C1, equivalent to that produced by scrapie resistant ARR/ARR sheep had the ability to inhibit PrP fibrillisation and production of PK resistant PrP^{Sc} *in vitro*, indicating that α-cleavage may be a defining factor in susceptibility to scrapie in sheep. During the study for this thesis, variations were identified in antibody binding to PrP^C from different *PRNP* genotypes. Novel recombinant proteins were produced representing variants of C1, C2 all of which will be pivotal to future studies.

Should the role of C1 as an inhibitor of conversion and fibrillisation with a significant genetic component be confirmed for sheep *in vivo*, it may represent a potential therapeutic target in the treatment of prion disease. C1 is also likely to have important roles in normal cellular function such as myelin maintenance. α-Cleavage may have wider implications which will be further understood as the function and role of PrP^C in other diseases becomes better comprehended.

7.1. SUMMARY

This thesis has shown that levels of full length PrP^C in the brain do not directly correlate to susceptibility to scrapie in sheep, with similar levels of PrP^C expression in the most susceptible and resistant genotypes. Proteolytic processing of PrP^C does vary between these genotypes with both higher levels of α-cleavage fragment C1 and lower frequency of sheep with C2 fragment associated with scrapie resistant genotype ARR/ARR. PrP^C processing and expression in ovine transgenic mice, ovine PrP^C expressing cell lines and primary neuronal cell lines produced from ovine transgenic mice were compared to sheep and these were assessed as models. To investigate the protease responsible for α-cleavage, ADAM proteases were inhibited in primary neuronal cells. With no direct reduction in C1 levels it is unlikely that ADAM proteases are directly involved in this event in neurons, although, this experiment does not rule out ADAM involvement in other cell types or tissues. Novel truncated recombinant C1 and C2 proteins were expressed in bacteria, purified and characterised. It has been shown for the first time that C1 proteins have the potential to form amyloid fibrils *in vitro*. These C1 fibrils have reduced toxicity to SMB cells and are made up of different sized populations of smaller aggregates, when compared to full length PrP^C. All PrP fibrils showed no toxicity to N2a cells indicating that fibril toxicity may be cell type specific. The presence of 171R in absence of the N-terminal results in a reduced potential to form amyloid fibrils. Addition of truncated proteins with 171R but not 171Q to fibrillisation reactions inhibited fibrillisation of full length PrP, both ovine and murine. In contrast, both C1 171R and 171Q inhibited *in-vitro* conversion of full length PrP^{VRQ}, highlighting that formation of amyloid fibrils and the conversion of full length PrP^C. to PrP^{Sc} may involve separate misfolding pathways. A preliminary experiment indicated that application of $C1^{ARR}$ exogenously to cells in culture may reduce PrP^{Sc} accumulation when infected with SSBP/1 scrapie.

In conclusion, this work has emphasised the importance of proteolytic processing of the cellular prion protein in resistance to TSE disease in sheep and shown that the C1 protein can act as an inhibitor of PrP^{C} conversion to PrP^{Sc} and should be further investigated as a possible therapeutic in the treatment of prion disease.

7.2. PrP^{C} EXPRESSION AND SUCEPTIBILITY TO SCRAPIE

To investigate PrP^{C} expression and processing in the ovine brain, seven brains areas were tested. Due to both physiological and functional regional variation and the high diversity of neuronal and glial cell types in the brain, it was speculated that different ovine brain regions would have different levels of PrP^{C} expression. However, this study suggests that there is an absence of correlation between neural cell density and levels of PrP^{C}, indicating that both neural and glial cell types express similar levels despite probable variations in mRNA expression, as has been shown for mice (Ford, Burton et al. 2002). It is obvious that a study in sheep of the transcriptional and post-transcriptional regulation of PrP is required to investigate this disconnection between mRNA, protein and cell type.

In mouse models PrP^{C} expression has been shown to directly positively correlate to disease susceptibility (Vilotte, Soulier et al. 2001). However, in this study PrP^{C} was found be highest in the cortex, with lowest levels found in the pons and the midbrain which are target areas of prion pathology. Hence, we have shown that PrP^{C} expression alone in sheep is unlikely to solely determine the pattern of PrP^{Sc} deposition or spread of disease throughout the brain (Chapter 4). Similarly, in Alzheimer's disease there is no direct correlation between expression and areas characteristic for protein deposition of the amyloid precursor protein (APP). Instead, like PrP, APP is expressed throughout both

human and rat brains at similar levels (Goedert 1987, Mita, Schon et al. 1989). If PrP^{C} expression does not correlate with PrP^{Sc} accumulation in sheep, other factors must be considered. As the cell surface is the primary site of conversion (Goold, Rabbanian et al. 2011), perhaps there are differences in PrP^{C} surface expression between neuronal cell types and/or between PrP^{C} with certain polymorphisms, which would account for area specific differences in PrP^{Sc} accumulation and genotype specific susceptibility. Furthermore, there may be differences in PrP^{C} glycosylation patterns between both cell types and PrP^{C} from different *PRNP* genotypes. Through the use of ovine glycosylation mutants, glycosylation has been shown to be important in the trafficking of PrP^{VRQ}, with the majority of unglycosylated PrP^{C} remaining intracellular. These cell lines displayed resistance to challenge with scrapie suggesting that cellular localisation as a result of altered glycosylation can effect cellular susceptibility to scrapie (Salamat, Dron et al. 2011). Murine models expressing only unglycosylated PrP^{C} also have increased incubation periods when experimentally infected with scrapie, highlighting that this is not specific to ovine PrP^{C} (Tuzi, Cancellotti et al. 2008). Along with a detailed comparison of PrP^{C} biochemical profiles of healthy sheep of different *PRNP* genotypes in the absence of PNGase F, the surface expression of PrP^{C} both in different primary cell types and in the brains of sheep of different *PRNP* genotypes could be studied by ICC/IHC and/or immunogold labeling of PrP^{C} and electron microscopy. Independent of PrP^{Sc} accumulation, contrasting cellular susceptibility to neurotoxic forms of misfolded PrP could in part account for brain area specific differences in neuronal loss. We have shown that fibril associated neurotoxicity may be cell type dependent (Chapter 6), hence varying neuronal loss during disease could be partially explained by host cell susceptibility to these misfolded aggregates. Experiments that measure the toxicity of PrP^{C} amyloid fibrils to different primary neuronal cell types would aid in deciphering variable cellular toxicity.

For future study it will be important to not only look at PrP^C expression in the brain, but also the periphery, in which varied levels of PrP^C could determine the initial success of infection and the spread of PrP^{Sc} to the brain. Along with differing conversion abilities of each of protein allotype (Bossers, Belt et al. 1997, Sabuncu, Petit et al. 2003) and variations in levels of proteolytic processing (Chapter 4), *PRNP* genotype specific expression levels in the initial sites of infection such as gastrointestinal tract and spleen, like those reported in ovine blood (Halliday, Houston et al. 2005) may play a part in creating the protective effect associated with certain PrP^C alleles.

7.3. PrP^C PROTEOLYTIC PROCESSING IN THE OVINE BRAIN

7.3.1 α-Cleavage levels in the ovine brain

We have shown that there is a lack of regional variation in levels of α-cleavage suggesting that most neural cell types undergo α-cleavage at similar levels. This leads us to speculate that the C1 and N1 are involved in general cell survival, rather than being responsible for a single specialised function. This work has also shown that the protease responsible for α-cleavage is expressed throughout the ovine brain and in neurons it is unlikely to be a member of the ADAM protease family. Other enzymes have been suggested such as plasmin, a serine protease which can cleave recombinant PrP^C *in-vitro* (Praus, Kettelgerdes et al. 2003) and also has a role in regulation of the metalloproteinase protein family. Calpain is another candidate secretase, the activity of which has been shown as essential for α-cleavage and processing of PrP^C in cell culture (Hachiya, Komata et al. 2011). In order to identify the PrP-secretase large-scale protease studies are required, perhaps making use of tagged recombinant protein models in an ELISA style assay. It appears that α-cleavage of PrP^C is not a simple enzymatic reaction, but may instead involve a complex

network of pathways, perhaps involving many of the discussed candidate proteases. Moreover, if the production of C1 and/or N1 is essential there may be substitute cleavage mechanism(s), which can 'step in' when one or more of these pathways are compromised.

Although there was little regional variation of C1 levels within the ovine brain animal-to-animal variation was high. This can be partly explained by polymorphisms in the *PRNP* gene, specifically at amino acid position 171, of which 171R is associated with higher residual C1. The higher propensity for PrP^{ARR} to undergo α-cleavage currently remains unexplained. However, possible influencing factors include: greater structural flexibility in comparison to PrP^{ARQ} and PrP^{VRQ} (Rezaei, Choiset et al. 2002, Wong, Thackray et al. 2004, Bujdoso, Burke et al. 2005), leading to increased presentation of the cleavage site to the PrP-secretase; a higher potential to form protein dimers as homodimerisation of PrP^{C} has been shown to increase α-cleavage in cell culture (Béland, Motard et al. 2012); varied cellular localisation, for example co-localisation with the Golgi apparatus increasing the chance of interacting with the PrP-secretase. In agreement with this speculation, glycosylation deficient transgenic mice with more Golgi-associated PrP^{C} and high levels of C1 (Kayleigh Iremonger, Ph.D. Thesis, University of Edinburgh) are more resistant to TSE disease than both wild type and other glycosylation mutants (Cancellotti, Bradford et al. 2010).

Prior to investigating these hypotheses, cleavage levels should be examined in unrelated ARR homozygote sheep. As this analysis was performed within a closed flock the influence of other heritable genetic factors cannot be ruled out. Although homozygous tissue was not available, analysis of ARR heterozygotes from an unrelated Norwegian flock failed to show the elevated C1 levels observed in ARR heterozygous sheep from The Roslin

Institute flock (Wilfred Goldmann and Michael Tranulis, personal communication). If α-cleavage is, in fact, controlled by a gene independent of *PRNP*, these ARR/ARR homozygote sheep may be an interesting model for gene expression studies. Identification of such a gene would be fundamental in identifying the unknown PrP-secreatase, or possible pathways that could be targeted to manipulate levels of α-cleavage.

Aside from explaining the reasons for such variation in cleavage levels, differences in levels of PrP^C, C1 and N1 may have important functional repercussions in brain and if consistent, also the periphery. Lower levels of full length PrP^C in brain, such as those seen in the ARQ/ARQ genotype, may affect normal functions, such as copper homeostasis. Although *in vivo* functions associated specifically and exclusively with truncated PrP^C proteins C1 and C2 are more or less unknown; the most probable *in vivo* role for α-cleavage is in myelin maintenance in the peripheral nervous system. Presence of C1 on neurons is essential for myelin trophic function, driving communication between neurons and Schwann cells involved in myelin maintenance (Bremer, Baumann et al. 2010). Very low natural residual levels of C1 may over time result in a reduction in myelin maintenance and in the development of peripheral neuropathies. Correspondingly, low levels of N1 may reduce the cell's ability to protect against p53 dependent apoptosis, leading to a higher rate of neuronal loss.

7.3.2 β-cleavage in the ovine brain

Many sheep tested during this study had levels of C2 representing 1 % or less of total PrP^C. β-cleavage, the production of C2/N2 fragments occurs in response to increases in reactive oxygen species (ROS) (Watt, Taylor et al. 2005), signifying that this event could be unregulated at times of abnormal cellular homeostasis. Such factors were not taken into account when selecting this data set, in which 'healthy' was defined as lack of scrapie infection. Age may also be an important factor when we consider that levels of oxidative

stress and accumulation of ROS can increase with age (Finkel and Holbrook 2000). C2 may also be an intermediate in the formation of PrP^{Sc} and we have found an increased frequency of this band in scrapie infected ovine brain, in agreement with others (Owen, Rees et al. 2007, Dron, Moudjou et al. 2010). However, it is unclear if this an additional susceptibility-enhancing factor, or produced as a result of elevated levels of ROS during disease, as shown using murine models of prion infection (Guentchev, Voigtlander et al. 2000) and in other neurodegenerative diseases, such as Alzheimer's disease, Parkinson's disease and Multiple Sclerosis (Christen 2000, Uttara, Singh et al. 2009). Unlike C1 and N1, there are no functions associated with the truncated fragments produced by β- cleavage. It is speculated that the lack of known function in comparison to C1 is unlikely to be a result of higher turnover/degradation or cellular localisation, as C2 is thought to reside on the cell surface alongside C1 but may instead be attributed to the addition of amino acids 92-114.

7.3.3 α-Cleavage and susceptibility to scrapie

Higher levels of α-cleavage are associated with scrapie resistant genotypes in sheep (Chapter 3) and cell lines with higher levels of C1 have been shown to have enhanced resistance to infection in cell culture compared to lines with lower levels of C1 (Lewis, Hill et al. 2009). It has been previously postulated that α-cleavage could be linked to resistance via two mechanisms. Firstly, more cleavage would result in less full length PrP^{C} to act as a template for conversion during TSE infection, as C1 cannot convert. Secondly, C1 can act as an inhibitor of conversion (Chapter 6), (Westergard, Turnbaugh et al. 2011). Work presented in this thesis suggests that the first may not necessarily be true in sheep, as levels of full length PrP^{C} and C1 were not found to be directly correlated.

For the first time this study has shown that all variants of C1 (ARR, ARQ and VRQ) and C2 (ARR and VRQ) have potential to misfold and form amyloid fibrils under certain conditions (Chapter 4). The N-terminal is therefore not essential for PrP fibril formation *in vitro*. The decreased potential of N-terminally truncated 171R variants to form amyloid fibrils suggests the primary binding site of PrP-to-PrP interaction is situated in the N-terminal of the protein. However, in the absence of this binding site, for example, in truncated C1 and C2, a secondary binding site may be adopted. If this site is in close proximity to amino acid 171, then polymorphisms at this position could be important in defining interaction and binding. Returning to our previous hypothesis (see section X.X.) that 171R has a higher potential to form homodimers due to its comparatively flexible structure and hence outwards facing dimer binding sites, it may be possible to explain the link with 171R and increased lag time of nucleation. If once dimerised PrP proteins are more stable and less likely to misfold, so ARR variants which readily form dimers in solution at a higher rate than other variants would take longer to nucleate.

Although Westergard and colleagues have shown that expression of C1 alone is not sufficient to support TSE infection in mice and that C1 can act as an inhibitor of disease (Westergard, Turnbaugh et al. 2011), they have used models in which C1 is unphysiologically overexpressed, meaning that these inhibitory effects may be greatly exaggerated. This thesis aimed to determine if proteolytic cleavage of PrP^{C} has a role in the conversion of PrP^{C} to PrP^{Sc} during TSE disease, by assessing the potential for ovine truncated proteins to take part in the conversion of PrP^{C} to PrP^{Sc}, using *in vitro* conversion assays. We have shown that C1 can act as an inhibitor to *in vitro* conversion at levels found *in vivo* and reduce the formation of toxic PrP^{C} species (Chapter 6). These assays have also shown that the ratio of C1: full length PrP is crucial for successful inhibition, indicating

that variations in levels of C1 observed in ovine brain would be sufficient to lead to altered disease prognosis.

The mechanism by which, C1 can inhibit the conversion of PrP^{C} to PrP^{Sc} is currently unknown. However, this work has shown that *in vitro* it likely involves two separate mechanisms, occurring individually or in unison, in which C1 binds to PrP^{C} prior to misfolding and/or C1 binds to PrP^{C} fibrils preventing further extension. Furthermore, a small pilot experiment in cell culture suggests that C1 may interact with PrP^{Sc} rather than PrP^{C} on the cell surface, inadvertently preventing both binding to other PrP^{C} molecules and also delay internalization, as C1 in absence of the N-terminal likely has a longer presence at the cell membrane as we known that the N-terminal possesses the ability to interact with a variety of protein involved in endocytosis.

High levels of C1, although appearing protective against conventional scrapie in sheep, may not play the same role during atypical disease. ARR/ARR sheep resistant to classical infection and with high levels of C1 are the most susceptible to infection with atypical scrapie (Benestad, Arsac et al. 2008). This raises the possibility that either C1 cannot bind atypical PrP^{Sc} due to conformational differences in the misfolded protein, which would nullify inhibitory effect, or that interaction with atypical PrP^{Sc} can induce misfolding of C1. Currently, attempts to amplify atypical scrapie *in vitro* have been unsuccessful (Thorne, Holder et al. 2012), although development of these assays would allow for the role of $C1^{ARR}$ to be investigated and compared to the inhibitory effects on conversion in classical disease.

Until now it had been assumed that increased incubation periods of heterozygous sheep and resistance of homozygous sheep with the ARR allele was a result of a reduced 'convertibility' of PrP^C with said mutations. The association of higher levels of C1 in scrapie resistant ARR/ARR sheep and the enhanced inhibitory effects of $C1^{ARR}$ suggest that α-cleavage may also play a crucial part in the *PRNP* genotype associated resistance in sheep. As there is similar genetic resistance in other TSE diseases such as vCJD and CWD, C1 levels as a factor of *PRNP* polymorphisms need to be fully investigated in these species using a similar approach to that of sheep, with both *in vivo* analysis and *in vitro* modeling.

7.4 C1 AS A POSIBLE THERAPUTIC IN THE TREATMENT OF PRION DISEASE

This work has revealed that C1 has the ability to inhibit both fibrillisation and conversion of full length PrP^C *in-vitro,* while Westergard and colleagues have shown that C1 plays a similar role when expressed *in vivo* (Westergard, Turnbaugh et al. 2011). As the C1 protein also does not act as a sufficient substrate for conversion to PK resistant PrP^{Sc} during disease, it may be a possible treatment for prion disease through the binding to PrP^{Sc}, preventing misfolding of PrP^C. Similar inhibitory effects have been illustrated in cell culture with the use of monoclonal antibodies specific to cellular PrP^C, which bind to PrP^C on the cell surface and block interaction and binding to incoming PrP^{Sc} (Peretz, Williamson et al. 2001). *In vivo,* murine models infected intraperitoneally showed a marked decrease in PrP^{Sc} accumulation, after treatment with PrP^C conformation dependent monoclonal antibodies (Sigurdsson, Sy et al. 2003, White, Enever et al. 2003). Mice infected intracranially or those treated after the onset of clinical signs showed no such clearance of infection (White, Enever et al. 2003), indicating that monoclonal antibodies may be useful in the clearance of infection from the periphery. However, as they cannot cross the blood brain barrier they are inert once infection has reached the brain. Although they may be

considered a useful tool treat those which have been exposed to a known risk factor, monoclonal antibodies could not be used to improve prognosis for those with clinical prion infection. It is for this reason that C1 may be considered as an alternative or combination therapy. C1 is normally expressed in the brain and over expression of C1 has been shown to have no neurotoxic effects, indicating that increasing the amount of C1 in the brain as a treatment is unlikely to have negative implications (Westergard, Turnbaugh et al. 2011). Furthermore, as the mechanism of C1 is likely to involve binding to PrP^{Sc} and not to cellular PrP^{C}, it is unlikely to interfere with cellular PrP^{C} function or recycling. There are several possible application strategies. The first of these would involve the identification of the protease responsible for cleavage in the brain and the manipulation of activity through pharmacological activation. The main problems with this approach are the lack of possible protease candidates and, if successful, the possible downstream effects on other proteins leading to functional implications in the brain. The second option is to artificially introduce C1 into the brain with a viral vector such as lentivirus, to deliver and express C1 in brain cells. This has been a successful delivery system for PrP 167R, which prolonged incubation times and alleviated behavioral symptoms in infected mouse models (Toupet, Compan et al. 2008).

A scaled up cell culture experiment, similar to that presented in this thesis, in which cells are treated with C1 at both different concentrations and at different time points may be very useful to determine the potential of C1 as a therapeutic in the treatment of prion disease.

7.4. IMPLICATIONS OF VARYING LEVELS OF PrP^C FRAGMENTS IN DEVELOPMENT OF DISEASE

7.4.1 Cancer

With the knowledge that truncated PrP^C proteins account for such a large percentage of total PrP^C in the brain, it would be interesting to measure proteolytic processing in peripheral tissues, such as the gastrointestinal tract and investigate the influence of such fragments on anti-apoptotic functions. PrP^C domain function in carcinogenic cellular invasion has been investigated through the production of deletion mutants PrPΔ4-90, PrPΔ51-90 and PrPΔ96-230. Only the deletion of the N-terminal from amino acids 4-90 had an inhibitory effect on the invasion ability of these cells (Pan, Zhao et al. 2006). If we assume that α-cleavage occurs in these tissues it is likely that N1 expression and secretion will not only promote cellular invasion but also have a anti-apoptotic effect, similar to that associated with expression of full length PrP^C. N1 has been shown to reduce staurosporin-stimulated caspase activation by down regulating p53 and subsequently protecting neuronal cells from apoptosis (Guillot-Sestier, Sunyach et al. 2009). Furthermore, removal of the PrP^C octopeptide repeat and C-terminal mutations, specifically, T183A and D178N, can reduce or ablate anti-apoptotic function in neuronal cells (Bounhar, Zhang et al. 2001). Speculatively, if these mutations in the C-terminal can result in functional alterations perhaps common polymorphisms in the human *PRNP* gene and ovine polymorphisms such as those at amino acid positions 136, 154 and 171 also have such an effect on anti-apoptotic functions and subsequently have a determining role in the development and treatment of both breast and gastric cancers.

7.4.2 Alzheimer's disease

If we consider the amino acids of PrP^C we known to be essential to involvement in the development of Alzheimer's disease it is difficult to predict if either α- or β- cleavage would hinder these functions. Both cleavage events leave the regions essential to binding intact (Figure 7.1, ovine amino acid numbering). *In vitro* peptides encompassing the region of amino acids 96-114 can inhibit fibril formation of Aβ (Younan, Sarell et al. 2013) implying that the smaller N-terminal binding site is not required in unison. We can speculate therefore that N1 and C2 truncated protein fragments could potentially be involved in the binding of misfolded Aβ peptides during Alzheimer's Disease. In fact, both Fluharty and colleagues (Fluharty, Biasini et al. 2013) and Béland and colleagues (Béland, Motard et al. 2012) have shown that N1 can bind Aβ oligomers and reduce Aβ-mediated cell death and toxicity both in cell culture and using murine models of Alzheimer's, perhaps through down regulation of the caspase 3 pathway. This indicates that α-cleavage not only plays a protective role in prion disease but also during Alzheimer's disease.

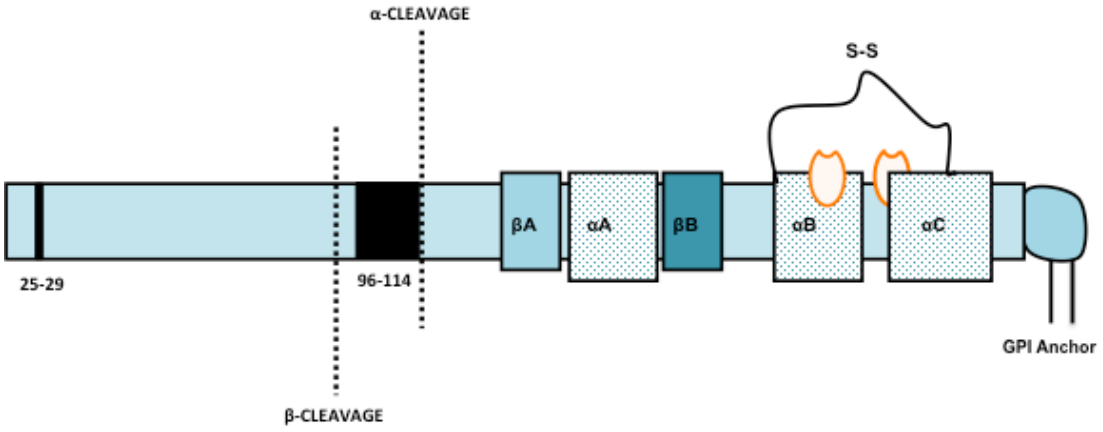

Figure 7.1 – PrP^C domains involved in the binding to Aβ. A linear model of ovine PrP^C with both α- and β- cleavage sites. The domains implicated in binding to Aβ peptides (numbering converted from murine PrP) are highlighted in black.

7.6. FUTURE DIRECTIONS

The most common natural route of infection in sheep is through oral ingestion, when PrP^{Sc} is imported to the CNS via the lymphoid system. Therefore α-cleavage levels may be important in predicting the outcome of early stages of infection. High levels of C1 in the periphery could stop PrP^{Sc} accumulation and infection of the brain. Measurement of α-cleavage in the periphery and lymphoid system of sheep with varying resistance to TSE disease would identify if similar genotypic variations are present as identified in the brain. A correlation in cleavage levels between the periphery and the brain would allow for tissue sampling and molecular analysis to be performed alongside genotyping to predict the susceptibility of a particular animal to scrapie infection. If performed prior to experimental infection, the influence of C1 levels in parallel with *PRNP* genotype on outcome of infection could be explored. Along with *in vivo* analysis, further *in vitro* conversion assays could be performed to investigate the role of C1 in conversion. Further cell free conversion assays should be performed in which $C1^{ARR}$ and C1 representing cleavage fragments with resistance polymorphisms from other species could be mixed with both murine and human recombinant PrP to assess inhibitory effects. In parallel, PMCA could also be implemented. PMCA uses brain homogenate as both substrate and inoculum, meaning all cellular cofactors will be present and unlike both cell free conversion and fibrillisation reactions, PrP is the native, mammalian expressed protein with post-translational modifications. Addition of C1 into these assays would help to close the current gap between *in vitro* and *in vivo* inhibitory functions. Following on from these experiments, large scale cell infection experiments could be set up to further investigate whether exogenous application of recombinant C1, post infection can decrease PrP^{Sc} accumulation. If findings mimic the outcomes of the small-scale preliminary experiment

then perhaps C1's ability to inhibit conversion could be investigated in mouse models of infection. Mice could be dosed with scrapie and subsequently administered C1 directly into the brain at different time points post infection. Both PrP^{Sc} accumulation, histology and survival time could be monitored.

REFERENCES

Alfa Cisse, M., K. Louis, U. Braun, B. Mari, M. Leitges, B. E. Slack, A. Fisher, P. Auberger, F. Checler and B. Vincent (2008). "Isoform-specific contribution of protein kinase C to prion processing." Mol Cell Neurosci **39**(3): 400-410.
Alfa Cisse, M., C. Sunyach, B. E. Slack, A. Fisher, B. Vincent and F. Checler (2007). "M1 and M3 muscarinic receptors control physiological processing of cellular prion by modulating ADAM17 phosphorylation and activity." J Neurosci **27**(15): 4083-4092.
Allinson, T. M., E. T. Parkin, A. J. Turner and N. M. Hooper (2003). "ADAMs family members as amyloid precursor protein alpha-secretases." J Neurosci Res **74**(3): 342-352.
Almstedt, K., S. Nystrom, K. P. Nilsson and P. Hammarstrom (2009). "Amyloid fibrils of human prion protein are spun and woven from morphologically disordered aggregates." Prion **3**(4): 224-235.
Alper, T., D. A. Haig and M. C. Clarke (1966). "The exceptionally small size of the scrapie agent." Biochem Biophys Res Commun **22**(3): 278-284.
Altmeppen, H. C., J. Prox, B. Puig, M. A. Kluth, C. Bernreuther, D. Thurm, E. Jorissen, B. Petrowitz, U. Bartsch, B. De Strooper, P. Saftig and M. Glatzel (2011). "Lack of a-disintegrin-and-metalloproteinase ADAM10 leads to intracellular accumulation and loss of shedding of the cellular prion protein in vivo." Mol Neurodegener **6**: 36.
Alvarez-Martinez, M. T., P. Fontes, V. Zomosa-Signoret, J. D. Arnaud, E. Hingant, L. Pujo-Menjouet and J. P. Liautard (2011). "Dynamics of polymerization shed light on the mechanisms that lead to multiple amyloid structures of the prion protein." Biochim Biophys Acta **1814**(10): 1305-1317.
Amos, S., M. Mut, C. G. diPierro, J. E. Carpenter, A. Xiao, Z. A. Kohutek, G. T. Redpath, Y. Zhao, J. Wang, M. E. Shaffrey and I. M. Hussaini (2007). "Protein kinase C-alpha-mediated regulation of low-density lipoprotein receptor related protein and urokinase increases astrocytoma invasion." Cancer Res **67**(21): 10241-10251.
Andreoletti, O., P. Berthon, D. Marc, P. Sarradin, J. Grosclaude, L. van Keulen, F. Schelcher, J. M. Elsen and F. Lantier (2000). "Early accumulation of PrP(Sc) in gut-associated lymphoid and nervous tissues of susceptible sheep from a Romanov flock with natural scrapie." J Gen Virol **81**(Pt 12): 3115-3126.
Andréoletti, O., L. Orge, S. L. Benestad, V. Beringue, C. Litaise, S. Simon, A. Le Dur, H. Laude, H. Simmons, S. Lugan, F. Corbière, P. Costes, N. Morel, F. Schelcher and C. Lacroux (2011). "Atypical/Nor98 scrapie infectivity in sheep peripheral tissues." PLoS Pathog **7**(2): e1001285.
Apetri, A. C., D. L. Vanik and W. K. Surewicz (2005). "Polymorphism at residue 129 modulates the conformational conversion of the D178N variant of human prion protein 90-231." Biochemistry **44**(48): 15880-15888.
Asai, M., C. Hattori, B. Szabo, N. Sasagawa, K. Maruyama, S. Tanuma and S. Ishiura (2003). "Putative function of ADAM9, ADAM10, and ADAM17 as APP alpha-secretase." Biochem Biophys Res Commun **301**(1): 231-235.

Azevedo, F. A., L. R. Carvalho, L. T. Grinberg, J. M. Farfel, R. E. Ferretti, R. E. Leite, W. Jacob Filho, R. Lent and S. Herculano-Houzel (2009). "Equal numbers of neuronal and nonneuronal cells make the human brain an isometrically scaled-up primate brain." J Comp Neurol **513**(5): 532-541.
Balkema-Buschmann, A., C. Fast, M. Kaatz, M. Eiden, U. Ziegler, L. McIntyre, M. Keller, B. Hills and M. H. Groschup (2011). "Pathogenesis of classical and atypical BSE in cattle." Prev Vet Med **102**(2): 112-117.
Barron, R. M., S. L. Campbell, D. King, A. Bellon, K. E. Chapman, R. A. Williamson and J. C. Manson (2007). "High titers of transmissible spongiform encephalopathy infectivity associated with extremely low levels of PrPSc in vivo." J Biol Chem **282**(49): 35878-35886.
Baskakov, I., P. Disterer, L. Breydo, M. Shaw, A. Gill, W. James and A. Tahiri-Alaoui (2005). "The presence of valine at residue 129 in human prion protein accelerates amyloid formation." FEBS Lett **579**(12): 2589-2596.
Baylis, M., C. Chihota, E. Stevenson, W. Goldmann, A. Smith, K. Sivam, S. Tongue and M. B. Gravenor (2004). "Risk of scrapie in British sheep of different prion protein genotype." J Gen Virol **85**(Pt 9): 2735-2740.
Baylis, M. and W. Goldmann (2004). "The genetics of scrapie in sheep and goats." Curr Mol Med **4**(4): 385-396.
Béland, M., J. Motard, A. Barbarin and X. Roucou (2012). "PrP(C) homodimerization stimulates the production of PrPC cleaved fragments PrPN1 and PrPC1." J Neurosci **32**(38): 13255-13263.
Bellesia, G. and J. E. Shea (2009). "Diversity of kinetic pathways in amyloid fibril formation." J Chem Phys **131**(11): 111102.
Benestad, S. L., J. N. Arsac, W. Goldmann and M. Nöremark (2008). "Atypical/Nor98 scrapie: properties of the agent, genetics, and epidemiology." Vet Res **39**(4): 19.
Benestad, S. L., P. Sarradin, B. Thu, J. Schonheit, M. A. Tranulis and B. Bratberg (2003). "Cases of scrapie with unusual features in Norway and designation of a new type, Nor98." Vet Rec **153**(7): 202-208.
Beringue, V., G. Mallinson, M. Kaisar, M. Tayebi, Z. Sattar, G. Jackson, D. Anstee, J. Collinge and S. Hawke (2003). "Regional heterogeneity of cellular prion protein isoforms in the mouse brain." Brain **126**(Pt 9): 2065-2073.
Biancalana, M. and S. Koide (2010). "Molecular mechanism of Thioflavin-T binding to amyloid fibrils." Biochim Biophys Acta **1804**(7): 1405-1412.
Birkett, C. R., R. M. Hennion, D. A. Bembridge, M. C. Clarke, A. Chree, M. E. Bruce and C. J. Bostock (2001). "Scrapie strains maintain biological phenotypes on propagation in a cell line in culture." EMBO J **20**(13): 3351-3358.
Bishop, M. T., P. Hart, L. Aitchison, H. N. Baybutt, C. Plinston, V. Thomson, N. L. Tuzi, M. W. Head, J. W. Ironside, R. G. Will and J. C. Manson (2006). "Predicting susceptibility and incubation time of human-to-human transmission of vCJD." Lancet Neurol **5**(5): 393-398.
Bocharova, O. V., L. Breydo, A. S. Parfenov, V. V. Salnikov and I. V. Baskakov (2005). "In vitro conversion of full-length mammalian prion protein produces amyloid form with physical properties of PrP(Sc)." J Mol Biol **346**(2): 645-659.
Bocharova, O. V., N. Makarava, L. Breydo, M. Anderson, V. V. Salnikov and I. V. Baskakov (2006). "Annealing prion protein amyloid fibrils at high temperature

results in extension of a proteinase K-resistant core." J Biol Chem **281**(4): 2373-2379.
Borchelt, D. R., M. Rogers, N. Stahl, G. Telling and S. B. Prusiner (1993). "Release of the cellular prion protein from cultured cells after loss of its glycoinositol phospholipid anchor." Glycobiology **3**(4): 319-329.
Bosque, P. J. and S. B. Prusiner (2000). "Cultured cell sublines highly susceptible to prion infection." J Virol **74**(9): 4377-4386.
Bosques, C. J. and B. Imperiali (2003). "The interplay of glycosylation and disulfide formation influences fibrillization in a prion protein fragment." Proc Natl Acad Sci U S A **100**(13): 7593-7598.
Bossers, A., P. Belt, G. J. Raymond, B. Caughey, R. de Vries and M. A. Smits (1997). "Scrapie susceptibility-linked polymorphisms modulate the in vitro conversion of sheep prion protein to protease-resistant forms." Proc Natl Acad Sci U S A **94**(10): 4931-4936.
Bossers, A., R. de Vries and M. A. Smits (2000). "Susceptibility of sheep for scrapie as assessed by in vitro conversion of nine naturally occurring variants of PrP." J Virol **74**(3): 1407-1414.
Bossers, A., B. E. Schreuder, I. H. Muileman, P. B. Belt and M. A. Smits (1996). "PrP genotype contributes to determining survival times of sheep with natural scrapie." J Gen Virol **77 (Pt 10)**: 2669-2673.
Bounhar, Y., Y. Zhang, C. G. Goodyer and A. LeBlanc (2001). "Prion protein protects human neurons against Bax-mediated apoptosis." J Biol Chem **276**(42): 39145-39149.
Bremer, J., F. Baumann, C. Tiberi, C. Wessig, H. Fischer, P. Schwarz, A. D. Steele, K. V. Toyka, K. A. Nave, J. Weis and A. Aguzzi (2010). "Axonal prion protein is required for peripheral myelin maintenance." Nat Neurosci **13**(3): 310-318.
Breydo, L., N. Makarava and I. V. Baskakov (2008). "Methods for conversion of prion protein into amyloid fibrils." Methods Mol Biol **459**: 105-115.
Brockes, J. P. (1999). "Topics in prion cell biology." Curr Opin Neurobiol **9**(5): 571-577.
Brown, D. R. (1999). "Prion protein expression aids cellular uptake and veratridine-induced release of copper." J Neurosci Res **58**(5): 717-725.
Bruce, M., A. Chree, I. McConnell, J. Foster, G. Pearson and H. Fraser (1994). "Transmission of bovine spongiform encephalopathy and scrapie to mice: strain variation and the species barrier." Philos Trans R Soc Lond B Biol Sci **343**(1306): 405-411.
Bruce, M. E., K. L. Brown, N. A. Mabbott, C. F. Farquhar and M. Jeffrey (2000). "Follicular dendritic cells in TSE pathogenesis." Immunol Today **21**(9): 442-446.
Bucalossi, C., G. Cosseddu, C. D'Agostino, M. A. Di Bari, B. Chiappini, M. Conte, F. Rosone, L. De Grossi, G. Scavia, U. Agrimi, R. Nonno and G. Vaccari (2011). "Assessment of the genetic susceptibility of sheep to scrapie by PMCA and comparison with experimental scrapie transmission studies." J Virol.
Bueler, H., A. Aguzzi, A. Sailer, R. A. Greiner, P. Autenried, M. Aguet and C. Weissmann (1993). "Mice devoid of PrP are resistant to scrapie." Cell **73**(7): 1339-1347.

Bujdoso, R., D. F. Burke and A. M. Thackray (2005). "Structural differences between allelic variants of the ovine prion protein revealed by molecular dynamics simulations." Proteins-Structure Function and Bioinformatics **61**(4): 840-849.
Cancellotti, E., B. M. Bradford, N. L. Tuzi, R. D. Hickey, D. Brown, K. L. Brown, R. M. Barron, D. Kisielewski, P. Piccardo and J. C. Manson (2010). "Glycosylation of PrPC determines timing of neuroinvasion and targeting in the brain following transmissible spongiform encephalopathy infection by a peripheral route." J Virol **84**(7): 3464-3475.
Cancellotti, E., S. P. Mahal, R. Somerville, A. Diack, D. Brown, P. Piccardo, C. Weissmann and J. C. Manson (2013). "Post-translational changes to PrP alter transmissible spongiform encephalopathy strain properties." EMBO J **32**(5): 756-769.
Cancellotti, E., F. Wiseman, N. L. Tuzi, H. Baybutt, P. Monaghan, L. Aitchison, J. Simpson and J. C. Manson (2005). "Altered glycosylated PrP proteins can have different neuronal trafficking in brain but do not acquire scrapie-like properties." J Biol Chem **280**(52): 42909-42918.
Caplazi, P. A., K. I. O'Rourke and T. V. Baszler (2004). "Resistance to scrapie in PrP ARR/ARQ heterozygous sheep is not caused by preferential allelic use." J Clin Pathol **57**(6): 647-650.
Capobianco, R., C. Casalone, S. Suardi, M. Mangieri, C. Miccolo, L. Limido, M. Catania, G. Rossi, G. Di Fede, G. Giaccone, M. G. Bruzzone, L. Minati, C. Corona, P. Acutis, D. Gelmetti, G. Lombardi, M. H. Groschup, A. Buschmann, G. Zanusso, S. Monaco, M. Caramelli and F. Tagliavini (2007). "Conversion of the BASE prion strain into the BSE strain: the origin of BSE?" PLoS Pathog **3**(3): e31.
Cardone, F., Q. G. Liu, R. Petraroli, A. Ladogana, M. D'Alessandro, C. Arpino, M. Di Bari, G. Macchi and M. Pocchiari (1999). "Prion protein glycotype analysis in familial and sporadic Creutzfeldt-Jakob disease patients." Brain Res Bull **49**(6): 429-433.
Casalone, C., G. Zanusso, P. Acutis, S. Ferrari, L. Capucci, F. Tagliavini, S. Monaco and M. Caramelli (2004). "Identification of a second bovine amyloidotic spongiform encephalopathy: molecular similarities with sporadic Creutzfeldt-Jakob disease." Proc Natl Acad Sci U S A **101**(9): 3065-3070.
Chabry, J., S. A. Priola, K. Wehrly, J. Nishio, J. Hope and B. Chesebro (1999). "Species-independent inhibition of abnormal prion protein (PrP) formation by a peptide containing a conserved PrP sequence." J Virol **73**(8): 6245-6250.
Chandler, R. L. and J. Fisher (1963). "Experimental transmission of scrapie to rats." Lancet **2**(7318): 1165.
Chen, S. G., D. B. Teplow, P. Parchi, J. K. Teller, P. Gambetti and L. Autilio-Gambetti (1995). "Truncated forms of the human prion protein in normal brain and in prion diseases." J Biol Chem **270**(32): 19173-19180.
Chen, S. G., S. P. Yadav and W. K. Surewicz (2010). "Interaction between Human Prion Protein and Amyloid-beta (A beta) Oligomers role of N-terminal residues." Journal of Biological Chemistry **285**(34): 26377-26383.
Chesebro, B. (2003). "Introduction to the transmissible spongiform encephalopathies or prion diseases." Br Med Bull **66**: 1-20.

Chianini, F., N. Fernandez-Borges, E. Vidal, L. Gibbard, B. Pintado, J. de Castro, S. A. Priola, S. Hamilton, S. L. Eaton, J. Finlayson, Y. Pang, P. Steele, H. W. Reid, M. P. Dagleish and J. Castilla (2012). "Rabbits are not resistant to prion infection." Proc Natl Acad Sci U S A **109**(13): 5080-5085.
Christen, Y. (2000). "Oxidative stress and Alzheimer disease." American Journal of Clinical Nutrition **71**(2): 621S-629S.
Cisse, M. A., C. Sunyach, S. Lefranc-Jullien, R. Postina, B. Vincent and F. Checler (2005). "The disintegrin ADAM9 indirectly contributes to the physiological processing of cellular prion by modulating ADAM10 activity." J Biol Chem **280**(49): 40624-40631.
Clarke, M. C. and D. A. Haig (1970). "Evidence for the multiplication of scrapie agent in cell culture." Nature **225**(5227): 100-101.
Clouscard, C., P. Beaudry, J. M. Elsen, D. Milan, M. Dussaucy, C. Bounneau, F. Schelcher, J. Chatelain, J. M. Launay and J. L. Laplanche (1995). "Different allelic effects of the codons 136 and 171 of the prion protein gene in sheep with natural scrapie." J Gen Virol **76 (Pt 8)**: 2097-2101.
Collinge, J., M. A. Whittington, K. C. Sidle, C. J. Smith, M. S. Palmer, A. R. Clarke and J. G. Jefferys (1994). "Prion protein is necessary for normal synaptic function." Nature **370**(6487): 295-297.
Collins, S., C. A. McLean and C. L. Masters (2001). "Gerstmann-Sträussler-Scheinker syndrome,fatal familial insomnia, and kuru: a review of these less common human transmissible spongiform encephalopathies." J Clin Neurosci **8**(5): 387-397.
Compton, L. A. and W. C. Johnson, Jr. (1986). "Analysis of protein circular dichroism spectra for secondary structure using a simple matrix multiplication." Anal Biochem **155**(1): 155-167.
Criado, J. R., M. Sanchez-Alavez, B. Conti, J. L. Giacchino, D. N. Wills, S. J. Henriksen, R. Race, J. C. Manson, B. Chesebro and M. B. Oldstone (2005). "Mice devoid of prion protein have cognitive deficits that are rescued by reconstitution of PrP in neurons." Neurobiol Dis **19**(1-2): 255-265.
Crozet, C., F. Beranger and S. Lehmann (2008). "Cellular pathogenesis in prion diseases." Vet Res **39**(4): 44.
Dealler, S. and N. G. Rainov (2003). "Pentosan polysulfate as a prophylactic and therapeutic agent against prion disease." IDrugs **6**(5): 470-478.
Diaz-San Segundo, F., F. J. Salguero, A. de Avila, J. C. Espinosa, J. M. Torres and A. Brun (2006). "Distribution of the cellular prion protein (PrPC) in brains of livestock and domesticated species." Acta Neuropathol **112**(5): 587-595.
Dron, M., M. Moudjou, J. Chapuis, M. K. Salamat, J. Bernard, S. Cronier, C. Langevin and H. Laude (2010). "Endogenous proteolytic cleavage of disease-associated prion protein to produce C2 fragments is strongly cell- and tissue-dependent." J Biol Chem **285**(14): 10252-10264.
Du, J., Y. Pan, Y. Shi, C. Guo, X. Jin, L. Sun, N. Liu, T. Qiao and D. Fan (2005). "Overexpression and significance of prion protein in gastric cancer and multidrug-resistant gastric carcinoma cell line SGC7901/ADR." Int J Cancer **113**(2): 213-220.
Eiden, M., E. O. Soto, T. C. Mettenleiter and M. H. Groschup (2011). "Effects of polymorphisms in ovine and caprine prion protein alleles on cell-free conversion." Vet Res **42**(1): 30.

Elfrink, K., J. Ollesch, J. Stohr, D. Willbold, D. Riesner and K. Gerwert (2008). "Structural changes of membrane-anchored native PrP(C)." Proc Natl Acad Sci U S A **105**(31): 10815-10819.
Endres, K., G. Mitteregger, E. Kojro, H. Kretzschmar and F. Fahrenholz (2009). "Influence of ADAM10 on prion protein processing and scrapie infectiosity in vivo." Neurobiol Dis **36**(2): 233-241.
Espinosa, J. C., M. E. Herva, O. Andréoletti, D. Padilla, C. Lacroux, H. Cassard, I. Lantier, J. Castilla and J. M. Torres (2009). "Transgenic mice expressing porcine prion protein resistant to classical scrapie but susceptible to sheep bovine spongiform encephalopathy and atypical scrapie." Emerg Infect Dis **15**(8): 1214-1221.
Finkel, T. and N. J. Holbrook (2000). "Oxidants, oxidative stress and the biology of ageing." Nature **408**(6809): 239-247.
Ford, M. J., L. J. Burton, H. Li, C. H. Graham, Y. Frobert, J. Grassi, S. M. Hall and R. J. Morris (2002). "A marked disparity between the expression of prion protein and its message by neurones of the CNS." Neuroscience **111**(3): 533-551.
Foster, J. D., W. A. McKelvey, M. J. Mylne, A. Williams, N. Hunter, J. Hope and H. Fraser (1992). "Studies on maternal transmission of scrapie in sheep by embryo transfer." Vet Rec **130**(16): 341-343.
Genoud, N., A. Behrens, I. Arrighi and A. Aguzzi (2003). "Prion proteins and infertility: insight from mouse models." Cytogenet Genome Res **103**(3-4): 285-289.
Geoghegan, K. F., H. B. Dixon, P. J. Rosner, L. R. Hoth, A. J. Lanzetti, K. A. Borzilleri, E. S. Marr, L. H. Pezzullo, L. B. Martin, P. K. LeMotte, A. S. McColl, A. V. Kamath and J. G. Stroh (1999). "Spontaneous alpha-N-6-phosphogluconoylation of a "His tag" in Escherichia coli: the cause of extra mass of 258 or 178 Da in fusion proteins." Anal Biochem **267**(1): 169-184.
Gibbons, R. A. and G. D. Hunter (1967). "Nature of the scrapie agent." Nature **215**(5105): 1041-1043.
Gibbs, C. J. and D. C. Gajdusek (1973). "Experimental subacute spongiform virus encephalopathies in primates and other laboratory animals." Science **182**(4107): 67-68.
Gimbel, D. A., H. B. Nygaard, E. E. Coffey, E. C. Gunther, J. Lauren, Z. A. Gimbel and S. M. Strittmatter (2010). "Memory Impairment in Transgenic Alzheimer Mice Requires Cellular Prion Protein." Journal of Neuroscience **30**(18): 6367-6374.
Goedert, M. (1987). "Neuronal localization of amyloid beta protein precursor mRNA in normal human brain and in Alzheimer's disease." EMBO J **6**(12): 3627-3632.
Goldmann, W. (1993). "PrP gene and its association with spongiform encephalopathies." Br Med Bull **49**(4): 839-859.
Goldmann, W. (2008). "PrP genetics in ruminant transmissible spongiform encephalopathies." Vet Res **39**(4): 30.
Goldmann, W., N. Hunter, G. Benson, J. D. Foster and J. Hope (1991). "Different scrapie-associated fibril proteins (PrP) are encoded by lines of sheep selected for different alleles of the Sip gene." J Gen Virol **72 (Pt 10)**: 2411-2417.

Goldmann, W., N. Hunter, J. D. Foster, J. M. Salbaum, K. Beyreuther and J. Hope (1990). "Two alleles of a neural protein gene linked to scrapie in sheep." Proc Natl Acad Sci U S A **87**(7): 2476-2480.
Goldmann, W., N. Hunter, G. Smith, J. Foster and J. Hope (1994). "PrP genotype and agent effects in scrapie: change in allelic interaction with different isolates of agent in sheep, a natural host of scrapie." J Gen Virol **75 (Pt 5)**: 989-995.
Goldmann, W., T. Martin, J. Foster, S. Hughes, G. Smith, K. Hughes, M. Dawson and N. Hunter (1996). "Novel polymorphisms in the caprine PrP gene: a codon 142 mutation associated with scrapie incubation period." J Gen Virol **77 (Pt 11)**: 2885-2891.
Goldmann, W., K. Ryan, P. Stewart, D. Parnham, R. Xicohtencatl, N. Fernandez, G. Saunders, O. Windl, L. Gonzalez, A. Bossers and J. Foster (2011). "Caprine prion gene polymorphisms are associated with decreased incidence of classical scrapie in goat herds in the United Kingdom." Vet Res **42**(1): 110.
Graham, J. F., S. Agarwal, D. Kurian, L. Kirby, T. J. Pinheiro and A. C. Gill (2010). "Low density subcellular fractions enhance disease-specific prion protein misfolding." J Biol Chem **285**(13): 9868-9880.
Graham, J. F., D. Kurian, S. Agarwal, L. Toovey, L. Hunt, L. Kirby, T. J. Pinheiro, S. J. Banner and A. C. Gill (2011). "Na+/K+-ATPase is present in scrapie-associated fibrils, modulates PrP misfolding in vitro and links PrP function and dysfunction." PLoS One **6**(11): e26813.
Guentchev, M., T. Voigtlander, C. Haberler, M. H. Groschup and H. Budka (2000). "Evidence for oxidative stress in experimental prion disease." Neurobiology of Disease **7**(4): 270-273.
Guillot-Sestier, M. V., C. Sunyach, C. Druon, S. Scarzello and F. Checler (2009). "The alpha-secretase-derived N-terminal product of cellular prion, N1, displays neuroprotective function in vitro and in vivo." J Biol Chem **284**(51): 35973-35986.
Hachiya, N., Y. Komata, S. Harguem, K. Nishijima and K. Kaneko (2011). "Possible involvement of calpain-like activity in normal processing of cellular prion protein." Neurosci Lett **490**(2): 150-155.
Haïk, S., K. Peoc'h, J. P. Brandel, N. Privat, J. L. Laplanche, B. A. Faucheux and J. J. Hauw (2004). "Striking PrPsc heterogeneity in inherited prion diseases with the D178N mutation." Ann Neurol **56**(6): 909-910; author reply 910-901.
Haire, L. F., S. M. Whyte, N. Vasisht, A. C. Gill, C. Verma, E. J. Dodson, G. G. Dodson and P. M. Bayley (2004). "The crystal structure of the globular domain of sheep prion protein." Journal of Molecular Biology **336**(5): 1175-1183.
Halliday, S., F. Houston and N. Hunter (2005). "Expression of PrPC on cellular components of sheep blood." J Gen Virol **86**(Pt 5): 1571-1579.
Harries-Jones, R., R. Knight, R. G. Will, S. Cousens, P. G. Smith and W. B. Matthews (1988). "Creutzfeldt-Jakob disease in England and Wales, 1980-1984: a case-control study of potential risk factors." J Neurol Neurosurg Psychiatry **51**(9): 1113-1119.
Harris, D. A. (1999). "Cellular biology of prion diseases." Clin Microbiol Rev **12**(3): 429-444.
Harris, D. A. (2003). "Trafficking, turnover and membrane topology of PrP." Br Med Bull **66**: 71-85.

Holscher, C., H. Delius and A. Burkle (1998). "Overexpression of nonconvertible PrPc delta114-121 in scrapie-infected mouse neuroblastoma cells leads to trans-dominant inhibition of wild-type PrP(Sc) accumulation." J Virol **72**(2): 1153-1159.
Hornshaw, M. P., J. R. McDermott and J. M. Candy (1995). "Copper binding to the N-terminal tandem repeat regions of mammalian and avian prion protein." Biochem Biophys Res Commun **207**(2): 621-629.
Houston, F., W. Goldmann, A. Chong, M. Jeffrey, L. Gonzalez, J. Foster, D. Parnham and N. Hunter (2003). "Prion diseases: BSE in sheep bred for resistance to infection." Nature **423**(6939): 498.
Hsiao, K., H. F. Baker, T. J. Crow, M. Poulter, F. Owen, J. D. Terwilliger, D. Westaway, J. Ott and S. B. Prusiner (1989). "Linkage of a prion protein missense variant to Gerstmann-Sträussler syndrome." Nature **338**(6213): 342-345.
Huber, R., T. Deboer and I. Tobler (2002). "Sleep deprivation in prion protein deficient mice sleep deprivation in prion protein deficient mice and control mice: genotype dependent regional rebound." Neuroreport **13**(1): 1-4.
Hunter, N. (2007). "Scrapie: uncertainties, biology and molecular approaches." Biochim Biophys Acta **1772**(6): 619-628.
Hunter, N., W. Goldmann, G. Smith and J. Hope (1994). "The association of a codon 136 PrP gene variant with the occurrence of natural scrapie." Arch Virol **137**(1-2): 171-177.
Iannuzzi, L., R. Palomba, G. P. Di Meo, A. Perucatti and L. Ferrara (1998). "Comparative FISH-mapping of the prion protein gene (PRNP) on cattle, river buffalo, sheep and goat chromosomes." Cytogenet Cell Genet **81**(3-4): 202-204.
Jacobs, J. G., A. Bossers, H. Rezaei, L. J. van Keulen, S. McCutcheon, T. Sklaviadis, I. Lantier, P. Berthon, F. Lantier, F. G. van Zijderveld and J. P. Langeveld (2011). "Proteinase K resistant material in ARR/VRQ sheep brain affected with classical scrapie is mainly composed of VRQ prion protein." J Virol.
Jimenez-Huete, A., P. M. Lievens, R. Vidal, P. Piccardo, B. Ghetti, F. Tagliavini, B. Frangione and F. Prelli (1998). "Endogenous proteolytic cleavage of normal and disease-associated isoforms of the human prion protein in neural and non-neural tissues." Am J Pathol **153**(5): 1561-1572.
Kang, Y. S., X. Zhao, J. Lovaas, E. Eisenberg and L. E. Greene (2009). "Clathrin-independent internalization of normal cellular prion protein in neuroblastoma cells is associated with the Arf6 pathway." J Cell Sci **122**(Pt 22): 4062-4069.
Karapetyan, Y. E., G. F. Sferrazza, M. Zhou, G. Ottenberg, T. Spicer, P. Chase, M. Fallahi, P. Hodder, C. Weissmann and C. I. Lasmézas (2013). "Unique drug screening approach for prion diseases identifies tacrolimus and astemizole as antiprion agents." Proc Natl Acad Sci U S A **110**(17): 7044-7049.
Kellett, K. A. B. and N. M. Hooper (2009). "Prion protein and Alzheimer disease." Prion **3**(4): 190-194.
Kirby, L., S. Agarwal, J. F. Graham, W. Goldmann and A. C. Gill (2010). "Inverse correlation of thermal lability and conversion efficiency for five prion protein polymorphic variants." Biochemistry **49**(7): 1448-1459.
Kirby, L., W. Goldmann, F. Houston, A. C. Gill and J. C. Manson (2006). "A novel, resistance-linked ovine PrP variant and its equivalent mouse variant modulate the in vitro cell-free conversion of rPrP to PrP(res)." J Gen Virol **87**(Pt 12): 3747-3751.

Kocisko, D. A., J. H. Come, S. A. Priola, B. Chesebro, G. J. Raymond, P. T. Lansbury and B. Caughey (1994). "Cell-free formation of protease-resistant prion protein." Nature **370**(6489): 471-474.
Kocisko, D. A., S. A. Priola, G. J. Raymond, B. Chesebro, P. T. Lansbury and B. Caughey (1995). "Species specificity in the cell-free conversion of prion protein to protease-resistant forms: a model for the scrapie species barrier." Proc Natl Acad Sci U S A **92**(9): 3923-3927.
Komolka, K., S. Ponsuksili and M. Schwerin (2013). "Healthy sheep that differ in scrapie associated PRNP genotypes exhibit significant differences of expression pattern associated with immune response and cell-to-cell signalling in retropharyngeal lymph nodes." Vet Immunol Immunopathol **152**(3-4): 370-380.
Konold, T., A. Davis, G. Bone, J. Bracegirdle, S. Everitt, M. Chaplin, G. C. Saunders, S. Cawthraw and M. M. Simmons (2007). "Clinical findings in two cases of atypical scrapie in sheep: a case report." BMC Vet Res **3**: 2.
Kramer, M. L., H. D. Kratzin, B. Schmidt, A. Romer, O. Windl, S. Liemann, S. Hornemann and H. Kretzschmar (2001). "Prion protein binds copper within the physiological concentration range." J Biol Chem **276**(20): 16711-16719.
Kuczius, T., J. Grassi, H. Karch and M. H. Groschup (2007). "Binding of N- and C-terminal anti-prion protein antibodies generates distinct phenotypes of cellular prion proteins (PrPC) obtained from human, sheep, cattle and mouse." FEBS J **274**(6): 1492-1502.
Kuczius, T., R. Koch, K. Keyvani, H. Karch, J. Grassi and M. H. Groschup (2007). "Regional and phenotype heterogeneity of cellular prion proteins in the human brain." Eur J Neurosci **25**(9): 2649-2655.
Laffont-Proust, I., B. A. Faucheux, R. Hassig, V. Sazdovitch, S. Simon, J. Grassi, J. J. Hauw, K. L. Moya and S. Haik (2005). "The N-terminal cleavage of cellular prion protein in the human brain." FEBS Lett **579**(28): 6333-6337.
Laffont-Proust, I., R. Hassig, S. Haik, S. Simon, J. Grassi, C. Fonta, B. A. Faucheux and K. L. Moya (2006). "Truncated PrP(c) in mammalian brain: interspecies variation and location in membrane rafts." Biol Chem **387**(3): 297-300.
Lampo, E., M. Van Poucke, K. Hugot, H. Hayes, A. Van Zeveren and L. J. Peelman (2007). "Characterization of the genomic region containing the Shadow of Prion Protein (SPRN) gene in sheep." BMC Genomics **8**: 138.
Laplanche, J. L., J. Chatelain, D. Westaway, S. Thomas, M. Dussaucy, J. Brugere-Picoux and J. M. Launay (1993). "PrP polymorphisms associated with natural scrapie discovered by denaturing gradient gel electrophoresis." Genomics **15**(1): 30-37.
Laude, H., D. Vilette, A. Le Dur, F. Archer, S. Soulier, N. Besnard, R. Essalmani and J. L. Vilotte (2002). "New in vivo and ex vivo models for the experimental study of sheep scrapie: development and perspectives." C R Biol **325**(1): 49-57.
Lawson, V. A., S. J. Collins, C. L. Masters and A. F. Hill (2005). "Prion protein glycosylation." J Neurochem **93**(4): 793-801.
Lawson, V. A., S. A. Priola, K. Meade-White, M. Lawson and B. Chesebro (2004). "Flexible N-terminal region of prion protein influences conformation of protease-resistant prion protein isoforms associated with cross-species scrapie infection in vivo and in vitro." J Biol Chem **279**(14): 13689-13695.

Lawson, V. A., S. A. Priola, K. Wehrly and B. Chesebro (2001). "N-terminal truncation of prion protein affects both formation and conformation of abnormal protease-resistant prion protein generated in vitro." J Biol Chem **276**(38): 35265-35271.
Lee, Y. J., R. Savtchenko, V. G. Ostapchenko, N. Makarava and I. V. Baskakov (2011). "Molecular structure of amyloid fibrils controls the relationship between fibrillar size and toxicity." PLoS One **6**(5): e20244.
Legname, G., I. V. Baskakov, H. O. Nguyen, D. Riesner, F. E. Cohen, S. J. DeArmond and S. B. Prusiner (2004). "Synthetic mammalian prions." Science **305**(5684): 673-676.
Lewis, P. A., M. H. Tattum, S. Jones, D. Bhelt, M. Batchelor, A. R. Clarke, J. Collinge and G. S. Jackson (2006). "Codon 129 polymorphism of the human prion protein influences the kinetics of amyloid formation." J Gen Virol **87**(Pt 8): 2443-2449.
Lewis, V., A. F. Hill, C. L. Haigh, G. M. Klug, C. L. Masters, V. A. Lawson and S. J. Collins (2009). "Increased proportions of C1 truncated prion protein protect against cellular M1000 prion infection." J Neuropathol Exp Neurol **68**(10): 1125-1135.
Liang, J., W. Wang, D. Sorensen, S. Medina, S. Ilchenko, J. Kiselar, W. K. Surewicz, S. A. Booth and Q. Kong (2012). "Cellular prion protein regulates its own alpha-cleavage through ADAM8 in skeletal muscle." J Biol Chem.
Ligios, C., M. Jeffrey, S. J. Ryder, S. J. Bellworthy and M. M. Simmons (2002). "Distinction of scrapie phenotypes in sheep by lesion profiling." J Comp Pathol **127**(1): 45-57.
Linden, R., V. R. Martins, M. A. Prado, M. Cammarota, I. Izquierdo and R. R. Brentani (2008). "Physiology of the prion protein." Physiol Rev **88**(2): 673-728.
Liu, Q., J. Zhang, H. Tran, M. M. Verbeek, K. Reiss, S. Estus and G. Bu (2009). "LRP1 shedding in human brain: roles of ADAM10 and ADAM17." Mol Neurodegener **4**: 17.
Lu, X., P. L. Wintrode and W. K. Surewicz (2007). "Beta-sheet core of human prion protein amyloid fibrils as determined by hydrogen/deuterium exchange." Proc Natl Acad Sci U S A **104**(5): 1510-1515.
Mabbott, N. A., C. F. Farquhar, K. L. Brown and M. E. Bruce (1998). "Involvement of the immune system in TSE pathogenesis." Immunol Today **19**(5): 201-203.
Manavalan, P. and W. C. Johnson, Jr. (1987). "Variable selection method improves the prediction of protein secondary structure from circular dichroism spectra." Anal Biochem **167**(1): 76-85.
Mange, A., F. Beranger, K. Peoc'h, T. Onodera, Y. Frobert and S. Lehmann (2004). "Alpha- and beta- cleavages of the amino-terminus of the cellular prion protein." Biol Cell **96**(2): 125-132.
Manson, J. C., A. R. Clarke, P. A. McBride, I. McConnell and J. Hope (1994). "PrP gene dosage determines the timing but not the final intensity or distribution of lesions in scrapie pathology." Neurodegeneration **3**(4): 331-340.
Martin, S., M. Jeffrey, L. González, S. Sisó, H. W. Reid, P. Steele, M. P. Dagleish, M. J. Stack, M. J. Chaplin and A. Balachandran (2009). "Immunohistochemical and biochemical characteristics of BSE and CWD in experimentally infected European red deer (Cervus elaphus elaphus)." BMC Vet Res **5**: 26.

Mays, C. E., J. Yeom, H. E. Kang, J. Bian, V. Khaychuk, Y. Kim, J. C. Bartz, G. C. Telling and C. Ryou (2011). "In vitro amplification of misfolded prion protein using lysate of cultured cells." PLoS One **6**(3): e18047.
McCutcheon, S., N. Hunter and F. Houston (2005). "Use of a new immunoassay to measure PrP Sc levels in scrapie-infected sheep brains reveals PrP genotype-specific differences." J Immunol Methods **298**(1-2): 119-128.
Meslin, F., R. Conforti, C. Mazouni, N. Morel, G. Tomasic, F. Drusch, M. Yacoub, J. C. Sabourin, J. Grassi, S. Delaloge, M. C. Mathieu, S. Chouaib, F. Andre and M. Mehrpour (2007). "Efficacy of adjuvant chemotherapy according to prion protein expression in patients with estrogen receptor-negative breast cancer." Annals of Oncology **18**(11): 1793-1798.
Mita, S., E. A. Schon and J. Herbert (1989). "Widespread expression of amyloid beta-protein precursor gene in rat brain." Am J Pathol **134**(6): 1253-1261.
Mitteregger, G., M. Vosko, B. Krebs, W. Xiang, V. Kohlmannsperger, S. Nolting, G. F. Hamann and H. A. Kretzschmar (2007). "The role of the octarepeat region in neuroprotective function of the cellular prion protein." Brain Pathol **17**(2): 174-183.
Monleon, E., M. Monzon, P. Hortells, R. Bolea, C. Acin, F. Vargas and J. J. Badiola (2005). "Approaches to Scrapie diagnosis by applying immunohistochemistry and rapid tests on central nervous and lymphoreticular systems." J Virol Methods **125**(2): 165-171.
Moore, R. A., I. Vorberg and S. A. Priola (2005). "Species barriers in prion diseases--brief review." Arch Virol Suppl(19): 187-202.
Moore, R. C., I. Y. Lee, G. L. Silverman, P. M. Harrison, R. Strome, C. Heinrich, A. Karunaratne, S. H. Pasternak, M. A. Chishti, Y. Liang, P. Mastrangelo, K. Wang, A. F. Smit, S. Katamine, G. A. Carlson, F. E. Cohen, S. B. Prusiner, D. W. Melton, P. Tremblay, L. E. Hood and D. Westaway (1999). "Ataxia in prion protein (PrP)-deficient mice is associated with upregulation of the novel PrP-like protein doppel." J Mol Biol **292**(4): 797-817.
Moudjou, M., Y. Frobert, J. Grassi and C. La Bonnardiere (2001). "Cellular prion protein status in sheep: tissue-specific biochemical signatures." J Gen Virol **82**(Pt 8): 2017-2024.
Moum, T., I. Olsaker, P. Hopp, T. Moldal, M. Valheim and S. L. Benestad (2005). "Polymorphisms at codons 141 and 154 in the ovine prion protein gene are associated with scrapie Nor98 cases." J Gen Virol **86**(Pt 1): 231-235.
Neale, M. H., S. J. Mountjoy, J. C. Edwards, D. Vilette, H. Laude, O. Windl and G. C. Saunders (2010). "Infection of cell lines with experimental and natural ovine scrapie agents." J Virol **84**(5): 2444-2452.
Nicolas, O., R. Gavin and J. A. del Rio (2009). "New insights into cellular prion protein (PrPc) functions: the "ying and yang" of a relevant protein." Brain Res Rev **61**(2): 170-184.
Nicot, S. and T. G. Baron (2010). "Strain-specific proteolytic processing of the prion protein in prion diseases of ruminants transmitted in ovine transgenic mice." J Gen Virol **91**(Pt 2): 570-574.
Noinville, S., J. F. Chich and H. Rezaei (2008). "Misfolding of the prion protein: linking biophysical and biological approaches." Vet Res **39**(4): 48.

Novak, U. (2004). "ADAM proteins in the brain." J Clin Neurosci **11**(3): 227-235.
Novitskaya, V., O. V. Bocharova, I. Bronstein and I. V. Baskakov (2006). "Amyloid fibrils of mammalian prion protein are highly toxic to cultured cells and primary neurons." J Biol Chem **281**(19): 13828-13836.
Nystrom, S., R. Mishra, S. Hornemann, A. Aguzzi, K. P. Nilsson and P. Hammarstrom (2012). "Multiple substitutions of methionine 129 in human prion protein reveal its importance in the amyloid fibrillation pathway." J Biol Chem **287**(31): 25975-25984.
Oliveira-Martins, J. B., S. Yusa, A. M. Calella, C. Bridel, F. Baumann, P. Dametto and A. Aguzzi (2010). "Unexpected tolerance of alpha-cleavage of the prion protein to sequence variations." PLoS One **5**(2): e9107.
Owen, J. P., H. C. Rees, B. C. Maddison, L. A. Terry, L. Thorne, R. Jackman, G. C. Whitelam and K. C. Gough (2007). "Molecular profiling of ovine prion diseases by using thermolysin-resistant PrPSc and endogenous C2 PrP fragments." J Virol **81**(19): 10532-10539.
Pan, Y. L., L. N. Zhao, J. Liang, J. Liu, Y. Q. Shi, N. Liu, G. Y. Zhang, H. F. Jin, J. Gao, H. H. Xie, J. Wang, Z. G. Liu and D. M. Fan (2006). "Cellular prion protein promotes invasion and metastasis of gastric cancer." Faseb Journal **20**(11): 1886-+.
Pankiewicz, J., F. Prelli, M. S. Sy, R. J. Kascsak, R. B. Kascsak, D. S. Spinner, R. I. Carp, H. C. Meeker, M. Sadowski and T. Wisniewski (2006). "Clearance and prevention of prion infection in cell culture by anti-PrP antibodies." Eur J Neurosci **23**(10): 2635-2647.
Panza, G., L. Luers, J. Stöhr, L. Nagel-Steger, J. Weiss, D. Riesner, D. Willbold and E. Birkmann (2010). "Molecular interactions between prions as seeds and recombinant prion proteins as substrates resemble the biological interspecies barrier in vitro." PLoS One **5**(12): e14283.
Parkin, E. T., N. T. Watt, I. Hussain, E. A. Eckman, C. B. Eckman, J. C. Manson, H. N. Baybutt, A. J. Turner and N. M. Hooper (2007). "Cellular prion protein regulates beta-secretase cleavage of the Alzheimer's amyloid precursor protein." Proc Natl Acad Sci U S A **104**(26): 11062-11067.
Parkin, E. T., N. T. Watt, A. J. Turner and N. M. Hooper (2004). "Dual mechanisms for shedding of the cellular prion protein." J Biol Chem **279**(12): 11170-11178.
Pattison, I. H. (1965). "RESISTANCE OF THE SCRAPIE AGENT TO FORMALIN." J Comp Pathol **75**: 159-164
Pearson, G. R., J. M. Wyatt, T. J. Gruffydd-Jones, J. Hope, A. Chong, R. J. Higgins, A. C. Scott and G. A. Wells (1992). "Feline spongiform encephalopathy: fibril and PrP studies." Vet Rec **131**(14): 307-310.
Peden, A. H., M. W. Head, D. L. Ritchie, J. E. Bell and J. W. Ironside (2004). "Preclinical vCJD after blood transfusion in a PRNP codon 129 heterozygous patient." Lancet **364**(9433): 527-529.
Peretz, D., R. A. Williamson, K. Kaneko, J. Vergara, E. Leclerc, G. Schmitt-Ulms, I. R. Mehlhorn, G. Legname, M. R. Wormald, P. M. Rudd, R. A. Dwek, D. R. Burton and S. B. Prusiner (2001). "Antibodies inhibit prion propagation and clear cell cultures of prion infectivity." Nature **412**(6848): 739-743.

Perrier, V., J. Solassol, C. Crozet, Y. Frobert, C. Mourton-Gilles, J. Grassi and S. Lehmann (2004). "Anti-PrP antibodies block PrPSc replication in prion-infected cell cultures by accelerating PrPC degradation." J Neurochem **89**(2): 454-463.
Peters, P. J., A. Mironov, Jr., D. Peretz, E. van Donselaar, E. Leclerc, S. Erpel, S. J. DeArmond, D. R. Burton, R. A. Williamson, M. Vey and S. B. Prusiner (2003). "Trafficking of prion proteins through a caveolae-mediated endosomal pathway." J Cell Biol **162**(4): 703-717.
Piccardo, P., J. C. Manson, D. King, B. Ghetti and R. M. Barron (2007). "Accumulation of prion protein in the brain that is not associated with transmissible disease." Proc Natl Acad Sci U S A **104**(11): 4712-4717.
Praus, M., G. Kettelgerdes, M. Baier, H. G. Holzhütter, P. R. Jungblut, M. Maissen, G. Epple, W. D. Schleuning, E. Köttgen, A. Aguzzi and R. Gessner (2003). "Stimulation of plasminogen activation by recombinant cellular prion protein is conserved in the NH2-terminal fragment PrP23-110." Thromb Haemost **89**(5): 812-819.
Premzl, M., J. E. Gready, L. S. Jermiin, T. Simonic and J. A. Marshall Graves (2004). "Evolution of vertebrate genes related to prion and Shadoo proteins--clues from comparative genomic analysis." Mol Biol Evol **21**(12): 2210-2231.
Prusiner, S. B. (1998). "Prions." Proc Natl Acad Sci U S A **95**(23): 13363-13383.
Prusiner, S. B., M. P. McKinley, D. F. Groth, K. A. Bowman, N. I. Mock, S. P. Cochran and F. R. Masiarz (1981). "Scrapie agent contains a hydrophobic protein." Proc Natl Acad Sci U S A **78**(11): 6675-6679.
Rezaei, H., Y. Choiset, F. Eghiaian, E. Treguer, P. Mentre, P. Debey, J. Grosclaude and T. Haertle (2002). "Amyloidogenic unfolding intermediates differentiate sheep prion protein variants." Journal of Molecular Biology **322**(4): 799-814.
Rigter, A. and A. Bossers (2005). "Sheep scrapie susceptibility-linked polymorphisms do not modulate the initial binding of cellular to disease-associated prion protein prior to conversion." J Gen Virol **86**(Pt 9): 2627-2634.
Rigter, A., J. Priem, D. Timmers-Parohi, J. P. Langeveld, F. G. van Zijderveld and A. Bossers (2009). "Prion protein self-peptides modulate prion interactions and conversion." BMC Biochem **10**: 29.
Rogers, M., F. Yehiely, M. Scott and S. B. Prusiner (1993). "Conversion of truncated and elongated prion proteins into the scrapie isoform in cultured cells." Proc Natl Acad Sci U S A **90**(8): 3182-3186.
Sabuncu, E., S. Petit, A. Le Dur, T. Lan Lai, J. L. Vilotte, H. Laude and D. Vilette (2003). "PrP polymorphisms tightly control sheep prion replication in cultured cells." J Virol **77**(4): 2696-2700.
Sajnani, G., M. A. Pastrana, I. Dynin, B. Onisko and J. R. Requena (2008). "Scrapie prion protein structural constraints obtained by limited proteolysis and mass spectrometry." Journal of Molecular Biology **382**(1): 88-98.
Sales, N. (2006). "What can we learn from the oral intake of prions by sheep?" J Pathol **209**(1): 1-3.
Sanghera, N., M. Wall, C. Vénien-Bryan and T. J. Pinheiro (2008). "Globular and pre-fibrillar prion aggregates are toxic to neuronal cells and perturb their electrophysiology." Biochim Biophys Acta **1784**(6): 873-881.
Shyng, S. L., J. E. Heuser and D. A. Harris (1994). "A glycolipid-anchored prion protein is endocytosed via clathrin-coated pits." J Cell Biol **125**(6): 1239-1250.

Shyng, S. L., M. T. Huber and D. A. Harris (1993). "A prion protein cycles between the cell surface and an endocytic compartment in cultured neuroblastoma cells." J Biol Chem **268**(21): 15922-15928.
Shyng, S. L., K. L. Moulder, A. Lesko and D. A. Harris (1995). "The N-terminal domain of a glycolipid-anchored prion protein is essential for its endocytosis via clathrin-coated pits." J Biol Chem **270**(24): 14793-14800.
Sigurdsson, E. M., M. S. Sy, R. L. Li, H. Scholtzova, R. J. Kascsak, R. Kascsak, R. Carp, H. C. Meeker, B. Frangione and T. Wisniewski (2003). "Anti-prion antibodies for prophylaxis following prion exposure in mice." Neuroscience Letters **336**(3): 185-187.
Simmons, M. M., T. Konold, H. A. Simmons, Y. I. Spencer, R. Lockey, J. Spiropoulos, S. Everitt and D. Clifford (2007). "Experimental transmission of atypical scrapie to sheep." BMC Vet Res **3**: 20.
Simmons, M. M., S. J. Moore, T. Konold, L. Thurston, L. A. Terry, L. Thorne, R. Lockey, C. Vickery, S. A. Hawkins, M. J. Chaplin and J. Spiropoulos (2011). "Experimental oral transmission of atypical scrapie to sheep." Emerg Infect Dis **17**(5): 848-854.
Somerville, R. A. (1999). "Host and transmissible spongiform encephalopathy agent strain control glycosylation of PrP." J Gen Virol **80 (Pt 7)**: 1865-1872.
Somerville, R. A. (2002). "TSE agent strains and PrP: reconciling structure and function." Trends Biochem Sci **27**(12): 606-612.
Spiropoulos, J., C. Casalone, M. Caramelli and M. M. Simmons (2007). "Immunohistochemistry for PrPSc in natural scrapie reveals patterns which are associated with the PrP genotype." Neuropathol Appl Neurobiol **33**(4): 398-409.
Sreerama, N. and R. W. Woody (2000). "Estimation of protein secondary structure from circular dichroism spectra: comparison of CONTIN, SELCON, and CDSSTR methods with an expanded reference set." Anal Biochem **287**(2): 252-260.
Sreerama, N. and R. W. Woody (2004). "Computation and analysis of protein circular dichroism spectra." Methods Enzymol **383**: 318-351.
Stanton, J. B., D. A. Schneider, K. D. Dinkel, B. F. Balmer, T. V. Baszler, B. A. Mathison, D. W. Boykin and A. Kumar (2012). "Discovery of a novel, monocationic, small-molecule inhibitor of scrapie prion accumulation in cultured sheep microglia and Rov cells." PLoS One **7**(11): e51173.
Stewart, L. A., L. H. Rydzewska, G. F. Keogh and R. S. Knight (2008). "Systematic review of therapeutic interventions in human prion disease." Neurology **70**(15): 1272-1281.
Stewart, P., L. Campbell, S. Skogtvedt, K. A. Griffin, J. M. Arnemo, M. Tryland, S. Girling, M. W. Miller, M. A. Tranulis and W. Goldmann (2012). "Genetic predictions of prion disease susceptibility in carnivore species based on variability of the prion gene coding region." PLoS One **7**(12): e50623.
Stewart, P., C. Shen, D. Zhao and W. Goldmann (2009). "Genetic analysis of the SPRN gene in ruminants reveals polymorphisms in the alanine-rich segment of shadoo protein." J Gen Virol **90**(Pt 10): 2575-2580.
Stohr, J., K. Elfrink, N. Weinmann, H. Wille, D. Willbold, E. Birkmann and D. Riesner (2011). "In vitro conversion and seeded fibrillization of posttranslationally modified prion protein." Biol Chem **392**(5): 415-421.

Stohr, J., K. Elfrink, N. Weinmann, H. Wille, D. Willbold, E. Birkmann and D. Riesner (2011). "In vitro conversion and seeded fibrillization of posttranslationally modified prion protein." Biological Chemistry **392**(5): 415-421.
Sunyach, C., M. A. Cisse, C. A. da Costa, B. Vincent and F. Checler (2007). "The C-terminal products of cellular prion protein processing, C1 and C2, exert distinct influence on p53-dependent staurosporine-induced caspase-3 activation." J Biol Chem **282**(3): 1956-1963.
Tagliavini, F., F. Prelli, M. Porro, M. Salmona, O. Bugiani and B. Frangione (1992). "A soluble form of prion protein in human cerebrospinal fluid: implications for prion-related encephalopathies." Biochem Biophys Res Commun **184**(3): 1398-1404.
Tan, B. C., A. R. Blanco, E. F. Houston, P. Stewart, W. Goldmann, A. C. Gill, C. de Wolf, J. C. Manson and S. McCutcheon (2012). "Significant differences in incubation times in sheep infected with bovine spongiform encephalopathy result from variation at codon 141 in the PRNP gene." J Gen Virol **93**(Pt 12): 2749-2756.
Taylor, D. R., E. T. Parkin, S. L. Cocklin, J. R. Ault, A. E. Ashcroft, A. J. Turner and N. M. Hooper (2009). "Role of ADAMs in the ectodomain shedding and conformational conversion of the prion protein." J Biol Chem **284**(34): 22590-22600.
Terry, L. A., L. Howells, J. Hawthorn, J. C. Edwards, S. J. Moore, S. J. Bellworthy, H. Simmons, S. Lizano, L. Estey, V. Leathers and S. J. Everest (2009). "Detection of PrPsc in blood from sheep infected with the scrapie and bovine spongiform encephalopathy agents." J Virol **83**(23): 12552-12558.
Thackray, A. M., T. J. Fitzmaurice, L. Hopkins and R. Bujdoso (2006). "Ovine plasma prion protein levels show genotypic variation detected by C-terminal epitopes not exposed in cell-surface PrPC." Biochem J **400**(2): 349-358.
Thackray, A. M., S. Yang, E. Wong, T. J. Fitzmaurice, R. J. Morgan-Warren and R. Bujdoso (2004). "Conformational variation between allelic variants of cell-surface ovine prion protein." Biochem J **381**(Pt 1): 221-229.
Tobler, I., S. E. Gaus, T. Deboer, P. Achermann, M. Fischer, T. Rulicke, M. Moser, B. Oesch, P. A. McBride and J. C. Manson (1996). "Altered circadian activity rhythms and sleep in mice devoid of prion protein." Nature **380**(6575): 639-642.
Toupet, K., V. Compan, C. Crozet, C. Mourton-Gilles, N. Mestre-Francés, F. Ibos, P. Corbeau, J. M. Verdier and V. Perrier (2008). "Effective gene therapy in a mouse model of prion diseases." PLoS One **3**(7): e2773.
Tuzi, N. L., E. Cancellotti, H. Baybutt, L. Blackford, B. Bradford, C. Plinston, A. Coghill, P. Hart, P. Piccardo, R. M. Barron and J. C. Manson (2008). "Host PrP glycosylation: a major factor determining the outcome of prion infection." PLoS Biol **6**(4): e100.
Tveit, H., C. Lund, C. M. Olsen, C. Ersdal, K. Prydz, I. Harbitz and M. A. Tranulis (2005). "Proteolytic processing of the ovine prion protein in cell cultures." Biochem Biophys Res Commun **337**(1): 232-240.
Tycko, R., R. Savtchenko, V. G. Ostapchenko, N. Makarava and I. V. Baskakov (2010). "The alpha-Helical C-Terminal Domain of Full-Length Recombinant PrP Converts to an In-Register Parallel beta-Sheet Structure in PrP Fibrils: Evidence from Solid State Nuclear Magnetic Resonance." Biochemistry **49**(44): 9488-9497.

Uttara, B., A. V. Singh, P. Zamboni and R. T. Mahajan (2009). "Oxidative stress and neurodegenerative diseases: a review of upstream and downstream antioxidant therapeutic options." Curr Neuropharmacol **7**(1): 65-74.
van Keulen, L. J., A. Bossers and F. van Zijderveld (2008). "TSE pathogenesis in cattle and sheep." Vet Res **39**(4): 24.
van Keulen, L. J., B. E. Schreuder, R. H. Meloen, M. Poelen-van den Berg, G. Mooij-Harkes, M. E. Vromans and J. P. Langeveld (1995). "Immunohistochemical detection and localization of prion protein in brain tissue of sheep with natural scrapie." Vet Pathol **32**(3): 299-308.
Vilette, D., O. Andreoletti, F. Archer, M. F. Madelaine, J. L. Vilotte, S. Lehmann and H. Laude (2001). "Ex vivo propagation of infectious sheep scrapie agent in heterologous epithelial cells expressing ovine prion protein." Proc Natl Acad Sci U S A **98**(7): 4055-4059.
Vilotte, J. L., S. Soulier, R. Essalmani, M. G. Stinnakre, D. Vaiman, L. Lepourry, J. C. Da Silva, N. Besnard, M. Dawson, A. Buschmann, M. Groschup, S. Petit, M. F. Madelaine, S. Rakatobe, A. Le Dur, D. Vilette and H. Laude (2001). "Markedly increased susceptibility to natural sheep scrapie of transgenic mice expressing ovine prp." J Virol **75**(13): 5977-5984.
Vincent, B. (2004). "ADAM proteases: protective role in Alzheimer's and prion diseases?" Curr Alzheimer Res **1**(3): 165-174.
Vincent, B., E. Paitel, Y. Frobert, S. Lehmann, J. Grassi and F. Checler (2000). "Phorbol ester-regulated cleavage of normal prion protein in HEK293 human cells and murine neurons." J Biol Chem **275**(45): 35612-35616.
Vincent, B., E. Paitel, P. Saftig, Y. Frobert, D. Hartmann, B. De Strooper, J. Grassi, E. Lopez-Perez and F. Checler (2001). "The disintegrins ADAM10 and TACE contribute to the constitutive and phorbol ester-regulated normal cleavage of the cellular prion protein." J Biol Chem **276**(41): 37743-37746.
Walmsley, A. R., N. T. Watt, D. R. Taylor, W. S. Perera and N. M. Hooper (2009). "alpha-cleavage of the prion protein occurs in a late compartment of the secretory pathway and is independent of lipid rafts." Mol Cell Neurosci **40**(2): 242-248.
Watt, N. T. and N. M. Hooper (2005). "Reactive oxygen species (ROS)-mediated beta-cleavage of the prion protein in the mechanism of the cellular response to oxidative stress." Biochem Soc Trans **33**(Pt 5): 1123-1125.
Watt, N. T., D. R. Taylor, A. Gillott, D. A. Thomas, W. S. Perera and N. M. Hooper (2005). "Reactive oxygen species-mediated beta-cleavage of the prion protein in the cellular response to oxidative stress." J Biol Chem **280**(43): 35914-35921.
Weissmann, C., H. Bueler, M. Fischer, A. Sauer and M. Aguet (1994). "Susceptibility to scrapie in mice is dependent on PrPC." Philos Trans R Soc Lond B Biol Sci **343**(1306): 431-433.
Weissmann, C., H. Bueler, A. Sailer, M. Fischer, M. Aguet and A. Aguzzi (1993). "Role of PrP in prion diseases." Br Med Bull **49**(4): 995-1011.
Wemheuer, W. M., S. L. Benestad, A. Wrede, W. E. Wemheuer, B. Brenig, B. Bratberg and W. J. Schulz-Schaeffer (2011). "PrPSc spreading patterns in the brain of sheep linked to different prion types." Vet Res **42**(1): 32.
Westaway, D., V. Zuliani, C. M. Cooper, M. Da Costa, S. Neuman, A. L. Jenny, L. Detwiler and S. B. Prusiner (1994). "Homozygosity for prion protein alleles

encoding glutamine-171 renders sheep susceptible to natural scrapie." Genes Dev **8**(8): 959-969.
Westergard, L., J. A. Turnbaugh and D. A. Harris (2011). "A naturally occurring C-terminal fragment of the prion protein (PrP) delays disease and acts as a dominant-negative inhibitor of PrPSc formation." J Biol Chem **286**(51): 44234-44242.
White, A. R., P. Enever, M. Tayebi, R. Mushens, J. Linehan, S. Brandner, D. Anstee, J. Collinge and S. Hawke (2003). "Monoclonal antibodies inhibit prion replication and delay the development of prion disease." Nature **422**(6927): 80-83.
Whitmore, L. and B. A. Wallace (2004). "DICHROWEB, an online server for protein secondary structure analyses from circular dichroism spectroscopic data." Nucleic Acids Res **32**(Web Server issue): W668-673.
Whitmore, L. and B. A. Wallace (2008). "Protein secondary structure analyses from circular dichroism spectroscopy: methods and reference databases." Biopolymers **89**(5): 392-400.
Wilham, J. M., C. D. Orrú, R. A. Bessen, R. Atarashi, K. Sano, B. Race, K. D. Meade-White, L. M. Taubner, A. Timmes and B. Caughey (2010). "Rapid end-point quantitation of prion seeding activity with sensitivity comparable to bioassays." PLoS Pathog **6**(12): e1001217.
Will, R. G. (1993). "Epidemiology of Creutzfeldt-Jakob disease." Br Med Bull **49**(4): 960-970.
Williams, E. S. (2005). "Chronic wasting disease." Vet Pathol **42**(5): 530-549.
Wong, E., A. M. Thackray and R. Bujdoso (2004). "Copper induces increased beta-sheet content in the scrapie-susceptible ovine prion protein PrPVRQ compared with the resistant allelic variant PrPARR." Biochem J **380**(Pt 1): 273-282.
Yadavalli, R., R. P. Guttmann, T. Seward, A. P. Centers, R. A. Williamson and G. C. Telling (2004). "Calpain-dependent endoproteolytic cleavage of PrPSc modulates scrapie prion propagation." J Biol Chem **279**(21): 21948-21956.
Younan, N. D., C. J. Sarell, P. Davies, D. R. Brown and J. H. Viles (2013). "The cellular prion protein traps Alzheimer's Abeta in an oligomeric form and disassembles amyloid fibers." FASEB J **27**(5): 1847-1858.
Zhao, H., M. Klingeborn, M. Simonsson and T. Linne (2006). "Proteolytic cleavage and shedding of the bovine prion protein in two cell culture systems." Virus Res **115**(1): 43-55.
Zhou, G. P. (2009). "Some insights into conversion process of the PrP(c) to PrP(beta)." Biochem Biophys Res Commun.